EXPLOITING mTOR CELLULAR SIGNALLING TO PROMOTE RETINAL GANGLION CELL SURVIVAL AND AXON REGENERATION AFTER TRAUMATIC OPTIC NEUROPATHY

by

Peter John Morgan-Warren

A thesis submitted to the University of Birmingham for the degree of
DOCTOR OF PHILOSOPHY

Neurotrauma Research Group
School of Clinical and Experimental Medicine
College of Medical and Dental Sciences
University of Birmingham
July 2015

UNIVERSITY OF
BIRMINGHAM

University of Birmingham Research Archive

e-theses repository

This unpublished thesis/dissertation is copyright of the author and/or third parties. The intellectual property rights of the author or third parties in respect of this work are as defined by The Copyright Designs and Patents Act 1988 or as modified by any successor legislation.

Any use made of information contained in this thesis/dissertation must be in accordance with that legislation and must be properly acknowledged. Further distribution or reproduction in any format is prohibited without the permission of the copyright holder.

ABSTRACT

Retinal ganglion cell (RGC) apoptosis and failure of optic nerve (ON) axon regeneration contribute to profound visual loss after traumatic optic neuropathy (TON), for which clinically effective treatments are lacking. Experimental manipulations of cellular signalling have identified phosphoinositide-3-kinase (PI3K) and its downstream mediators mTOR and GSK3β as important regulators of neuronal survival and axon regeneration. This study aimed to promote RGC neuroprotection and axon regeneration in an animal model of TON, using targeted siRNA to knock-down key negative regulators of cellular signalling, and to investigate underlying mechanisms using retinal cultures. Intravitreal treatment with siRNA targeting RTP801, a stress-induced inhibitor of mTOR, promoted RGC survival and axon elongation after ON crush (ONC), and potentiated reactive gliosis. *In vitro*, siRTP801-induced neuroprotection was direct, but required $GFAP^+$ activated retinal glia to stimulate neurite elongation. siRTP801 also potentiated levels of glial-derived Trk-dependent neurotrophic factors. Knock-down of the axon growth cone/apoptosis regulator GSK3β was also neuroprotective, promoted modest axon elongation after ONC, and increased neurite sprouting *in vitro*. GSK3β suppression counteracted neurite growth-inhibition induced by CNS myelin-derived Nogo. Combined treatment with siRTP801/siGSK3β augmented axon regeneration after ONC. These findings support a clinically translatable siRNA approach targeting PI3K/mTOR signalling as the basis for development of novel neuroprotective/axogenic therapies.

ACKNOWLEDGMENTS

I would like to thank my supervisors, Professor Ann Logan and Wg Cdr Professor Rob Scott, for giving me the opportunity to undertake this PhD research project and for their invaluable guidance, advice and support throughout the process.

I would also like to thank Professor Martin Berry, who has provided exceptional intellectual input and practical advice during the course of this project.

In addition, I wish to acknowledge the support and contributions of friends and colleagues in the Neurotrauma Research Group, and in the wider University of Birmingham, who have provided practical guidance, help with experiments, administrative support and general encouragement.

This research has been funded by the Medical Research Council and Royal College of Ophthalmologists John Lee Fellowship (MRC Grant MR/J011584/1). I am honoured to be the recipient of the inaugural John Lee Fellowship, and am grateful to the Royal College of Ophthalmologists and its supporters for their backing. I hope my work will contribute to the development of future novel sight-saving therapies to benefit patients.

Thank you also to Quark Pharmaceuticals Inc. (Ness Ziona, Israel), who kindly provided the small interfering ribonucleic acid (siRNA) reagents used in this research project, and also contributed relevant supporting data and information.

I wish to acknowledge my line management at HQ Air, Royal Air Force High Wycombe, and Dr Amarjit Samra, Director of Research at the Royal Centre for Defence Medicine (RCDM, Birmingham), for supporting this research project and appreciating its military potential.

Finally, I wish to thank my friends and family, especially Claire, for their encouragement and support, without which this project would not have been possible.

CONTENTS

1 INTRODUCTION……1

1.1 Overview of the visual system……2

1.1.1 Structure of the retina…… 2

1.1.2 RGC sub-types and classification…… 5

1.1.3 Optic nerve and central projections…… 5

1.1.4 Comparative anatomy between human and rodent visual systems…… 6

1.2 Traumatic optic neuropathy…… 7

1.2.1 Pathophysiology…… 7

1.2.2 Epidemiology…… 7

1.2.3 Clinical features…… 9

1.2.4 Management of TON…… 9

1.2.4.1 Corticosteroids…… 9

1.2.4.2 Surgical optic canal decompression…… 10

1.2.4.3 Requirement for novel therapeutic options…… 11

1.3 Rodent optic nerve crush model and anatomical assessment of RGC survival and axon regeneration…… 11

1.4 Response to injury and optic nerve regenerative failure…… 11

1.4.1 ON injury response…… 14

1.4.2 RGC death by apoptosis…… 15

1.4.3 RGC axon regenerative failure due to the inhibitory CNS milieu…… 17

1.5 RGC survival and axon regeneration are promoted by inflammatory stimulation…

……19

1.5.1 Activated macrophages and neutrophils are key mediators of inflammatory stimulation…… 20

1.5.2 Glial activation and trophic factor signalling…… 21

1.6 Intrinsic determinants of RGC regenerative ability…… 22

1.6.1 Developmental down-regulation of RGC regenerative ability…… 22

1.6.1.1 cAMP……23

1.6.1.2 Transcription factors……23

1.6.2 Mammalian Target of Rapamycin (mTOR)…… 24

1.7 Activation of mTOR activity by the PI3K/Akt signalling pathway..... 24
1.7.1 mTOR forms two distinct functional complexes with different substrates and cellular effects..... 26
1.7.2 Other downstream effectors of PI3K/Akt signalling and links to alternative pathways..... 27
1.7.2.1 Glycogen synthase kinase 3 beta (GSK3β)..... 27
1.7.2.2 ERK/MAPK signalling pathway..... 28
1.7.2.3 Cytokine signalling and the Wnt pathway..... 28
1.8 Extrinsic mechanisms of mTOR activity regulation..... 29
1.8.1 Hypoxia..... 29
1.8.2 Energy deprivation..... 30
1.8.3 Nutrient availability..... 30
1.9 Manipulating mTOR signalling to promote RGC survival and axon regeneration 32
1.9.1 Deletion of the *pten* gene promotes RGC survival and robust axon regeneration..... 32
1.9.2 Combining *pten* deletion with other approaches further enhances RGC survival and axon regeneration..... 35
1.10 Translation of molecular biology for clinical use..... 35
1.10.1 RNA interference: principles and mechanisms..... 36
1.10.2 Delivery and stability of siRNA..... 37
1.10.3 Off-target effects of RNAi..... 38
1.11 Project aims and hypotheses..... 39
1.11.1 Overall project aim..... 39
1.11.2 Overall project hypothesis..... 40
1.11.3 Chapter overview..... 41

2 MATERIALS AND METHODS..... 43

2.1 Overview of experimental methods..... 44
2.2 siRNA..... 46
2.3 *In vivo* methods..... 46
2.3.1 Animals and animal surgery..... 46
2.3.2 Anaesthesia and peri-operative care..... 47

2.3.2 ONC..... 48
2.3.3 Intravitreal injections..... 50
2.3.4 Tissue preparation..... 50
2.3.5 Immunofluorescence..... 51
2.3.5.1 Principles of immunofluorescence..... 51
2.3.5.2 Immunohistochemistry protocol..... 53
2.3.5.3 Fluorescence microscopy..... 54
2.3.6 Quantification of *in vivo* responses..... 55
2.3.6.1 Quantification of RGC survival..... 55
2.3.6.2 Quantification of RGC axon regeneration..... 56
2.3.6.3 Quantification of retinal glial activation..... 57
2.3.6.4 Quantification of cellular detection of signalling mediators..... 57
2.3.6.5 Quantification of immunostaining intensity..... 58
2.4 *In vitro* methods..... 60
2.4.1 Retinal cell culture..... 60
2.4.1.1 Principles of retinal cell culture studies..... 60
2.4.1.2 Retinal cell culture protocol..... 61
2.4.2 siRNA transfection..... 64
2.4.3 Treatment of retinal cultures with inhibitors..... 67
2.4.3.1 Rapamycin..... 67
2.4.3.2 K252a..... 67
2.4.3.3 Chir99021..... 68
2.4.4 Preparation of retinal cultures in the presence of Nogo growth-inhibitory substrate..... 68
2.5 Immunocytochemistry..... 69
2.6 Quantification of retinal cultures..... 70
2.6.1 Quantification of RGC survival..... 71
2.6.2 Quantification of RGC neurite outgrowth..... 71
2.6.2.1 Quantification of neurite outgrowth initiation..... 71
2.6.2.2 Quantification of neurite outgrowth elongation..... 72
2.6.3 Quantification of retinal astrocytes and Müller glia..... 72
2.6.4 Quantification of cellular signalling markers in RGC and glia..... 72
2.7 Enzyme linked immunosorbent assay (ELISA)...... 74

2.7.1 Principles of ELISA..... 74
2.7.2 ELISA protocols..... 76
2.7.2.1 CNTF (and NGF, NT-3 and GDNF) ELISA..... 76
2.7.2.2 BDNF ELISA..... 77
2.7.2.3 PEDF ELISA..... 79
2.7.3 ELISA analysis..... 80
2.8 Polymerase chain reaction (PCR)..... 82
2.8.1 Principles of PCR..... 82
2.8.2 qPCR protocols..... 85
2.8.2.1 Sample preparation..... 86
2.8.2.2 RNA extraction, quantification and quality control..... 86
2.8.2.3 Reverse transcription..... 88
2.8.2.4 Primer preparation..... 88
2.8.2.5 qPCR reaction protocol..... 89
2.8.2.6 Confirmation of qPCR reaction specificity..... 90
2.8.2.7 Selection of endogenous control (reference) gene..... 93
2.8.2.8 Gene expression quantification..... 93
2.9 Statistics..... 94

3 INVESTIGATING siRNA-MEDIATED KNOCK-DOWN OF RTP801 ON RGC SURVIVAL AND AXON REGENERATION..... 96

3.1 Introduction / rationale..... 97
3.2 Hypothesis..... 98
3.3 Aims..... 99
3.4 Experimental design..... 99
3.4.1 Confirmation of siRNA specificity and knock-down with qPCR..... 99
3.4.2 Assessment of siRTP801 on retinal expression of RTP801 and on RGC survival and axon regeneration after ONC *in vivo*..... 100
3.4.3 Assessment of siRTP801 on retinal cellular localisation of RTP801 and on RGC survival and neurite outgrowth in dissociated mixed retinal cultures..... 100
3.5 Results..... 101
3.5.1 Characterisation of specific activity of siRTP801 and target knock-down.. 101

3.5.1.1 Confirmation of specificity of siRTP801 and target knock-down *in vitro*…… 101
3.5.1.2 Confirmation of siRTP801 specificity and the lack of induction of non-specific pro-inflammatory effects of siRTP801 *in vivo*……103
3.5.2 Characterisation of retinal expression of RTP801 and the effects of siRTP801 …… 105
3.5.2.1 Retinal expression of RTP801 was increased after ONC and reduced by siRTP801 treatment……105
3.5.2.2 RTP801 cellular localisation and target knock-down in RGC and other retinal cell populations *in vitro*……110
3.5.3 Effects of siRTP801 on RGC survival and axon regeneration after ONC *in vivo* …… 118
3.5.3.1 siRTP801 promoted RGC survival up to 24d after ONC…… 118
3.5.3.2 siRTP801 promoted longer growth of regenerating RGC axons up to 1200µm beyond the injury site without affecting the initiation of axon sprouting after ONC…… 121
3.5.4 Effect of siRTP801 on RGC survival and neurite outgrowth in cultured retinal cells *in vitro*…… 123
3.5.4.1 siRTP801 was RGC neuroprotective in primary retinal cultures from uninjured animals…… 123
3.5.4.2 siRTP801 neither initiated RGC neurite outgrowth nor increased RGC neurite length in primary retinal cultures from uninjured animals….. ……123
3.5.5 Summary of results……126
3.6 Discussion……128
3.6.1 Specificity and efficacy of siRNA-mediated knock-down of RTP801 and lack of non-specific pro-inflammatory response…… 128
3.6.2 RTP801 expression in the retina, response to injury, and siRTP801-induced knock-down……131
3.6.3 Neuroprotective effect of RTP801 knock-down…… 134
3.6.4 Axon regeneration/elongation after RTP801 knock-down…… 138

4 INVESTIGATING THE CONTRIBUTION OF mTOR SIGNALLING AND GLIAL-DEPENDENT FACTORS TO RGC SURVIVAL AND AXON/NEURITE GROWTH AFTER RTP801 KNOCK-DOWN..... 143

4.1 Introduction / rationale.....144
4.2 Hypotheses..... 145
4.3 Aims.....145
4.4 Experimental design..... 146
4.4.1 Characterisation of RGC expression of pS6 and the effects of siRTP801 *in vivo*..... 146
4.4.2 Characterisation of RGC expression of pS6 and the effects of siRTP801 *in vitro*..... 147
4.4.3 Assessment of the effects of siRTP801 on activation of retinal glia after ONC *in vivo*..... 147
4.4.4 Assessment of the effects of siRTP801 on activation of retinal glia *in vitro*, on RGC survival and neurite outgrowth in the presence of activated retinal glia, and the contribution of mTORC1- and Trk-dependent signalling..... 147
4.4.5 Assessment of the effects of siRTP801 on the production of retinal glial-derived NTF..... 148
4.5 Results.....149
4.5.1 Effect of siRTP801 on RGC mTORC1 activity.....149
4.5.1.1 Injury-induced reduction in RGC pS6 expression was prevented by siRTP801..... 149
4.5.1.2 siRTP801 increased RGC expression of pS6 in retinal cultures established from uninjured adult rats.....149
4.5.1.3 Expression of pS6 was reduced in cultured RGC after ONC injury, but maintained after siRTP801 treatment..... 152
4.5.1.4 RGC pS6 activity was not mandatory for neurite outgrowth, and pS6 was detected in non-RGC retinal cells.....152
4.5.2 Effect of siRT801 on retinal glial activity.....156
4.5.2.1 Retinal glial activation after ONC *in vivo* was potentiated by siRTP801 without affecting retinal glial proliferation.....156

4.5.2.2 Activated GFAP$^+$ retinal glia were present *in vitro* after prior ONC, and RTP801 expression in activated glia was knocked-down by siRTP801..... 156
4.5.3 Effect of siRTP801 on RGC survival and neurite outgrowth in the presence of activated retinal glia, and the role of mTORC1- and Trk-dependent signalling. 162
4.5.3.1 siRTP801 promoted RGC survival and neurite elongation in the presence of activated retinal glia in vitro, without affecting neurite growth initiation..... 162
4.5.3.2 The contribution of mTORC1-dependent signalling to siRTP801-induced neuroprotection and neurite elongation *in vitro*..... 162
4.5.3.3 The contribution of Trk-dependent signalling to siRTP801-induced RGC neuroprotection and neurite elongation *in vitro*..... 163
4.5.4 Effect of siRTP801 on the production of NTF *in* vitro..... 167
4.5.4.1 Effect of siRTP801 on the production of neurotrophins and other NTF in the absence and presence of activated retinal glia..... 167
4.5.4.2 Neurotrophic factor production both from RGC and glia..... 170
4.5.5 Summary of results..... 170
4.6 Discussion..... 172
4.6.1 The role of mTOR activity in siRTP801-mediated RGC survival and axon/neurite growth..... 173
4.6.2 The role of activated retinal glia in siRTP801-mediated RGC survival and axon/neurite growth..... 179

5 EVALUATION OF THE EFFECTS OF GSK3β INHIBITION ON RGC SURVIVAL AND AXON/NEURITE REGENERATION..... 186

5.1 Introduction / rationale..... 187
5.2 Hypotheses..... 191
5.3 Aims..... 191
5.4 Experimental design..... 192
5.4.1 Assessment of the effects of Chir99021 on RGC survival, neurite outgrowth and GSK3β expression *in vitro*..... 192

5.4.2 Assessment of the effects of siGSK3β on RGC survival, neurite outgrowth and GSK3β expression *in vitro*……. 193
5.4.3 Confirmation of siRNA specificity and target knock-down with qPCR…….. 193
5.4.4 *In vivo* assessment of the effects of siGSK3β on RGC survival, axon regeneration and retinal glial activation, and of combination treatment with siGSK3β and siRTP801 on RGC survival and axon regeneration after ONC.194
5.4.5 In vitro assessment of the effects of siGSK3β on RGC survival and neurite outgrowth in the presence of activated retinal glia and the evaluation of the underlying cellular signalling mechanisms…… 194
5.4.6 Assessment of combined siRNA treatment with siGSK3β and siRTP801 on RGC survival and axon/neurite growth…… 195
5.5 Results……196
5.5.1 Effects of GSK3β inhibition using the pharmacological inhibitor Chir99021 on RGC survival, neurite outgrowth and RGC expression of GSK3β in the absence of activated retinal glia *in vitro*…….. 196
5.5.1.1 Chir99021 was RGC neuroprotective in a concentration-dependent manner in retinal cultures in the absence of activated retinal glia196
5.5.1.2 Chir99021 promoted RGC neurite initiation but did not affect neurite length in retinal cultures in the absence of activated retinal glia..197
5.5.1.3 Chir99021 did not affect RGC localisation of GSK3β *in vitro*……. 197
5.5.2 Effects of siGSK3β on RGC expression of GSK3β and knock-down *in vitro*.200
5.5.3 Effects of siGSK3β on RGC survival and neurite outgrowth in the absence of activated retinal glia *in vitro*…… 200
5.5.3.1 siGSK3β was RGC neuroprotective in primary retinal cultures…... 200
5.5.3.2. siGSK3β promoted RGC neurite growth initiation in the absence of activated retinal glia *in vitro*…… 201
5.5.3.3 siGSK3β did not affect RGC neurite elongation in the absence of activated retinal glia *in vitro*…… 204
5.5.4 Confirmation of siRNA-mediated knock-down of GSK3β mRNA in retinal cells …….. 204
5.5.5 Effects of siGSK3β on RGC survival and axon regeneration 24d after ONC *in vivo*…… 206
5.5.5.1 siGSK3β was RGC neuroprotective 24d after ONC…….. 206

5.5.5.2 siGSK3β promoted elongation of regenerating RGC axons beyond the injury site without affecting initiation of axon sprouting at 24d after ONC…… 206
5.5.6 Effects of siGSK3β on RGC survival, neurite outgrowth and mTORC1 activity in the presence of activated retinal glia *in vitro*…… 210
5.5.6.1 siGSK3β was RGC neuroprotective in the presence of activated retinal glia *in vitro*, and the effects were dependent upon mTORC1 signalling……210
5.5.6.2 siGSK3β increased RGC neurite outgrowth initiation in the presence of activated retinal glia *in vitro*, independent of mTORC1 signalling…. ……..211
5.5.6.3 siGSK3β promoted RGC neurite elongation in the presence of activated retinal glia *in vitro*, independent of mTORC1 signalling. 211
5.5.6.4 siGSK3β did not affect RGC expression of pS6 in the presence of activated retinal glia *in vitro*……212
5.5.7 Cellular localisation of GSK3β was limited to RGC and not present in activated retinal glia…… 215
5.5.8 siGSK3β did not affect reactive gliosis after ONC *in vivo*……215
5.5.9 Effects of siGSk3β on downstream substrates of GSK3β……218
5.5.9.1 Effects of siGSK3β on RGC cellular expression of pGSK3β ……..218
5.5.9.2 Effects of siGSK3β on RGC cellular expression of pCRMP2…… 218
5.5.9.3 Effects of siGSK3β on RGC cellular expression of pSmad1……..218
5.5.9.4 Effects of siGSK3β on RGC cellular expression of pMAP1B……219
5.5.10 Effects of GSK3β inhibition on overcoming Nogo inhibitory peptide *in vitro*… …… 224
5.5.10.1 GSK3β inhibition overcame the inhibitory effect of Nogo on RGC neurite outgrowth initiation *in vitro*……224
5.5.10.2 GSK3β inhibition overcame the inhibitory effect of Nogo on RGC neurite elongation *in vitro*…… 224
5.5.11 Effects of combined siGSK3β/siRTP801 on RGC survival, neurite outgrowth and target knock-down in the presence of activated retinal glia *in vitro*… 227

5.5.11.1 Combined siGSK3β (50nM) + siRTP801 (20nM) did not induce dual target knock-down, nor promoted RGC survival or neurite outgrowth *in vitro*..... 227

5.5.11.2 Combined siGSK3β (25nM) + siRTP801 (25nM) enabled dual target knock-down, was RGC neuroprotective and promoted neurite outgrowth initiation and elongation *in vitro*..... 229

5.5.12 Effects of combined siGSK3β/siRTP801 on RGC survival and axon regeneration after ONC *in vivo*..... 232

5.5.12.1 Effects of combined siGSK3β/siRTP801 treatment on RGC survival after ONC *in vivo*..... 232

5.5.12.2 Effects of combined siGSK3β/siRTP801 treatment on axon regeneration after ONC *in vivo*..... 232

5.5.13 Summary of results..... 235

5.6 Discussion..... 236

5.6.1 GSK3β and neuroprotection..... 237

5.6.2 GSK3β and axon regeneration..... 242

5.6.3 Mechanisms of siGSK3β-induced axon growth..... 245

5.6.4 Combined siRNA approach for RGC neuroprotection and axon regeneration 250

6 SUMMARY, GENERAL DISCUSSION, FUTURE DIRECTIONS AND CONCLUSIONS.... 255

6.1 Consideration of project hypotheses..... 256

6.1.1 Hypothesis 1: siRNA-mediated knock-down of the stress-induced mTOR negative regulator RTP801 promotes RGC survival and axon regeneration in a rat model of TON..... 257

6.1.2 Hypothesis 2: RGC survival and axon growth effects are mediated *via* increased mTORC1 activity..... 258

6.1.3 Hypothesis 3: The presence of activated retinal glia is required to mediate the axon growth effects of siRTP801, *via* the enhanced production of NTF… 259

6.1.4 Hypothesis 4: Inhibition of GSK3β promotes RGC survival and axon growth…. 259

6.1.5 Hypothesis 5: Combined siRNA mediated knock-down of both RTP801 and GSK3β potentiates RGC survival and axon regeneration..... 260
6.2 Challenges for clinical translation of cellular signalling based therapies..... 262
6.2.1 Optimising conditions for RGC survival and axon regeneration after TON 262
6.2.2 Unlocking axon regeneration in non-responding RGC.....263
6.2.3 Forming the right connections: axon guidance and synaptogenesis.....264
6.2.4 Translating molecular biology to the clinic: clinical potential for siRNA therapy.....265
6.2.5 Potential adverse effects of up-regulating PI3K/Akt/mTOR signalling..... 266
6.3 Experimental limitations..... 267
6.3.1 Limitations of *in vivo* procedures.....267
6.3.2 Limitations of *in vitro* procedures.....269
6.4 Future directions.....270
6.4.1 Development of an optimal targeted combination treatment..... 270
6.4.2 Measurement of anatomical and functional outputs..... 272
6.5 Conclusions.....272

REFERENCES..... 274

APPENDIX.....307

LIST OF FIGURES

Chapter 1 Introduction

1.1 Structure of the eye and retina……4

1.2 Traumatic optic neuropathy…… 8

1.3 RGC death and regenerative failure after optic nerve injury…… 13

1.4 Schematic diagram of the rodent ONC model for investigating RGC survival and axon regeneration……14

1.5 Cellular mechanisms of apoptosis……16

1.6 Contribution of myelin- and glia-scar derived factors to inhibitory signalling……18

1.7 Signalling of the mTOR pathway, with links to related signalling pathways…… 25

1.8 Regulation of mTOR signalling by external factors…… 31

1.9 Deletion of *pten* promotes RGC axon regeneration…… 33

1.10 Mechanism of RNA interference (RNAi)…… 37

1.11 Project hypothesis…… 40

Chapter 2 Materials and Methods

2.1 Overview of experimental approach of *in vivo* and *in vitro* studies……45

2.2 Optic nerve crush (ONC) procedure……49

2.3 Principles of immunofluorescence……52

2.4 *In vivo* quantification techniques…… 59

2.5 Quantification of the yield of cells obtained in retinal cell culture studies…… 63

2.6 Transfection of retinal cultures with siRNA…… 66

2.7 Quantification of retinal cultures…… 70

2.8 Identification of retinal cells in culture……73

2.9 Enzyme linked immunosorbent assay (ELISA)…… 75

2.10 Principles of polymerase chain reaction (PCR)…… 83

2.11 Quantitative polymerase chain reaction (qPCR)…… 85

2.12 Example of melt curve analysis for qPCR specificity validation…… 92

Chapter 3 Investigating siRNA-mediated knock-down of RTP801 on RGC survival and axon regeneration

3.1 Target specificity and knock-down efficacy of siRTP801……102
3.2 Confirmation of siRTP801 target specificity and lack of induction of non-specific pro-inflammatory response……103
3.3 RTP801 expression in the retinal GCL after ONC, and siRTP801-mediated target knock-down in RGC and other GCL cells……107
3.4 RTP801 expression and localisation with Müller glia in retinal sections, and siRTP801-mediated target knock-down in the INL……108
3.5 RTP801 cellular localisation and siRTP801-mediated target knock-down in retinal cultures established from uninjured animals……111
3.6 Lack of $GFAP^+$ or $CRALBP^+$ activated retinal glia in cultures established from uninjured intact animals……115
3.7 RTP801 expression in $calbindin^+$ horizontal cells *in vitro*, and lack of target knock-down by siRTP801……116
3.8 RTP801 expression in $S100\beta^+$ retinal glia *in vitro* and siRTP801-mediated target knock-down……117
3.9 $\beta III\text{-}tubulin^+$ RGC survival after ONC *in vivo*……119
3.10 $Brn3a^+$ RGC survival after ONC *in vivo*……120
3.11 Enhanced RGC axon elongation by siRTP801 after ONC without affecting initiation of axon regeneration……122
3.12 RGC survival and neurite outgrowth in cultured retinal cells in the absence of activated retinal glia……124

Chapter 4 Investigating the contribution of mTOR signalling and glial-dependent factors to RGC survival and axon/neurite growth after RTP801 knock-down

4.1 Maintenance of RGC expression of mTORC1 substrate pS6 after ONC *in vivo*……150
4.2 Effect of siRTP801 on RGC pS6 expression in retinal cultures established from uninjured animals……151
4.3 Maintenance of RGC pS6 expression after injury *in vitro*……154

4.4 Expression of pS6 does not correlate with RGC neurite outgrowth, and is present in non-neuronal cells..... 155
4.5 Retinal astrocyte/Müller glial response after ONC *in vivo*..... 158
4.6 $GFAP^+$ activated retinal glia and RTP801 knock-down in activated glia in retinal cultures established 5d after ONC..... 159
4.7 $CRALBP^+$ activated retinal glia and RTP801 knock-down in activated glia in retinal cultures established 5d after ONC..... 160
4.8 $S100\beta^+$ retinal glia and RTP801 knock-down in activated glia in retinal cultures established 5d after ONC..... 161
4.9 RGC survival and neurite outgrowth in cultured retinal cells in the presence of activated retinal glia..... 164
4.10 Effects of mTORC1 inhibitor Rapamycin and pan-Trk receptor antagonist K252a on RGC survival and neurite outgrowth in glial-activated retinal cultures..... 165
4.11 Effects of siRTP801 treatment on NTF titres in the absence and presence of activated retinal glia..... 168
4.12 NTF detection in RGC and non-neuronal cells in glial-activated retinal cultures..... 171

Chapter 5 Evaluation of the effects of GSK3β inhibition on RGC survival and axon/neurite regeneration

5.1 Regulation and substrates of GSK3β activity..... 190
5.2 Effects of GSK3β inhibitor Chir99021 on RGC survival and neurite outgrowth in cultured retinal cells in the absence of activated retinal glia..... 198
5.3 Effects of siGSK3β on cellular localisation of GSK3β, RGC survival and neurite outgrowth in cultured retinal cells in the absence of activated retinal glia..... 202
5.4 Target specificity and knock-down efficacy of siGSK3β..... 205
5.5 $Brn3a^+$ RGC survival after ONC *in vivo*..... 208
5.6 Enhanced RGC axon elongation by siGSK3β without affecting initiation of axon regeneration after ONC *in vivo*..... 209
5.7 Effects of siGSK3β on RGC survival, neurite outgrowth and mTORC1 activity in the presence of activated retinal glia *in vitro*..... 213
5.8 Cellular localisation of GSK3β was limited to RGC with no detectable expression in glia... 216

5.9 Effect of siGSK3β on retinal astrocyte/Müller glial response after ONC *in vivo*..... 217
5.10 Effect of siGSK3β on RGC cellular localisation of pGSK3β.....220
5.11 Effect of siGSK3β on RGC cellular localisation of pCRMP2..... 221
5.12 Effect of siGSK3β on RGC cellular localisation of pSmad1..... 222
5.13 Effect of siGSK3β on RGC cellular localisation of pMAP1B..... 223
5.14 Effect of GSK3β inhibition on overcoming Nogo growth-inhibitory peptide in cultured retinal cells..... 225
5.15 Effects of combined siGSK3β (50nM) and siRTP801 (20nM) RGC survival, neurite outgrowth and target knock-down in cultured retinal cells.....228
5.16 Effects of combined siGSK3β (25nM) and siRTP801 (25nM) RGC survival, neurite outgrowth and target knock-down in cultured retinal cells.....230
5.17 Effect of combined siGSK3β/siRTP801 treatment on $Brn3a^{+}$ RGC survival after ONC *in vivo*.....233
5.18 Effect of combined siGSK3β/siRTP801 treatment on $GAP43^{+}$ axon regeneration after ONC *in vivo*.....234

LIST OF TABLES

Table 1.1 Comparison of reported experimental approaches to promote RGC survival and axon regeneration.....34

Table 2.1 Immunohistochemistry and immunocytochemistry reagents..... 54
Table 2.2 Primary and secondary antibodies used in immunohistochemistry (IHC) and immunocytochemistry (ICC)..... 55
Table 2.3 Reagents and buffers for CNTF, NGF, NT-3 and GDNF ELISAs.....81
Table 2.4 Reagents and buffers for BDNF ELISA.....81
Table 2.5 Reagents and buffers for PEDF ELISA.....81
Table 2.6 Details of primers used in qPCR for target genes..... 89
Table 2.7 Reaction mix for qPCR experiments..... 90

Table 3.1 Effects of siRTP801 on RGC survival after ONC (Quark/Neuregenix)..... 127
Table 3.2 Effects of siRTP801 on axon regeneration after ONC (Quark/Neuregenix) 127

ABBREVIATIONS

4E-BP1	eukaryotic translation initiation factor 4E-binding protein
ADB	antibody diluting buffer
AMP	adenosine monophosphate
AMPK	AMP activated kinase
ANOVA	analysis of variance
AOI	albumin ovomucoid inhibitor
APC	adenomatosis polyposis coli
ATP	adenosine triphosphate
BB	blocking buffer
BDNF	brain derived neurotrophic factor
cAMP	cyclic adenosine monophosphate
cDNA	complementary DNA
CNS	central nervous system
CNTF	ciliary neurotrophic factor
CRALBP	cellular retinaldehyde binding protein
CREB	cyclic AMP response element binding protein
CRMP2	collapsin response mediator protein 2
CSPG	chondroitin sulphate proteoglycans
CST	corticospinal tract
Ct	cycle threshold
DAPI	4',6-diamidino-2-phenylindole
DDIT4	DNA damage inducible transcript 4
DNA	deoxyribonucleic acid
DNase 1	deoxyribonuclease 1
DRG	dorsal route ganglion
dsDNA	double stranded DNA
EBSS	Earle's balanced salt solution
EGFP	enhanced green fluorescent protein
EGFR	epidermal growth factor receptor
eIF4E	eukaryotic translation initiation factor 4E
ELISA	enzyme linked immunosorbent assay
Epac	exchange protein activated by cAMP

ERK	extracellular signal related kinase
FGF-2	fibroblast growth factor 2
GAP43	growth associated protein 43
GAPDH	glyceraldehyde 3-phosphate dehydrogenase
GCL	ganglion cell layer
GDNF	glial derived neurotrophic factor
GFAP	glial fibrillary acidic protein
GM-CSF	granulocyte macrophage colony stimulating factor
gp130	glycoprotein 130
GSK3β	glycogen synthase kinase 3β
GTP	guanosine triphosphate
HIF1α	hypoxia inducible factor 1α
IL-1	interleukin-1
IL-6	interleukin-6
INL	inner nuclear layer
IONTS	International Optic Nerve Trauma Study
IPL	inner plexiform layer
ipRGC	intrinsically photosensitive retinal ganglion cell(s)
JAK	janus kinase(s)
KLF	Krüppel like factor
LGN	lateral geniculate nucleus
LIF	leukaemia inhibitory factor
MAG	myelin associated glycoprotein
MAP1B	microtubule associated protein 1B
MAPK	mitogen activated protein kinase
mRNA	messenger RNA
mTOR	mammalian target of Rapamycin
mTORC1	mammalian target of Rapamycin complex 1
mTORC2	mammalian target of Rapamycin complex 2
NFL	nerve fibre layer
NF-κB	nuclear factor κB
NGF	nerve growth factor
NgR	Nogo receptor

NT-3	neurotrophin 3
NT-4/5	neurotrophin 4/5
NTF	neurotrophic factor(s)
Ocm	Oncomodulin
OCT	optical coherence tomography
OMgp	oligodendrocyte myelin glycoprotein
ON	optic nerve
ONC	optic nerve crush
ONH	optic nerve head
ONL	outer nuclear layer
OPL	outer plexiform layer
$p75^{NTR}$	neurotrophin receptor p75
PBS	phosphate buffered saline
PCR	polymerase chain reaction
pCRMP2	phosphorylated CRMP2
PD	Parkinson's disease
PDK1	phosphatidylinositol dependent protein kinase 1
PEDF	pigment epithelium derived factor
PFA	Paraformaldehyde
pGSK3β	phosphorylated GSK3β
PI3K	phosphoinositide-3-kinase
PIP2	phosphatidylinositol (4,5) bisphosphate
PIP3	phosphatidylinositol (3,4,5) triphosphate
PKA	protein kinase A
PKCα	protein kinase Cα
pMAP1B	phosphorylated MAP1B
PN	peripheral nerve
PNS	peripheral nervous system
pS6	phosphorylated S6
pSmad1	phosphorylated Smad1
PTEN	phosphatase and tensin homolog deleted on chromosome ten
qPCR	quantitative polymerase chain reaction
RB	rinsing buffer

Redd1	regulated in development and DNA damage responses 1
RGC	retinal ganglion cell(s)
Rheb	Ras homolog enriched in brain
RhoA	Ras homolog gene A
RISC	RNA induced silencing complex
RNA	ribonucleic acid
RNAi	ribonucleic acid interference
ROCK	Rho associated kinase
ROP	retinopathy of prematurity
RTP801	(alternative name for DDIT4 / Redd1)
S6	ribosomal S6 kinase
SC	spinal cord
SCI	spinal cord injury
SCN	suprachiasmatic nucleus
SEM	standard error of the mean
shRNA	short hairpin ribonucleic acid
siEGFP	siRNA targeting EGFP
siGSK3β	siRNA targeting GSK3β
siRNA	short interfering ribonucleic acid
siRTP801	siRNA targeting RTP801
sNBA	supplemented Neurobasal A
SOCS3	suppressor of cytokine signalling 3
STAT	signal transducer and activator of transcription
TGF-β	transforming growth factor β
TLR	toll-like receptor
Tm	melting temperature
TNF-α	tumour necrosis factor α
TON	traumatic optic neuropathy
Trk	receptor tyrosine kinase
TSC1	tuberous sclerosis complex 1
TSC2	tuberous sclerosis complex 2
VEGF	vascular endothelial growth factor

CHAPTER 1

INTRODUCTION

Elements of work presented in this Chapter have been published in:

Morgan-Warren PJ, Berry M, Ahmed Z, Scott RAH, Logan A. Exploiting mTOR signaling: a novel translatable treatment strategy for traumatic optic neuropathy? *Invest Ophthalmol Vis Sci.* 2013; 54: 6903-6916

1.1 OVERVIEW OF THE VISUAL SYSTEM

Processing of visual information begins in the eye, the visual sensory organ, which is responsible for detecting and focussing light, and converting light information into neural signals for transmission to the visual centres of the brain. The eye is derived embryologically from both ectoderm and mesoderm and, once developed, the eyeball consists of: (1) an outer fibrous layer, the sclera, with the transparent cornea forming the anterior one-sixth of the eyeball surface; (2) the highly vascular pigmented layer, consisting of the choroid, ciliary body and iris; and (3) the neural layer, the retina. After travelling through the ocular media of the anterior eye (tear film, cornea, anterior chamber, lens and vitreous chamber), light passes through the transparent inner layers of the retina to the photoreceptors in the outer retina where the visual signal is transduced, and relayed *via* bipolar cells to retinal ganglion cells (RGC), which extend axons across the retinal surface that become the optic nerve (ON) upon exiting the eye. The ON connects the eye to central targets, enabling further visual processing and the perception of visual stimuli (Snell, 1998).

1.1.1 Structure of the retina

The retina is derived from the neuroectoderm, and consists of an outer pigmented layer, the retinal pigment epithelium (RPE), which provides metabolic and structural support, and absorbs excess intraocular light to reduce light scatter, and an inner neurosensory layer (Prasad and Galetta, 2011). The neurosensory component is stratified into several distinct anatomical layers, and consists of three main neuronal elements: (1) the rod and cone photoreceptors with somata in the outer nuclear layer (ONL), that transduce the light stimulus into an electrical signal; (2) bipolar cells, which are orientated radially with somata in the inner nuclear layer (INL) and dendrites that extend outwards through the outer plexiform layer (OPL) to synapse with the photoreceptors and a single axon

inwards through the inner plexiform layer (IPL) to relay signals; and (3) RGC, whose somata are in the ganglion cell layer (GCL), which receive input from the bipolar cell axons and extend non-myelinated axons in the retinal nerve fibre layer (NFL), which converge at the optic disc and pass through the lamina cribrosa (a fenestrated opening in the sclera) to become the ON (LeVere, 1978). In addition, the retina also contains horizontal cells and amacrine cells in the INL, which modify and integrate the visual relay from bipolar cells to RGC (Prasad and Galetta, 2011). In addition to neurons, the retina contains supporting glia. The principal retinal glia are the radially oriented Müller cells. Müller glial somata are situated in the INL and they extend long bi-directional processes spanning almost the entire thickness of the neural retina, outward through the OPL to the photoreceptors, and inward through the IPL to the GCL. Müller glia contribute both structural support for the retina and metabolic nourishment of neurons, produce neurotrophic factors (NTF), regulate electrolyte homeostasis and take-up excess neurotransmitters (Newman and Reichenbach, 1996). The retina also contains astrocytes in the GCL, which regulate synaptic transmission and become reactive after injury (Pekny and Nilsson, 2005). A schematic representation of the eye and retinal architecture is shown in Figure 1.1.

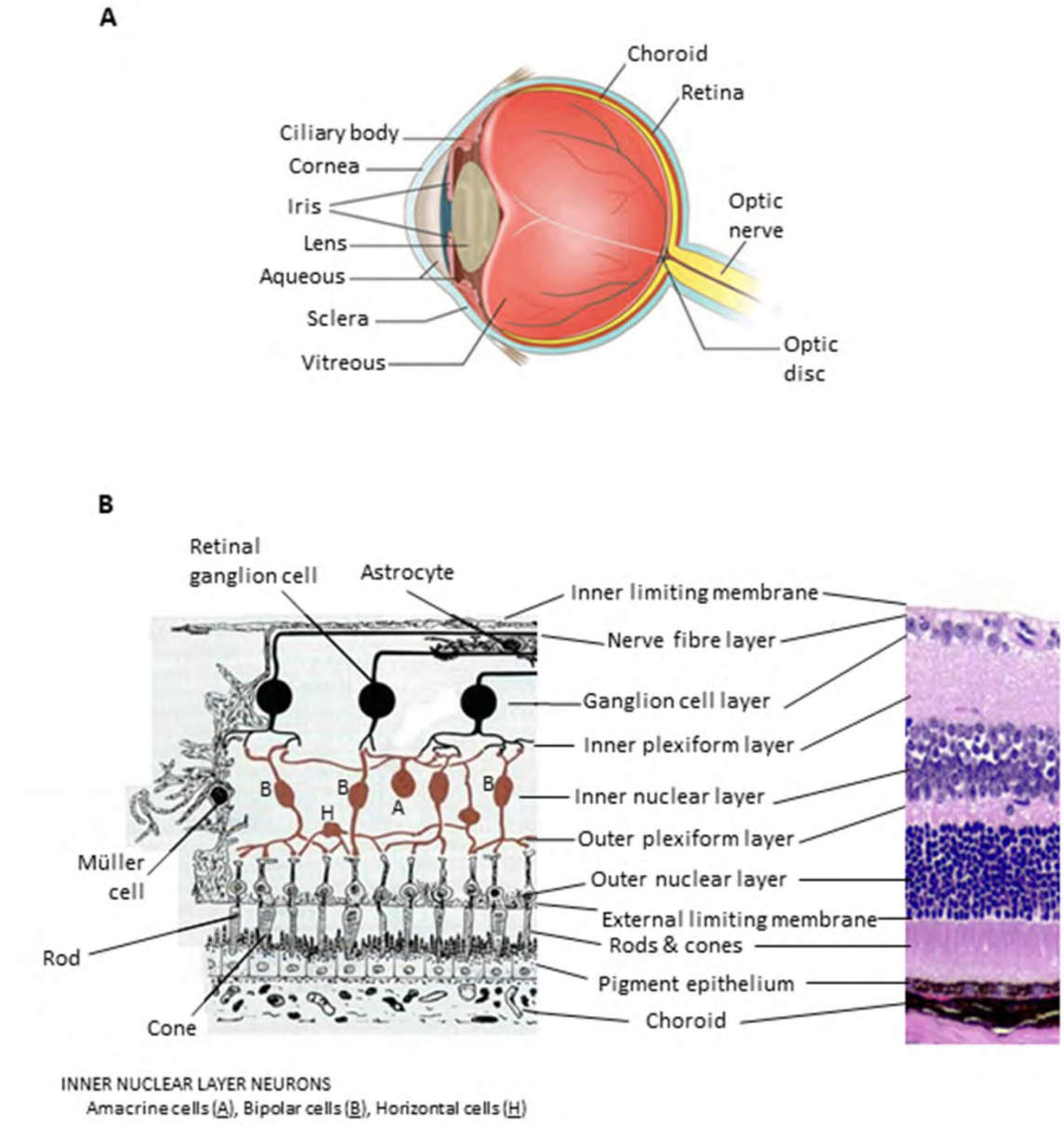


Figure 1.1: Structure of the eye and retina. (A) Schematic cross-section of the human eye. Adapted from http://www.freedom-eyecare.com/medical-eye-care/eye-diagram (Accessed 2 July 2015).
(B) Cross-sectional schematic (left) and histological (right) representation of the ultrastructure of the retina. Adapted from http://instruct.uwo.ca/anatomy/530/retina.jpg (schematic; accessed 2 July 2015) and http://histology-world.com/photoalbum/displayimage.php?album=21&pid=1104 (histology; accessed 2 July 2015).

1.1.2 RGC sub-types & classification

RGC have historically been classified into three main types, based on anatomical features underlying important functional differences (Prasad and Galetta, 2011). Midget RGC account for approximately 80% of RGC, have a very narrow dendritic tree and small receptive field size, receiving input from a single bipolar cell, and are spectrally sensitive. These cells form the "P" (parvocellular) pathway, projecting to the parvocellular layers of the lateral geniculate nucleus (LGN), and are implicated in mediating high acuity, colour vision and stereopsis. Parasol RGC are larger, with complex dendritic arbours and receiving input from multiple bipolar cells. These RGC constitute around 10% of RGC, and form the "M" (magnocellular) pathway, particularly associated with edge and motion detection. The remaining 10% include less well-defined sub-types, including "K" (koniocellular) RGC, which may play a role in colour vision (Prasad and Galetta, 2011). More recent classifications of RGC using morphological, physiological and molecular criteria have identified at least 30 distinct RGC sub-types (Sanes and Masland, 2015). An additional, distinct, group of melanopsin containing intrinsically-photosensitive RGC (ipRGC) was discovered in 2002, exhibiting a direct response to light and directly connecting to the suprachiasmatic nucleus (SCN) where they are thought to mediate circadian rhythms (Hattar *et al.*, 2002). These ipRGC account for approximately 1% of the total RGC population, and have also been classified, with M1-M6 sub-types defined based on multiple features (Cui *et al.*, 2015). RGC sub-type may determine resistance to injury and capability for axon regeneration after axotomy (see later) (Cui *et al.*, 2015; Duan *et al.*, 2015; Li *et al.*, 2006; Li *et al.*, 2008).

1.1.3 Optic nerve and central projections

The ON commences at the optic disc and comprises RGC axons, which become myelinated caudal to the lamina cribrosa, and a full complement of glia, including oligodendrocytes, astrocytes, microglia

and synantocytes (NG2 glia) (Berry *et al.*, 2008). There are approximately 1.2 million RGC axons in the adult human ON (Prasad and Galetta, 2011), and the glial processes are interspersed throughout the axon bundles (Berry *et al.*, 2008). The ON courses postero-medially through the orbital cavity, through the optic canal of the sphenoid, and then passes intracranially to the optic chiasm. The ON is surrounded by three meningeal sheaths: the dura, arachnoid and pia mater, each in continuity with the corresponding brain meninges. The ON vascular supply is from the ophthalmic artery, itself a branch of the internal carotid artery. The optic chiasm is the site of RGC axon decussation, with approximately 53% crossing to the contralateral optic tract and 47% remaining ipsilateral (Prasad and Galetta, 2011). From here, the optic tracts connect with the LGN and superior colliculus on each side and the midline pretectum, which each relay visual information to the occipital cortex for visual perception, brainstem nuclei for visually-guided responses and pupillary/accommodation reflexes (Berry *et al.*, 2008).

1.1.4 Comparative anatomy between human and rodent visual systems

The rodent visual system is a widely used experimental model, and there are a few key differences in the visual anatomy between humans and rats. The typical axial ocular diameter of a mature rat is approximately 6.4mm and, in contrast to humans, the lens makes up a relatively greater proportion of the intraocular contents (LeVere, 1978). The histological structure of the rat retina and ON is largely similar to that of humans, although the rat retina lacks a macula, and the ON contains approximately 80-100,000 RGC axons (Joos *et al.*, 2010; LeVere, 1978), of which the majority (>90-95%) decussate at the chiasm. The proportion of uncrossed fibres at the chiasm is slightly higher in pigmented compared to albino rodents (Marcus *et al.*, 1996; Lund, 1965). The retinal artery travels centrally within the human ON, but runs within the dural sheath in the rat, which enables the rat ON to be transected as a model for ON injury without damaging the retinal blood supply.

1.2 TRAUMATIC OPTIC NEUROPATHY

1.2.1 Pathophysiology

Traumatic optic neuropathy (TON) refers to dysfunction of the ON secondary to a traumatic insult, which may be as a result of direct injury to the ON or *via* an indirect mechanism. The ON can be damaged directly by penetrating injury from an object or projectile, avulsion from the globe after violent rotational injury, or crush/laceration injury from fragments of bone following an impact (Thanos *et al.*, 2012; Steinsapir and Goldberg, 2011; Jacobs and Van Stavern, 2013). More commonly, TON results from an indirect mechanism, whereby the ON is injured from non-penetrating effects of trauma. The shockwave following an orbital or facial impact can be transmitted to, and concentrated at, the optic canal where the ON dural sheath is closely adherent to the periosteum and consequently vulnerable to damage (Steinsapir and Goldberg, 2011; Jacobs and Van Stavern, 2013) (Figure 1.2A), with injury to RGC axons as a result of shearing forces as a primary pathological insult, possibly followed by ON compression from secondary oedema and subsequent ischaemia. Mechanical disruption to RGC axons results in RGC death, with resultant visual loss (Steinsapir and Goldberg, 2011; Jacobs and Van Stavern, 2013). Furthermore, a local inflammatory response with up-regulation of pro-inflammatory mediators such as IL-1, IL-6 and TNF-α, also contributes to RGC degeneration (Lin and Wen, 2013).

1.2.2 Epidemiology

TON occurs is reported in up to 5-12% of patients after head trauma (Steinsapir and Goldberg, 1994; Van Stavern *et al.*, 2001; Sharma *et al.*, 2014), and more commonly when there are associated craniofacial fractures (Steinsapir and Goldberg, 2011). The prevalence of TON in the general

population of the United Kingdom is around 1 in 1000000 (Lee *et al.*, 2010), and the majority of patients are young males with injuries sustained after motor vehicle or bicycle accidents (49%), falls (27%) and assaults (13%) (Yu-Wai-Man and Griffiths, 2013a). In the paediatric setting, TON is usually a result of sports injuries, falls or motor vehicle accidents (Mahapatra and Tandon, 1993). In the military population, ocular injury is reported in 10% of major trauma cases (Blanch *et al.*, 2011) and TON has been reported to account for nearly 20% of ocular injuries in combat (Weichel *et al.*, 2008).

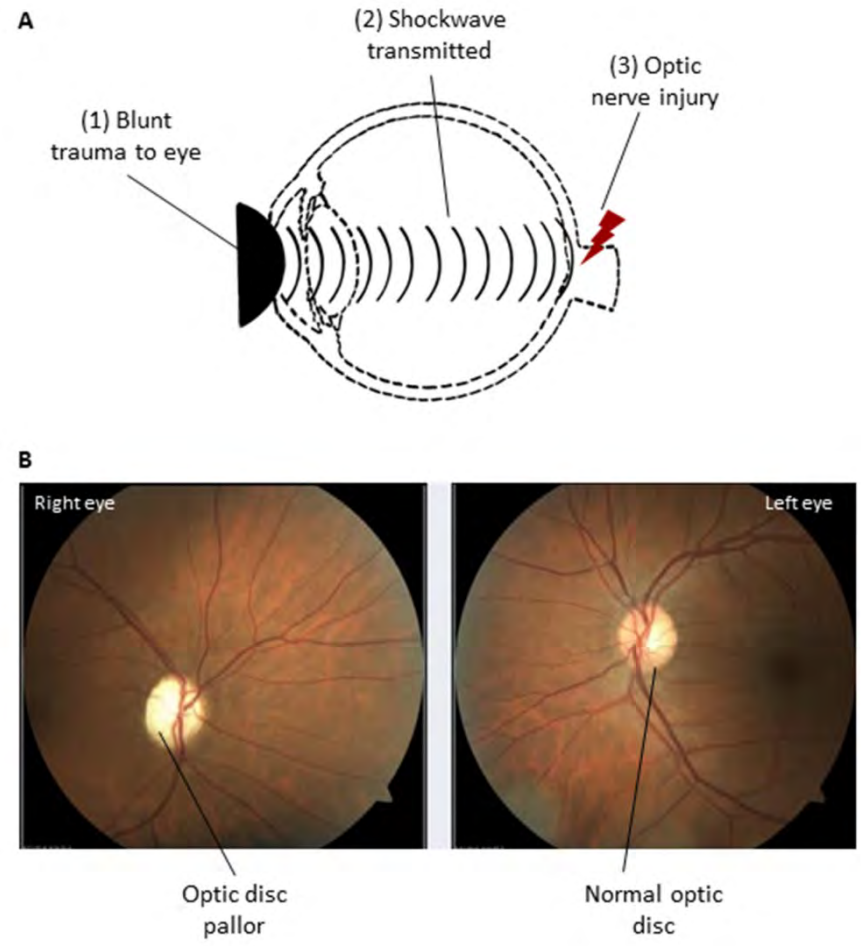


Figure 1.2: Traumatic optic neuropathy. (A) Schematic representation of the mechanism of optic nerve injury after blunt ocular trauma. Adapted from http://80.36.73.149/almacen/medicina/oftalmologia/enciclopedias/duane/pages/v3/v3c031.html (accessed 2 July 2015). (B) Retinal photographs demonstrating optic disc pallor after traumatic optic neuropathy (right eye) compared to a normal, healthy looking optic disc in the fellow eye of the same patient (left eye). Adapted from http://www.pattyvisioncenters.com/index.php/eye_atlas/condition/traumatic_optic_neuropathy (accessed 2 July 2015).

1.2.3 Clinical features

The diagnosis of TON is based on clinical features with a supporting history of direct or indirect facial or head trauma, with unilateral or bilateral (usually asymmetrical) involvement. Other clinical features include: visual loss, which may be as severe as loss of light perception or worse in 40-60% patients; a relative afferent pupillary defect (except in cases of bilateral injury of equal severity); visual field defect of variable degree and impairment of colour vision (Lee *et al.*, 2010; Yu-Wai-Man and Griffiths, 2013a). The clinical appearance of the optic disc depends on the anatomical site of the ON injury, with disc swelling and associated retinal haemorrhages in the case of anterior ON injuries, and often normal appearances in the acute stages of more posterior injuries. The development of optic atrophy with pallor of the ON head is usually evident by 6 weeks after the injury (Yu-Wai-Man and Griffiths, 2013a) (Figure 1.2B).

1.2.4 Management of TON

Spontaneous improvement in vision has been reported in around 30-60% patients with TON, although reported visual improvements may not reach pre-injury levels (Wolin and Lavin, 1990; Levin *et al.*, 1999). In addition to conservative management, current treatment options for TON include corticosteroids and surgical optic canal decompression.

1.2.4.1 Corticosteroids

The rationale for use of corticosteroids in the management of TON was based on the observation from clinical trials that patients with spinal cord injury (SCI) treated with corticosteroids had a significant improvement in neurological recovery compared to placebo (Bracken *et al.*, 1990). The

International Optic Nerve Trauma Study (IONTS) is the largest prospective TON study reported to date (Levin *et al.*, 1999). Initially intended to be a randomised controlled trial, the IONTS was converted to an observational study, and was significantly biased toward treatment. Of 133 patients analysed, 125 received corticosteroids of varying doses and 33 also had surgery. There was no significant difference in outcome between the groups, with visual improvement reported in 57% of the untreated patients, 52% of the steroid group and 33% of the surgery group (p=0.22) (Levin *et al.*, 1999). A recent systematic review concluded that there was insufficient evidence that corticosteroids provided additional benefit over observation alone (Yu-Wai-Man and Griffiths, 2013a). Furthermore, both preclinical models (Steinsapir *et al.*, 2000) and clinical studies (Roberts *et al.*, 2004) indicate that corticosteroids are associated with an unacceptable risk of side effects and complications.

1.2.4.2 Surgical optic canal decompression

The rationale for surgical decompression is based on the hypothesis that TON results in ON swelling within the fixed confines of the optic canal, with consequent tissue ischemia and further damage to the ON (Steinsapir and Goldberg, 2011). As mentioned, the surgical group in the IONTS had no improvement in visual outcome compared to observation or corticosteroid treatment, and the majority of surgical patients were also treated with corticosteroids, thus confounding the analysis (Levin *et al.*, 1999). Moreover, 10% of patients undergoing surgery in the IONTS suffered post-operative cerebrospinal fluid leak, with one developing meningitis (Levin *et al.*, 1999), highlighting the potential significant risks associated with surgical intervention. A recent systematic review of published case series concluded that there was insufficient evidence that any form of surgical decompression improved visual outcomes in TON (Yu-Wai-Man and Griffiths, 2013b).

1.2.4.3 Requirement for novel therapeutic options

The lack of a proven effective treatment, and the risks associated with current management options, mean that amelioration of the long-term morbidity associated with TON represents an unmet clinical need. There is, therefore, a requirement for the development of novel therapeutic options for TON to provide clinicians with an opportunity to limit visual loss or even restore sight after injury.

1.3 RODENT OPTIC NERVE CRUSH MODEL AND ANATOMICAL ASSESSMENT OF RGC SURVIVAL AND AXON REGENERATION

The optic nerve crush (ONC) model is a commonly used paradigm to study RGC responses to injury (Berry *et al.*, 2008; Blanch *et al.*, 2012). In the model, the adult rat ON is exposed surgically and axotomised within the meningeal sheath, thereby disconnecting RGC from central targets, separating the proximal (ocular side) and distal (chiasm side) axon segments at the crush site, whilst preserving retinal vascular perfusion through the retinal artery in the dural sheath. A detailed description of the ONC method is given in Chapter 2. Surviving RGC can be detected using RGC phenotypic markers, such as βIII-tubulin and Brn3, while axon tracers, such as fluorogold or cholera toxin, and axon regeneration-associated proteins such as growth-associated protein-43 (GAP43) immunohistochemistry are used to evaluate RGC axon regeneration (Berry *et al.*, 2008; Nadal-Nicolas *et al.*, 2009; Mead *et al.*, 2014; Gao *et al.*, 2012).

1.4 RESPONSE TO INJURY AND OPTIC NERVE REGENERATIVE FAILURE

Unlike the peripheral nervous system (PNS), in which axon regeneration after injury is associated with limited functional recovery (Chen *et al.*, 2007; Fenrich and Gordon, 2004), most axons of the

adult mammalian CNS compromised by injury or disease do not regenerate. ON regenerative failure is a major barrier to functional recovery after TON, and has been attributed to a combination of multiple underlying mechanisms, including axotomy-induced apoptotic RGC death, loss of target-derived trophic support, the inhibitory myelin microenvironment of the ON, suboptimal stimulation of regenerative responses, and a lack of intrinsic axogenic capacity of mature RGC (Fischer and Leibinger, 2012; Moore and Goldberg, 2010) (Figure 1.3). The prevailing dogma for many decades was that mammalian CNS neurons were inherently incapable of regenerating axons after injury, although the classical experiments of Aguayo and colleagues in the 1980s demonstrated that CNS axons grew into implanted segments of peripheral nerve (PN), and were therefore capable of regrowth in favourable conditions (Aguayo *et al.*, 1987; Bray *et al.*, 1987a; David and Aguayo, 1985; Richardson *et al.*, 1980). Several specific experimental manipulations have demonstrated that RGC can survive and regenerate axons *in vivo* after injury, for example through PN grafts sutured to the transected end of the ON (Aguayo *et al.*, 1987; Bray *et al.*, 1987b; Vidal-Sanz *et al.*, 1987), and after intravitreal implantation of a PN fragment (Berry *et al.*, 1996; Berry *et al.*, 1999), lens injury (Fischer *et al.*, 2000; Leon *et al.*, 2000), induction of intraocular inflammation (Yin *et al.*, 2003), intravitreal delivery of neurotrophic factors (Logan *et al.*, 2006) and targeted gene deletion (Park *et al.*, 2008; Smith *et al.*, 2009; Sun *et al.*, 2011) (Figure 1.4). The molecular basis of these RGC survival and pro-regenerative paradigms is becoming increasingly clear, with selected modulation of the intracellular signalling pathways that mediate changes in RGC gene expression profile emerging as the basis for a class of novel therapeutics.

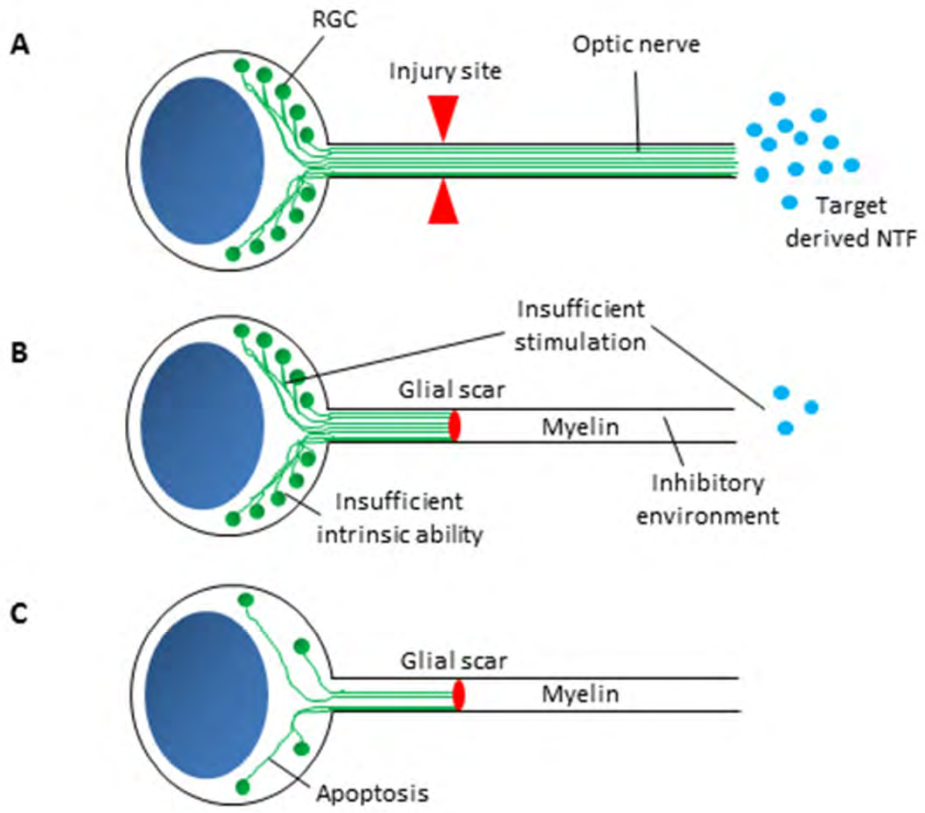


Figure 1.3: RGC death and regenerative failure after optic nerve injury. (A) Schematic diagram of a rodent eye representing RGC somata in the retina with axons projecting in the ON and receiving trophic support from target-derived factors. (B) After ON injury, axons distal to the lesion site degenerate, and regenerative failure is attributed to loss of target-derived trophic support, the inhibitory CNS environment including the developing glial scar, and an insufficient intrinsic RGC regenerative capacity. (C) In the absence of experimental intervention to promote RGC survival and/or axon regeneration, RGC die by apoptosis and fail to regenerate axons, associated with the development of a glial scar. Figure adapted from: Fischer D and Leibinger M. Promoting optic nerve regeneration. *Prog Retin Eye Res* 2012;31:688-701.

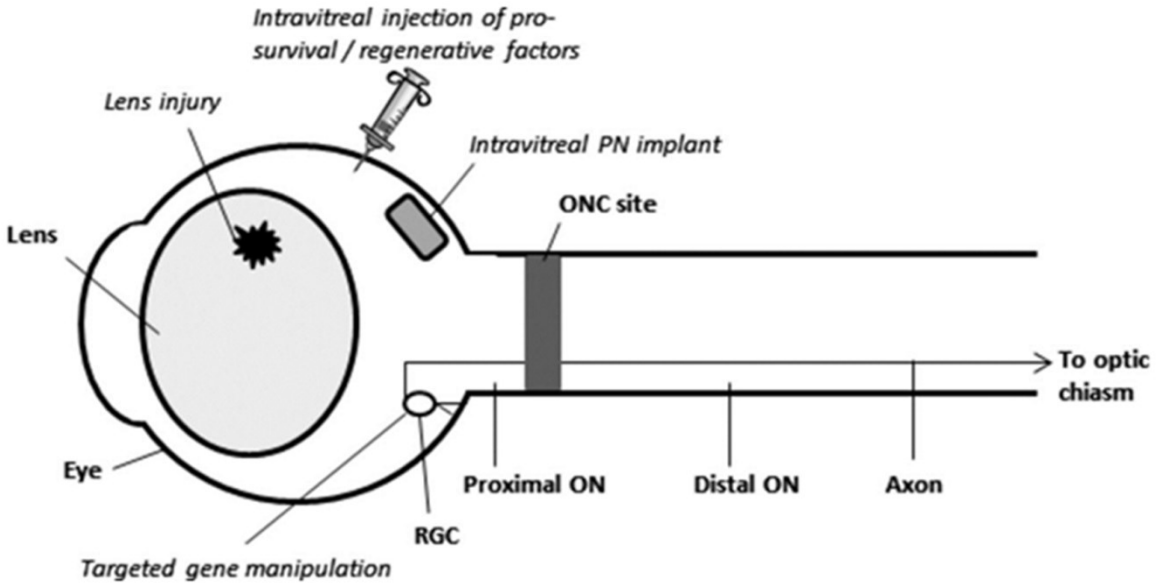


Figure 1.4: Schematic diagram of the rodent ONC model for investigating RGC survival and axon regeneration. The RGC axons arising in the retina are crushed at the ONC site. Experimental manipulations to promote RGC survival and axon regeneration include lens injury, intravitreal delivery of putative survival/regenerative factors, implantation of a PN fragment, and targeted gene manipulation. Figure adapted from Berry M, *et al*. Regeneration of axons in the visual system. *Restor Neurol Neurosci* 2008; 26: 147-174.

1.4.1 ON injury response

After axotomy in the adult rat ON, RGC axons initially retract back from the lesion site within 6h of injury, remaining retracted 30-200μm from the lesion for up to 24h (Selles-Navarro *et al.*, 2001). After this initial response, RGC axons sprout at the proximal lesion edge, and largely fail to traverse the wound to progress into the distal ON, and a glial scar develops at the lesion site within 8d, which matures and contracts over the next 10d (Berry *et al.*, 2008; Logan and Berry, 2002). A small minority of sprouting axons, particularly at the periphery of the ON, may grow past the centre of the lesion for up to 100μm, although this is usually considered to be within the region of the lesion site (Selles-Navarro *et al.*, 2001). Axotomy-induced RGC death by apoptosis commences within 5-7d after

intraorbital ON injury in rats, with fewer than 10% surviving by 14d (Berkelaar *et al.*, 1994). However, the pattern of neuronal loss is determined by the site of the lesion along the visual pathway, as intracranial injury 8-9mm behind the eye delays the onset of apoptosis to 8d, with RGC survival of approximately 80% at 4 weeks after injury, suggesting that ON glia- or target-derived retrogradely-transported neurotrophic signals are short-term regulators of RGC viability (Berkelaar *et al.*, 1994; Fischer and Leibinger, 2012).

1.4.2 RGC death by apoptosis

RGC death after ON injury occurs predominantly by axotomy-induced apoptosis, associated with induction of activated caspase signalling, which ultimately results in cleavage of intracellular proteins that maintain cellular integrity (Berry *et al.*, 2008; Fischer and Leibinger, 2012). Caspase-mediated apoptotic cell death is induced by intrinsic and extrinsic pathways: the intrinsic pathway is mediated by caspase-9 in response to cellular stress, which *via* caspase-8 cleaves and activates caspase-3; the extrinsic pathway is induced by ligand-activated recruitment of the fas-associated death domain (FADD), which complexes with and cleaves procaspase-8, which in turn activates caspase-3 to engage common executioner caspases (Berry *et al.*, 2008) (Figure 1.5). Activation of caspases-2, -3, -6, -8 and -9 have all been reported in association with ON injury (Ahmed *et al.*, 2011; Vigneswara *et al.*, 2014; Vigneswara *et al.*, 2012; Kermer *et al.*, 2000; Kermer *et al.*, 1999; Weishaupt *et al.*, 2003; Monnier *et al.*, 2011; Cheung *et al.*, 2004). The critical role of caspases in mediating injury-induced apoptosis is evidenced by significantly enhanced RGC survival after caspase-2 inhibition by intravitreal delivery of either a modified short interfering RNA (siRNA) or the pharmacological inhibitor z-VDVAD after ONC injury (Ahmed *et al.*, 2011; Vigneswara *et al.*, 2012).

The Bcl family of proteins tightly regulates RGC survival. There is up-regulation of pro-apoptotic factors and a decrease in the levels of anti-apoptotic Bcl-2 in the retina after ON injury, and over-expression of Bcl-2 in transgenic mice protects RGC from axotomy-induced RGC loss both in neonatal and adult rodent models (Bonfanti *et al.*, 1996; Cenni *et al.*, 1996). Over-expression of Bcl-XL is similarly highly anti-apoptotic (Malik *et al.*, 2005), and neutralization of pro-apoptotic Bax provides 95% RGC neuroprotection after ON transection (Qin *et al.*, 2004). Strategies that limit RGC apoptosis after injury in adults have routinely failed to elicit axon regenerative responses (Berry *et al.*, 2008). Whilst RGC survival is a pre-requisite for axon regeneration, neuroprotection alone is insufficient to promote ON axon regeneration in adults in the absence of a specific axogenic stimulus, therefore indicating that different cellular mechanisms mediate these separate events.

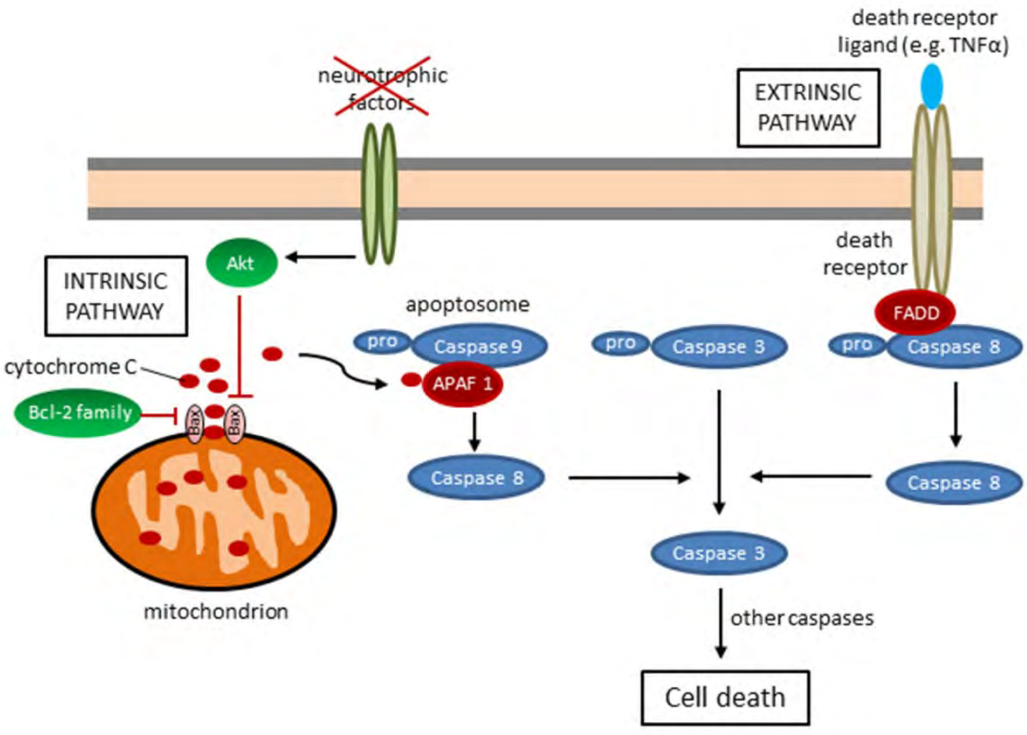


Figure 1.5: Cellular mechanisms of apoptosis. The induction of apoptosis is mediated by: (1) the extrinsic pathway, whereby ligand-receptor activation recruits the fas-associated death domain (FADD) to activate caspase signalling; (2) the intrinsic pathway is activated by cellular stress, for example by deprivation of neurotrophic factors, and subsequent activation of caspase signalling. Both pathways culminate in activation of common executioner caspases to induce cell death. Figure adapted from: Fischer D and Leibinger M. Promoting optic nerve regeneration. *Prog Retin Eye Res* 2012; 31: 688-701.

1.4.3 RGC axon regenerative failure due to the inhibitory CNS milieu

As mentioned, the classical experiments of Aguayo demonstrated that axotomised RGC, which are normally unable to regenerate, can grow axons into the permissive environment of a PN graft anastomosed to the transected ON stump (Aguayo *et al.*, 1987; Vidal-Sanz *et al.*, 1987). However, RGC that survive axotomy do not regenerate axons spontaneously, due in part to the inhibitory myelin surround of the CNS. Transected RGC axons are exposed to growth-inhibitory ligands derived from degenerate CNS myelin and the incipient glial scar, which initiate receptor-activated signalling pathways to destabilise the actin cytoskeleton of axonal growth cones. Several myelin-derived inhibitory ligands have been characterised, including Nogo-A, myelin-associated glycoprotein (MAG) and oligodendrocyte-myelin glycoprotein (OMgp), which bind with similar affinity to the Nogo receptor (NgR) (Yiu and He, 2003; Yiu and He, 2006). Ligand-receptor signalling through NgR requires recruitment of transmembrane co-receptors $p75^{NTR}$/TROY, LINGO-1/AMIGO-3 (Mi *et al.*, 2008; Wang *et al.*, 2002; Ahmed *et al.*, 2013; Shao *et al.*, 2005), and subsequent signalling converges on the Ras homolog gene A/rho-associated kinase (RhoA/ROCK) pathway, leading to axonal growth cone collapse (Berry *et al.*, 2008; Tan *et al.*, 2011) (Figure 1.6). Furthermore, formation of a glial scar at the lesion site after ON transection is associated with transforming hypertrophy and proliferation of astrocytes, and recruitment of meningeal fibroblasts, which secrete inhibitory molecules, most notably chondroitin sulfate proteoglycans (CSPG), ephrins and semaphorins, which also signal RhoA-mediated growth inhibition through their cognate receptors (Silver and Miller, 2004; Niederost *et al.*, 1999; Tang, 2003). Myelin- and scar-derived inhibitors induce growth cone collapse through the LIMK/cofilin and glycogen synthase kinase (GSK3β) pathways (Sandvig *et al.*, 2004; Zhou and Snider, 2005a; Liu *et al.*, 2012).

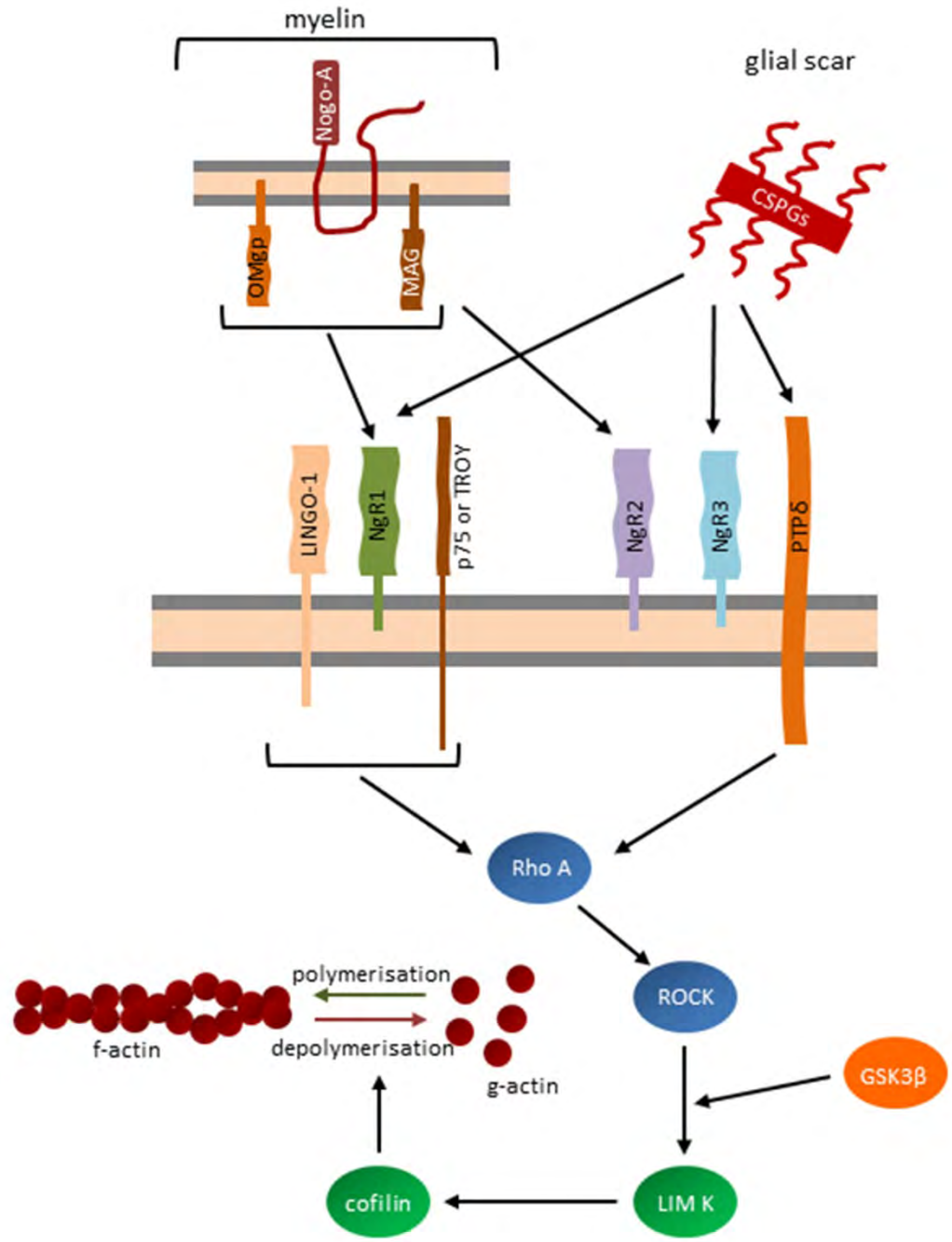


Figure 1.6: Contribution of myelin- and glial-scar derived factors to inhibitory signalling. Diagrammatic representation of myelin- and glial-scar derived factors leading to actin depolymerisation and collapse in axonal growth cones. Chondroitin sulphate proteoglycans (CSPG) from the glial scar, and myelin-derived factors , including NogoA, myelin associated glycoprotein (MAG) and oligodendrocyte myelin glycoprotein (OMgp), activate cognate receptors which induce signalling that converges on the RhoA-ROCK pathway to induce actin depolymerisation. GSK3β activity is thought to promote growth cone collapse through a variety of mechanisms, including interaction with Rho/ROCK pathway. Figure adapted from: Fischer D and Leibinger M. Promoting optic nerve regeneration. *Prog Retin Eye Res* 2012; 31: 688-701.

Experimental strategies to overcome the growth-inhibitory CNS environment promote only modest axon regeneration (Yiu and He, 2006). Inactivation of RhoA/ROCK signalling with pharmacological inhibitors or gene knock-down blocks the effect of inhibitory ligands on RGC *in vitro*, and *in vivo* enables a small number of RGC axons to cross a lesion site and grow into the distal ON segment, an effect that is enhanced with inflammatory stimulation (Lehmann *et al.*, 1999; Bertrand *et al.*, 2005; Fischer *et al.*, 2004b; Ahmed *et al.*, 2009; Lingor *et al.*, 2007; Lingor *et al.*, 2008; Koch *et al.*, 2014b; Koch *et al.*, 2014a). Inhibition of NgR is insufficient to promote axon regeneration in the absence of an axogenic inflammatory stimulus (Fischer *et al.*, 2004a; Chen *et al.*, 2009; Cui *et al.*, 2014). Regulated intramembranous proteolysis (RIP) of $p75^{NTR}$/TROY by neurotrophic factors (Ahmed *et al.*, 2006), and pharmacological inhibition of GSK3β (Goold and Gordon-Weeks, 2004; Arevalo and Rodriguez-Tebar, 2006) both paralyse inhibitory signalling, promoting axogenesis by protecting against growth cone collapse. Multiple extrinsic inhibitory mechanisms, therefore, combine to arrest the growth of mature CNS axons, and although blockade of inhibitory signals does enable some axon growth, additional strategies are required if functional RGC axon regeneration is to be achieved.

1.5 RGC SURVIVAL AND AXON REGENERATION ARE PROMOTED BY INFLAMMATORY STIMULATION

The observation of abortive axon sprouting about the lesion site after ON injury suggests that RGC are not incapable of initiating an axon regenerative response. Although neutralisation of the myelin- and scar-derived inhibitory ligands enables very limited axon regeneration though the lesion, the effect is enhanced in the presence of an axogenic stimulus. Thus, CNS axon regenerative failure has also been attributed, in part, to the lack of an effective axogenic stimulus after injury.

RGC survival and axon regeneration can be promoted experimentally by lens injury (Leon *et al.*, 2000; Fischer *et al.*, 2000); intravitreal injection of lens crystallin proteins (Fischer *et al.*, 2008); intravitreal delivery of toll-like receptor 2 agonists, such as the yeast cell wall extract zymosan (Yin *et al.*, 2003) or Pam3Cys (Hauk *et al.*, 2010); and intravitreal implantation of a PN segment (Berry *et al.*, 1996; Berry *et al.*, 1999). Intraocular inflammation is a common feature of all these approaches (Lorber *et al.*, 2008). The 'regenerative state' is associated with up-regulation of growth-associated proteins, such as GAP43 and SPRR1A (Fischer *et al.*, 2004b), when RGC axon growth is possible through the normally inhibitory environment of the crushed ON. The pro-regenerative effects of inflammatory stimulation are enhanced when combined with strategies to overcome inhibitory ligands, like blocking NgR and RhoA signalling (Fischer *et al.*, 2004a; Fischer *et al.*, 2004b).

1.5.1 Activated macrophages and neutrophils are key mediators of inflammatory stimulation

Influx of neutrophils and activated macrophages is a key event underlying the pro-survival and regenerative effects of inflammatory stimulation (Yin *et al.*, 2003; Cui *et al.*, 2009; Benowitz and Popovich, 2011; Benowitz and Yin, 2010; Kurimoto *et al.*, 2013). Neutrophils and macrophages are thought to be the source of oncomodulin (Ocm), a 12kDa calcium binding protein that rapidly accumulates in the inflamed eye, and is presumed to be involved in receptor binding in a cyclic adenosine monophosphate (cAMP)-dependent manner (Yin *et al.*, 2006; Yin *et al.*, 2009; Kurimoto *et al.*, 2013). Both an Ocm peptide antagonist and a neutralising anti-Ocm antibody reportedly suppress inflammation-induced axon regeneration (Yin *et al.*, 2006; Yin *et al.*, 2009), although the precise role of Ocm is debated (Hauk *et al.*, 2008; Cui *et al.*, 2008). The axon growth effects of Ocm may be mediated through intracellular Mst3b, a purine sensitive kinase, and linked to the mitogen activated protein kinase (MAPK) signalling pathway (Irwin *et al.*, 2006; Lorber *et al.*, 2009b).

1.5.2 Glial activation and trophic factor signalling

Intraocular inflammation activates retinal astrocytes and Müller cells (Lorber *et al.*, 2008), stimulating them to produce multiple factors, including cytokines, such as ciliary neurotrophic factor (CNTF), leukaemia inhibitory factor (LIF) and interleukin-6 (IL-6), and the neurotrophins brain derived neurotrophic factor (BDNF), nerve growth factor (NGF), neurotrophin 3 (NT3) and neurotrophin 4/5 (NT4/5) (Ahmed *et al.*, 2010). RGC dependence on glial factors after inflammatory stimulation is implied by the failure of axon growth through an ON lesion in response to macrophage accumulation within the glial-free lesion site (David *et al.*, 1990; Ahmed *et al.*, 2010). Furthermore, both vitreal and ON inflammation are RGC neuroprotective after ON injury, but only the former is axogenic, indicating that neuroprotective factors are transported retrogradely to RGC somata to prevent apoptosis, but induction of a growth stimulus depends on retinal glial activation by vitreal inflammation (Ahmed *et al.*, 2010). CNTF and LIF expression is up-regulated in retinal astrocytes by inflammation (Muller *et al.*, 2007), and the neuroprotective and axogenic effects of inflammatory stimulation are absent in mice deficient for CNTF and LIF, demonstrating a pivotal role for these cytokines (Leibinger *et al.*, 2009). CNTF and LIF enhance neurite outgrowth *in vitro* (Leibinger *et al.*, 2009; Jo *et al.*, 1999; Muller *et al.*, 2009), although the effects of recombinant CNTF after ON injury are less robust than those induced by inflammation (Lingor *et al.*, 2008; Muller *et al.*, 2009). Other NTF, including the neurotrophins, supplied individually *in vivo* promote limited RGC survival and axon regeneration, whereas a combination of fibroblast growth factor 2 (FGF-2), NT3 and BDNF acts synergistically to induce robust axogenesis that is equivalent to that seen after intravitreal inflammation (Logan *et al.*, 2006).

Cytokines, such as CNTF and LIF, act upon receptor complexes with a shared gp130 protein (Taga and Kishimoto, 1997), leading to association with janus kinases (JAKs), and recruitment of signal

transducers and activators of transcription (STAT) proteins, particularly STAT3, and the protein tyrosine phosphatase SHP-2 (Rane and Reddy, 2000). Activated STAT3 translocates to the nucleus, binding to specific DNA response elements in the promoter region of target genes (Stahl *et al.*, 1994), and activated SHP-2 leads to signalling *via* the phosphoinositide-3-kinase (PI3K)/Akt pathway (see later) and MAPK/extracellular signal regulated kinase (ERK) pathways (Fischer and Leibinger, 2012; Muller *et al.*, 2009) (Figure 1.7). The JAK/STAT system is finely regulated, and one of the genes up-regulated by STAT3 activation is the suppressor of cytokine signalling 3 (*socs3*), a negative-feedback regulator that prevents prolonged stimulation of this pathway. Deletion of *socs3* enables RGC axon regeneration after ON injury, and significantly enhances the regenerative effects of exogenous CNTF (Smith *et al.*, 2009), whereas viral-mediated over-expression of *socs3* prevents axon growth (Hellstrom *et al.*, 2011). Expression of *socs3* is also increased in mature axotomised RGC and, therefore, may be acting as an intrinsic brake to cytokine-mediated axon regeneration (Fischer and Leibinger, 2012).

1.6 INTRINSIC DETERMINANTS OF RGC REGENERATIVE ABILITY

1.6.1 Developmental down-regulation of RGC regenerative ability

During development, axons are guided to their targets, and growth capacity of axons is reduced during the transition from embryo to adulthood to enable stabilisation of synaptogenesis (Yang and Yang, 2012). Embryonic RGC axon growth rates are high, but these decrease significantly over the later stages of development, and further in adult RGC that become exquisitely sensitive to axotomy (Goldberg *et al.*, 2002a; Goldberg *et al.*, 2002b). Rather than merely reflecting the maturation of the inhibitory CNS environment, the development-dependent down-regulation of growth ability is an intrinsic property of CNS neurons (Goldberg, 2003; Liu *et al.*, 2011).

1.6.1.1 cAMP

There is a direct correlation between the age-dependent decline in neuronal cAMP and the onset of neurite growth inhibition by CNS myelin-associated factors (Cai *et al.*, 2001). cAMP stimulates the accumulation of growth factor receptors to the cell surface (Meyer-Franke *et al.*, 1998), down-regulates the growth inhibitory SOCS3 (Park *et al.*, 2009), and potentiates the effect of Ocm in mediating axon growth (Yin *et al.*, 2009; Yin *et al.*, 2006). RGC exhibit a decrease in cAMP after injury, although exogenous cAMP does not increase neuronal survival in the absence of NTF (Shen *et al.*, 1999; Monsul *et al.*, 2004). Neuronal responses to cAMP depend on differential signalling through protein kinase A (PKA) and exchange protein activated by cAMP (Epac) (Peace and Shewan, 2011). Axonal growth cones demonstrate either attraction or repulsion, based on development-dependent cAMP-mediated signalling *via* Epac and PKA, respectively, and Epac signalling promotes axon regeneration in neurons of the adult spinal cord (Murray and Shewan, 2008; Murray *et al.*, 2009).

1.6.1.2 Transcription factors

Krüppel-like factors (KLF, a set of transcription factors) have been identified as development-dependent regulators of axonal growth. Gene expression analysis in zebrafish, which mount a robust RGC regenerative response after ON injury, found that a host of genes are up-regulated in regenerating RGC, including KLF6 and KLF7, knock-down of which significantly reduced axon growth (Veldman *et al.*, 2007). KLF4 is a potent inhibitor of axon growth in embryonic RGC, and RGC lacking KLF4 show increased axon growth *in vitro* and after ON injury *in vivo* (Moore *et al.*, 2009). Pro-regenerative KLF6 and KLF7 are down-regulated after birth, whereas growth inhibitory KLF4 and KLF9 are up-regulated post-natally (Moore *et al.*, 2009), indicating that key RGC intrinsic elements regulate axon growth characteristics.

1.6.2 Mammalian Target of Rapamycin (mTOR)

The serine-threonine kinase mammalian target of Rapamycin (mTOR) was discovered as a target for the antifungal macrolide Rapamycin, produced by *Streptomyces hygroscopicus* (Vezina *et al.*, 1975). Highly active during development, but down-regulated in the mature CNS, mTOR is implicated in numerous cellular processes, including regulation of protein synthesis and axonal growth in development (Jaworski and Sheng, 2006; Ma and Blenis, 2009), and much interest has developed in the role of mTOR as a determinant of neuronal survival and axon growth in response to injury (Don *et al.*, 2012; Tsang *et al.*, 2007). The residual mTOR activity in adult neurons is reduced further by axotomy (Liu *et al.*, 2010a; Park *et al.*, 2010) and, although the mechanism for the two-step reduction in activity is not fully understood, this correlates with the reduced ability of CNS axons to initiate the protein synthesis that is required for axon regeneration. In contrast, some injured adult PNS neurons maintain high levels of mTOR and their axons regenerate well (Abe *et al.*, 2010), although mTOR-independent PNS regeneration also occurs (Christie *et al.*, 2010). Inadequate mTOR signalling may be a major intrinsic obstacle to neuronal survival and axon regeneration in the CNS. Genetic manipulation of signalling pathways to up-regulate mTOR activity is associated with some of the most significant degrees of axon regeneration achieved so far in the CNS (see later, and Table 1.1).

1.7 ACTIVATION OF mTOR ACTIVITY BY THE PI3K/AKT SIGNALLING PATHWAY

The intracellular signalling pathways mediating mTOR activity and regulation are increasingly well understood. Therefore, manipulating mTOR to provide neuroprotection and rekindle axon growth makes this pathway an attractive target for potential translatable therapy for TON and other optic neuropathies. mTOR activity is determined by a balance in intracellular signalling cascades; the lipid kinase PI3K is activated by neurotrophins acting upon cell membrane receptor tyrosine kinases (Trk),

leading to a well described canonical pathway to up-regulate mTOR activity (Figure 1.7) (Laplante and Sabatini, 2013).

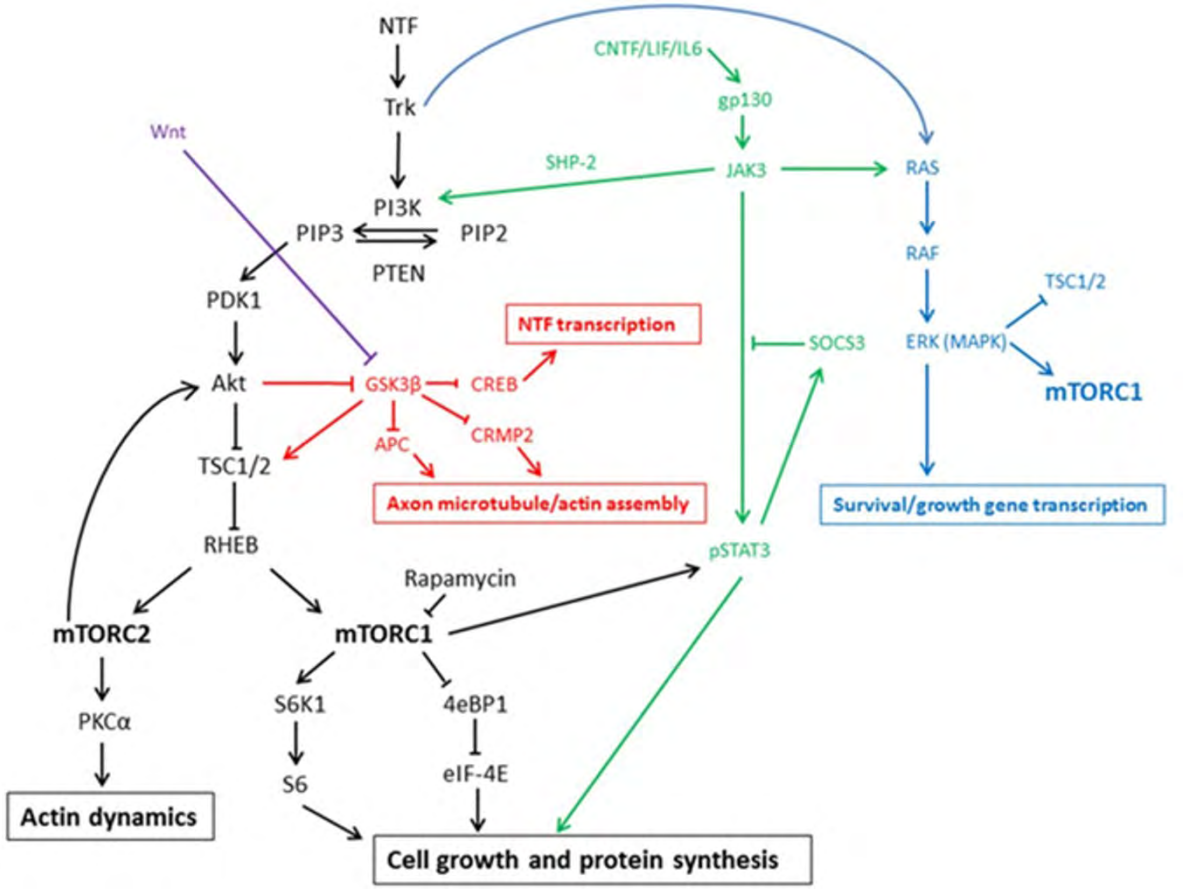


Figure 1.7: Signalling of the mTOR pathway, with links to related signalling pathways. Neurotrophic factors (NTF) acting upon cell membrane receptor tyrosine kinases (Trk) induce activity of the lipid kinase PI3K, which phosphorylates and activates the conversion of phosphatidylinositol (4,5) bisphosphate (PIP2) to phosphatidylinositol (3,4,5) triphosphate (PIP3). Phosphatase and tensin homolog deleted on chromosone ten (PTEN) catalyses the reverse reaction. PIP3 recruits and activates phosphatidylinositol-dependent protein kinase 1 (PDK1), which in turn activates Akt that phosphorylates and inhibits the tuberous sclerosis complex (TSC), a heterodimer comprising TSC1 and TSC2 complexes. These act as GTPase activating proteins to stimulate the Ras homolog enriched in brain (Rheb) to upregulate mTOR activity. The mTOR forms two distinct complexes to influence cellular activity (see text). Akt also inhibits GSK3β, which in turn disinhibits CREB-mediated NTF transcription, and disinhibits APC and CRMP2 to promote growth cone assembly. Activation of Trk also stimulates the ERK/MAPK signalling pathway, which is linked to mTOR signalling. Cytokines such as CNTF/LIF/IL-6 activate gp130-mediated signalling through the JAK-STAT pathway to promote STAT3 activity, which is negatively regulated by SOCS3 (see text). mTORC1 also activates STAT3, linking PI3K/Akt/mTOR signalling at a downstream level. Connections between pathways enable significant cross-talk to influence multiple cellular processes.

Receptor activation by NTF induces activity of the lipid kinase PI3K, which phosphorylates and activates the conversion of phosphatidylinositol (4,5) bisphosphate (PIP2) to phosphatidylinositol (3,4,5) triphosphate (PIP3). Phosphatase and tensin homolog deleted on chromosome ten (PTEN) catalyses the reverse reaction. PIP3 recruits and activates phosphatidylinositol-dependent protein kinase 1 (PDK1), which in turn activates Akt, that phosphorylates and inhibits tuberous sclerosis complex (TSC), a heterodimer comprising TSC protein 1 (TSC1) and TSC2. This complex acts as a GTPase activating protein, converting Rheb-GTP to Rheb-GDP (Laplante and Sabatini, 2013). The active Rheb-GTP binds to and stimulates mTOR, and therefore TSC1/2 acts to impair mTOR activity by converting Rheb to its inactive, GDP-bound state (Inoki *et al.*, 2003a). Thus, NTF-induced activity through the PI3K pathway acts to up-regulate Akt, which inhibits TSC1/2, thereby disinhibiting Rheb and ultimately leading to enhanced mTOR activity (Figure 1.7).

1.7.1 mTOR forms two distinct complexes with different substrates and cellular effects

mTOR exerts multiple effects on cellular function by forming two distinct functional complexes that act on downstream substrates to influence cell survival and growth. The mTOR complex 1 (mTORC1) includes mTOR and the proteins Raptor, PRAS40, Deptor, and GβL (Maiese *et al.*, 2013), and is sensitive to Rapamycin, which binds the FK506-binding protein FKBP12 and physically interacts with the complex to decrease its activity (Johnson *et al.*, 2013). The second complex, mTORC2, also contains mTOR, Deptor and GβL, and additionally Rictor, mSIN1, and Protor-1 (Maiese *et al.*, 2013). In contrast to mTORC1, mTORC2 is Rapamycin resistant, although chronic exposure to Rapamycin may inhibit mTORC2 assembly (Johnson *et al.*, 2013; Sarbassov *et al.*, 2006; Ma and Blenis, 2009).

The two main targets of mTORC1 are ribosomal S6 kinase (S6), and eukaryotic translation initiation factor 4E-binding protein (4E-BP1), with up-regulation of mTOR activity promoting translation and

protein synthesis *via* these two effectors (Laplante and Sabatini, 2013). Activation of S6 by phosphorylation stimulates translation of mRNA coding proteins involved in ribosome biogenesis and protein synthesis (Meyuhas, 2000; Jefferies *et al.*, 1997). 4E-BP1 is active in its hypophosphorylated form and blocks protein translation though an interaction with eukaryotic translation initiation factor 4 epsilon (eIF4E), and mTORC1 acts to repress 4E-BP1 by phosphorylation, which in turn dissociates from eIF4E to enable initiation of protein translation (Gingras *et al.*, 1998). Thus, mTORC1 increases the protein synthesis capacity of the cell, a key requirement in cell survival and axon regeneration. Lipid synthesis, repressed cellular degradation by autophagy, glucose metabolism and mitochondrial function are amongst other processes linked to mTORC1 activity (Johnson *et al.*, 2013). The downstream outputs and effects of mTORC2 are less well understood, although it activates protein kinase C alpha (PKCα) to control actin dynamics (Ma and Blenis, 2009; Hoeffer and Klann, 2010), and activates Akt through a positive feedback pathway, thereby sustaining mTOR activation and promoting actin/microtubule assembly by inhibiting GSK3β (Figure 1.7; also see below) (Jacinto *et al.*, 2006).

1.7.2 Other downstream effectors of PI3K/Akt signalling and links to alternative pathways

1.7.2.1 Glycogen synthase kinase 3 beta (GSK3β)

mTORC1 and mTORC2 are not the only downstream effectors of the PI3K/Akt pathway. GSK3β negatively regulates growth cone microtubule assembly and is inactivated by Akt (Zhou and Snider, 2005b). Inhibition of GSK3β promotes actin/microtubule assembly after disinhibition of collapsing response mediator protein 2 (CRMP2) and the microtubule binding protein adenomatosis polyposis coli (APC) (Fukata *et al.*, 2002; Trivedi *et al.*, 2005). GSK3β also directly phosphorylates TSC1/2 to down-regulate mTOR activity (Inoki *et al.*, 2006) (Figure 1.7), therefore signalling through the

PI3K/Akt pathway acts both to up-regulate Akt activity (and subsequent mTOR activity) directly, and disinhibit mTOR *via* inhibition of GSK3β. Protection against growth cone collapse and stimulation of growth cone dynamics by GSK3β inhibition are required for neurotrophin-induced axon growth (Zhou *et al.*, 2004). GSK3β is also heavily implicated as a key regulator of gene transcription and neuronal survival (Hur and Zhou, 2010; Jacobs *et al.*, 2012).

1.7.2.2 ERK/MAPK signalling pathway

The ERK/MAPK pathway regulates protein synthesis, cell survival and axon growth (Figure 1.7) (Polleux and Snider, 2010), and is also activated by Trk ligands. ERK directly activates mTORC1 by phosphorylation (Carriere *et al.*, 2011), acts upon TSC1/2 to disinhibit mTORC1 activity (Ma *et al.*, 2005), and is important for the kinetics of S6 phosphorylation (Razmara *et al.*, 2013). ERK/MAPK and PI3K/Akt-mediated signalling may mediate distinct aspects of neuronal growth, such as axon elongation, axon calibre and branching (Park *et al.*, 2010; Goldberg, 2003; Polleux and Snider, 2010), effects that are enhanced by mTOR-induced axogenic protein synthesis.

1.7.2.3 Cytokine signalling and the Wnt Pathway

CNTF/LIF signalling *via* the gp130 receptor complex acts through SHP-2 (JAK1) to stimulate the PI3K/Akt and ERK/MAPK pathways (Figure 1.7) (Rane and Reddy, 2000; Fischer and Leibinger, 2012). Furthermore, mTORC1 phosphorylates STAT3 in a CNTF-dependent manner (Yokogami *et al.*, 2000). Wnt protein signalling is associated with multiple cellular processes, including cellular development and survival, and can increase mTORC1 activity by blocking the effect of GSK3β on the TSC1/2 complex (Maiese *et al.*, 2008; Arevalo and Rodriguez-Tebar, 2006).

These alternative and linked pathways highlight opportunities for downstream cross-talk of multiple different ligand-receptor interactions, leading to myriad effects on cellular processes. The complexity of intracellular signalling *via* multiple pathways is a significant challenge in identifying key survival/regeneration mediators and targeting appropriate regulatory points to achieve potential therapeutic effects.

1.8 EXTRINSIC MECHANISMS OF mTOR ACTIVITY REGULATION

In addition to developmental down-regulation, mTOR activity is modulated by the metabolic conditions of the cellular environment, with adverse conditions, such as hypoxia, energy deprivation, and reduced nutrient availability all inhibiting mTOR activity, with consequent restriction of protein synthesis (Figure 1.8) (Hay and Sonenberg, 2004; Laplante and Sabatini, 2012; Malik *et al.*, 2012; Arsham *et al.*, 2003). The TSC1/2 complex is a key nodal point, upstream of mTORC1/2, integrating signals from multiple sources to regulate mTOR-dependent protein synthesis.

1.8.1 Hypoxia

Hypoxia down-regulates 4E-BP1 and S6 phosphorylation (Arsham *et al.*, 2003; Brugarolas *et al.*, 2004) *via* the induction of RTP801 (otherwise known as Redd1), which acts directly on the TSC1/2 complex (Figure 1.8) (Brugarolas *et al.*, 2004; Corradetti *et al.*, 2005). RTP801 transcription is up-regulated rapidly by hypoxia inducible factor 1 alpha (HIF1α) (Shoshani *et al.*, 2002), although RTP801 is also induced by hypoxia in HIF1α-deficient cells, indicating that other HIF family members or HIF-independent mechanisms may also play a role in hypoxia-mediated suppression of mTOR activity (Shoshani *et al.*, 2002). The hypoxic response is thought to promote ATP production in oxygen-

limited conditions by encouraging a shift in metabolism toward lactic acid fermentation and glycolysis (Johnson *et al.*, 2013).

1.8.2 Energy deprivation

Down-regulation of mTOR in response to energy deprivation acts through the AMP-activated kinase (AMPK), a metabolic regulator that is stimulated by impaired cellular energy production (ATP depletion, or increased AMP:ATP ratio) (Brugarolas *et al.*, 2004; Inoki *et al.*, 2003b), and negatively regulates mTORC1 by direct phosphorylation of TSC2 and the Raptor domain of mTORC1 (Inoki *et al.*, 2003b; Gwinn *et al.*, 2008) (Figure 1.8). The tumour suppressor proteins liver kinase B1 and p53 also act upon AMPK to inhibit mTORC1 in a TSC-independent manner (Chong *et al.*, 2012; Budanov and Karin, 2008). Moreover, AMPK can itself activate RTP801 (DeYoung *et al.*, 2008), highlighting the close interaction of mTORC1 regulation in response to hypoxic and metabolic stressors.

1.8.3 Nutrient availability

The availability of amino acids is also an important determinant of mTOR function (Jewell and Guan, 2013). Activation of mTORC1 by amino acids (especially leucine and arginine) is independent of TSC1/2 and relies on small GTPases, named Ras-related GTP binding proteins (Rags), which bind directly to the Raptor component of mTORC1 to stimulate protein synthesis (Hara *et al.*, 1998). Furthermore, amino acids also up-regulate mTORC2 activity directly (Tato *et al.*, 2011) (Figure 1.8).

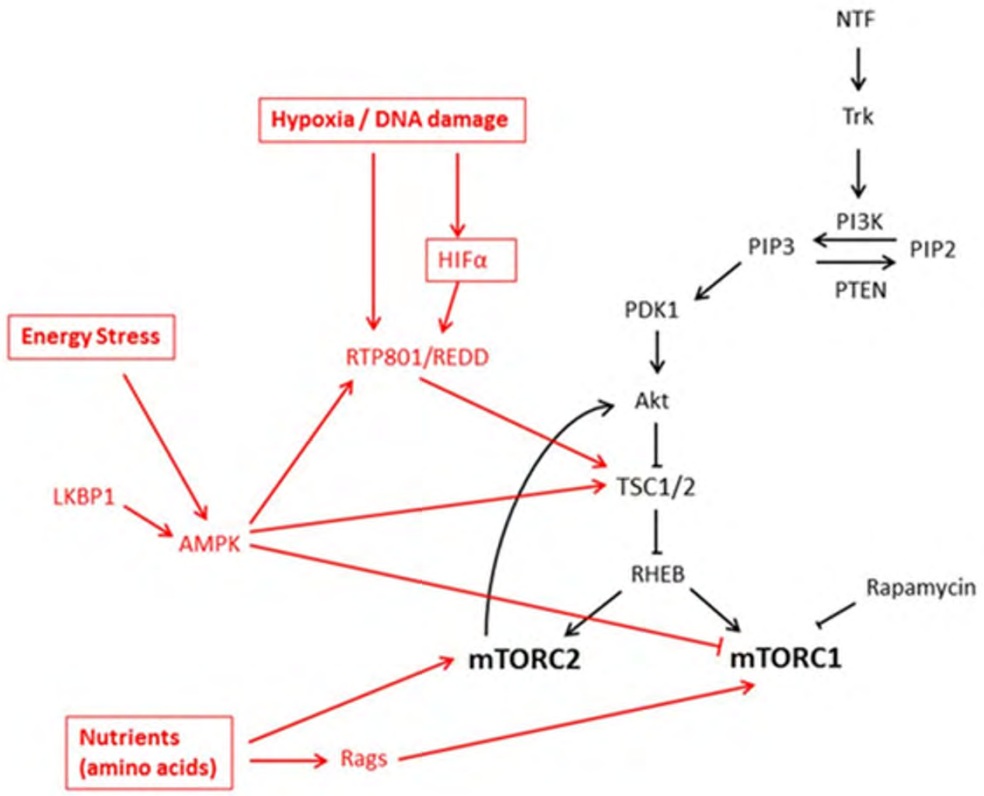


Figure 1.8: Regulation of mTOR signalling by external factors. Cellular stress, such as hypoxia and DNA damage induce RTP801 *via* HIF1α-dependent and independent pathways. RTP801 promotes TSC activity and results in mTOR down-regulation. AMPK is activated in response to impaired cellular energy production, acting directly on TSC to negatively regulate mTOR, and also up-regulates RTP801 and directly inhibits mTORC1. Nutrient availability (e.g. amino acids required for protein synthesis) is signalled via Rag proteins to influence mTOR activity. Targeting negative regulators of mTOR pathway signalling represents an opportunity to promote mTOR activity, which is associated with neuronal survival and growth (see text).

1.9 MANIPULATING mTOR SIGNALLING TO PROMOTE RGC SURVIVAL AND AXON REGENERATION

1.9.1 Deletion of the *pten* gene promotes RGC survival and robust axon regeneration

There is good evidence that up-regulation of mTOR signalling is a viable strategy to promote RGC survival and axon regeneration after ON injury. A conditional *pten* gene deletion paradigm, preventing RGC apoptosis in an ONC model with approximately 45% RGC survival at 14d after ONC, also promotes ON axon regeneration, allowing approximately 8% to 10% of the surviving RGC to regenerate axons beyond the lesion site, with a small subset regenerating several mm as far as the optic chiasm (Figure 1.9) (Park *et al.*, 2008). Conditional deletion of *tsc1* also promotes axon regeneration, although the effect is less pronounced than with *pten* knock-down (Park *et al.*, 2008). Similarly, deletion of either *pten* or *tsc1/2* enhances the regenerative potential of corticospinal tract (CST) neurons and peripheral sensory neurons (Liu *et al.*, 2010a; Abe *et al.*, 2010; Christie *et al.*, 2010).

The conversion of PIP3 to PIP2 is blocked by *pten* deletion, leading to accumulation of PIP3, activation of Akt and mTORC1/mTORC2, and inhibition of GSK3β, with consequent stimulation of axon protein synthesis and growth cone dynamics, respectively (Figure 1.7). Using a phospho-S6 (pS6) antibody (as a marker of mTOR activity), the pS6 signal is completely abolished in RGC at 1, 3 and 7d after axotomy in wild-type animals, suggesting a rapid and sustained down-regulation of mTORC1 activity (Park *et al.*, 2008). By contrast, there is activation of mTORC1 in $pS6^{+}$ RGC, correlated with axon growth after *pten* deletion, while Rapamycin reduces pS6 expression and diminishes the pro-regenerative effects of *pten* deletion after axotomy (Park *et al.*, 2008).

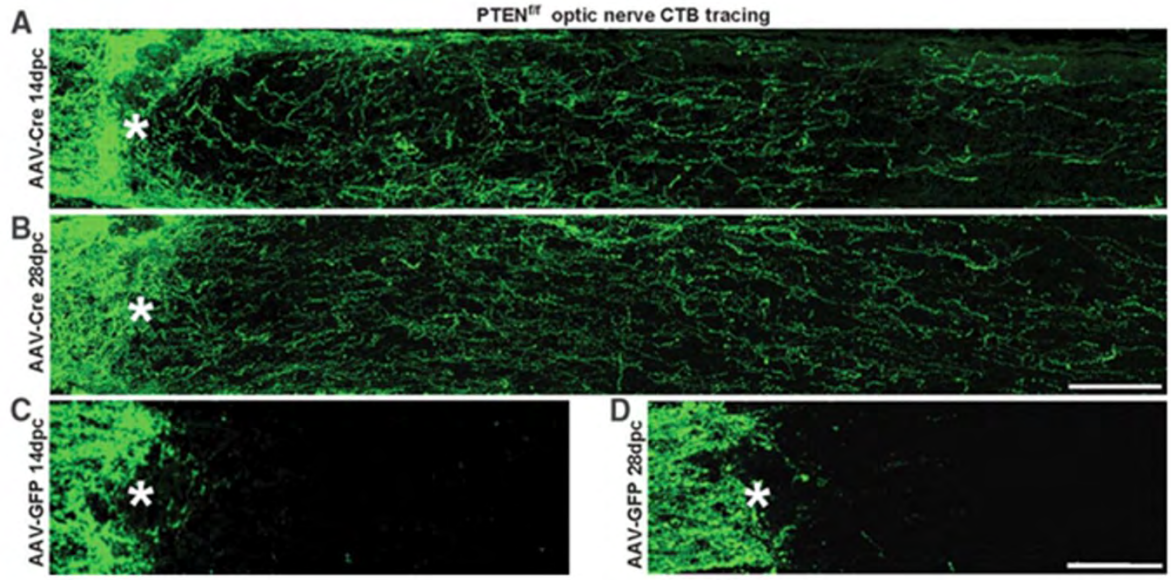


Figure 1.9: Deletion of *pten* promotes RGC axon regeneration. (A-D) Confocal images of optic nerves showing cholera toxin β (CTB)-labelled fibres around the lesion sites (*) at 14d (A, C) or 28d (B, D) after injury from PTEN$^{f/f}$ mice injected with AAV-Cre (treatment, [A, B] or AAV-GFP (control, [C, D]). Scale bar 100µm. (see text for details) Reprinted with permission from Park KK, *et al.* Promoting axon regeneration in the adult CNS by modulation of the PTEN/mTOR pathway. *Science* 2008; 322: 963-66. Copyright 2008 AAAS.

Intervention	Species	RGC Survival	Axon Regeneration Beyond Lesion	Comment	Reference
Lens injury	Rat	~24% at 2 wk	~1500-1900 axons at 0.5 mm*		Leon *et al.*, 2000; Fischer *et al.*, 2000
Intravitreal zymosan	Rat	Increased x 2 vs control	~1200 axons at 0.5 mm†	Axon growth up to 4.7 mm	Yin *et al.*, 2003
Intravitreal Pam3Cys	Rat	No increase vs control *in vitro*	~700 axons at 0.5 mm†	2 injections, 7 d apart for max effect	Hauk *et al.*, 2010
Intravitreal neurotrophic factors	Rat	Increased x 2 vs control *in vitro*	~1000 axons at 2 mm*	FGF2/NT3/BDNF transfected fibroblasts	Logan *et al.*, 2006
RhoA blockade	Rat	No increase vs lens injury alone	~250 axons at 0.5 mm†		Fischer *et al.*, 2004
RhoA blockade + lens injury	Rat	No increase vs lens injury alone	~1500 axons at 0.5 mm†		Fischer *et al.*, 2004
PTEN deletion	Mouse	~45% at 2 wk	~1500-1700 axons at 0.5 mm†	Few fibres >3 mm to chiasm by 4 wk	Park *et al.*, 2008
TSC deletion	Mouse	~50% at 2 wk	~1200-1500 axons at 0.5 mm†		Park *et al.*, 2008
SOCS3 deletion	Mouse	~40% at 2 wk	~500 axons at 0.5 mm†	No significant regeneration >1.5 mm	Smith *et al.*, 2009
SOCS3 deletion + CNTF	Mouse		~1500 axons at 0.5 mm†	Few fibres 2-2.5 mm	Smith *et al.*, 2009
PTEN/SOCS3 deletion + CNTF	Mouse	~60% at 2 wk	~1500-1900 axons at 0.5 mm†	~20% regenerating fibres to chiasm, few to optic tract, hypothalamus and SCN	Sun *et al.*, 2011
PTEN deletion + cAMP + zymosan	Mouse	~36% at 10 wk	~325 axons at 2.5 mm‡	Axons to SCN, LGN, olivary pretectal nucleus, and restitution of some visual behaviours	de Lima *et al.*, 2012
PTEN deletion + cAMP + zymosan	Mouse	~54% at 2 wk	~800 axons at 0.5 mm†	~1% to LGN at 6 wk	Kurimoto *et al.*, 2010

* 3 wk post-lesion
† 2 wk post-lesion
‡ 6 wk post-lesion

Table 1.1: Comparison of reported experimental approaches to promote RGC survival and axon regeneration.

1.9.2 Combining *pten* deletion with other approaches further enhances RGC survival and axon regeneration

Given the multiple mechanisms acting in concert to regulate neuronal survival and axonal regrowth, as described, it follows that combinatorial approaches consistently yield stronger RGC survival and axon regenerative responses than do individual manipulations (Table 1.1). Deletion of the *pten* gene in combination with inflammatory stimulation promotes long-distance regeneration over 5mm, and some target re-innervation (Kurimoto *et al.*, 2010), and may be sufficient even to partially regain some visually dependent behaviour (de Lima *et al.*, 2012). Combined deletion of *pten* and *socs3*, together with CNTF administration, promotes a 10-fold increase in the number of regenerating axons at 2mm beyond the ONC site compared to deletion of either gene alone (Sun *et al.*, 2011). Thus, development of a therapeutic intervention may need to target multiple points in cellular signalling pathways in order to elicit a robust and clinically relevant effect.

1.10 TRANSLATION OF MOLECULAR BIOLOGY FOR CLINICAL USE

Once the optimal biochemical conditions for RGC survival and axon regeneration are elucidated in laboratory experiments, a major challenge remains in translating them into a clinical approach. Conditional gene deletion is not translatable, and gene therapy is in its infancy. Furthermore, induction of an intraocular inflammatory response would result in unacceptable clinical side effects, such as increased intraocular pressure and cataract formation. Ribonucleic acid interference (RNAi) is a promising strategy for targeted knock-down of specific genes, and the eye represents an easily accessible system for the investigation of RNAi-based therapies for ocular disease (Guzman-Aranguez *et al.*, 2013).

1.10.1 RNA interference: principles and mechanism

RNAi is an evolutionarily conserved mechanism that leads to post-transcriptional gene silencing by suppressing mRNA translation. First demonstrated in the nematode *Caenorhabditis elegans* (Fire *et al.*, 1998), the RNAi machinery was also shown to be present in mammalian cells shortly after (Elbashir *et al.*, 2001). The sequence-specific gene silencing RNAi pathway can be induced by either microRNA (miRNA), endogenous non-coding double-stranded RNA (dsRNA) molecules which modulate gene expression, or exogenously synthesised small interfering RNAs (siRNAs), 18-25 nucleotide duplexes that can be directly delivered to the cell or tissue of interest (Guzman-Aranguez *et al.*, 2013).

The mechanism of RNAi is summarised in Figure 1.10. Endogenous ds-RNA are cleaved by the RNase III enzyme Dicer into shorter siRNA fragments (Ketting *et al.*, 2001). In cell cytoplasm, endogenously synthesised or exogenously delivered siRNA are subsequently incorporated into a multi-protein complex called the RNA-induced silencing complex (RISC), incorporating an ATP-helicase enzyme that dissociates the two RNA strands by cleaving and unwinding the sense strand, leaving the anti-sense strand associated with an endonuclease, Argonaute 2 (AGO2) (Rand *et al.*, 2004). This complex hybridizes to, and subsequently hydrolyses, the target complementary mRNA sequence, thus preventing translation of the cleaved mRNA transcript and resulting in 'knock-down' of the target gene. RNAi is a very potent process, as the activated RISC is capable of binding to and cleaving many complementary mRNA transcripts, thereby efficiently suppressing target gene expression (Guzman-Aranguez *et al.*, 2013).

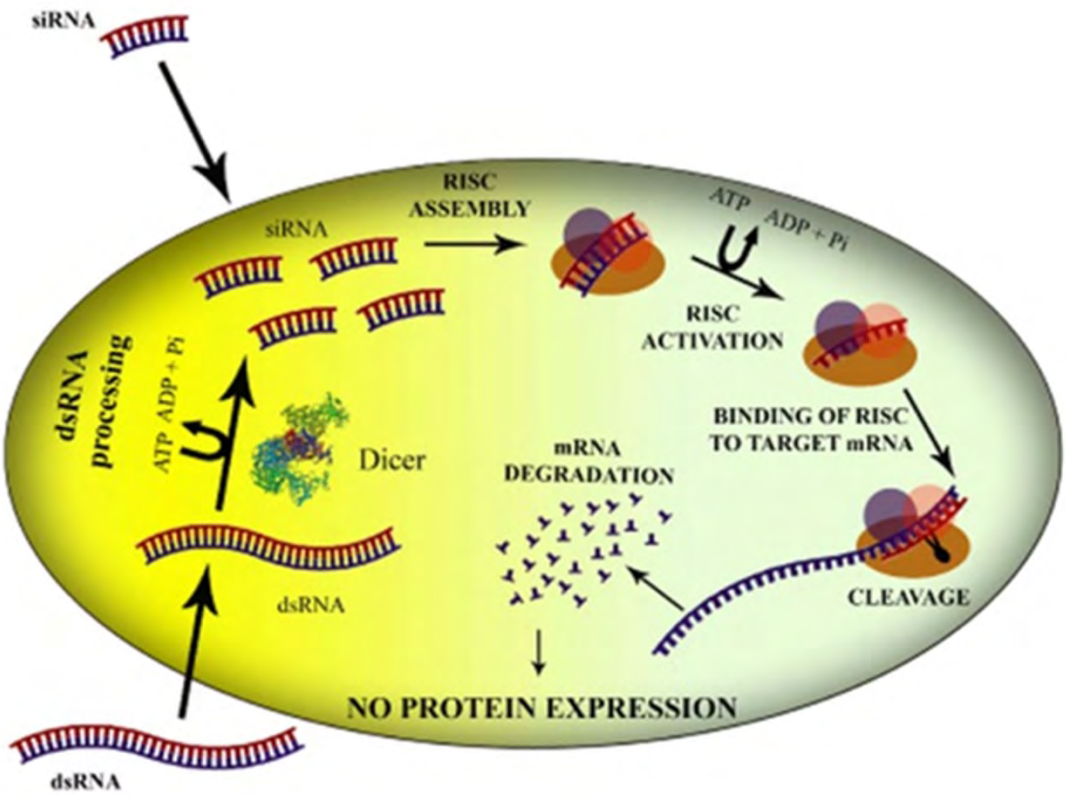


Figure 1.10: Mechanism of RNA interference (RNAi). Schematic representation of RNAi. Long dsRNA molecules are cleaved into siRNA fragments by the Dicer RNase III enzyme. Alternatively, synthetically constructed 18-25 base-pair siRNA are directly introduced into the cell. The siRNAs are integrated in to the RNA-induced silencing complex (RISC), which unwinds the dsRNA, associates with the complementary target mRNA, and hydrolyses the target mRNA sequence resulting in specific gene knock-down. Figure reproduced from Guzman-Aranguez *et al. Br J Pharmacol* 2013; 170:730-47, with permission.

1.10.2 Delivery and stability of siRNA

A major limitation to siRNA use is their inability to cross cell membranes to reach the cytoplasm to access the RNAi machinery and exert gene knock-down. Negatively charged phosphate groups on the siRNA backbone repel the similarly negatively charged membrane lipids, preventing movement into

the cells (Thakur *et al.*, 2012). A variety of delivery strategies are available to overcome this problem, such as non-viral carriers that act as transfection reagents to enhance siRNA cellular uptake (Thakur *et al.*, 2012). One commonly used approach, particularly for cell culture, is to form complexes between siRNA and cationic lipids ("lipoplexes"). A detailed description of siRNA transfection used in experiments is given in Chapter 2.

Gene silencing induced by siRNA is only transient, typically lasting for 3-7d before siRNA degradation (Guzman-Aranguez *et al.*, 2013). A number of chemical modifications have been described in order to resist siRNA hydrolysis *in vivo* including, for example, 2'-O-methylation of the ribose structure (Czauderna *et al.*, 2003), although even chemically modified siRNA are susceptible to eventual degradation by extracellular endonucleases, such as those found in the vitreous (Guzman-Aranguez *et al.*, 2013).

1.10.3 Off-target effects of RNAi

Although specificity is a key feature underlying the gene silencing effect of RNAi, off-target effects can also occur. Partial hybridization of siRNA/RISC to sequences other than the specific target mRNA may result in unintended knock-down of genes sharing similar homology with the siRNA (Thakur *et al.*, 2012). Furthermore, specific nucleotide motifs have been associated with cellular toxicity (Fedorov *et al.*, 2006). In addition to non-specific gene silencing, siRNA may trigger an immune response. In particular, exposure to long dsRNA (>30 nucleotides) may activate Toll-like Receptors (TLR), such as TLR3 and TLR7/8, and protein kinase R (PKR), with subsequent production of cytokines, interferon release and alterations of gene expression (Kleinman *et al.*, 2008; Forsbach *et al.*, 2008).

1.11 PROJECT AIMS AND HYPOTHESES

As described above, the cellular signalling pathways involved in mediating RGC survival and axon regeneration after ON injury in experimental studies are becoming increasingly well understood, and manipulation of these pathways may be the best opportunity for development of novel therapeutic treatments for translation in to clinical practice. In particular, the PI3K/Akt signalling pathway and the downstream effector mTOR complexes are heavily implicated in RGC survival and axon regeneration, and up-regulation of this pathway is associated with robust results in animal models of TON. Moreover, much of the focus of targeting signalling pathways has only considered the RGC themselves as the prime targets for intervention, when it is increasingly clear that retinal glia also play a role in determining RGC responses to injury and regenerative potential.

1.11.1 Overall project aim

The aim of the experimental work described here was to use a clinically translatable siRNA approach to manipulate intracellular signalling of the PI3K pathway at key nodal regulatory points, including knock-down of the mTOR negative regulator RTP801 and the cell survival/axonal growth cone modulator GSK3β, in order to promote RGC survival and axon regeneration after ONC *in vivo*, and act as the basis for the development of a novel therapy to restore sight to patients. In addition, *in vitro* cell culture models were used to evaluate the underlying cellular mechanisms associated with targeted siRNA-mediated gene knock-down, to enable a deeper understanding of cellular signalling in relation to RGC survival and axon growth, and optimise the formulation of novel treatment strategies.

1.11.2 Overall project hypothesis

siRNA-mediated knock-down of key negative regulatory targets in the PI3K signalling pathway promotes mTOR activity to enhance RGC survival and axon regeneration after ON injury. A schematic representation of the project hypothesis is given in Figure 1.11.

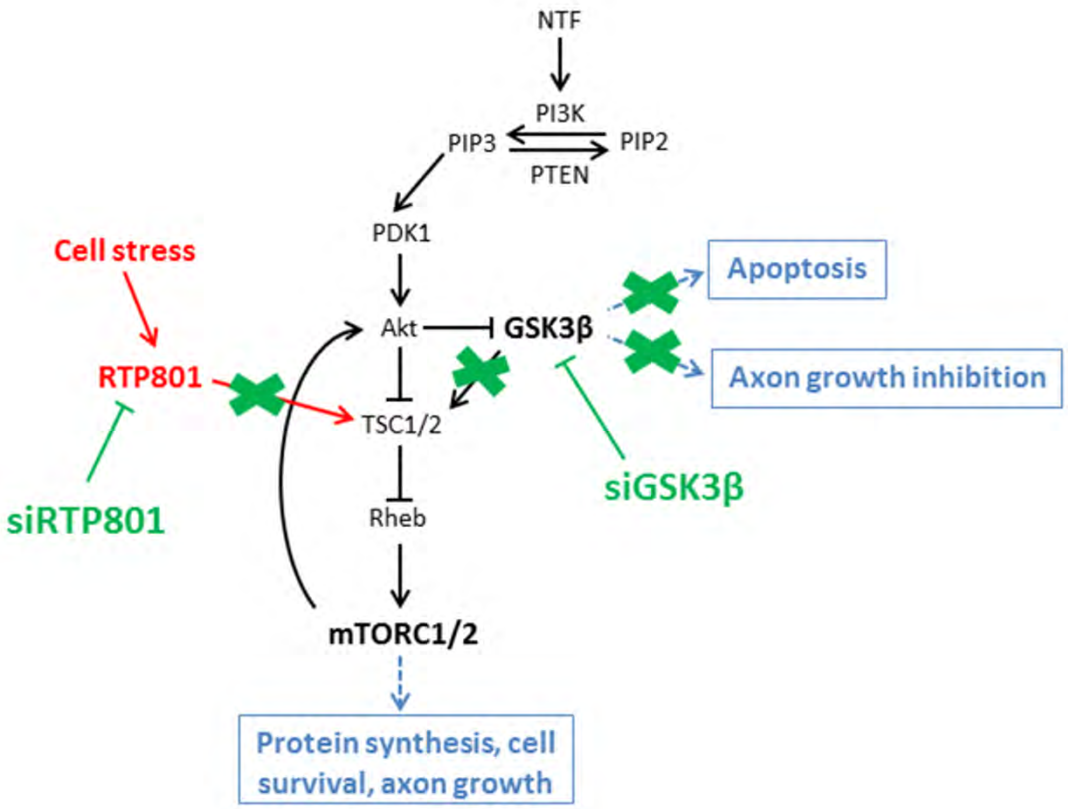


Figure 1.11: Project hypothesis. siRNA-mediated knock-down of key negative regulatory targets in the PI3K signalling pathway promotes mTOR activity to enhance RGC survival and axon regeneration after ON injury. RTP801 is a stress-induced negative regulator of mTOR activity, and it was hypothesised that siRTP801 promotes RGC survival and axon regeneration after ONC by promotion of mTOR activity (discussed in detail in Chapters 3 and 4). GSK3β activity is implicated in neuronal apoptosis and axonal growth cone collapse, and it was hypothesised that siGSK3β promotes RGC survival and disinhibited axon growth, and that combination treatment with both siRTP801 and siGSK3β further enhances these effects (discussed in detail in Chapter 5).

1.11.3 Chapter overview

A detailed description of materials and experimental methods is provided in Chapter 2, including the ONC model and the evaluation of RGC survival, axon regeneration and glial responses using immunohistochemistry and fluorescence microscopy after intravitreal delivery of targeted siRNA. The principles and methods of the *in vitro* retinal cell culture experiments are also described, as well as immunocytochemistry, enzyme-linked immunosorbent assay (ELISA) and quantitative polymerase chain reaction (qPCR) techniques employed.

Chapter 3 describes experiments investigating the effects of siRNA-mediated knock-down of RTP801, a stress-induced negative regulator of mTOR activity. The aim of Chapter 3 was to characterise the expression of RTP801 in retinal cells, including the effects of ON injury and target knock-down in response to siRNA treatment, and to investigate the effects of siRTP801 on RGC survival and axon regeneration both *in vivo* after ONC and in a dissociated retinal cell culture model. It was hypothesised that siRNA-mediated target knock-down of RTP801 promotes RGC neuroprotection and axon regeneration.

In Chapter 4, further experiments are described that investigated in more detail the cellular mechanisms underlying the results obtained in initial studies, and examined the relationship between direct effects of RTP801 knock-down on RGC, and indirect sequelae as a result of effects on retinal glia. Specifically, the effects of siRTP801 on activation of retinal glia were investigated both after ONC *in vivo*, and in retinal cell culture studies, along with ELISA analysis of NTF production, and the effects of RTP801 knock-down on mTOR activity investigated. It was hypothesised that siRTP801 promotes both up-regulation of mTOR activity and the activation of retinal glia to enhance the production of NTF, which in turn contribute to RGC survival and axon regeneration.

Experiments described in Chapter 5 investigated the effects of GSK3β inhibition with a pharmacological inhibitor on RGC survival and neurite growth in a retinal culture model, and siRNA-mediated knock-down of GSK3β on RGC survival and axon regeneration both *in vivo* and *in vitro*. In addition, experiments were undertaken to evaluate whether a combinatorial siRNA approach targeting both RTP801 and GSK3β enabled enhanced effects. It was hypothesised that inactivation of GSK3β promotes RGC survival and axon regeneration, *via* potentiated mTOR activity and by overcoming the external inhibitory environment, and that combined siGSK3β/siRTP801 treatment further enhances RGC survival and axon regeneration.

In Chapter 6, an overall summary and discussion of the results, their implications for future research and for the potential development of novel translatable treatments is presented.

CHAPTER 2

MATERIALS AND METHODS

2.1 OVERVIEW OF EXPERIMENTAL METHODS

The experiments described in this thesis utilised both *in vivo* and *in vitro* techniques. Specific details of the experimental groups are given in the experimental Chapters 3-5. *In vivo* studies using the adult rat ONC model and intravitreal injections of test and control siRNA were designed to evaluate the effects of siRNA-mediated target knock-down on RGC survival, axon regeneration and glial responses, using immunohistochemical analysis of retinal and ON tissue sections (Figure 2.1A). Studies on retinal cultures were undertaken to investigate the cellular mechanisms underlying the effects seen *in vivo*. Dissociated mixed cell cultures were obtained from adult rat retinae, either uninjured ('intact') or 5d after ONC *in vivo* to activate retinal glia (and before significant RGC death occurred) (Figure 2.1B). Cultured cells were transfected with siRNA or appropriate controls, in the presence or absence of selected inhibitors. Cell cultures were analysed by immunocytochemistry for RGC survival, neurite outgrowth, cellular detection and knock-down of specific siRNA targets, effects on other intracellular signalling markers of interest and effects on glia. Conditioned medium from siRNA-treated cell cultures was assayed for neurotrophic factor titres by enzyme-linked immunosorbent assay (ELISA) (described in Chapter 4), and RNA obtained from cultured cells was subjected to quantitative polymerase chain reaction (qPCR) experiments to evaluate siRNA target mRNA knock-down.

All reagents were obtained from Sigma (Poole, UK) unless otherwise stated.

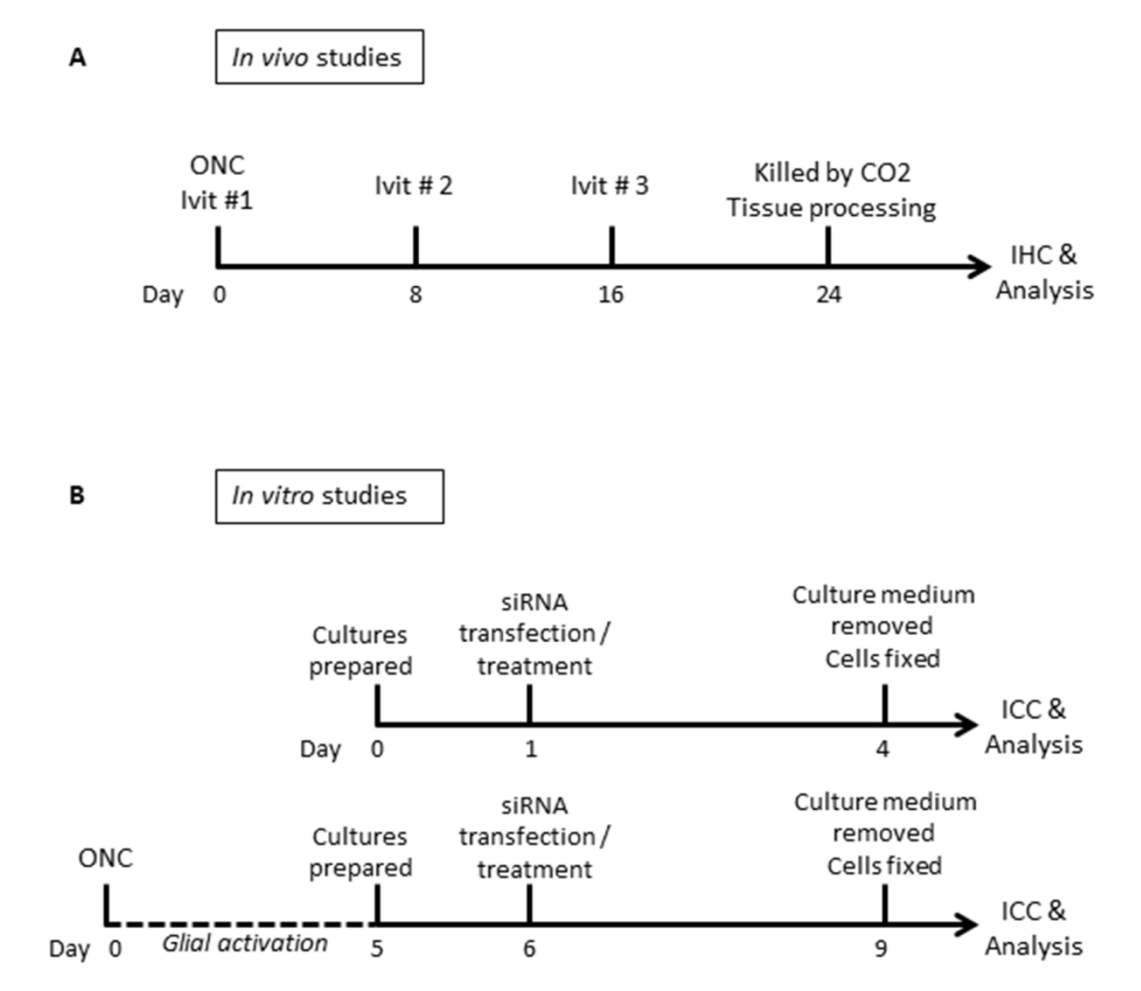


Figure 2.1: Overview of experimental approach of (A) *in vivo*, and (B) *in vitro* studies.

2.2 siRNA

All siRNA were supplied by Quark Pharmaceuticals Inc. (Ness Ziona, Israel) for no cost under a Material Transfer Agreement with the University of Birmingham. All siRNA were stabilised for *in vivo* use by alternating 2'O-methylation (Czauderna *et al.*, 2003), and were synthesised at BioSpring (Frankfurt, Germany). The siRNA studied included those targeting RTP801 (siRTP801), with sequence 5'-GUGCCAACCUGAUGCAGCU-3' (sense strand) as previously published (Rittenhouse *et al.*, 2014), GSK3β (siGSK3β, sequence held by Quark Pharmaceuticals Inc.), and control siRNA against enhanced green fluorescent protein (EGFP; siEGFP), with sequence 5'-GGCUACGUCCAGGAGCGCACC-3' (sense strand) as previously published (Hamar *et al.*, 2004). The siRNA were supplied in powder form, and were prepared for use by spinning in a centrifuge at 17000rpm for 3min, incubated in a tissue culture hood for 30min at room temperature, then dissolved in sterile phosphate buffered saline (PBS) to stock concentration of 20µg/µl. The siRNA stock solutions were stored at -20°C until use.

2.3 *IN VIVO* METHODS

2.3.1 Animals and animal surgery

Adult male Wistar rats (Charles River, Kent, UK), weighing 200-250g at the commencement of experiments, were housed at 21°C/55% humidity in a 12h light and dark cycle with *ad libitum* access to food and water. All surgery was carried out in accordance with the UK Home Office regulations for the care and use of experimental animals and the UK Animals (Scientific Procedures) Act 1986, and approved by the University of Birmingham Ethical Review Committee. Surgical procedures for experiments described in Chapter 3 were performed by [redacted], with administration of analgesia, anaesthetic, and peri-operative care by me. Surgical procedures for experiments

described in Chapters 4 and 5 were performed by me, with assistance for peri-operative care from colleagues in the Neurotrauma Research Group.

2.3.2 Anaesthesia and peri-operative care

Analgesia with subcutaneous injection of buprenorphine (0.1ml/100g; National Veterinary Supplies, Stoke, UK) was administered 30-60min before the start of surgery. Inhalational general anaesthesia was induced with 5% isoflurane in 1.5L/min O_2 (National Veterinary Supplies) and maintained at 3% throughout surgery. After induction of anaesthesia animals were placed on a warming mat and secured in a head supporting frame to maintain position and stability, with EMLA Cream 5% (topical 2.5% lidocaine/2.5% prilocaine; Astra Zeneca, Macclesfield, UK) applied to the ear-bars to prevent discomfort (Figure 2.2A). Physiological parameters were continuously monitored during surgery with a respiratory monitor, pulse oximeter, and rectal thermometer. Animals were also monitored for signs of return to consciousness, including return of return of blink and pedal reflexes. After surgery, lubricating Carbomer Gel 0.2% eye lubricant (Blumont Healthcare, Grantham, UK) was applied to protect the ocular surface, and animals recovered from surgery in heated cages under supervision of trained animal technicians for 24h until the emergence of normal behaviour, when they were returned to home cages. In accordance with the Home Office Licence, all experimental animals were monitored at least twice daily for 3d and then daily for potential adverse effects of surgery, including: local effects, such as ocular infection, lens injury (cataract) and skin wound infection/dehiscence; and general effects, including weight loss, inadequate body temperature, lethargy, inappetence, and starey coat/hunched appearance. A Named Veterinary Surgeon (NVS) was available for advice if any concern was identified.

2.3.3 ONC

A midline scalp incision was made over the dorsum of the skull, the skin reflected laterally to expose the orbital margin and subcutaneous fascia divided. The temporalis muscle was identified, and a 2-3mm vertical incision made in the muscle belly with microscissors (Figure 2.2B), extended superiorly to the orbital margin and rostrally around the orbital margin to the medial canthus, with care to maintain haemostasis. The supraorbital neurovascular bundle was identified and clamped with forceps for several seconds before being divided between the clamp sites to expose the underlying Harderian gland (Figure 2.2C). The superficial lobe of the Harderian gland was mobilised by opening the capsule and reflecting it rostrally toward the medial canthus to expose the deep lobe (Figure 2.2D). The overlying capsule was divided between the superior and lateral rectus muscles and the deep lobe of the Harderian gland reflected rostrally to expose the underlying ON in its dural sheath, with the adjacent lateral rectus muscle lying caudally. Sterile paper retractors were placed rostrally between the ON sheath, the deep lobe of Harderian gland and the superior rectus, and caudally between the ON sheath and lateral rectus, to enable easy access to the ON (Figure 2.2E). The retractor bulbi muscle, dura mater and arachnoid mater were divided longitudinally to expose the underlying ON, with care taken to preserve the retinal artery within the medial aspect of the dural sheath. The ON was crushed for 5-10s with fine forceps approximately 2mm posterior to the lamina cribrosa, transecting all axons whilst preserving the pia mater with its associated vasculature (Figure 2.2F). The ON sheath, retractor bulbi muscle, rectus muscles and lobes of the Harderian gland were sequentially replaced into position, and the procedure repeated on the contralateral eye. Once complete, the skin incision was closed with interrupted Ethicon 6-0 coated Vicryl (polyglactin 910) absorbable sutures (Johnson and Johnson Medical Limited, Livingstone, UK). In experiments where intravitreal injections were performed, these were undertaken immediately after skin closure, prior to cessation of anaesthesia.

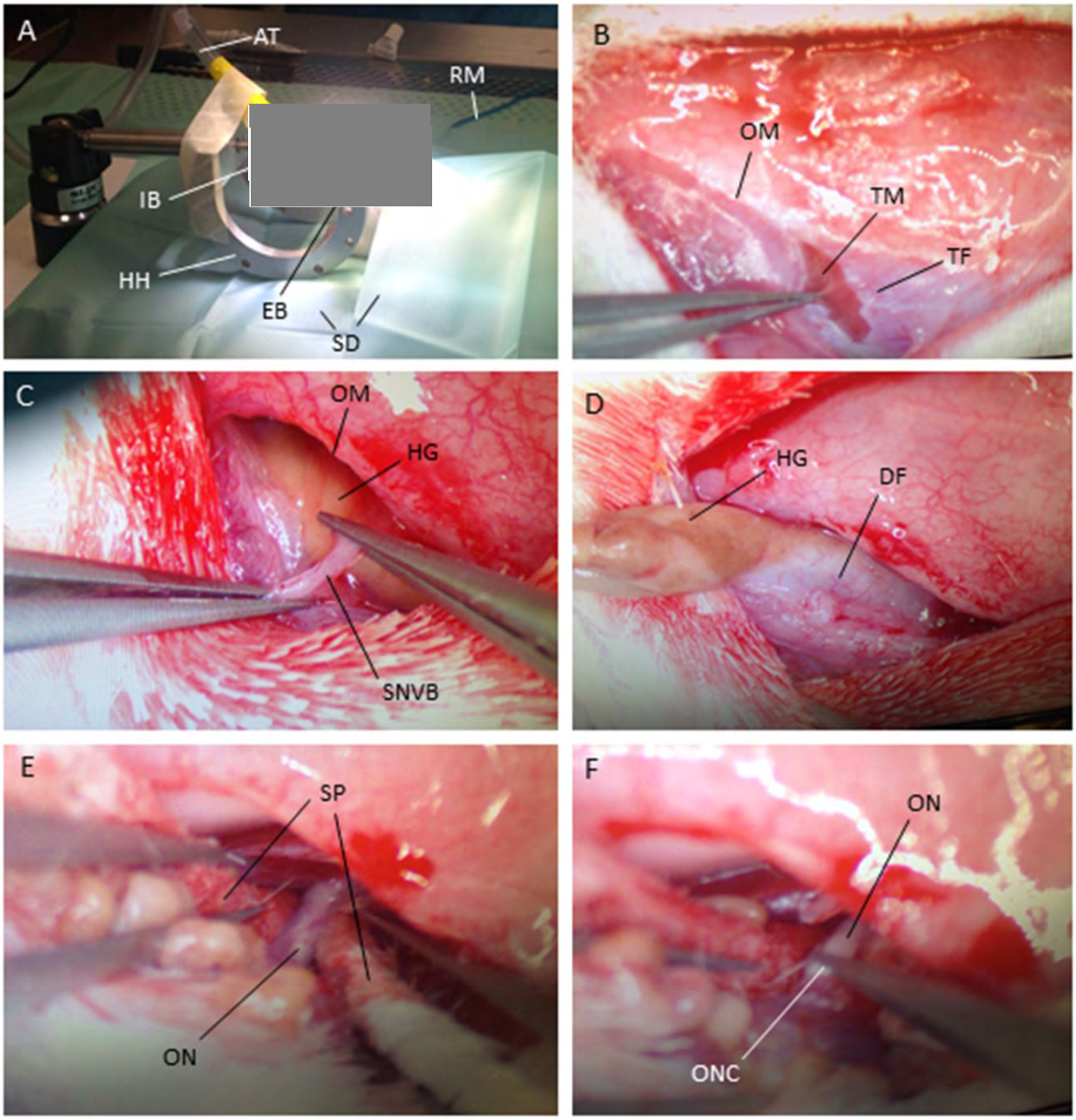


Figure 2.2: Optic nerve crush (ONC) procedure. (A) Operative set-up for animal surgery (AT, anaesthetic tube; EB, ear bar; HH, head holder; IB incisor bar; RM, respiratory monitoring; SD, sterile drapes). (B) Midline cutaneous incision and exposure of the orbital margin (OM), temporalis fascia (TF) and temporalis muscle (TM). (C) Identification and clamping of the superior orbital neurovascular bundle (SNVB) prior to division to expose the underlying superficial lobe of the Harderian gland (HG). (D) The superficial lobe of the Harderian gland (HG) is reflected rostrally to expose deep fascia (DF) covering the deep lobe of the Harderian gland, beneath which is the ON. (E) Tissues adjacent to the optic nerve (ON) are retracted with sterile paper (SP) to enable easy access to the ON. (F) The ON is exposed for the optic nerve crush (ONC) with fine forceps. See text for a full description of the ONC surgery.

2.3.4 Intravitreal injections

Intravitreal injections allow rapid local delivery of therapeutic substances to RGC and other cells of the retina, whilst minimising systemic absorption. Intravitreal injections were administered using glass micropipettes (produced in-house using glass capillary rods [Harvard Apparatus, Kent, UK] and a Flaming-Brown micropipette puller [Sutter Instruments, Novato, CA, USA]) inserted immediately posterior to the limbus. Care was taken to avoid damaging the lens. Animals underwent bilateral intravitreal injections (10µl/eye) of siRNA (20µg dissolved in sterile PBS) or PBS control, according to the treatment schedules prescribed for each eye, immediately after bilateral ONC, and then repeat injections were administered 8d and 16d after ONC. Treatment groups are described in the experimental Chapters.

2.3.5 Tissue preparation

At 24d after ONC, animals were killed by rising concentration of CO_2. After confirmation of death by cessation of respiratory or cardiac effort, each animal was transferred to a fume hood, placed supine, and a midline skin incision made from the abdomen to the neck. The jugular bulbs were identified and cut. The abdominal cavity was opened with surgical scissors and the diaphragm separated from the abdominal wall to expose the thoracic cavity. Pericardial adhesions were divided, and the descending thoracic aorta identified and clamped with an artery clip. The left ventricle was punctured and the animal perfused with PBS *via* a giving set until the blood exiting the jugular bulbs was clear, and then with 4% paraformaldehyde (PFA; TAAB, Reading, UK) until the animal was rigid. Eyes and ON were dissected from the head and post-fixed in 4% PFA for 2h. Tissue was washed in PBS for 10min, and subsequently cryoprotected sequentially in 10%, 20% and 30% sucrose solution in PBS for 24h each at 4°C. Tissue samples were embedded in Optimal Cutting Temperature medium

(Thermo Sandon, Runcorn, UK), frozen rapidly on dry ice and then stored at -80°C. Radial eye sections (10µm thick) and longitudinal ON sections (15µm thick) were cut using a cryostat (Bright Instrument Company, Huntingdon, UK), mounted on Superfrost Plus microscope slides (Fisher Scientific, Loughborough, UK) and stored at -20°C until analysis. Radial ocular sections taken through the ON head and ON sections that contained the ONC injury site were selected for analysis.

2.3.6 Immunofluorescence

Ocular and ON sections were analysed for RGC survival, axon regeneration, glial response and expression of specific antibody markers using immunohistochemistry.

2.3.6.1 Principles of immunofluorescence

Immunofluorescence techniques include immunohistochemistry and immunocytochemistry, which utilise specific antibodies to detect antigens of interest in tissue sections and cellular samples, respectively. Several variations in technique are described, but studies undertaken here utilised indirect immunofluorescence, in which specific primary antibodies with a high affinity and avidity for a target antigenic epitope bind specifically in the tissue or cell sample. A fluorophore-labelled secondary antibody, directed against the species from which the primary antibody was generated, is then used to detect the primary antibody by fluorescence microscopy. The specimen is illuminated with light at one wavelength, known as the excitation wavelength, which is absorbed by the fluorophore, which emits light at a longer wavelength, the emission wavelength (Lichtman and Conchello, 2005) (Figure 2.3). Immunofluorescence is highly specific, so detection of a signal enables correlation with its location in a particular tissue or cell; and is very sensitive, as multiple fluorophore-tagged secondary antibodies can bind to each primary antibody, thus amplifying the

fluorescence signal (Odell and Cook, 2013). Detection of multiple antigens is possible by incubating the sample with separate primary antibodies raised in different species, and then incubating with appropriate secondary antibodies tagged with different fluorophores, reactive at different wavelengths.

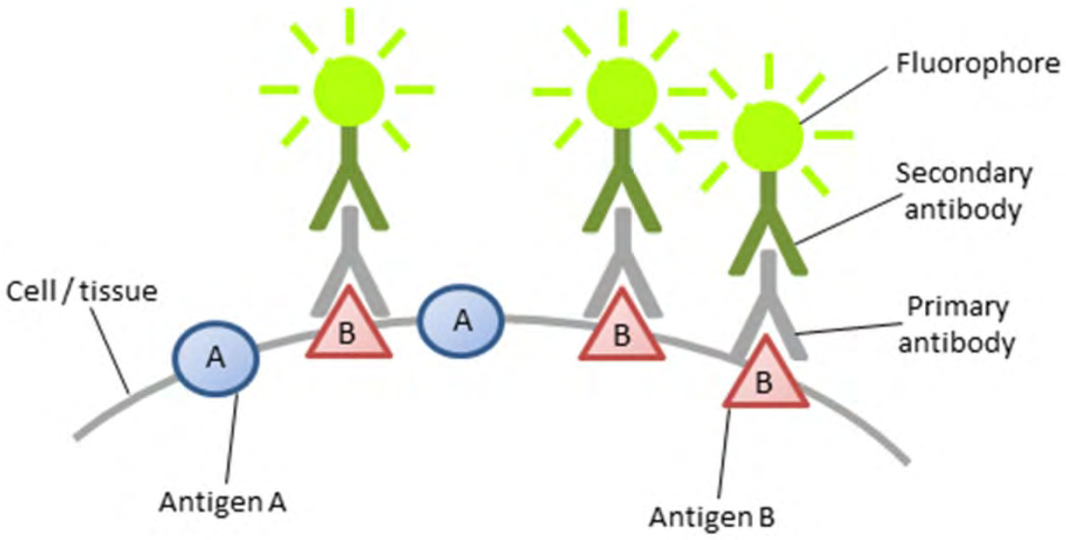


Figure 2.3: Principles of immunofluorescence. A specific primary antibody binds to the antigen of interest (Antigen B in the illustrated case), followed by binding of a fluorophore-labelled secondary antibody, specific to the species in which the primary antibody was raised. Upon illumination at the excitation wavelength, fluorescence at the emission wavelength is detected.

Successful immunofluorescence requires proper sample preparation and adherence to specific protocol steps to detect the target of interest with the maximum signal-to-noise ratio (Ramos-Vara, 2011). Although generally very specific for the target epitope, primary antibodies may bind weakly to 'reactive' sites on non-specific proteins with resemblance to the epitope of interest, resulting in 'background' staining which may mask identification of the true target. Incubation of the tissue/cellular sample with a suitable buffer that blocks the non-specific reactive sites is commonly

undertaken to reduce the background staining in immunofluorescence techniques. Examples of buffers that are used for this process include normal serum from the same species as the secondary (fluorophore-tagged) antibody and bovine serum albumin. Furthermore, the signal obtained from immunofluorescence may degrade over time with light exposure, known as 'photobleaching'. Samples can be protected for long-term use by using a mounting medium and coverslip, using only short exposure to as much fluorescent light as necessary when visualising samples, and storing samples in the dark when not in use (Ramos-Vara, 2011).

2.3.6.2 Immunohistochemistry protocol

Reagents used for immunohistochemistry are detailed in Table 2.1, and antibodies in Table 2.2. Retinal and ON sections for immunohistochemistry were allowed to thaw at room temperature for 30min. Sections were washed in rinsing buffer (RB) for 3 x 5min, excess RB was aspirated and the slides dried around the tissue. A hydrophobic pen (ImmEdge™, Vector Laboratories, Peterborough, UK) was used to draw around each section, to create a hydrophobic barrier to contain subsequent reagents in proximity to the tissue section and prevent leakage. Blocking buffer (BB) was applied (100µl/section) and sections were incubated in a humidified chamber for 1h at room temperature to eliminate non-specific protein binding and therefore minimise later background fluorescence. BB was removed and sections incubated with primary antibodies (100µl/section) in antibody diluting buffer (ADB) in a humidified chamber overnight at 4°C. Additional sections were prepared in the absence of primary antibody solution to act as negative controls. The following day, primary antibody solution was removed and sections washed 3 x 5min in RB. Appropriate secondary antibodies (100µl/section) in ADB were applied and sections incubated in a humidified chamber for 1h at room temperature in the dark to eliminate bleaching of the secondary antibody fluorophore. Slides were then washed in RB (3 x 5min), excess buffer removed, followed by cover-slip mounting using Vectashield® Mounting

Medium with DAPI (Vector Laboratories) and storage at 4°C before microscopic analysis. A detailed protocol for immunocytochemistry is described in section 2.5.

2.3.6.3 Fluorescence Microscopy

Tissue sections prepared as above were viewed under an upright Axioplan-2 fluorescence microscope (Carl Zeiss Ltd, Cambridge, UK) at x200 or x400 magnification. Photomicrograph images were captured with an AxioCam microscope digital camera (Carl Zeiss Ltd), with equal exposure time for all sections of 800ms for green and red channels, and 15-20ms for the blue (DAPI) channel. Unless otherwise stated, photomicrograph images were analysed with AxioVision SE64 4.9.1 software (Carl Zeiss Ltd).

Reagent	**Constituents**	**Supplier**
Phosphate buffered saline (PBS)	1 tablet[1] per 100ml Milli-Q water	[1]Oxoid, Basingstoke, UK
Rinsing buffer (RB)	0.1% Triton X-100[2] in PBS	[2]Sigma-Aldrich, Gillingham, UK
Antibody diluting buffer (ADB)	3% Bovine Serum Albumin (BSA)[3] in RB	[3]Sigma-Aldrich, Gillingham, UK
Blocking buffer (BB)	10% normal goat[4]/donkey[5] serum + 3% BSA in RB	[4]Vector Laboratories, Peterborough, UK [5]Sigma Aldrich, Gillingham, UK
Vectashield Mounting Medium with DAPI	Glycerol-based mounting medium containing 4', 6-diamidino-2-phenylindole (DAPI)	Vector Laboratories, Peterborough, UK

Table 2.1: Immunohistochemistry and immunocytochemistry reagents

	Antigen	Species	Dilution (IHC)	Dilution (ICC)	Supplier
Primary	β_{III}-tubulin	Mouse	1:500	1:200	Sigma (Poole, UK)
	Brn3a	Goat	1:250	-	Santa Cruz (Heidelberg, Germany)
	BDNF	Rabbit	-	1:100	Santa Cruz (Heidelberg, Germany)
	Calbindin	Mouse	-	1:200	Sigma (Poole, UK)
	CRALBP	Mouse	-	1:100	Abcam (Cambridge, UK)
	GAP-43	Mouse	1:500	-	Invitrogen (Paisley, UK)
	GFAP	Mouse	1:250	1:200	Sigma (Poole, UK)
	GSK3β	Rabbit	1:100	1:100	Cell Signalling (Hitchin, UK)
	Laminin	Rabbit	1:500	-	Sigma (Poole, UK)
	NT-3	Rabbit	-	1:100	Merck Millipore (Hertfordshire, UK)
	Phospho-CRMP2 (T514)	Rabbit	-	1:500	Abcam (Cambridge, UK)
	Phospho-GSK3β (S9)	Rabbit	-	1:100	Cell Signalling (Hitchin, UK)
	Phospho-MAP1B (Thr1265)	Rabbit	-	1:500	Merck Millipore (Hertfordshire, UK)
	Phospho-S6 (S235/236)	Rabbit	1:75	1:100	Cell Signalling (Hitchin, UK)
	Phospho-Smad1 (S187)	Rabbit	-	1:100	Abcam (Cambridge, UK)
	RTP801 (DDIT4)	Rabbit	1:100	1:100	Abcam (Cambridge, UK)
	S100β	Mouse	1:250	1:200	Sigma (Poole, UK)
Secondary	Goat IgG Fluor 488	Donkey	1:500	-	Molecular Probes (Paisley, UK)
	Mouse IgG Fluor 488	Goat	1:500	1:400	Molecular Probes (Paisley, UK)
	Rabbit IgG Fluor 594	Goat	1:500	1:400	Molecular Probes (Paisley, UK)
	Rabbit IgG Fluor 594	Donkey	1:500	-	Molecular Probes (Paisley, UK)

Table 2.2: Primary and secondary antibodies used in immunohistochemistry (IHC) and immunocytochemistry (ICC).

2.3.7 Quantification of *in vivo* responses

2.3.7.1 Quantification of RGC survival

Analysis of RGC survival was undertaken using a method described previously (Mead *et al.*, 2013). RGC were identified using the RGC phenotypic markers βIII-tubulin and Brn3a (Mead *et al.*, 2014; Nadal-Nicolas *et al.*, 2009; Nadal-Nicolas *et al.*, 2012) and counted in a 250μm linear strip of the ganglion cell layer (GCL) in radial sections either side of the ON head (Figure 2.4A, B). For each experimental group, RGC counts were undertaken in 4 radial sections/retina, from n=5

animals/treatment group where possible, and results expressed as the mean number of RGC/250µm GCL (±SEM). Initial *in vivo* studies of siRTP801 used βIII-tubulin as the RGC marker, which was later superseded with Brn3a, considered a more specific RGC marker (Nadal-Nicolas *et al.*, 2009; Mead *et al.*, 2014). Estimation of RGC numbers using Brn3a immunostained retinal sections detects quantitatively similar RGC loss compared to Brn3a-stained retinal whole-mounts or FluoroGold back-labelled retinal whole-mounts, whilst avoiding the additional animal surgery required for FG studies, and simplifying retinal analysis compared to whole-mount preparations, thereby reducing animal usage and associated costs (Mead *et al.*, 2014). Thus, the use of Brn3a immunostained retinal sections is a preferred method for RGC survival analyses, yielding reliable results.

2.3.7.2 Quantification of RGC axon regeneration

Quantification of RGC axon regeneration in longitudinal ON sections was undertaken using a method described previously (Lorber *et al.*, 2005). Composite ON images were constructed from individual x200 magnification ON sections using Photoshop CS3 (Adobe Systems Inc., San Jose, CA, USA). The ONC site was identified using laminin^{+} immunostaining of scar tissue and axon regeneration was quantified by counting the number of GAP43^{+} regenerating axons extending 100, 200, 400, 800 and 1200µm from the centre of the ONC toward the optic chiasm (Figure 2.4C). The cross-sectional width of the ON was measured at the point at which each axon count was taken, and used to calculate the number of axons/mm ON width. This value was then employed to derive Σ*ad*, the total number of axons extending distance *d* in an ON with radius *r* using the following formula as described by others (Berry *et al.*, 1996):

$$\Sigma ad = \pi r^2 \times \frac{\text{average number of axons/mm width}}{\text{section thickness (0.015mm)}}$$

Axon counts were undertaken in 3 sections/ON, from n=5 animals/treatment group. Use of GAP43 to label regenerating axons is considered the gold standard for quantification of RGC axon regeneration in the distal segment of the rat ON, as the number of $GAP43^+$ axons correlates with the number of axons detected using the anterograde tracer Rhodamine B (Vigneswara *et al.*, 2014), with the advantage of fewer surgical interventions in experimental animals to obtain axon regeneration data.

2.3.7.3 Quantification of retinal glial activation

Astrocytes in the GCL/nerve fibre layer and Müller glial processes and somata were detected using GFAP and S100β immunohistochemistry (Figure 2.4D, E). Radial retinal sections through the ON head were immnostained for GFAP, an activated astrocyte/Müller cell phenotypic antibody marker (Riechenbach, 2013; Pekny and Nilsson, 2005; Lorber *et al.*, 2012). The number of $GFAP^+$ Müller cell processes intersecting a 250µm horizontal sampling line passing through the inner plexiform layer (IPL) was counted at the mid-point between the inner nuclear layer (INL) and GCL (Figure 2.4D), in 4 sections/retina, n=5 animals/treatment group. Results were expressed as the mean number of $GFAP^+$ processes/250µm IPL (± SEM). Retinal sections were also immunostained for the S100β protein, expressed by both activated and quiescent astrocytes/Müller glia (Adami *et al.*, 2001; Zimmer *et al.*, 1995). The number of $S100\beta^+$ Müller glia somata in the INL was quantified along a 250µm sample line (Figure 2.4E) of 4 sections/retina, n=5 animals/group, and expressed as the mean number of $S100\beta^+$ Müller glia/250µm INL (± SEM).

2.3.7.4 Quantification of cellular detection of signalling mediators

In experiments in which the cellular detection of particular antibody markers was of interest, retinal sections were double immunostained for the cell phenoyptic marker (e.g. Brn3a for RGC) and the

signalling marker of interest (e.g. RTP801/pS6). Cell counts were undertaken as described above, and the cells co-expressing the signalling marker were identified and reported as a percentage (± SEM) of the cell population in the sample.

2.3.7.5 Quantification of immunostaining intensity

For comparison of immunostaining intensity between treatment groups, colour photomicrograph images of retinal sections were converted to black and white using ImageJ v1.45s software (National Institutes of Health, Bethesda, MA, USA) and threshold brightness set (determined by images of retinal sections in the absence of primary antibody) for use across sections from all experimental groups. Measurements of immunostaining intensity (pixel count integrated density [arbitrary units] ± SEM) were undertaken both on whole retinal sections (encompassing all retinal layers), and also in 250 x 40µm samples of the INL (containing Müller glia somata), in 4 sections/retina from n=5 animals/group.

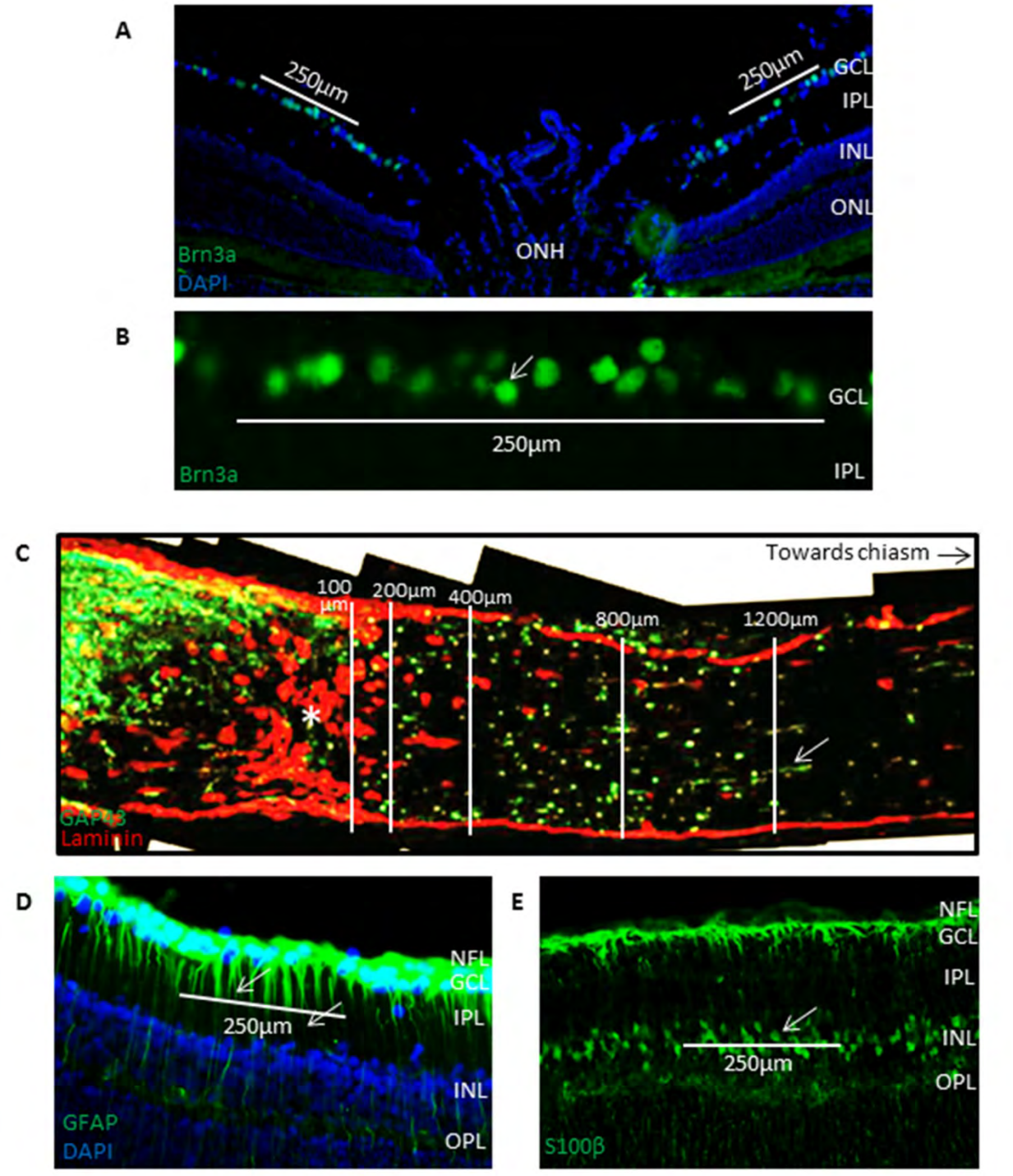


Figure 2.4: *In vivo* quantification techniques. (A) Radial retinal sections were obtained at the level of the ON head (ONH), and RGC counted in a linear 250µm sample of the GCL on either side of the ONH. (B) Higher magnification image of Brn3a$^+$ RGC (arrow) in the GCL. (C) Longitudinal ON section immunostained for laminin (red) to identify the ONC site (scar tissue, asterisk), and GAP43$^+$ regenerating axons (arrow) were counted at 100, 200, 400, 800 and 1200µm distal to the ONC site. (D) Quantification of GFAP$^+$ Müller glial processes (arrows) along a 250µm sample of the IPL in retinal sections. (E) Quantification of S100β$^+$ Müller glial somata (arrow) along a 250µm sample of the INL in retinal sections.

2.4 *IN VITRO* METHODS

2.4.1 Retinal cell culture

2.4.1.1 Principles of retinal cell culture studies

To investigate potential cellular mechanisms underlying the *in vivo* observations, studies on cultured retinal cells were undertaken. Mixed primary retinal cultures were prepared from adult rats by dissection of retinal tissue, which was then enzymatically dissociated and plated in appropriate media (Levin, 2005). Papain is considered superior to many other enzymes for dissociation of viable, intact postnatal neurons (Huettner and Baughman, 1986). Particular retinal cells, such as RGC, can be identified using a number of techniques, most commonly immunocytochemical detection of phenotypic antibody markers. Whilst the anatomical arrangement of RGC and supporting cells in culture is not maintained, dissociation of mixed retinal cells *in vitro* enables the neuronal and glial diversity to be maintained. Cell culture studies enable precise control of the cellular exposure to chemical factors, pharmacological agents and changes in the extracellular milieu, and enable study of the interactions of a variety of cell types. Furthermore, by controlling the cell culture medium, multiple conditions can be investigated in parallel in the same experiment, which is much more challenging *in vivo*. Retinal cultures are commonly used for the study of RGC neuroprotection and regeneration, as RGC in culture can regenerate axonal processes in culture (Lilley and Robbins, 2005; Wigley and Berry, 1988; Romano and Hicks, 2007). However, in order to facilitate the extension of axonal processes *in vitro*, neurons must be cultured on a growth permissive substrate, of which laminin is considered optimal (Manthorpe *et al.*, 1983; Bahr *et al.*, 1988). It is often not possible in culture to determine whether neuronal projections are axons or dendrites, and so the term ‘neurites’ is commonly used to refer to all neuronal extensions.

2.4.1.2 Retinal cell culture protocol

Retinal tissues from adult rats were dissociated into single cells using a Papain Dissociation System (Worthington Biochemicals, Lakewood, NJ, USA) in accordance with the manufacturer's instructions. Unless otherwise specified, all reagents used were provided with the kit. Animals were killed with rising concentration of CO_2, eyes were dissected and then washed in sterile Dulbecco's phosphate buffered saline (dPBS, Sigma). Corneal and iris tissues were removed by dissection around the limbus with microscissors, followed by lens and vitreous removal with microforceps. Retinal tissue was dissected from the scleral cup, and the retinae from both eyes of each animal were placed in a vial with 1.25ml sterile Earle's Balanced Salt Solution (EBSS) with bicarbonate and phenol red, containing 20 units/ml papain, 1mM L-cysteine with 0.5mM EDTA, and 0.005% deoxyribonuclease I (DNase I), and slightly minced in the vial with scissors. Vials were then equilibrated with 95% O_2:5% CO_2 in a humidified incubator at 37°C for 90min. After incubation, the mixture was gently triturated with a 10ml pipette, filling and emptying the pipette at a rate of approximately 5ml/sec. This step served to break up the retinal tissue fragments in the dissociation mix to enable a high yield of cells. The cell suspension was removed, placed in a 15ml tube, and centrifuged at 300 x g for 5min at room temperature. The supernatant was discarded and the cell pellet immediately re-suspended in a solution containing 1.35ml EBSS, 150µl reconstituted albumin ovomucoid inhibitor (AOI; ovomucoid protease inhibitor with bovine serum albumin, vial reconstituted with 32ml EBSS to yield a solution of containing 10mg/ml ovomucoid inhibitor and 10mg/ml albumin) and 75µl DNase I. A discontinuous density gradient was prepared by adding 2.5ml AOI solution to a 15ml tube and carefully layering the cell suspension on top. This tube was centrifuged at 70 x g for 6min at room temperature. This step served to pellet the dissociated cells at the bottom of the tube, with membrane fragments remaining at the interface of the two solutions. The supernatant was discarded and the cell pellet immediately re-suspended in 1ml supplemented Neurobasal-A (sNBA) culture

medium solution (24.2ml Neurobasal-A medium, supplemented with 500µl B27 supplement, 62.5µl L-glutamine [200mM] and 125µl gentamicin [all from Life Technologies Ltd, Paisley, UK]). Neurobasal-A is a serum-free culture medium formulated for culture of neuronal cells and B27 is a serum-free supplement used to support the growth and maintenance of neurons and glia in culture (Brewer, 1995). L-glutamine is an essential amino acid for cell culture, but is unstable at physiological pH and therefore is added to culture medium as a supplement immediately before use (Pasieka and Morgan, 1959); gentamicin is an effective antibiotic widely used in cell culture (Fischer, 1975).

To quantify the yield of dissociated cells for each animal, 25µl of cell suspension was added to an Eppendorf tube with an equal volume of the indicator dye trypan blue. Cells absorbing trypan blue become stained blue and are considered non-viable (Strober, 2001). This cell suspension-trypan blue solution was mixed and a 10µl aliquot of this solution immediately added to each side of a cell counting chamber (haemocytometer) under a coverslip. The number of viable (unstained) cells in the central $1mm^2$ area of the haemocytometer was counted (Figure 2.5), and then the cell count repeated for the second counting chamber. The cell yield was calculated as follows:

$$C = N \times 2 \times 10^4$$

where C = cells/ml

N = average cell count of two counting chambers

2 = multiplication factor to account for dilution of cell suspension with trypan blue

10^4 = volume conversion factor for $1mm^2$ counting area on haemocytometer

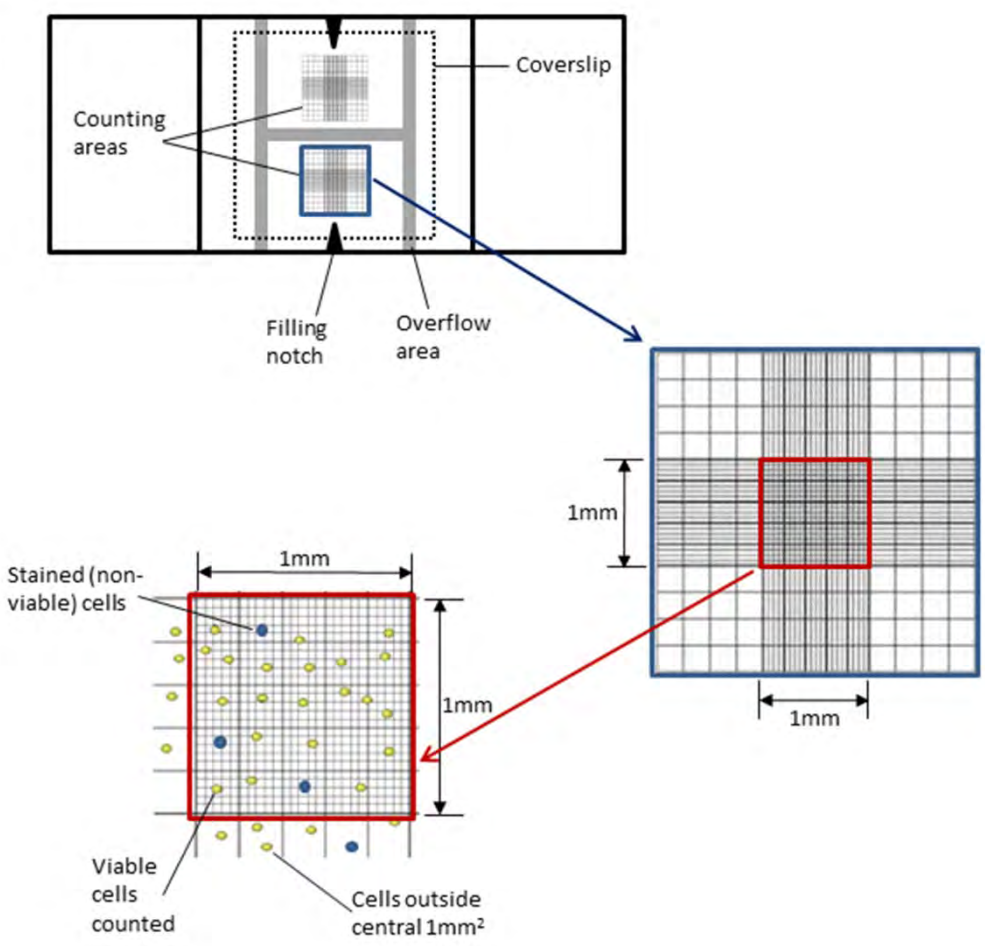


Figure 2.5: Quantification of the yield of cells obtained in retinal cell culture studies, before siRNA transfection/treatment. Cell suspension-trypan blue solution was added to each side of a haemocytometer (blue square) and cells counted in the central 1mm^2 counting area (red square). Viable cells are unstained and counted, whereas cells taking up trypan blue are non-viable and not counted. Cell counts obtained in this way enabled seeding of 125000 cells/well for *in vitro* studies.

Dissociated retinal cells were plated at a density of 125000 cells/well, at a final volume of 300µl/well in 8-well chamber slides (BD Biosciences, Erembodegem, Belgium). Chamber wells were pre-coated with 150µl poly-D-lysine (100µg/ml) for 1h, washed x 3 with sterile dPBS and then coated with 150µl laminin (20µg/ml). Laminin was removed and chamber wells washed with sterile PBS immediately prior to addition of cell culture medium. Chamber slides containing dissociated retinal cells were

incubated at 37°C/5% CO_2 overnight before siRNA transfection or other treatment. For a typical adult rat (2 retinae) used, average cell count was routinely approximately 100 cells/mm^2, corresponding to approximately 2000000 cells/ml. This enabled plating of 16 wells per animal for cell culture studies. Of the total retinal cell population present in the cultures, approximately 1% were RGC (~1250 RGC/well), with the remainder a mixture of interneurons, astrocytes, Müller glia, endothelial cells and fibroblasts (Suggate *et al.*, 2009).

Experiments described in Chapters 4 and 5 included investigation of siRNA effects in the presence of $GFAP^+$ activated retinal glia, which are not present in cultures prepared from uninjured, intact animals (see Chapter 3). To prepare cultures containing activated retinal glia, rats underwent bilateral ONC (as per Section 2.3.3) and were subsequently killed after 5d, at which point retinal cultures were prepared as described above. Retinal cultures established 5d after ONC contain $GFAP^+$ glia, but significant RGC death has not yet occurred (Ahmed *et al.*, 2010; Lorber *et al.*, 2008; Lorber *et al.*, 2012; Vigneswara *et al.*, 2014).

2.4.2 siRNA transfection

Retinal cultures were transfected with siRNA after incubation for 24h at 37°C/5% CO_2 as described above. The cationic liposomal transfection reagent Lipofectamine™ 2000 (Invitrogen, Paisley, UK) was used to transfect retinal cells *in vitro*, in accordance with the manufacturer's protocol (Figure 2.6), and as described previously (Suggate *et al.*, 2009). Transfections were undertaken using Opti-MEM® I Reduced Serum Medium (Invitrogen) to dilute siRNA/Lipofectamine, with a final transfection volume of 200µl/well.

A working stock solution of 10µM siRNA was prepared by dilution of 1µl primary siRNA stock solution (20µg/µl) in 160µl Opti-MEM. The treatment concentration of siRNA for particular wells depended on the individual experiments, as described in experimental Chapters, and was prepared by dilution of the working stock solution in Opti-MEM, sufficient for 100µl/well. The siRNA solution was gently mixed and left to stand for 5min at room temperature. During this time, Lipofectamine™ 2000 transfection reagent was prepared by diluting 2µl/well in 98µl/well Opti-MEM, and was also left to stand for 5min at room temperature. The Lipofectamine solution was then combined with the siRNA solution, giving a combined solution sufficient for 200µl/well, and was gently mixed by pipetting up-and-down and then stood for 20-25min at room temperature to enable Lipofectamine-siRNA complex formation. After this incubation, the sNBA culture medium was removed from the wells of the culture slides by gentle pipette aspiration and the Lipofectamine-siRNA complex solution added at 200µl/well. Cultures were incubated at 37°C/5% CO_2 for 5h for transfection to occur, and then sNBA culture medium was added to wells to a final volume of 500µl/well. After transfection, cultures were incubated at 37°C/5% CO_2 for a further 3d prior to analysis. Treatment siRNAs used were targeted against RTP801 (Chapters 3-5) and GSK3β (Chapter 5), and a control siRNA (siEGFP) was also used. Sham transfection with Lipofectamine™ 2000 combined with Opti-MEM/sNBA in the absence of siRNA acted as a negative control, and untreated (sNBA alone) wells were also used. All *in vitro* experiments comprised 2-3 wells/treatment condition (technical replicates) from at least 3 independent animals (biological replicates) (Lazic, 2010; Cumming *et al.*, 2007).

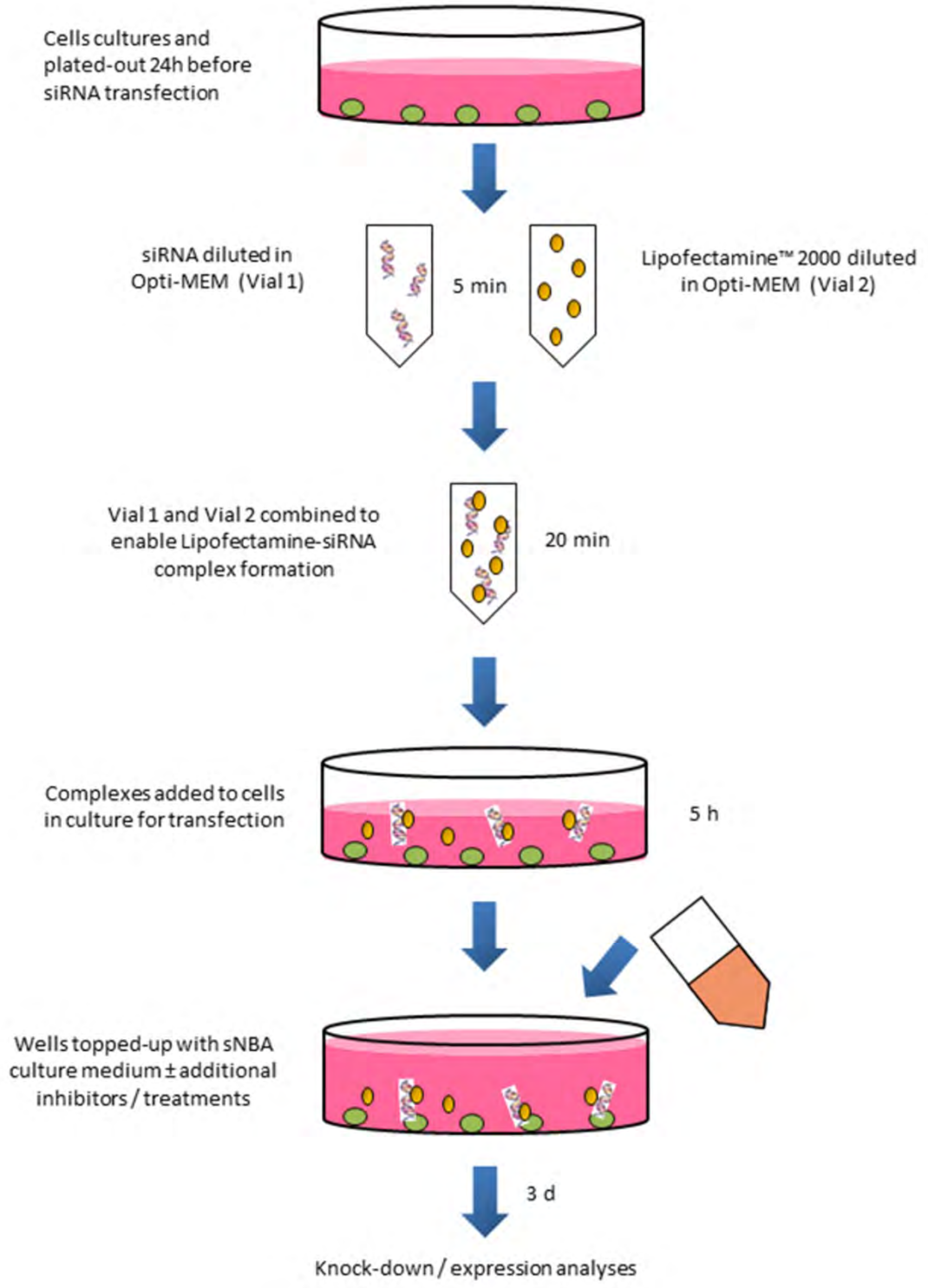


Figure 2.6: Transfection of retinal cultures with siRNA. Cultured cells are incubated for 24h before transfection. siRNA and Lipofectamine transfection reagent are prepared in Opti-MEM in separate tubes, and then combined to enable complex formation. siRNA-Lipofectamine complexes are added to the cell culture wells and left for 5h to transfect cells. After the transfection period, wells are topped-up with culture medium ± any additional inhibitors or treatments as per the experimental protocol. Treated cultures are incubated for 3d before analysis.

2.4.3 Treatment of retinal cultures with inhibitors

In certain experiments, retinal cell cultures were treated with specific cell signalling inhibitors. Specific preparation steps for individual inhibitors used are described below. Inhibitors were prepared during the siRNA transfection period and added to culture wells at the end of the 5h incubation.

2.4.3.1 Rapamycin

The mTORC1 inhibitor Rapamycin (Merck Millipore, Watford, UK) was administered at a treatment concentration of 10nM, in accordance with previous reports (Codeluppi *et al.*, 2009; Li *et al.*, 2015), in a final volume of 500µl/well. Rapamycin was provided as 1mg powder (molar mass 914.2) and prepared as a 1.1mM stock solution in 1000µl DMSO. As there was already 200µl/well transfection solution present, the treatment concentration of 10nM Rapamycin was prepared by dilution of 4.5µl Rapamycin stock solution in 300µl/well sNBA and added to wells at the end of the 5h transfection period.

2.4.3.2 K252a

The pan-Trk receptor antagonist K252a (Merck Millipore) was administered at a treatment concentration of 50nM, in accordance with previous studies (Mead *et al.*, 2013; Gao *et al.*, 2003; Douglas *et al.*, 2009) in a final volume of 500µl/well. K252a was supplied as a powder (100µg, molar mass 467.5) and prepared as a stock solution of 210µM in 1000µl DMSO. To attain the treatment concentration, a 500nM working stock solution was prepared by dilution of 2.4µl stock solution in 1000µl sNBA. As there was already 200µl/well transfection solution present, the treatment

concentration of 50nM K252a was prepared by dilution of 50µl working stock solution in 300µl/well sNBA and added to wells at the end of the 5h transfection period.

2.4.3.3 Chir99021

Experiments described in Chapter 5 investigated the effects of the GSK3β inhibitor 6-((2-((4-(2,4-Dichlorophenyl)-5-(4-methyl-1H-imidazol-2-yl)pyrimidin-2-yl)amino)ethyl)amino)nicotinonitrile (Chir99021, an ATP-competitive GSK3β inhibitor; Cambridge Bioscience Ltd, Cambridge, UK) on RGC survival and neurite growth *in vitro*. A dose-response assay was performed initially (see Chapter 5 for details), with further investigation using the optimal concentration as determined from the dose-response study. Chir99021 was supplied as a 5mg powder (molar mass 465.34) and prepared as a stock concentration of 10mM in 1074.5µl DMSO. Working stock solutions of 1mM and 10µM were prepared by addition of 200µl stock to 1800µl sNBA (1mM working stock), and then addition of 10µl of 1mM working stock to 990µl sNBA (10µl working stock). Chir99021 test concentrations of 30nM (0.03µM), 300nM (0.3µM), 3µM, 30µM and 300µM were prepared from the working stock solutions, in final volumes of 500µl/well. Addition of Chir99021 treatment to retinal cells *in vitro* was not administered in the presence of siRNA. Treatment was added to wells after the initial preparation of retinal cultures and overnight incubation as described above.

2.4.4 Preparation of retinal cultures in the presence of Nogo growth-inhibitory substrate

To evaluate the RGC neuroprotective and neurite-growth effects of certain test reagents in the presence of growth-inhibitory ligand (see Chapter 5), retinal cultures were prepared as described above, and treated with recombinant Nogo-P4 peptide (Alpha Diagnostics, San Antonio, TX, USA). Nogo-P4 peptide was added to wells at a concentration of 25µM in a final volume of 500µl/well. This

dose has been shown previously to be effective at inhibiting neurite outgrowth whilst not showing any RGC toxic effect (J O'Neill, University of Birmingham, unpublished observations). Nogo-P4 peptide was supplied as a 1mg powder (molar mass 2885) and prepared as a 347µM stock solution in 1000µl DMSO. As there was already 200µl/well transfection solution present, the inhibitory substrate of 25µM Nogo-P4 peptide was prepared by dilution of 36µl stock solution in 300µl/well sNBA and added to wells at the end of the 5h siRNA transfection period.

2.5 IMMUNOCYTOCHEMISTRY

Principles of immunofluorescence are described in section 2.3.6.1. Buffers/reagents used for immunocytochemistry are listed in Table 2.1 and antibodies used are listed in Table 2.2.

After incubation of retinal cultures for 3d, the culture medium was carefully removed from wells of the tissue culture slides by pipetting. For experiments where study of conditioned culture medium was required, the removed medium was transferred to an Eppendorf tube and stored at -20°C until further analysis. In order to fix the retinal cells to the microscope slide, 4% PFA (500µl/well) was added to each well and incubated at room temperature for 10min. The fixative was then removed and wells washed with rinsing buffer (RB) 3 x 5min. Blocking buffer (BB) was added to each well (150µl/well) and incubated at room temperature for 30min to reduce non-specific antibody binding. After removal of the BB, primary antibodies diluted to the relevant concentration in antibody diluting buffer (ADB) were added to each well (150µl/well) and incubated for 1h at room temperature. Primary antibody solution was removed, wells washed 3 x 5min with RB, and then secondary antibodies diluted in ADB were added to each well (150µl/well) and incubated for 1h at room temperature in the dark to prevent fluorophore bleaching. Secondary antibody solution was removed by pipetting and wells washed 3 x 5min with RB. The well dividing walls were removed from

the culture slides and coverslips mounted with Vectashield Mounting Medium with DAPI. Slides were stored in the dark at 4°C until fluorescence microscopy.

2.6 QUANTIFICATION OF RETINAL CULTURES

Immunostained retinal culture slides were viewed under an upright Axioplan-2 fluorescence microscope (Carl Zeiss Ltd, Cambridge, UK) at x200 magnification, and photomicrograph images captured with an AxioCam microscope digital camera and analysed with AxioVision SE64 4.9.1 software (both Carl Zeiss). Each well was divided into 9 equal squares, and four random photomicrographs were captured in each of the 9 grid squares, giving a total of 36 images/well (Figure 2.7).

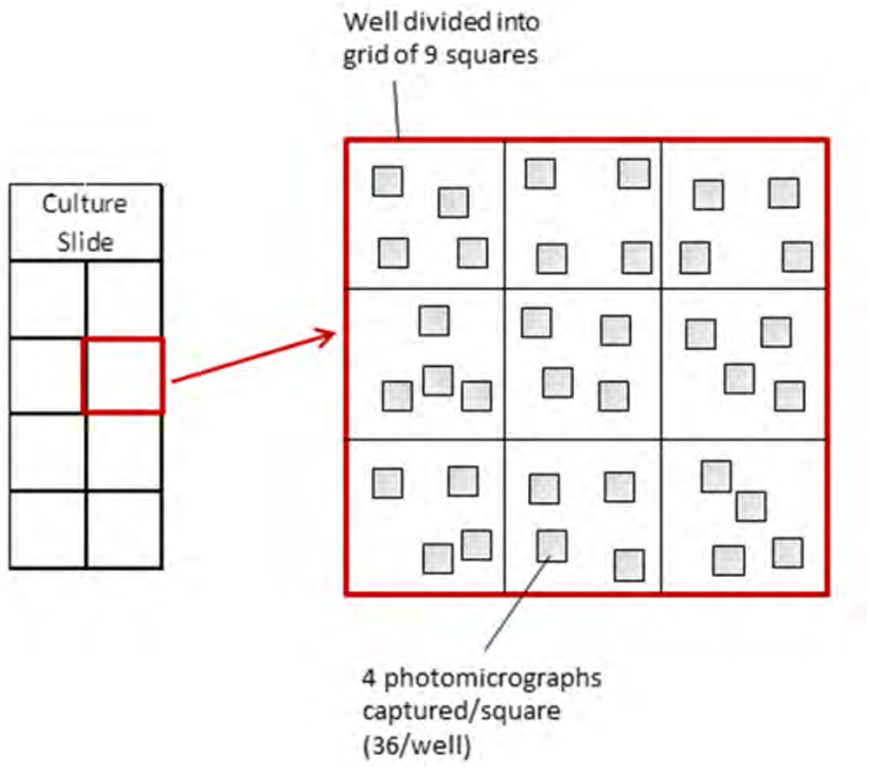


Figure 2.7: Quantification of retinal cultures. Each well of the culture slide (red square) was divided into 9 equal regions. Four photomicrographs were captured in each region, giving a total of 36 images/well. Cells of interested were counted in the photomicrographs obtained, and estimates of total cell number calculated (see text for details).

2.6.1 Quantification of RGC survival

Surviving RGC were identified by βIII-tubulin$^+$ immunostaining (Figure 2.8). RGC typically have somata larger than 10-12µm in diameter (Guenther *et al.*, 1994; Lilley and Robbins, 2005), enabling RGC to be identified from any other βIII-tubulin$^+$ cells in culture. The advantage of using βIII-tubulin rather than the more specific RGC marker Brn3a for RGC analyses *in vitro* is that whereas Brn3a is expressed only in RGC nuclei, βIII-tubulin immunostaining also permits visualisation of RGC neurites, enabling both survival and neurite outgrowth analyses to be undertaken in the same setting. RGC counts were undertaken in each of the 36 images/well and RGC survival was determined from these samples. The area captured by a single (x200 magnification) photomicrograph was 0.2475 mm^2 (550µm x 450µm) and the surface area of each well of the 8-well chamber slides was 69mm^2. The number of βIII-tubulin$^+$ RGC observed in 36 images/well (8.91 mm^2) was therefore multiplied by 7.74 to give an estimate of the total number of surviving RGC/well. RGC survival results for each treatment group were presented as the mean number of βIII-tubulin$^+$ RGC/well (± SEM).

2.6.2 Quantification of RGC neurite outgrowth

Quantification of RGC neurite outgrowth in retinal cultures was made by assessment of two parameters: (1) neurite outgrowth initiation, and (2) neurite elongation.

2.6.2.1 Quantification of neurite outgrowth initiation

The number of βIII-tubulin$^+$ RGC extending at least one neurite was evaluated in the photomicrographs obtained of each well. Neurites were classified as cytoplasmic extensions originating at the cell body, and extending for a length equivalent to at least the diameter of the

soma (Figure 2.8). The proportion of neurite-bearing RGC was determined as a percentage of the total number of βIII-tubulin$^+$ RGC. RGC neurite outgrowth initiation results for each treatment group were presented as the proportion (%) of RGC extending neurites (mean ± SEM).

2.6.2.2 Quantification of neurite outgrowth elongation

The longest neurite extending from each RGC was measured using Image Pro 6.2 (Media Cybernetics, Bethesda, MD, USA) and the average length of longest neurite determined from all neurite-bearing RGC identified in the images captured for each well. RGC neurite elongation results for each treatment group are presented as the mean length of longest neurite (± SEM).

2.6.3 Quantification of retinal astrocytes and Müller glia

Retinal astrocytes and Müller glia were identified in culture by immunocytochemistry for the phenotypic antibody markers GFAP (Figure 2.8E) and S100β. The total number of glia/well was determined by counting the number of GFAP$^+$ or S100β$^+$ cells in each photomicrograph obtained for each well, and multiplying the cell count by the multiplication factor 7.74, as described for quantification of RGC survival.

2.6.4 Quantification of cellular signalling markers in RGC and glia

In experiments where the detection of signalling pathway markers in RGC was of interest (for example RTP801, pS6, GSK3β), the number of βIII-tubulin$^+$ RGC co-expressing the relevant marker was evaluated in the photomicrographs obtained of each well. Quantification was determined as a proportion of the total number of βIII-tubulin$^+$ RGC. Quantification of signalling pathway markers in

glia was estimated as the proportion of $GFAP^+$ or $S100\beta^+$ cells co-localising the relevant marker in the photomicrographs obtained of each well.

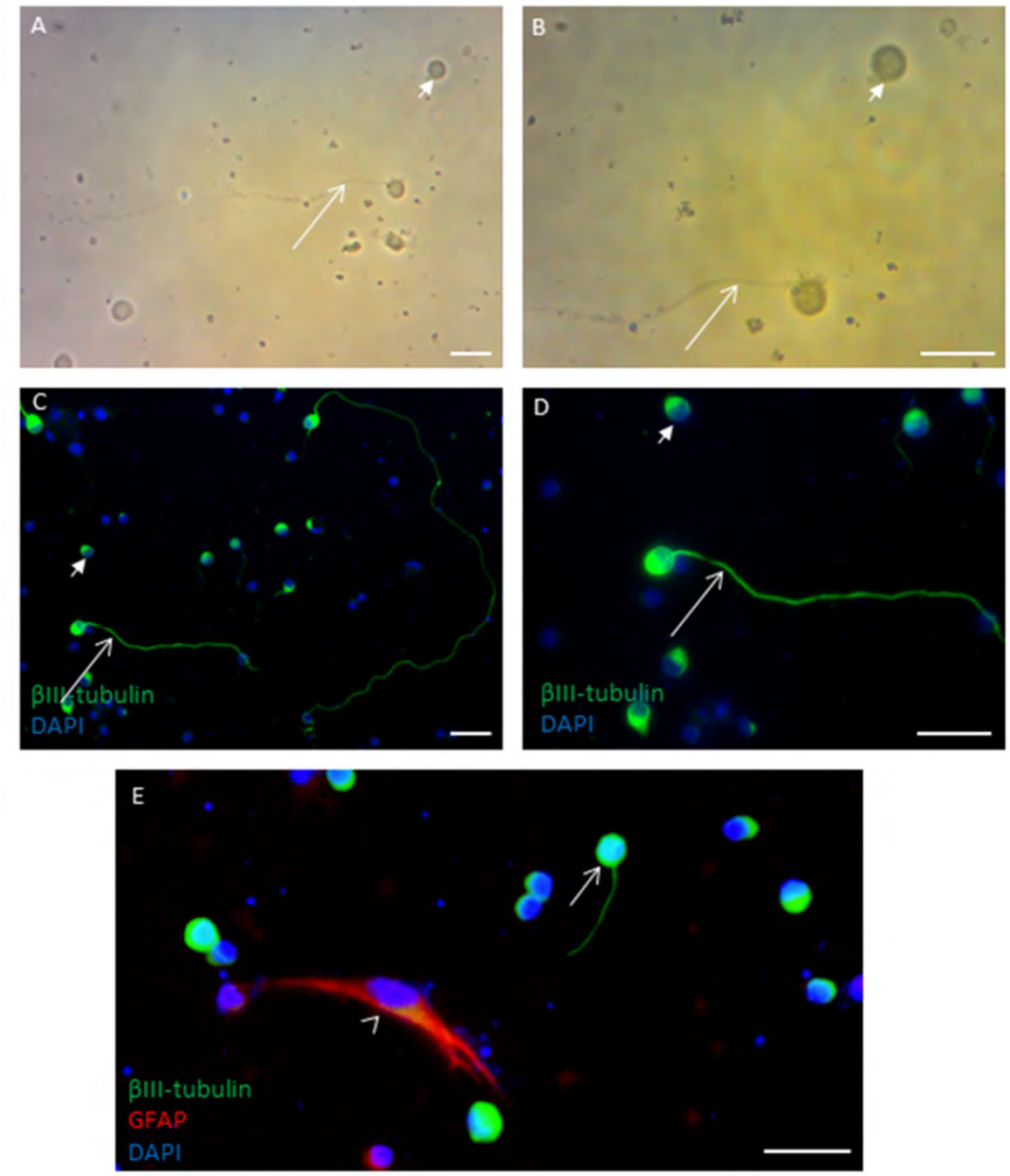


Figure 2.8: Identification of retinal cells in culture. (A) Light microscopy of dissociated primary retinal cells in culture, demonstrating RGC with neurite (long arrow) and RGC without neurite (short arrow). (B) Higher magnification of light microscopy image shown in (A). (C) Fluorescence microscopy image of retinal cells in culture (note: a different field compared to (A) and (B)), demonstrating βIII-tubulin$^+$ RGC with neurite (long arrow) and without neurites (short arrow), with DAPI as a nuclear counterstain. (D) Higher magnification view of image shown in (C). (E) Fluorescence microscopy image of glial-activated retinal cultures, demonstrating the presence of βIII-tubulin$^+$ RGC (arrow) and $GFAP^+$ activated glial cell (astrocyte/Müller cell, arrowhead). Scale bar = 20nm in all images.

2.7 ENZYME LINKED IMMUNOSORBENT ASSAY (ELISA)

2.7.1 Principles of ELISA

ELISA is a commonly utilised technique for the detection and quantification of an antigen in solution. In ELISA, the antigen to be measured is immobilised to a solid surface, and subsequently bound to a detection antibody that is linked directly or indirectly to an enzyme. Detection and quantification of the antigen is achieved by measuring the conjugated enzyme activity, *via* addition of a substrate solution to produce a measurable outcome (Crowther, 1995).

ELISA experiments undertaken in this study were designed to detect and quantify the presence of NTF in culture medium after treatment of retinal cultures with siRNA. Whilst several variations in technique have been described, the ELISA studies reported here used the 'sandwich ELISA' technique (Figure 2.9A). In this format, a 96-well plate is coated with a 'capture' antibody, specific for the antigen of interest to be quantified. The test solution is then added to the well and any antigen in the solution binds to the capture antibody. A 'detection' antibody is then added, which binds to the captured antigen, and then a tertiary antibody is added which is conjugated to an enzyme. Unbound conjugate is removed by washing and then a chromogenic substrate is added to the well and the colour change measured, with the intensity of the colour change proportional to the amount of antigen present in the test solution (Crowther, 1995). Quantitative results are obtained by comparison to a standard curve, generated by a serial dilution of a known quantity of purified antigen.

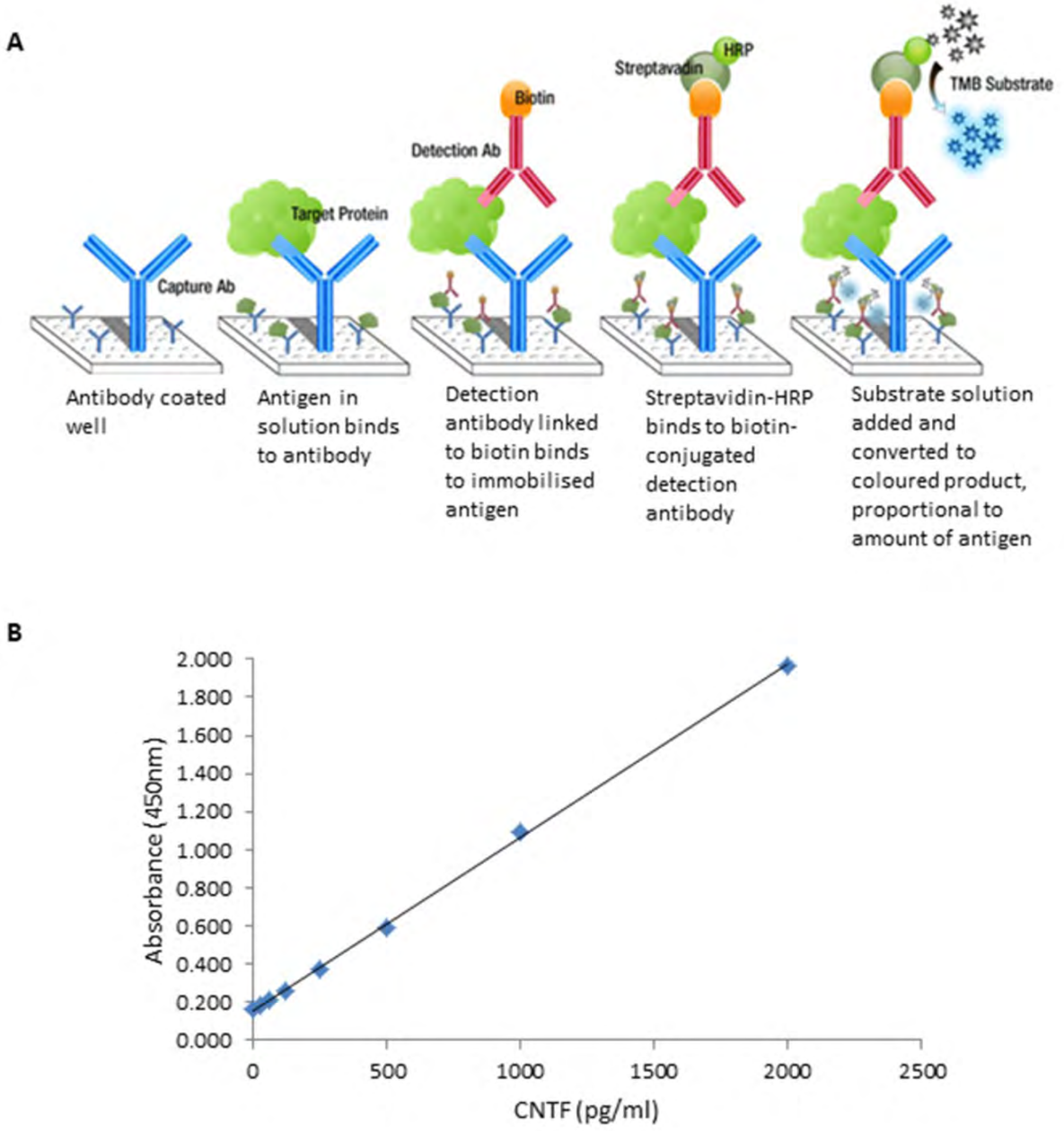


Figure 2.9: Enzyme linked immunosorbent assay (ELISA). (A) Principles of 'sandwich' ELISA. Image adapted from http://www.epitomics.com/images/products/sandwich.jpg (accessed 2 July 2015). (B) Standard curve for ELISA analysis, plotting absorbance (y-axis) against known concentration of standard (x-axis), and depicting a linear relationship. The concentration of antigen (e.g. neurotrophic factor) in a particular sample is determined from the measured absorbance (note dilution factor calculation required).

2.7.2 ELISA protocols

Reagents and buffers used for ELISA are documented in Tables 2.3, 2.4 and 2.5.

To obtain titres for the range of NTF of interest, three different brands of ELISA kit were utilised. ELISA kits to assay for rat-specific CNTF, NGF, NT-3 and GDNF were obtained from R & D Systems (Abingdon, UK) and the protocols were identical. ELISA kits to assay for rat BDNF (Promega UK, Southampton, UK) and pigment epithelial derived factor (PEDF; Millipore UK Ltd, Watford, UK) were different and described separately.

2.7.2.1 CNTF (and NGF, NT-3 and GDNF) ELISA

The ELISA protocol was performed according to the manufacturer's instructions, and the identical protocol was also followed for NGF, NT-3 and GDNF assays. Capture antibody was prepared to the working concentration (2µg/ml) in PBS and 100µl added to coat each well of a sterile 96-well plate (Scientific Laboratory Supplies, Nottingham, UK). The plate was then sealed with Parafilm sealing film (Fisher Scientific, Loughborough, UK) and incubated overnight at room temperature. The next morning, each well was aspirated and washed x 3 with wash buffer (WB), approximately 400µl/well, with a Bio-Plex Pro Wash Station automated plate washer (Bio-Rad Laboratories Ltd., Hemel Hempstead, UK). After the last wash, remaining WB was removed by inverting the plate and blotting it against clean absorbent paper. To prevent non-specific binding, the plate was blocked with 300µl/well Reagent Diluent (RD), and incubated for 1h at room temperature, before the aspiration/wash step was repeated using the automated plate washer. During the blocking period, the standards and samples were prepared, and then added to the plate (100µl/well) after the last wash step. To prepare the standards, the vial of recombinant CNTF was first reconstituted with 0.5ml

RD, giving a solution of 110ng/ml, which was allowed to sit for minimum of 15min with gentle agitation before making dilutions. The stock solution was diluted in RD to a working high standard of 2000pg/ml, and then a series of 1:2 dilutions undertaken to create a seven-point standard curve (i.e. 1000, 500, 250, 125, 62.5 and 31.25 pg/ml). The last well of the standard column was RD only (0 pg/ml standard). To prepare samples, each was initially diluted 1:2 in RD, to ensure that the detected concentration would fall within the standard curve generated by the standards. Serial 1:2 dilutions of the samples were then undertaken, and added to the plate. The plate was then sealed with Parafilm and incubated on a shaker at approximately 150rpm for 2h at room temperature. The aspiration/wash step was repeated with the automated plate washer, and then 100µl/well detection antibody was added to the plate, covered again with Parafilm and incubated for a further 2h at room temperature on a shaker. The aspiration/wash step was repeated with the automated plate washer, and then 100µl/well working concentration of Streptavidin-HRP was added. The plate was sealed again, incubated for 20min at room temperature away from direct light, and the aspiration/wash step subsequently repeated. Substrate solution (100µl/well) was then added, and the plate incubated for 20 min at room temperature away from direct light. At this point, a blue colour formed in standard and sample wells in proportion to the amount of detected protein. After this incubation, stop solution (50µl/well) was applied and the plate tapped gently to ensure thorough mixing. The blue colour turned yellow upon acidification. The optical density of each well was determined immediately, using a Victor 3 1420 Multilabel Plate Counter microplate reader (PerkinElmer, Buckinghamshire, UK) set to 450nm absorbance. Data were then analysed as described below.

2.7.2.2 BDNF ELISA

The ELISA protocol was performed according to the manufacturer's instructions. Capture antibody was prepared in carbonate coating buffer and 100µl added to coat each well of a sterile 96-well

plate. The plate was then sealed with Parafilm and incubated overnight at 4°C. The next morning each well was aspirated and washed x 3 with wash buffer (WB), approximately 400µl/well, with an automated plate washer. After the last wash step, remaining WB was removed by inverting the plate and blotting it against clean absorbent paper. To prevent non-specific binding, the plate was blocked with 200µl/well Block & Sample 1X Buffer (BSB), and incubated for 1h at room temperature, before the aspiration/wash step was repeated using the automated plate washer. During the blocking period, the standards and samples were prepared, and then added to the plate (100µl/well) after the last wash step. To prepare the standards, the vial of BDNF standard was first diluted 1:2000 in BSB to achieve a concentration of 500pg/ml. To do this, 10µl of undiluted standard was transferred into 390µl BSB (1:40 dilution), then 10µl of this solution was transferred into 490µl BSB (1:50 dilution), resulting in 1:2000 dilution of the standard. Next, 200µl diluted BDNF standard was added to the first well of two columns of the 96-well plate, immediately followed by serial 1:2 dilutions in BSB down the plate in the columns designated for the standard curve, generating a seven-point standard curve (500, 250, 125, 62.5 and 31.25, 15.6, 7.8 pg/ml). The last well of the standard column was BSB only (0pg/ml BDNF standard). To prepare the samples, each sample was initially diluted 1:4 in BSB, to ensure that the detected concentration would fall within the standard curve generated by the standards. Serial 1:2 dilutions of the samples were then undertaken, and added to the plate. The plate was then sealed and incubated on a shaker at approximately 150rpm for 2h at room temperature. The aspiration/wash step was repeated with the automated plate washer, and then 100µl/well detection antibody was added to the plate, sealed again with Parafilm and incubated for a further 2h at room temperature on a shaker. The aspiration/wash step was repeated with the automated plate washer, and then 100µl/well working concentration of anti-IgY HRP conjugate was added. The plate was sealed, incubated for 1h at room temperature, with shaking, and the aspiration/wash step subsequently repeated. TMB One solution (100µl/well) was then added, and the plate incubated for 10min at room temperature with shaking. At this point, a blue colour formed

in standard and sample wells in proportion to the amount of detected protein. After this incubation, stop solution (100µl/well) was applied and the plate tapped gently to ensure thorough mixing. The blue colour turned yellow upon acidification. The optical density of each well was determined immediately, using a microplate reader set to 450nm absorbance. Data were then analysed as described below.

2.7.2.3 PEDF ELISA

The ELISA protocol was performed according to the manufacturer's instructions. The kit provided a sealed 96-well plate pre-coated with anti-PEDF monoclonal 'capture' antibody. To prepare the standards, the vial of 250ng recombinant PEDF was first reconstituted with 500µl assay diluent (AD), giving a solution of 500ng/ml. The stock solution was diluted in AD to a working high standard of 62.5ng/ml, and then a series of 1:2 dilutions undertaken to create a seven-point standard curve (i.e. 31.3, 15.6, 7.8, 3.9, 1.95 and 0.98 ng/ml). The last well of the standard column was AD only (0 ng/ml PEDF standard). To prepare the samples, each sample was initially diluted 1:2 in AD, to ensure that the detected concentration would fall within the standard curve generated by the standards. Serial 1:2 dilutions of the samples were then undertaken, and added to the plate at 100µl/well. The plate was then sealed with Parafilm and incubated for 1h at 37°C. The plate was washed x 3 with WB with an automated plate washer. After the last wash step, remaining WB was removed by inverting the plate and blotting it against clean absorbent paper. Next, the detection antibody was added to the plate (100µl/well), the plate sealed again and incubated for a further 1h at 37°C. The aspiration/wash step was repeated with the automated plate washer, and then 100µl/well diluted streptavidin peroxidase conjugate was added. The plate was covered again, incubated for 1h at 37°C and the aspiration/wash step subsequently repeated. TMB/E substrate solution (100µl/well) was then added, and the plate incubated for 10min at room temperature with shaking. At this point a blue colour

formed in the standard wells and sample wells in proportion to the amount of detected protein. After this incubation, stop solution (100µl/well) was applied and the plate tapped gently to ensure thorough mixing. The blue colour turned yellow upon acidification. The optical density of each well was determined immediately, using a microplate reader set to 450nm absorbance. Data were then analysed as described below.

2.7.3 ELISA analysis

Analysis of the ELISA assays was undertaken by the same method for all the ELISA kit protocols described above. For each assay, a standard curve was constructed in Microsoft Excel, plotting the mean optical density (absorbance) for each standard on the y-axis against the known concentration of standard on the x-axis (Figure 2.9B). In each case, the standard curve resulted in a graph depicting a linear relationship between the concentrations of standards and the optical density (absorbance). The standard curve thus generated for each assay was used to determine the concentration of NTF in each sample. Where samples had been diluted, the concentration (as read from the standard curve) was multiplied by the dilution factor to determine the measured NTF titre. For each ELISA, samples of conditioned medium (n=3 independent samples/treatment condition) were tested, and NTF titres compared between treatment conditions.

Reagent	Constituents	Supplier
Phosphate buffered saline (PBS)	1 tablet[1] per 100ml Milli-Q water	[1]Oxoid, Basingstoke, UK
Wash buffer (WB)	0.05% Tween-20[2] in PBS	[2]Sigma-Aldrich, Gillingham, UK
Reagent diluent (RD)	1% Bovine Serum Albumin (BSA)[3] in PBS	[3]Sigma-Aldrich, Gillingham, UK
Substrate solution	1:1 mixture of Color Reagent A (H_2O_2) and Color Reagent B (Tetramethylbenzidine)	R&D Systems, Abingdon, UK
Stop solution	2N H_2SO_4	Scientific Lab. Supplies, Notts, UK
Capture antibody	2µg/ml in PBS	R&D Systems, Abingdon, UK
Detection antibody	200ng/ml in RD	R&D Systems, Abingdon, UK
Streptavidin-HRP	Diluted to working concentration as per specific ELISA protocol in RD	R&D Systems, Abingdon, UK

Table 2.3: Reagents and buffers for CNTF, NGF, NT-3 and GDNF ELISAs.

Reagent	Constituents	Supplier
Phosphate buffered saline (PBS)	1 tablet[1] per 100ml Milli-Q water	[1]Oxoid, Basingstoke, UK
Wash buffer (WB)	0.05% Tween-20[2] in PBS	[2]Sigma-Aldrich, Gillingham, UK
Carbonate Coating Buffer (CCB)	0.025M sodium bicarbonate and 0.025M sodium carbonate in Milli-Q water (pH 9.7)	
Block & Sample 1X Buffer (BSB)	10.6ml Block & Sample 5X Buffer in 42.4ml Milli-Q water	Promega UK, Southampton, UK
TMB One Solution	3,3',5,5'-tetramethylbenzidine in non-hazardous buffer	Promega UK, Southampton, UK
Stop solution	2N H_2SO_4	Scientific Lab. Supplies, Notts, UK
Capture antibody	10µl anti-BDNF mAb in 9.99ml CCB	Promega UK, Southampton, UK
Detection antibody	20µl anti-BDNF pAb in 9.98ml BSB	Promega UK, Southampton, UK
Anti-IgY HRP Conjugate	50µl anti-IgY HRP conjugate in 9.95ml BSB	Promega UK, Southampton, UK

Table 2.4: Reagents and buffers for BDNF ELISA.

Reagent	Constituents	Supplier
Phosphate buffered saline (PBS)	1 tablet[1] per 100ml Milli-Q water	[1]Oxoid, Basingstoke, UK
Wash buffer (WB)	100ml Wash Buffer 10X Concentrate in 1000ml Milli-Q water	Millipore UK Ltd, Watford, UK
Assay Diluent (AD)	60ml proprietary diluent	Millipore UK Ltd, Watford, UK
TMB/E Substrate Solution	3,3',5,5'-tetramethylbenzidine in non-hazardous buffer	Millipore UK Ltd, Watford, UK
Stop solution	2N H_2SO_4	Scientific Lab. Supplies, Notts, UK
Detection antibody	4µl anti-PEDF Ab in 9996µl AD	Millipore UK Ltd, Watford, UK
Streptavidin, HRP conjugated	10µl HRP-conjugated Streptavidin in 9990µl AD	Millipore UK Ltd, Watford, UK

Table 2.5: Reagents and buffers for PEDF ELISA.

2.8 POLYMERASE CHAIN REACTION (PCR)

2.8.1 Principles of PCR

PCR is a very powerful tool in molecular biology, enabling the amplification of specific sequences within a DNA template. Target mRNA sequences can be detected, but require reverse transcription into a complementary DNA (cDNA) template first, and this technique is known as reverse transcription PCR (RT-PCR). In quantitative PCR (qPCR, also known as real-time PCR), data are collected during the PCR reaction, combining both target amplification and detection into a single process (Taylor *et al.*, 2010). The PCR product is detected and measured at each cycle of the PCR reaction, which allows accurate determination of the initial quantity of the target. Using qPCR, it is therefore possible to compare gene expression between samples, for example treated *vs* untreated conditions.

An overview of the PCR process is given in Figure 2.10. PCR is driven by a thermostable DNA polymerase, which synthesises a complementary sequence of nucleotide bases to any single strand of DNA, provided there is a double-stranded starting point. The target of interest to be amplified by the PCR is specifically selected by adding 'primers', small pieces of DNA complimentary to the gene of interest, which provide a double-stranded DNA (dsDNA) scaffold for the DNA polymerase to bind to and initiate copying of the sequence. There are three major steps that make up each cycle of a PCR reaction, and reactions generally run for 40 cycles. First, the temperature is raised to 95°C, to denature ('melt') the DNA into single strands. Next, the temperature is lowered to around 60°C to enable the sequence-specific primers to 'anneal', and then the temperature adjusted for optimal activity of the DNA polymerase to copy the DNA strand (Life Technologies, 2012).

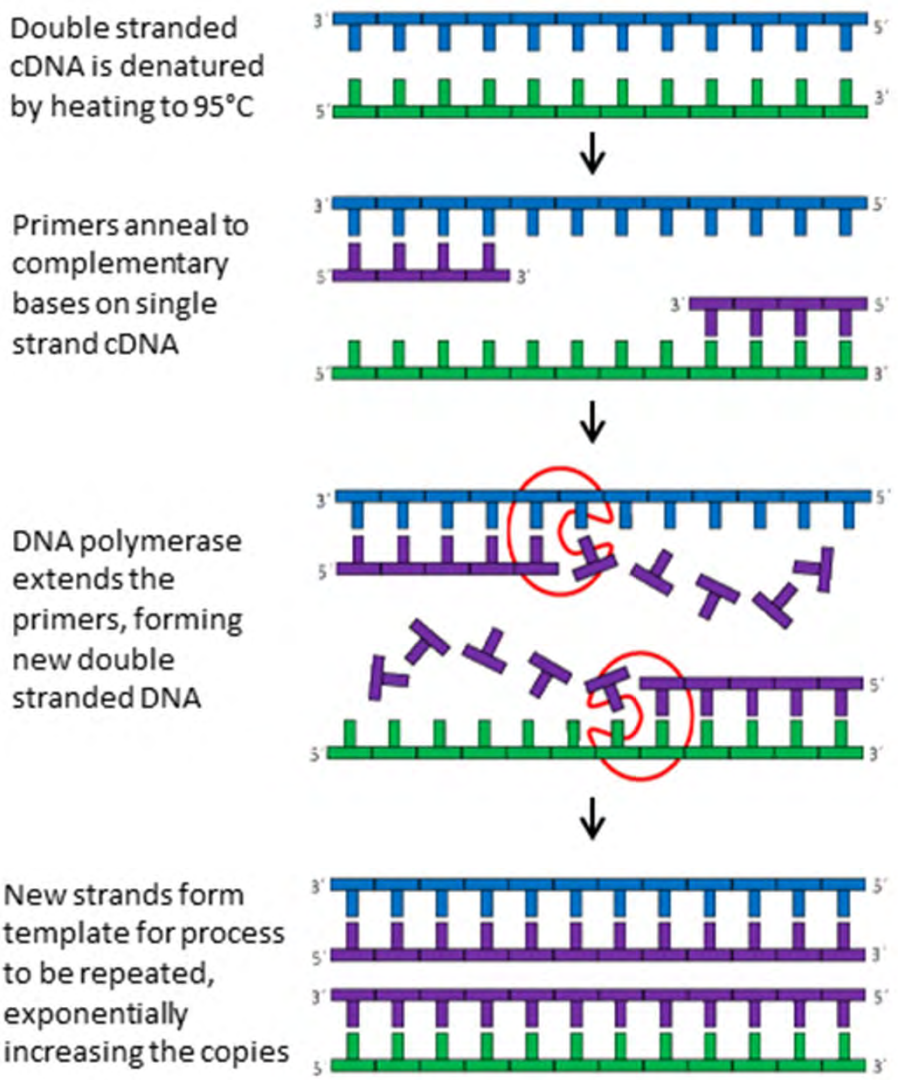


Figure 2.10: Principles of polymerase chain reaction (PCR). Figure adapted from https://www2.le.ac.uk/departments/emfpu/genetics/explained/images/PCR-process.gif/view (accessed 6 July 2015).

Detection of the qPCR product is linked to fluorescence chemistry, which correlates the concentration of PCR product to fluorescence intensity (Life Technologies, 2012). The SYBR® Green DNA intercalating dye is commonly used and was employed in experiments described in this thesis. SYBR® Green is fluorescent in its own right, but when bound to dsDNA produces a more intense fluorescent signal than when unbound. As the PCR reaction progresses and creates more DNA, more dye can bind with a corresponding increase in fluorescence (Wittwer *et al.*, 1997; Life Technologies, 2012). Consequently, the larger the quantity of the target DNA in the sample, the faster an increase in fluorescence can be detected.

A typical qPCR reaction is shown in Figure 2.11. During the early cycles of PCR (the linear ground phase), the PCR reaction is just beginning and fluorescence is at background/baseline levels. As PCR progresses, in the early exponential phase the amount of amplified target DNA increases and consequently the amount of fluorescence reaches a threshold significantly greater than background (typically 10X the standard deviation of the baseline). The PCR cycle at which the fluorescence signal is first detected is known as threshold cycle (C_t), which is representative of the amount of target DNA in the initial sample and is used to calculate experimental results (Wong and Medrano, 2005; Life Technologies, 2012). The reaction eventually reaches a plateau due to limitation of reaction components. Thus, comparison of the amount of target DNA between samples is possible, as a sample starting with a greater amount will amplify above threshold quicker than a sample with a smaller amount, and C_t will be lower.

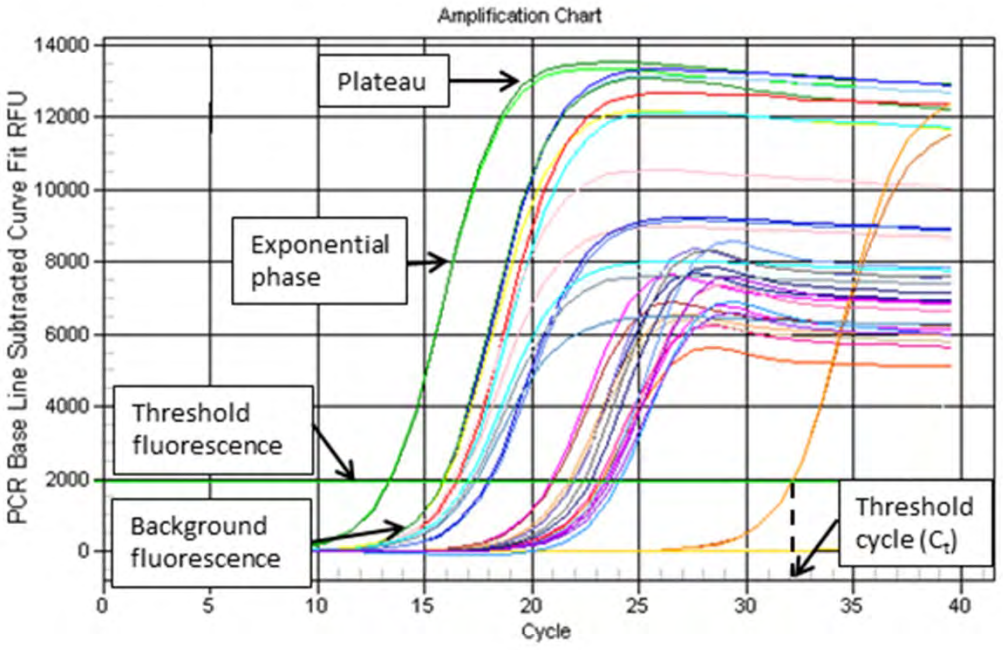


Figure 2.11: Quantitative polymerase chain reaction (qPCR). A typical qPCR amplification reaction is shown. Fluorescence is at background levels during the early cycles of PCR, and eventually reaches a threshold level. The cycle number at which fluorescence reaches a level significantly greater than background is the threshold cycle (C_t) and this value is recorded. PCR proceeds exponentially until the reaction reaches a plateau.

2.8.2 qPCR protocols

Experiments using qPCR were undertaken to confirm the specificity of siRNA of interest (siRTP801, used in experiments described in Chapters 3, 4 & 5; siGSK3β used in experiments described in Chapter 5) in achieving target knock-down. Protocols used for each of the following stages of the qPCR process are described below: (1) sample preparation and treatment; (2) RNA extraction, quantification and quality control; (3) reverse transcription; (4) preparation of primers; (5) qPCR process; (6) confirmation of qPCR reaction specificity; (7) selection of endogenous control; and (8) quantification.

2.8.2.1 Sample preparation

RNA to be used as the template for qPCR studies was extracted from retinal cells after siRNA treatment *in vitro*. Retinal cultures were prepared as described in Section 2.4.1. To facilitate the extraction of RNA from these cultures, dissociated retinal cells were plated in sNBA culture medium at a density of 1.5 million cells/well in 6-well culture plates. Transfection with siRNA was undertaken the following day (as per Section 2.4.2), although reagent volumes were scaled up accordingly due to the larger well size of 6-well plates compared to the 8-well plates usually used for culture studies. After siRNA transfection, plates were incubated at 37°C/5% CO_2 for 3d.

For experiments to confirm knock-down of RTP801 expression after siRTP801 treatment (Chapter 3), RNA was extracted from the following experimental groups: (1) sNBA culture medium (untreated); (2) Lipofectamine (transfection vehicle); (3) siEGFP (inactive siRNA); and (4) siRTP801-treated. For experiments to confirm knock-down of GSK3β expression after siGSK3β treatment (Chapter 5), RNA was extracted from the following experimental groups: (1) sNBA culture medium (untreated); (2) Lipofectamine (transfection vehicle); (3) siEGFP (inactive siRNA); and (4) siGSK3β -treated.

2.8.2.2 RNA extraction, quantification and quality control

RNA was extracted from retinal cells with the RNeasy Mini Kit (Qiagen Ltd., Manchester, UK) in accordance with the manufacturer's instructions. Buffers mentioned in this section were provided with the kit. For each well, culture medium was completely aspirated and cells washed once with warm sterile dPBS, disrupted (to release RNA in the sample) by addition of 600µl Buffer RLT, and the base of the well scraped with a cell scraper to remove cells from the base of the well. Cell lysate was transferred from each well to an Eppendorf. The cell lysate was homogenised using an IKA-T10

homogeniser (Cole-Parmer Instrument Co. Ltd., London, UK), with the blade cleaned with sterile dPBS between each sample to prevent contamination. An equal volume (600µl) of 70% ethanol was added to the homogenised cell lysate and mixed by pipetting up and down several times. For each sample, 700µl was transferred into an RNeasy spin column placed in a 2ml collection tube, and centrifuged at 10000rpm for 15s, and the flow-through discarded. The remainder of each sample was added to the RNeasy spin column, similarly centrifuged and the flow-through discarded. Next, 700µl Buffer RW1 was added to the RNeasy spin column and centrifuged at 10000rpm for 15s, and the flow-through discarded. Buffer RPE (500µl) was added to the spin column, and then centrifuged at 10000rpm for 15s, and the flow-through discarded. A further 500µl Buffer RPE was added to the spin column and then centrifuged at 10000rpm for 2min. The collection tube and flow-through was discarded and the RNeasy spin column placed in a new 2ml collection tube and centrifuged at 13000rpm for 1min. The RNeasy spin column was transferred to a new 1.5ml collection tube, and 50µl RNase-free water added directly to the spin column membrane. This was centrifuged at 10000rpm for 1min to elute the RNA.

The amount and purity of isolated RNA was checked using a ND-1000 Spectrophotometer (NanoDrop, Wilmington, DE, USA). Using the inbuilt nucleic acid protocol, a 2µl sample of nuclease-free water was added to the detector as a 'blank' run to prepare the system. Next, a 2µl sample of RNA was added to the detector, and the measured amount of RNA (ng/µl) and purity (260/280 ratio) was recorded. A 260nm/280nm absorbance ratio of 1.8-2.0 indicates good quality RNA that is not contaminated with protein or phenol and is considered acceptable for use in qPCR (Taylor *et al.*, 2010). A 'blank' sample of 2µl nuclease-free water was run between each RNA sample.

2.8.2.3 Reverse transcription

RNA was converted to cDNA for qPCR using the High Capacity cDNA Reverse Transcription Kit (Applied Biosystems, Paisley, UK) in accordance with the manufacturer's instructions. The kit components were allowed to thaw on ice, and then for each sample a 50µl Reverse Transcriptase Master Mix was prepared in a PCR tube, comprising 10µl 10X reverse transcriptase buffer, 4µl 25X dNTP mix, 10µl 10X random primers, 5µl Multiscribe™ Reverse Transcriptase (50 U/µl) and 21µl nuclease-free water. The RNA mix for each sample (50µl) was added to the Master Mix, and mixed by gentle pipetting. Tubes were loaded into an iCycler PCR machine (Bio-Rad Laboratories Ltd) and the following protocol followed:

1. 25°C for 10min
2. 37°C for 120min
3. 85°C for 5min to deactivate the reverse transcriptase enzyme
4. 4°C hold until sample collected

Quantity (ng/µl) and purity (260:280 ratio) of synthesised cDNA was checked using the ND-1000 Spectrophotometer, as described above. Samples were diluted to a working concentration of 20 ng/µl and stored at -20°C until qPCR the protocol was undertaken.

2.8.2.4 Primer preparation

Primers for target genes were supplied by Alta Biosciences (Birmingham, UK). The primer sequences for the RTP801 primers were kindly supplied by Quark Pharmaceuticals and the primer sequences for the GSK3β primers were as published previously (Mendes *et al.*, 2009) (Table 2.6). Primers were initially diluted to a stock concentration of 100pmole/µl in nuclease-free water and stored at -20°C

before use in qPCR. Primers were prepared in a working concentration of 10µM by combining 10µl each of the forward and reverse primer stock solution with 80µl nuclease-free water, and used at 300nM in the final reaction mixture.

Primers for reference genes were selected from the geNorm™ Reference Gene Selection Kit (Primer Design Ltd, Southampton, UK). Reference gene primers were initially reconstituted in 220µl nuclease-free water, in accordance with the manufacturer's instructions, and used at 300nM in the final reaction mixture.

Primer	Sequence	Melting temp. (°C)	Molecular weight (Da)
RTP801 (Fwd)	5'-GCC--GGA--GGA--AGA--CTC--CTC--AT-3'	60.5	6126
RTP801 (Rev)	5'-GCT--GCA--TCA--GGT--TGG--CAC--AC-3'	62.1	6117
GSK3b (Fwd)	5'-AGC--CTA--TAT--CCA--TTC--CTT--GG-3'	53.8	6042
GSK3b (Rev)	5'-CCT--CGG--ACC--AGC--TGC--TTT-3'	58.4	5426

Table 2.6: Details of primers used in qPCR for target genes.

2.8.2.5 qPCR reaction protocol

Each qPCR reaction was undertaken with a total reaction volume of 50µl/well in a sealed 96-well PCR plate (Starlab Ltd., Milton Keynes, UK). For each 50µl reaction, a qPCR Master Mix was prepared in accordance with the instructions provided with the LightCycler®480 SYBR Green 1 Master Mix (Roche Applied Science, West Sussex, UK), incorporating the SYBR Green Master Mix, 300nM primer mix and nuclease-free water (Table 2.7) and added to the PCR plate. Template cDNA, from siRNA treated samples and controls (100ng/5µl), was added to the wells and the plate loaded into an iQ5 Multicolor Real-Time PCR Detection System (Bio-Rad Laboratories) and the following qPCR protocol followed:

1. 50°C for 2min
2. 95°C for 10min to activate the Taq polymerase
3. 95°C for 15sec to denature
4. 60°C for 1min to anneal/extend (steps 3 & 4 repeated x 40)
5. 55-95°C in 0.5°C increments (30sec at each temperature) for melt curve

Each cDNA sample was run in duplicate, and for each primer mix a no template control (NTC; qPCR mix as described above without template cDNA) was run to ensure no contaminant DNA was present. At the end of the qPCR protocol, the C_t value for each well was recorded for analysis. Confirmation of qPCR amplification efficiency of 100% was provided by the software.

	Target Gene Primers	**Reference Gene Primers**
Component	**Volume**	**Volume**
SYBR Green Master Mix*	25 µl	25 µl
Primer mix (300nM)	1.5 µl	2.5 µl
Nuclease-free water	18.5 µl	17.5 µl
cDNA (100ng)	5 µl	5 µl
Total volume per reaction	**50 µl**	**50 µl**

*FastStart Taq DNA Polymerase, reaction buffer, dNTP mix, SYBR Green I dye, $MgCl_2$

Table 2.7: Reaction mix for qPCR experiments.

2.8.2.6 Confirmation of qPCR reaction specificity

A weakness of DNA intercalating dyes for the detection of PCR target products in qPCR is in their specificity. Dyes such as SYBR® Green do not bind to dsDNA in a sequence-specific fashion, and will

therefore bind to any amplified product, target or non-target, producing a single amplification plot (Life Technologies, 2012). The specificity of a qPCR reaction in amplifying the DNA target of interest, and therefore a measure of the specificity of the sequence-specific DNA primer, is undertaken with a dissociation analysis, or 'melt-curve' analysis (Ririe *et al.*, 1997). This is undertaken routinely as part of the qPCR protocol, and if an amplified target is of one specific sequence, it should possess a specific melting temperature (T_m), which is used to identify the target and differentiate it from non-target amplification, such as created by so-called "primer-dimers" where primers bind to themselves. In a melt curve analysis the PCR product is heated up to around 95°C, when the melting temperature of the PCR product is reached and the two DNA strands dissociate and release the SYBR® Green dye into solution, resulting in a sudden drop in fluorescence (Life Technologies, 2012). The qPCR machine automatically generates a melt-curve, plotting the rate-of-change of fluorescence against temperature. A single distinct peak in the melt curve indicates a single melting temperature of the PCR product, analogous to a distinct band on an electrophoresis gel, and is consistent with a specific PCR reaction (Taylor *et al.*, 2010). The presence of multiple amplified products, e.g. either from contaminants or primer-dimers, is identified by multiple peaks on the melt curve, or a melt curve with a wide base.

Before undertaking qPCR experiments to compare expression of target genes after siRNA transfection, the specificity of each qPCR primer was confirmed by undertaking melt curve analysis (Figure 2.12). To test the specificity of the RTP801 and GSK3β target gene primers, a qPCR master mix was prepared as described above, using cDNA samples obtained from untreated retinal cells as the template DNA for amplification. Each primer was tested in duplicate, and a melt curve was produced by the qPCR machine. The presence of a single peak for each well of the duplicate samples indicated a single melting temperature for the amplified product in each well, thereby confirming the absence of amplified non-target DNA or primer-dimers.

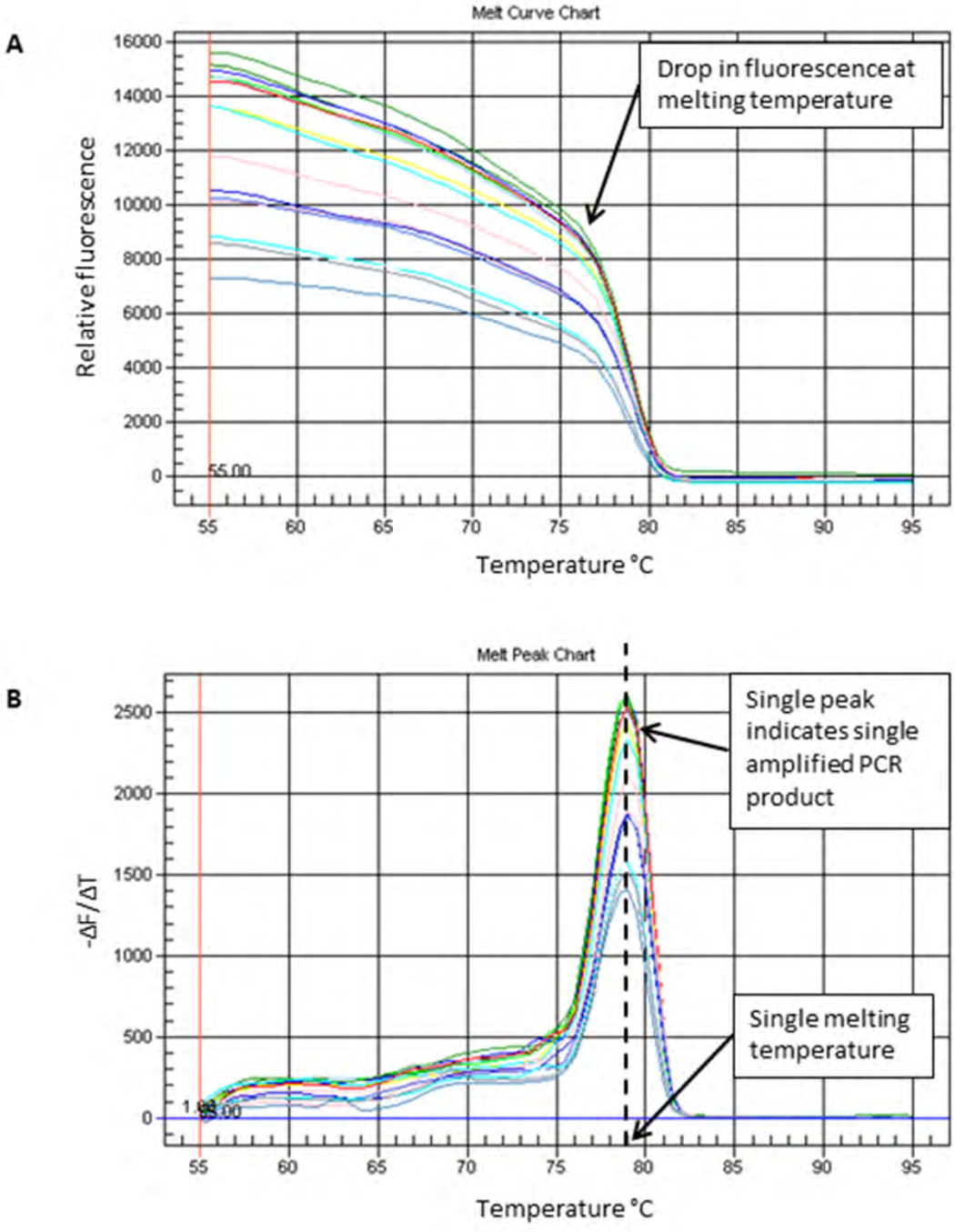


Figure 2.12: Example of melt curve analysis for qPCR specificity validation. (A) At the end of the qPCR programme, the temperature is raised to dissociate the dsDNA and release the SYBR Green dye into solution, resulting in a sudden drop in fluorescence. (B) Change in fluorescence per change in temperature (-ΔF/ΔT, y-axis) is plotted against temperature (x-axis). A single peak represents a single amplification product, confirming the absence of non-specific amplification.

2.8.2.7 Selection of endogenous control (reference) gene

For analysis of results obtained by qPCR experiments, relative quantification is commonly used. Changes in the expression of the target gene between samples are identified by normalising data to those of a stably expressed endogenous control (reference) gene that does not vary between experimental conditions (Wong and Medrano, 2005). Various 'housekeeping' genes are used as reference genes, such as glyceraldehyde phosphate dehydrogenase (GAPDH), although it is important that the expression of the reference gene is equally expressed in all the samples being analysed for a qPCR experiment.

For accurate comparison of target gene expression between siRNA-treated and control samples, it was important to normalise target gene expression to the expression of a reference gene that exhibited stability of expression between samples, regardless of experimental intervention. The following reference genes were assessed for stability across samples: *GAPDH, 18S, B2M* and *UBC*. For each treatment condition described above (sNBA culture medium ['untreated'], Lipofectamine, siEGFP and siRTP801-treated [Chapter 3] or siGSK3β-treated [Chapter 5]), a qPCR reaction was undertaken for each reference gene primer with cDNA templates from 5 independent samples, with each sample tested in duplicate. The C_t was recorded for each sample. The standard deviation of C_t values across all samples was smallest for *GAPDH*, suggesting this to be the most stable of the reference genes assessed. Thus, *GAPDH* was selected as the endogenous control gene.

2.8.2.8 Gene expression quantification

Comparison of target gene expression between experimental samples does not require quantification of absolute amounts of DNA. Rather, algorithms compare the fold-change in

expression of the target gene relative to that of the reference/housekeeping gene (Livak and Schmittgen, 2001). To determine the level of target gene expression, relative quantification was determined using the ΔΔCt method (Livak and Schmittgen, 2001). The relative expression of the target gene (RTP801 in Chapter 3, GSK3β in Chapter 5) in siRNA treated samples and in Lipofectamine/siEGFP control samples was compared to untreated (sNBA culture medium alone) samples, as follows:

$$\Delta Ct = Ct\ (target\ gene) - Ct\ (reference\ gene)$$

For each treatment condition described, the mean ΔCT was calculated from n=5 independent samples. Next, ΔΔCt was calculated, as follows:

$$\Delta\Delta Ct = \Delta Ct\ (test\ condition) - \Delta Ct\ (untreated\ control)$$

Target gene expression, represented as a 'fold-change' with reference to the endogenous control gene (*GAPDH*) was calculated, as follows:

$$Relative\ gene\ expression\ ('fold\text{-}change') = 2^{-\Delta\Delta Ct}$$

2.9 STATISTICS

Experimental data were recorded on Excel Spreadsheets (Microsoft Corp., Redmond, WA, USA) and statistical analyses undertaken with SPSS 19.0 (IBM SPSS Inc., Chicago, IL, USA). Data were presented as means ± standard errors of the mean (SEM). For *in vivo* studies, treatment groups of at least n=5 eyes/treatment were used where possible, as this has previously been shown to provide statistically

significant results between experimental groups in RGC survival and axon regeneration analyses (Mead *et al.*, 2014; Ahmed *et al.*, 2011), whilst fulfilling the requirements of the UK Home Office licences to use a minimum number of experimental animals. For retinal culture studies *in vitro*, all experimental results were derived from up to 3 wells/treatment (technical replicates) and repeated with cultures from at least n=3 independent animals (biological replicates) per experiment, based upon previous published experiments and statistical advice (Lorber *et al.*, 2012; Cumming *et al.*, 2007; Lazic, 2010; Vigneswara *et al.*, 2013; Ennos, 2007).

Where comparisons were undertaken between only two conditions, for example the analysis of axon regeneration between siRTP801-treated and siEGFP-control eyes after ONC in Chapter 3, the Students t-test was used. For all other experiments where comparisons were required between multiple groups/conditions, one-way analysis of variance (ANOVA) was undertaken, followed by *post hoc* testing with Tukey correction (comparison between multiple groups/conditions) or Dunnett correction (comparison of groups/conditions against a specific control) (Ennos, 2007). Differences between group means were considered statistically significant if the difference had a calculated probability (p) of occurring by chance of < 5% ($p<0.05$).

CHAPTER 3

INVESTIGATING siRNA-MEDIATED KNOCK-DOWN OF RTP801 ON RGC SURVIVAL AND AXON REGENERATION

Elements of work presented in this Chapter have been published in:

Morgan-Warren PJ, O'Neill J, De Cogan F, Spivak K, Ashush H, Kalinski H, Ahmed Z, Berry B, Feinstein E, Scott RAH, Logan A. siRNA mediated knockdown of the mTOR inhibitor RTP801 promotes retinal ganglion cell survival and axon elongation by direct and indirect mechanisms. *Invest Ophthalmol Vis Sci.* 2016 (in press). DOI:10.1167/iovs.15-17511

3.1 INTRODUCTION / RATIONALE

In seeking to develop novel translatable therapies to promote RGC survival and axon regeneration, the identification of key mediators of cellular signalling which regulate processes associated with neuronal survival and axon growth is vital. The PI3K-Akt-mTOR signalling pathway is now implicated as a major neuronal intrinsic determinant of survival and axon regenerative ability, and experimental manipulations to up-regulate mTOR signalling have proven successful in promoting RGC survival and significant axon regeneration after ONC in rodent models (Park *et al.*, 2008; Park *et al.*, 2010). In addition to the visual system, promotion of mTOR activity has enabled axon regeneration in other neuronal paradigms, such as in CST neurons, after spinal cord injury and in the PNS (Liu *et al.*, 2010a; Ohtake *et al.*, 2014; Ning *et al.*, 2010; Christie *et al.*, 2010). However, the experimental strategies used to date, such as conditional gene deletion, are not clinically translatable. The availability of siRNA drugs allow these cellular signalling targets to be accessed for potential therapeutic use.

Identified in 2002, RTP801 (also known as Redd1) is a 232 amino acid protein encoded by the DNA-damage-inducible transcript 4 (DDIT4) stress-responsive gene, and is expressed in numerous tissues where it localises to the nucleus, cytoplasm and cellular membranes (Shoshani *et al.*, 2002; Canal *et al.*, 2014). RTP801 is rapidly up-regulated in response to cellular stressors including hypoxia, energy deprivation, DNA damage and lack of nutrient availability (Brugarolas *et al.*, 2004; Laplante and Sabatini, 2012; Canal *et al.*, 2014), and its major role is in the down-regulation of mTOR activity which results in the limitation of protein synthesis (Brugarolas *et al.*, 2004; Corradetti *et al.*, 2005; Gordon *et al.*, 2015). RTP801 is activated in response to cellular stress and achieves suppression of mTOR *via* activation of the TSC1/2 complex (Figures 1.8 and 1.11) (Brugarolas *et al.*, 2004; Corradetti *et al.*, 2005). Whilst RTP801 is thought not to physically interact directly with TSC1 or TSC2, the exact mechanism underlying the inhibitory effect of RTP801 towards mTOR remains incompletely

understood, although may be by alteration of the activity of Akt towards TSC1/2 (DeYoung *et al.*, 2008; Vega-Rubin-de-Celis *et al.*, 2010; Dennis *et al.*, 2014).

Several factors implicate RTP801 as a potentially useful target to promote RGC survival and axon regeneration after ON injury. RTP801 is a negative regulator both of neuronal development in embryogenesis and of neuronal survival in mature animals. Knock-down of RTP801 promotes the differentiation of neural progenitors into neurons (Malagelada *et al.*, 2011). Induced over-expression of RTP801 promotes apoptosis in a neuronal cell line (Shoshani *et al.*, 2002), and RTP801 knock-out mice exhibit reduced apoptosis in retinal neurons in a model of retinopathy of prematurity (ROP) (Brafman *et al.*, 2004). RTP801 is associated with cell death in a murine Parkinson's disease model, in which RTP801 knock-down is neuroprotective (Malagelada *et al.*, 2008; Malagelada *et al.*, 2006). Furthermore, RTP801 inhibition protects RGC-5 neurons from apoptosis induced by cobalt chloride or blue light toxicity (del Olmo-Aguado *et al.*, 2013). Therefore, there is a clear rationale for RTP801 inhibition to represent a viable strategy to promote mTOR activity after injury, and enhance CNS neuroprotection and axogenesis, although to date there are no previous reports of the effects of RTP801 inhibition on RGC survival and axon growth after ON injury. Experiments described in this Chapter utilised a clinically translatable targeted siRNA against RTP801, in order to investigate whether knock-down of this mTOR inhibitor promoted RGC neuroprotection and axon regeneration, as the basis for a novel therapeutic approach for patients with TON.

3.2 HYPOTHESIS

siRNA mediated knock-down of the stress-induced mTOR negative regulator RTP801 promotes RGC survival and axon regeneration in a model of TON.

3.3 AIMS

The specific aims of experiments described in this chapter were to:

1. Confirm siRNA target specificity and knock-down;
2. Characterise retinal expression of RTP801 and its response to ONC, and investigate the effects of siRTP801 on RTP801 expression in retinal cells *in vivo* and *in vitro*;
3. Investigate the effects of siRTP801 on RGC survival and axon regeneration after ONC *in vivo*;
4. Investigate the effects of siRTP801 on RGC survival and neurite outgrowth in dissociated retinal cultures.

3.4 EXPERIMENTAL DESIGN

Details of specific experimental techniques and methodologies are described in Chapter 2.

3.4.1 Confirmation of siRNA specificity and knock-down with qPCR

RNA was obtained from mixed retinal cultures incubated with sNBA culture medium alone (untreated), and from cultures treated with siRTP801, siEGFP and Lipofectamine, as described in Section 2.8.2, with n=3 independently treated culture wells/condition. Specificity of the RTP801 primer was assessed by running a qPCR reaction with cDNA from an untreated sample in duplicate, and undertaking melt-curve analysis to confirm a single amplicon. RTP801 knock-down was evaluated by comparing RTP801 expression, as a fold-change relative to the housekeeping gene GAPDH, in samples from the different treatment conditions.

3.4.2 Assessment of siRTP801 on retinal expression of RTP801 and on RGC survival and axon regeneration after ONC *in vivo*

Adult rats underwent bilateral ONC as described previously (Section 2.3.3), followed by bilateral intravitreal injections consisting of unilateral injection with siRTP801 (20µg/10µl) and injection of siEGFP (20µg/10µl) to the fellow eye immediately after ONC and again 8d and 16d after ONC, in a total of n=5 animals. ON sections from these animals were prepared after 24d and analysed by IHC for the presence of $GAP43^+$ regenerating axons. Assessment of RGC survival and retinal expression of RTP801 was compared using retinal sections from these two treatment conditions, and also using retinal sections obtained from eyes of intact, uninjured animals (n=5 eyes/group).

3.4.3 Assessment of siRTP801 on retinal cellular localisation of RTP801 and on RGC survival and neurite outgrowth in dissociated mixed retinal cultures

Primary cultures containing mixed retinal cells were established from uninjured adult rats as described previously (Section 2.4.1). Culture wells (2-3 wells/condition, from n=3 independent animals) were incubated for 3d (37°C / 5% CO_2) in the following treatment conditions: sNBA culture medium alone; Lipofectamine transfection reagent; siEGFP at 10nM, 20nM and 50nM; siRTP801 at 10nM, 20nM and 50nM; and cultures were evaluated for βIII-$tubulin^+$ RGC survival, neurite outgrowth (initiation and elongation) and RTP801 expression. For further characterisation of cellular localisation of RTP801, cultures were established as described and incubated either untreated (sNBA alone) or treated with siEGFP (20nM) or siRTP801 (20nM), and subsequently double-immunostained to evaluate co-expression of RTP801 with GFAP, CRALBP, calbindin and S100β cell-phenotypic antibody markers. In all cases 2-3 wells/condition from n=3 independent animals were used for analysis (Cumming *et al.*, 2007).

3.5 RESULTS

3.5.1 Characterisation of specific activity of siRTP801 and target knock-down

3.5.1.1 Confirmation of specificity of siRTP801 and target knock-down in vitro

Quantitative PCR was undertaken to confirm the specificity of the siRNA targeting RTP801, in order to validate the fidelity of subsequent experiments. A melt curve analysis of the qPCR reaction, undertaken using the specific RTP801 primers on a cDNA sample obtained from untreated (sNBA alone) retinal cultures, demonstrated a single peak in the melt curve (Figure 3.1A), indicating a single PCR amplicon and the absence of non-specific amplification, thus confirming the specificity of the RTP801 primers. Compared to retinal cultures exposed to sNBA culture medium alone, there was no significant difference in the relative expression of RTP801 in retinal cultures after treatment with Lipofectamine transfection reagent or with siEGFP (Figure 3.1B). However, there was a significant reduction in RTP801 expression in cDNA prepared from retinal cultures treated with 20nM siRTP801, with a fold change of 0.49 ± 0.09 ($p=0.032$, Figure 3.1B). These data indicated that RTP801 expression was specifically knocked-down in mixed dissociated cultured retinal cells after siRTP801 treatment, with approximately 51% target knock-down, and that there was no RTP801 knock-down by the Lipofectamine or siEGFP controls.

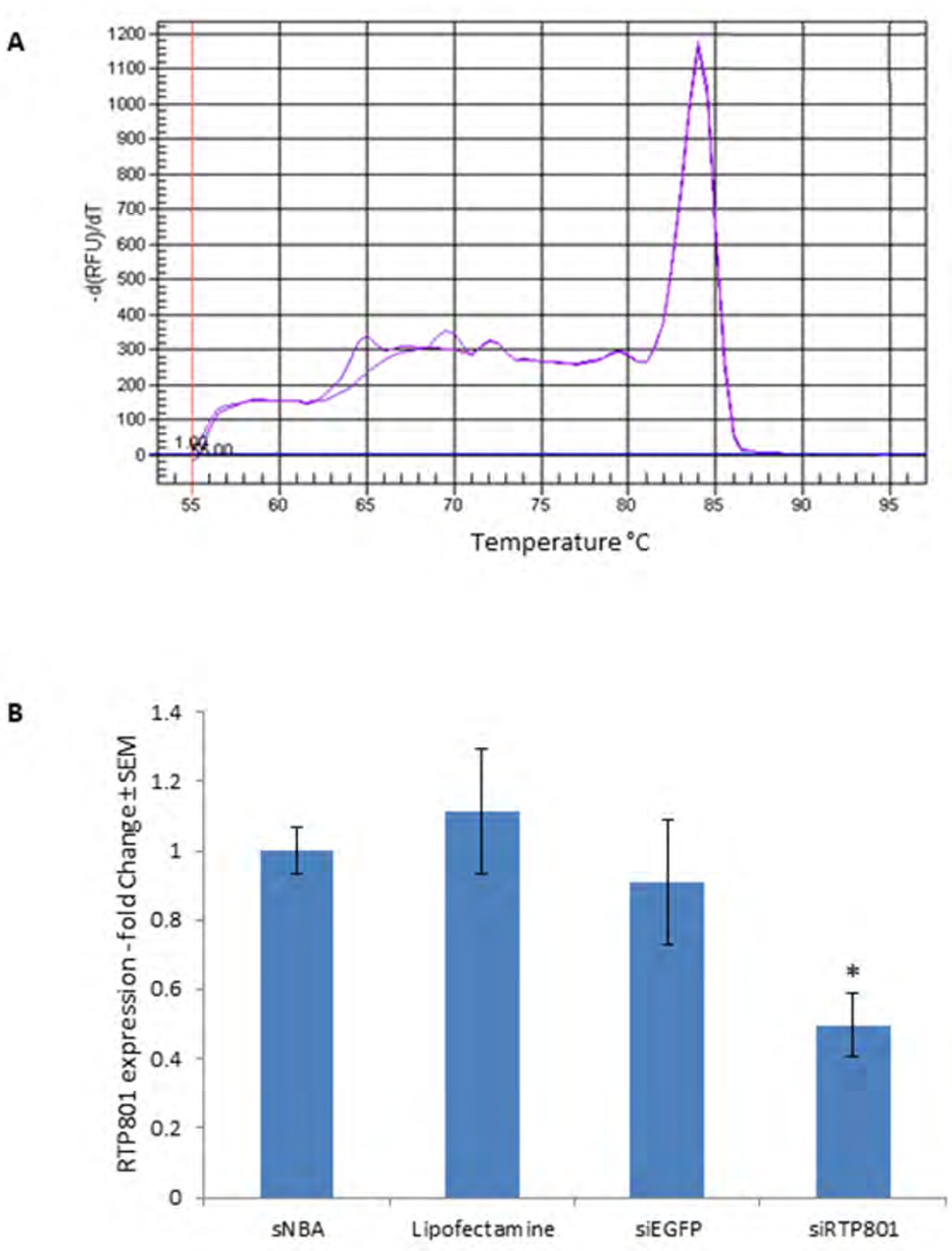


Figure 3.1: Target specificity and knock-down efficacy of siRTP801. (A) Melt curve analysis of qPCR reaction using RTP801-specific primers on cDNA samples obtained from uninjured retinal cultures. A single peak in the melt curve indicates a single PCR amplicon and the absence of non-specific amplification, confirming the specificity of the RTP801 primers. (B) RTP801 expression in cultured retinal cells after treatment with sNBA culture medium alone, Lipofectamine transfection reagent, control siEGFP (20nM) and siRTP801 (20nM), indicating target knock-down by siRTP801 (n=3; *p<0.05).

3.5.1.2 Confirmation of siRTP801 specificity and the lack of induction of non-specific pro-inflammatory effects of siRTP801 in vivo

Further data concerning the specificity of siRTP801 were kindly provided by Quark Pharmaceuticals. Detection of siRTP801-specific RTP801 mRNA cleavage by RLM-RACE in the rat retina after intravitreal siRTP801 delivery confirmed the specific activity of this siRNA *in vivo* (Figure 3.2A). The lack of induction of retinal expression of interferon-responsive genes IFIT and OAS 1B at 4 and 24h after intravitreal administration of siRTP801 confirmed the lack of pro-inflammatory (TLR-mediated) effects of this siRNA compound (Kleinman *et al.*, 2008; Forsbach *et al.*, 2008) (Figure 3.2B).

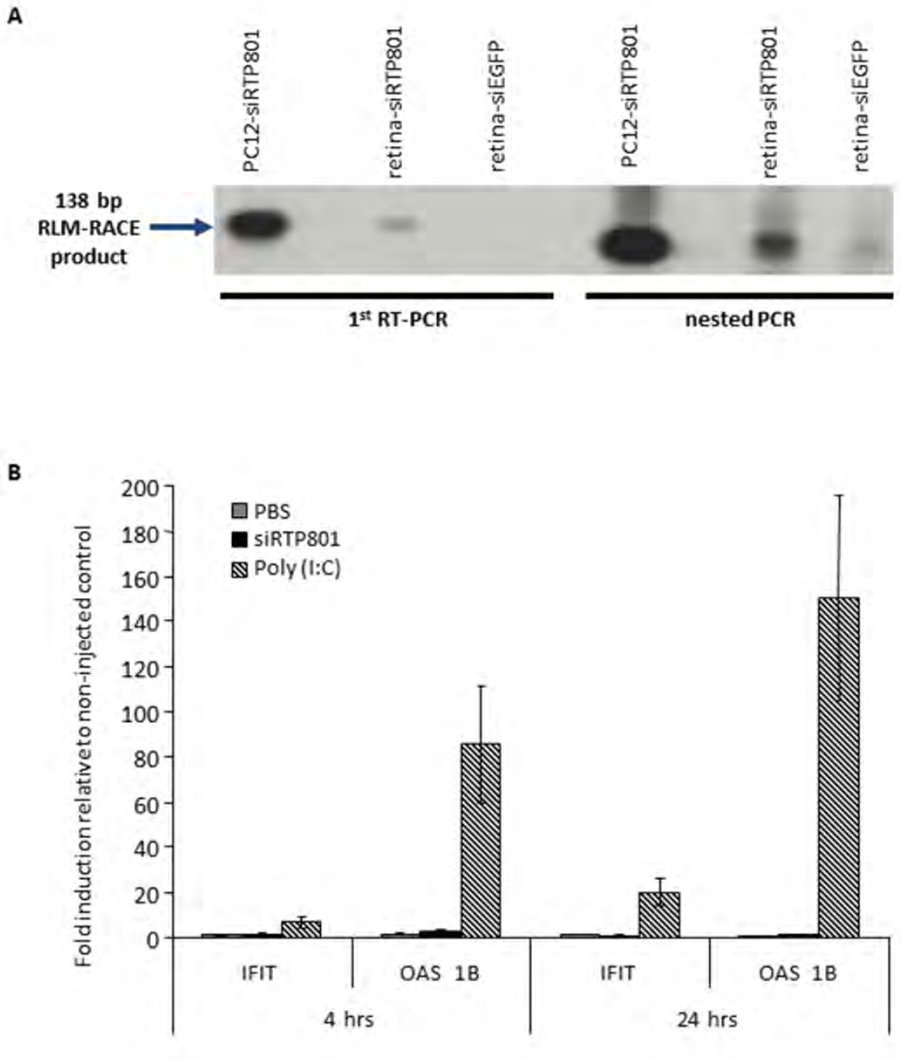


Figure 3.2: Confirmation of siRTP801 target specificity and lack of induction of non-specific pro-inflammatory response. (Legend continues on next page).

Figure 3.2: Confirmation of siRTP801 target specificity and lack of induction of non-specific pro-inflammatory response. (A) Detection of siRTP801-specific RTP801 mRNA cleavage by RLM-RACE in the retina *in vivo*. Adult male 180-220g Sprague-Dawley rats were subjected to a 20µg intravitreal injection of either siRTP801 or siEGFP in 10µl PBS/eye. Four hours later, retinae were harvested and extracted RNA was analysed using RLM-RACE to detect siRTP801 produced mRNA cleavage product using GeneRacer^{TM} kit (Invitrogen, Carlsbad, CA, USA), according to the manufacturer's instructions. RNA samples extracted from cultured PC12 cells transfected with siRTP801 were used a positive control. RACE products were separated on a 2% agarose gel, blotted and hybridised to the RACE-specific oligonucleotide probe (5'-GGAGTAGAAATGATGCAGCT-3') labelled with γ-^{33}P-ATP. After hybridisation, the membrane was washed and exposed to a KODAK BioMax film (Kodak, Rochester, NY, USA). The following primers were used for the amplification of the RTP801-RLM-RACE-product: 5' – GGCTGTAACCAGGGACCAAG-3' (RTP801-specific RT primer); 5' – ATGCCAGGCGCAGGAGTTCCTT-3' (RTP801-specific reverse PCR primer); 5' – AGGAGTTCCTTGCCCACCT-3' (RTP801-specific nested reverse PCR primer); 5' – CGACTGGAGCACGAGGACACTGCAT-3' (adapter-specific forward PCR primer); and 5'- GGACACTGCATGGACTGAAGGAGTA-3' (adapter-specific nested forward PCR primer). (B) Lack of induction of non-specific pro-inflammatory effects of siRTP801 in the retina after intravitreal injection. Lack of expression of interferon-responsive genes IFIT and OAS1, in the retina and choroid of rat eyes after intravitreal siRTP801 injection. Poly I:C is a positive control Toll-like receptor (TLR)-3 activator, and siRTP801is in a ~30-fold molar excess compared to poly I:C. Sprague-Dawley rats (n=6/treatment group) were injected intravitreally with either 20mg/eye of poly(I:C) (200-1000bp; Invivogen) in 10ml of PBS or 35mg of siRTP801 in 10ml of PBS (19bp; ~30-fold molar excess compared to poly (I:C)). Control animals were injected with 10 ml PBS (the vehicle). Four or 24h after injection, eyes were enucleated and retina/choroid complexes isolated for RNA extraction (EZ-RNA extraction kit, Biological Industries, Beth HaEmek, Israel) and assessment of expression of IFN-responsive genes using quantitative real-time RT-PCR (qPCR). The following amplification primers were used (official gene symbols are shown in parentheses): rat cyclophilin A (PPIA): forward: 5'-CGACTGTGGACAGCTCTAAT-3'; reverse: 5'-CCTGAGCTACAGAAGGAATG-3'; rat beta-actin (ACTB): forward: 5'-AGAGCTATGAGCTGCCTGAC-3'; reverse: 5'- AATTGAATGTAGTTTCATGGATG-3'; rat interferon-induced protein with tetratricopeptide repeats 1 (IFIT1): forward: 5' – GCCTACGTGAGACACCTGAA-3'; reverse: 5' – AGGTCACCAGGCTTCTCTTG-3'; rat 2'-5' oligoadenylate synthetase 1B (OAS1B): forward: 5'-TGATGTGCTTCCAGCCTATG-3'; reverse: 5'-TGCGCTCACTGATGAGATTG-3'. (Figure and legends kindly provided by Quark Pharmaceuticals, Ness Ziona, Israel).

Taken together, these data demonstrated that siRTP801 was target specific, achieved mRNA target knock-down both *in vivo* and *in vitro*, and that the effects of siRTP801 were attributed to this specific target knock-down rather than siRNA-induced activation of an immune response. These initial findings thus validated the fidelity of the siRNA under investigation in subsequent experiments.

3.5.2 Characterisation of retinal expression of RTP801 and the effects of siRTP801

3.5.2.1 Retinal expression of RTP801 was increased after ONC and reduced by siRTP801 treatment

There was a low level of RTP801 immunoreactivity in cells of retinal sections from intact uninjured animals, predominantly in the GCL (Figure 3.3A). Increased RTP801 expression was evident in GCL cells of retinal sections 24d after ONC and intravitreal siEGFP, which was attenuated in sections obtained from ONC + siRTP801 animals. Quantitatively, RTP801 expression was observed in 10.6 ± 1.1% $Brn3a^+$ RGC in uninjured controls, and significantly increased to 47.3 ± 3.1% ($p<0.001$) of remaining RGC after ONC + siEGFP. Treatment with siRTP801 significantly reduced the proportion of $RTP801^+$ RGC compared to siEGFP-injected eyes (21.9 ± 1.6%, $p<0.001$) (Figure 3.3B). In addition to RGC, RTP801 localised to $Brn3a^-$ cells in the GCL of intact animals, probably astrocytes/amacrine cells (0.7 ± 0.3 cells/250µm GCL), with increased RTP801 detection in these cells after ONC + siEGFP (3.5 ± 0.4 cells/250µm GCL, $p<0.001$), which was reduced after siRTP801 treatment (1.5 ± 0.3 cells, $p=0.001$) (Figure 3.3C).

In addition to the RTP801 expression in the GCL, immunostaining of retinal sections demonstrated increased RTP801 detection in cells of the INL after ONC and, using the glial cell markers GFAP and S100β, demonstrated some RTP801/S100β co-localisation in cells of the INL, suggesting RTP801 activity in activated astrocytes and Müller glia after ONC, with reduced immunoreactivity after

siRTP801 treatment (Figure 3.4A, B). To obtain a semi-quantitative measure of RTP801 activity in retinal sections as a whole, and to specifically examine the INL, the intensity of RTP801 immunostaining was compared using pixel counts. Using this analysis, it was observed that RTP801 immunoreactivity was minimal in the intact retina, significantly up-regulated in the retina after ONC, and attenuated after siRTP801 treatment, although not quite to the levels seen in uninjured animals (Figure 3.4C). Analysis of RTP801 immunostaining intensity in samples of the INL also demonstrated very low level expression in this retinal layer of uninjured animals, which was significantly up-regulated after ONC and reduced by siRTP801 treatment (Figure 3.4D). Taken together, these findings indicated that there was low constitutive activity of RTP801 in multiple cell types in the retina of intact uninjured animals, that ONC led to increased expression of RTP801 in RGC and non-neuronal cells in the GCL and also in cells of the INL (probably Müller glia), and that treatment with siRTP801 resulted in attenuation in RTP801 immunoreactivity in multiple retinal layers.

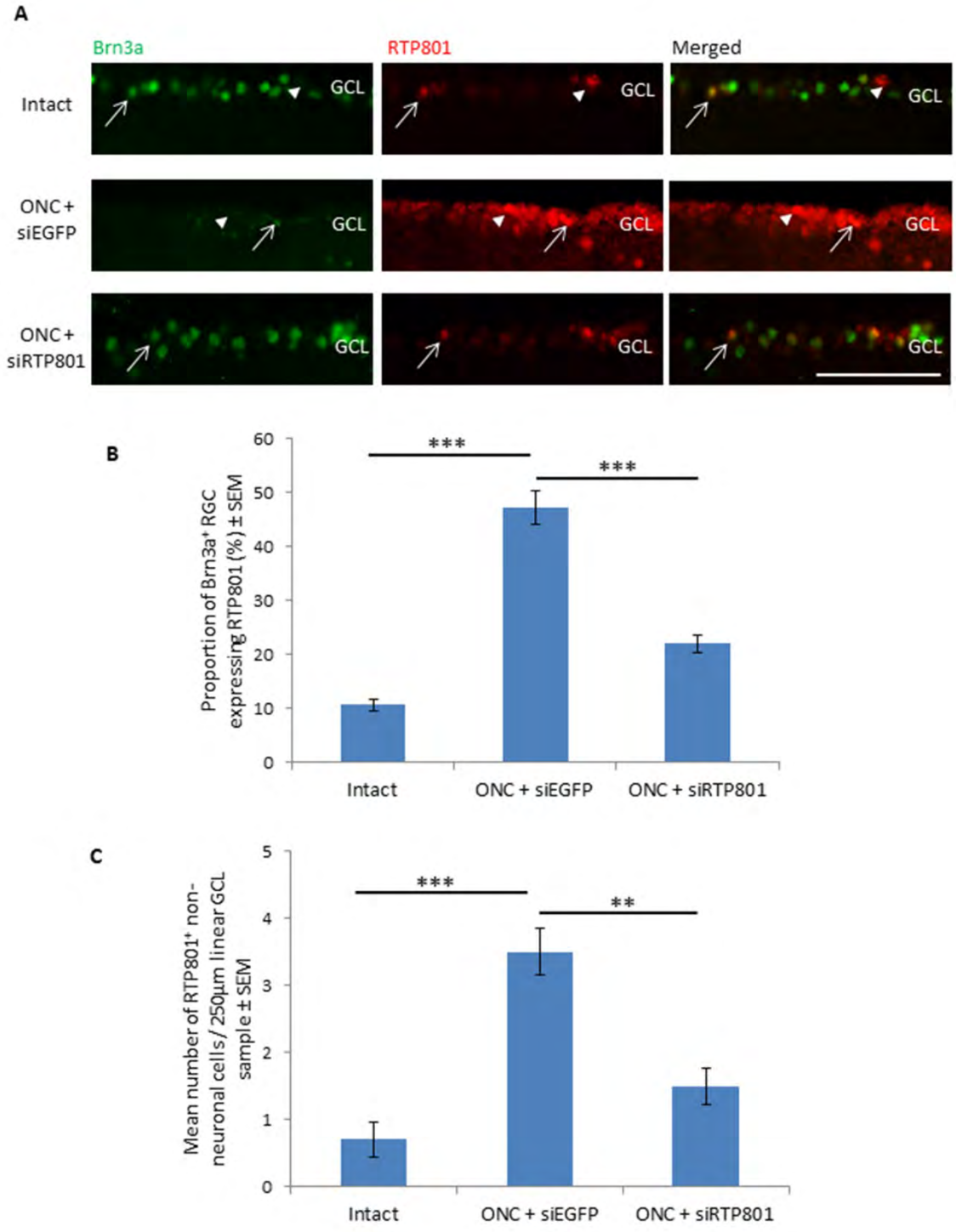


Figure 3.3: RTP801 expression in the retinal GCL after ONC, and siRTP801-mediated target knock-down in RGC and other GCL cells. (A) Retinal sections immunostained for Brn3a (green) and RTP801 (red) in the GCL of intact retinae (top row) and 24d after ONC + siEGFP (middle row) and ONC + siRTP801 (bottom row) (scale bar = 100µm). Note the presence of RTP801^{+} RGC (arrows) and also RTP801 expression in non-neuronal cells (arrowheads). (B) Quantification of RTP801^{+} RGC in a 250µm GCL linear region of the animals described in (A) (n=5 retinae/group; ***p<0.001), indicating target knock-down in RGC by siRTP801. (C) Quantification of RTP801 activity in Brn3a^{-} non-neuronal cells of the GCL for the groups described in (A) (n=5 retinae/group; **p<0.01, ***p<0.001), indicating target knock-down by siRTP801.

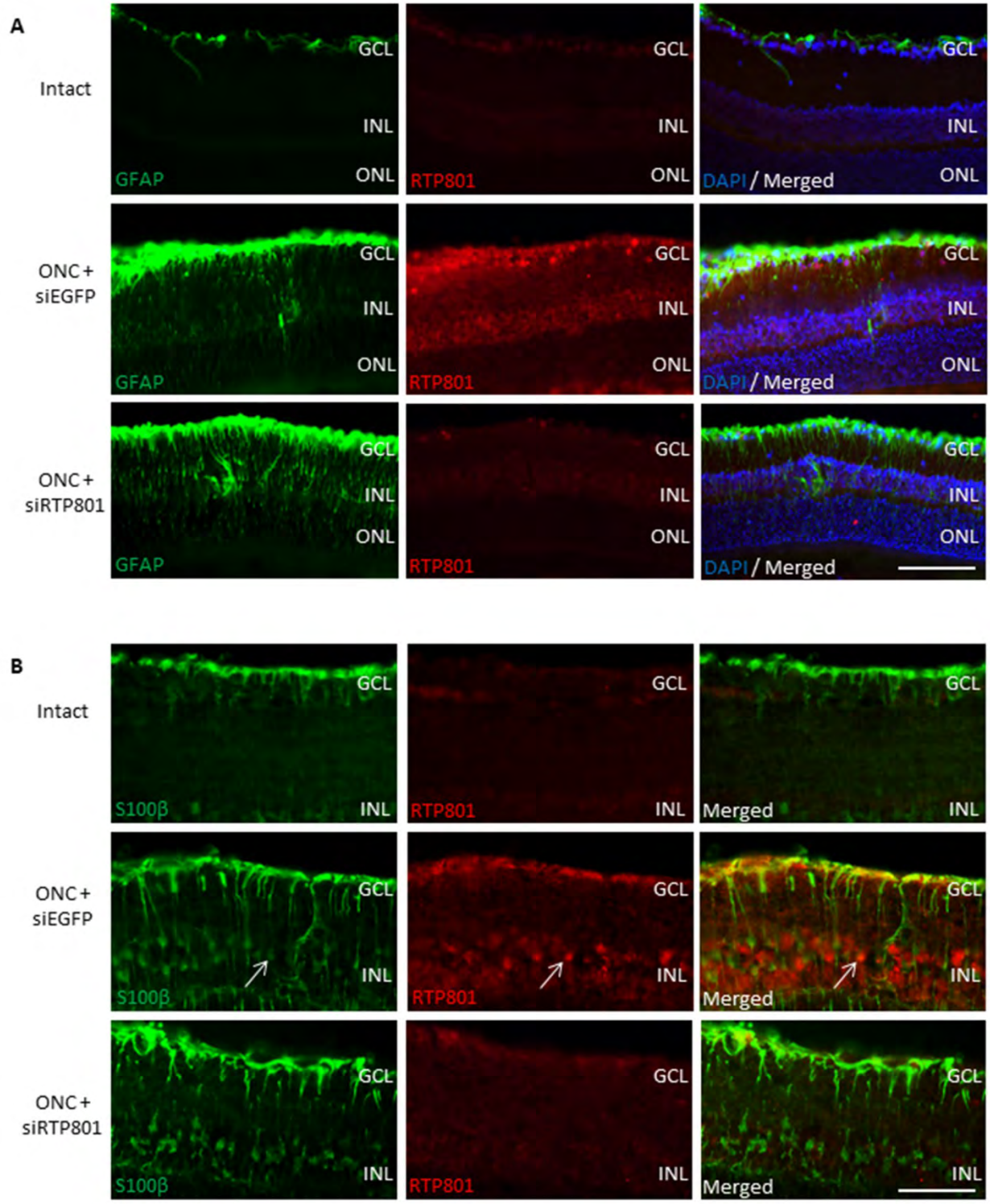


Figure 3.4: RTP801 expression and localisation with Müller glia in retinal sections, and siRTP801-mediated target knock-down in the INL. Retinal sections immunostained for RTP801 (red) and (A) GFAP (green), and (B) S100β (green) in intact retinae (top row) and 24d after ONC + siEGFP (middle row) and ONC + siRTP801 (bottom row) (scale bar = 100µm). Note the localisation of RTP801 expression with S100β^{+} Müller glia after ONC (arrow), which is reduced after siRTP801 treatment. Figure and legend continues on next page.

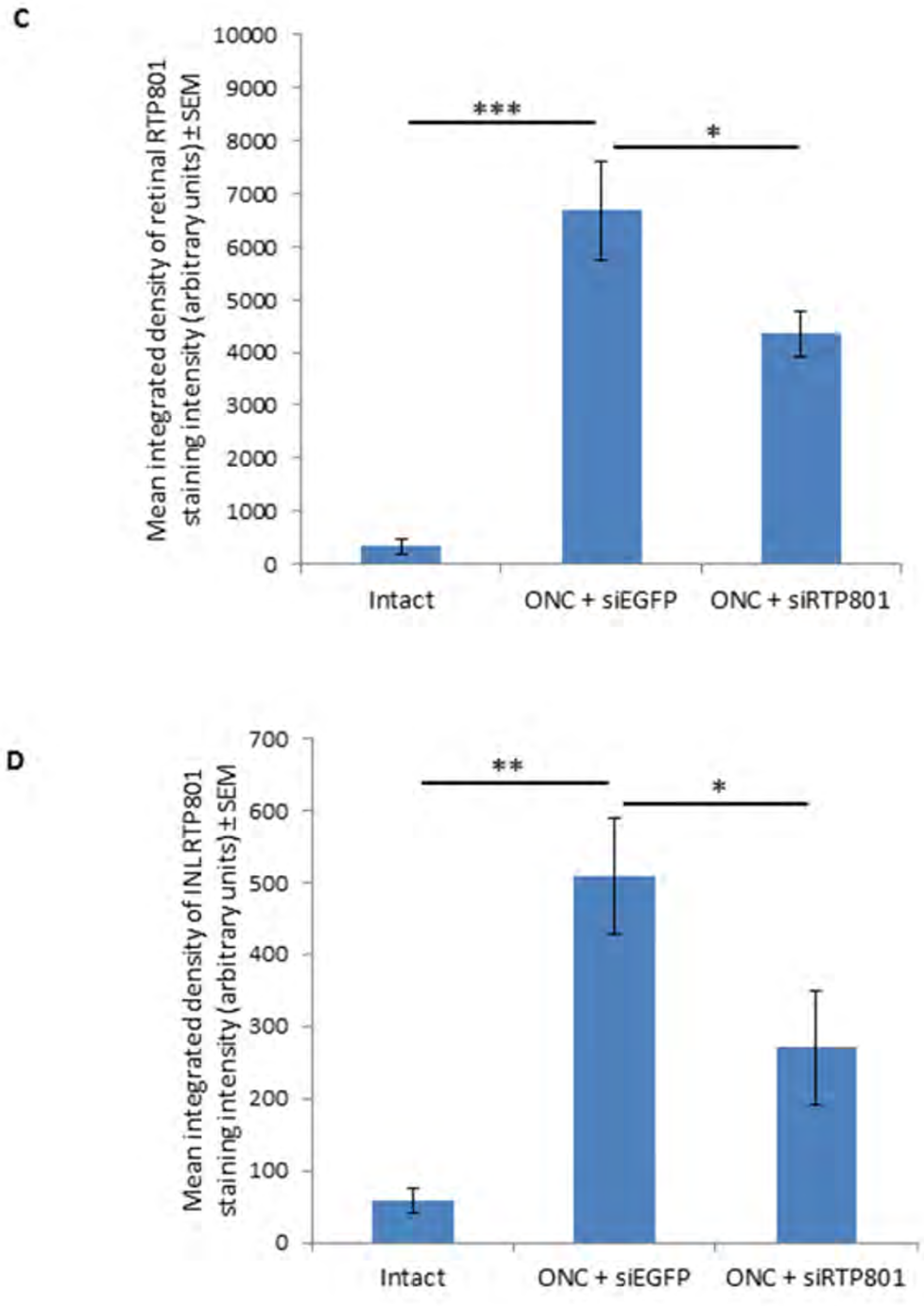


Figure 3.4: RTP801 expression and localisation with Müller glia in retinal sections, and siRTP801-mediated target knock-down in the INL. Continued from previous page. (C) Quantification of the immunostaining intensity of RTP801 in retinal sections of animals described in (A) and (B) (n=5 retinae/group; *p<0.05, ***p<0.001). (D) Quantification of the immunostaining intensity of RTP801 in the INL of retinal sections of animals described in (A) and (B) (n=5 retinae/group; *p<0.05, **p<0.01).

3.5.2.2 RTP801 cellular localisation and target knock-down in RGC and other retinal cell populations in vitro

To confirm the *in vivo* findings, retinal culture studies were undertaken to characterise the cellular localisation of RTP801 and the effects of siRTP801 transfection. RTP801 co-expression was observed in βIII-tubulin^{+} RGC in the primary retinal cultures (Figure 3.5A). The proportion of βIII-tubulin^{+} RGC expressing RTP801 in sNBA control wells (88.3 ± 12.1%) was significantly reduced by siRTP801 treatment of 10nM (25.6 ± 10.3%), 20nM (26.2 ± 12.5%) and 50nM (29.4 ± 10.9%) ($p<0.01$ at each test concentration, Figure 3.5B), confirming target knock-down in RGC. In control wells, there was no significant effect on RGC expression of RTP801 after incubation with either Lipofectamine solution or with siEGFP at 10, 20 or 50nM concentrations (Figure 3.5B).

In addition to RGC, it was evident from the retinal cultures that RTP801 activity was also detected in a population of βIII-tubulin^{-} cells (Figure 3.5A). The number of RTP801^{+}/βIII-tubulin^{-} cells in the sNBA control wells was 312.2 ± 23.9 cells, with no significant difference observed in Lipofectamine or siEGFP (10nM, 20nM or 50nM) control wells (Figure 3.5C). There was a significant reduction in the number of RTP801^{+}/βIII-tubulin^{-} cells in wells treated with siRTP801 at 10nM (134.2 ± 17.2 cells, $p<0.01$), 20nM (85.1 ± 14.5, $p<0.001$) and 50nM (113.5 ± 10.1 cells, $p<0.01$), demonstrating RTP801 target knock-down in non-neuronal cells (Figure 3.5C).

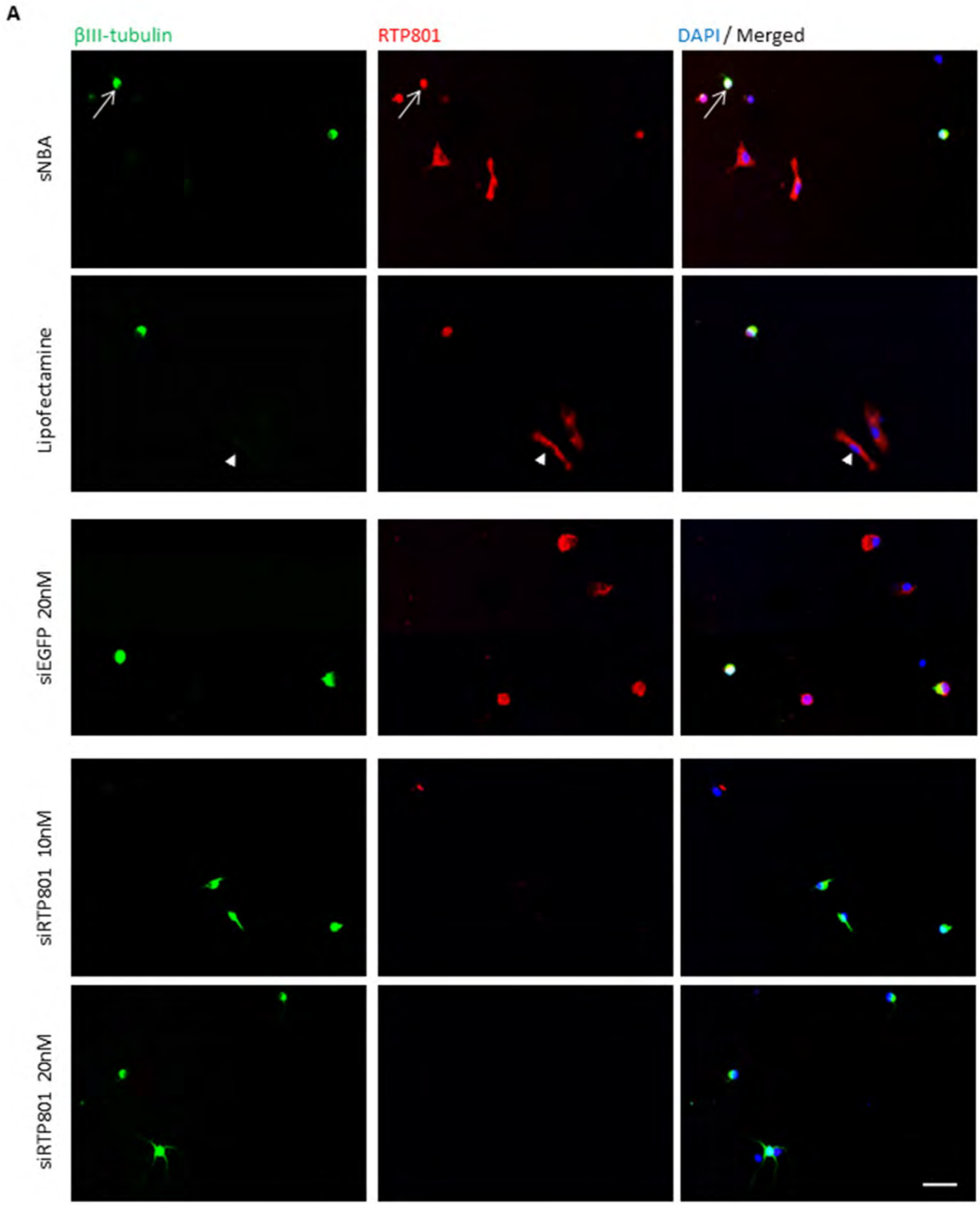


Figure 3.5: RTP801 cellular localisation and siRTP801-mediated target knock-down in retinal cultures established from uninjured animals. (A) Retinal cultures established from intact, uninjured animals, immunostained for βIII-tubulin (green) and RTP801 (red) with DAPI (blue) as a nuclear counterstain, after 3d incubation with sNBA culture medium (top row), Lipofectamine transfection reagent (2nd row), 20nM siEGFP (middle row) and siRTP801 (10nM and 20nM; 4th and 5th rows). Note the presence of RTP801^{+} RGC (arrows) and non-neuronal cells (arrowheads), and the reduced RTP801 expression in siRTP801-treated wells, indicating target knock-down (scale bar = 20µm). Figure and legend continues on the next page.

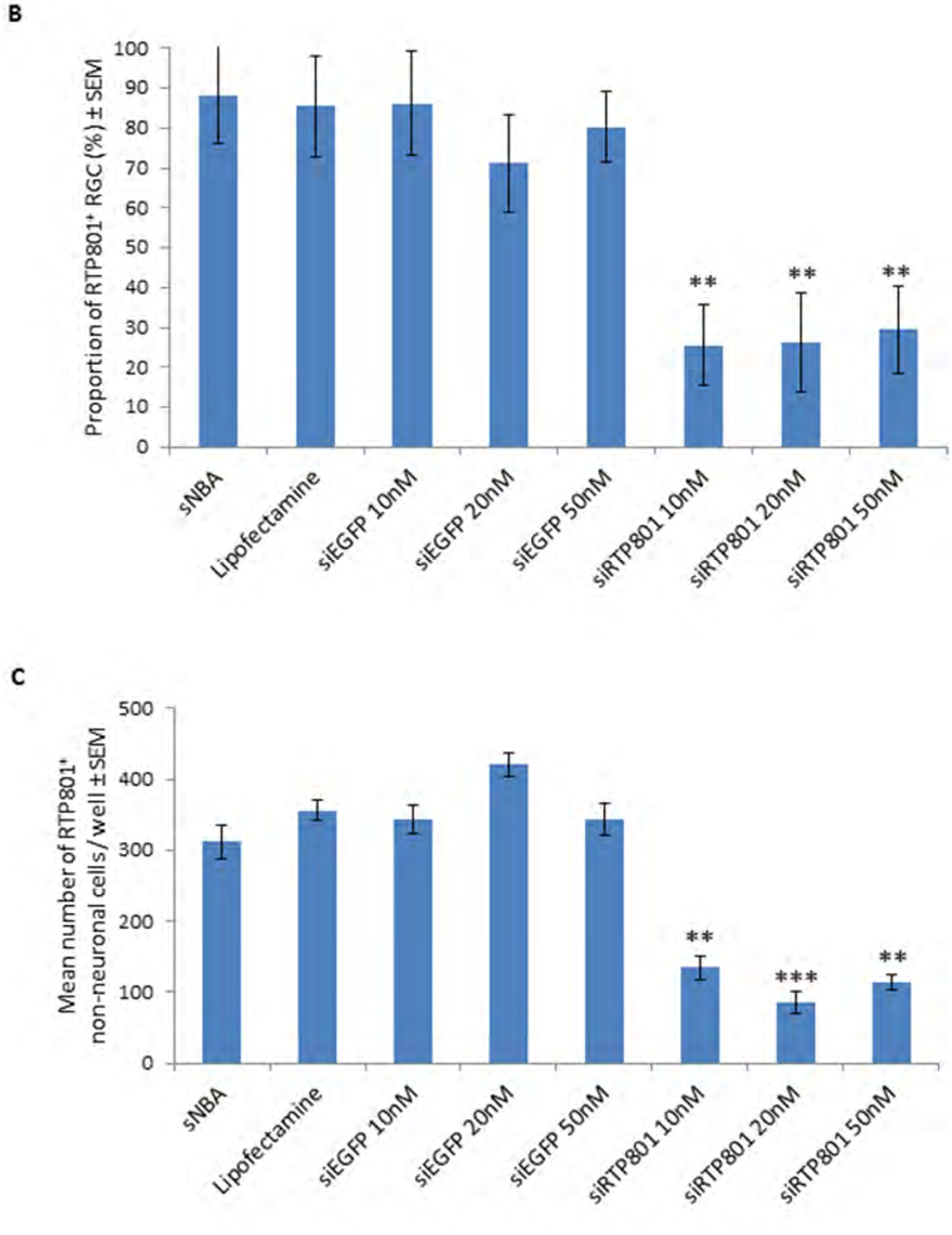


Figure 3.5: RTP801 cellular localisation and siRTP801-mediated target knock-down in retinal cultures established from uninjured animals. Continued from previous page. (B) Proportion of βIII-tubulin^{+} RGC co-expressing RTP801 in retinal cultures after siRTP801 treatment at concentrations of 10nM, 20nm and 50nM, and control wells (n=3; **p<0.01 vs sNBA control), indicating siRTP801-mediated target knock-down in RGC. (C) Quantification of RTP801^{+} non-neuronal cells in retinal cultures after siRTP801 treatment at concentrations of 10nM, 20nm and 50nM, and control wells (n=3; **p<0.01, ***p<0.001 vs sNBA control), indicating siRTP801-mediated target knock-down in non-neuronal retinal cells.

To characterise the cell population(s) expressing RTP801 in addition to RGC, further primary retinal cultures were undertaken and immunocytochemistry performed for the co-localisation of RTP801 with other phenotypic antibody markers. There were no $GFAP^+$ activated glia present after incubation of retinal cultures prepared from intact eyes in the presence of either sNBA culture medium alone, siEGFP or siRTP801 (Figure 3.6A), demonstrating an absence of activated astrocytes/Müller glia in this primary cell culture model (Riechenbach, 2013). Furthermore, immunocytochemistry with the activated Müller glial marker CRALBP (Wahlin *et al.*, 2004; Lindqvist *et al.*, 2010; Riechenbach, 2013; Wahlin *et al.*, 2000) demonstrated an absence of this cell population also (Figure 3.6B).

Immunostaining retinal cultures for calbindin, a phenotypic cell marker expressed by horizontal cells (Hamano *et al.*, 1990; Pochet *et al.*, 1991; Morquette *et al.*, 2014), demonstrated the presence of low numbers of $calbindin^+$ cells in untreated sNBA control wells (33.5 ± 11.2 cells), with no significant difference in this cell population after incubation with either siEGFP (20.6 ± 6.8 cells) or siRTP801 (25.8 ± 6.8) (Figure 3.7A, B). The proportion of $calbindin^+$ cells expressing RTP801 was 55.9 ± 9.8% in sNBA wells, and this was not significantly affected by either siEGFP (72.2 ± 14.7%) or siRTP801 (47.8 ± 7.8%) (Figure 3.7C), suggesting that whilst RTP801 was expressed in horizontal cells, treatment with siRTP801 neither affected the number of these cells, nor achieved measurable target knock-down in this cell population in this model.

Despite the absence of $GFAP^+$ or $CRALBP^+$ activated glia in these cultures, $S100\beta^+$ (quiescent) glia were present, with a total of 307.0 ± 33.5 cells in sNBA control wells, 263.2 ± 20.5 cells in siEGFP wells and 299.3 ± 15.7 cells in siRTP801-transfected wells, with no significant difference in total $S100\beta^+$ cell number between these groups (Figure 3.8A, B). In these wells, co-localisation of RTP801 was observed in 87.7 ± 5.2% and 84.4 ± 3.7% $S100\beta^+$ cells in sNBA and siEGFP wells, respectively,

numbers that were significantly reduced after treatment with siRTP801, which resulted in 36.7 ± 11.8% RTP801^{+}/S100β^{+} cells (p=0.008 *vs* sNBA control, p=0.012 *vs* siEGFP control) (Figure 3.8C). These data demonstrated that RTP801 was expressed in quiescent retinal glia, siRTP801 did not influence the number of S100β^{+} glia in these primary retinal cultures, and that siRTP801 significantly knocked-down RTP801 expression in these glial cells.

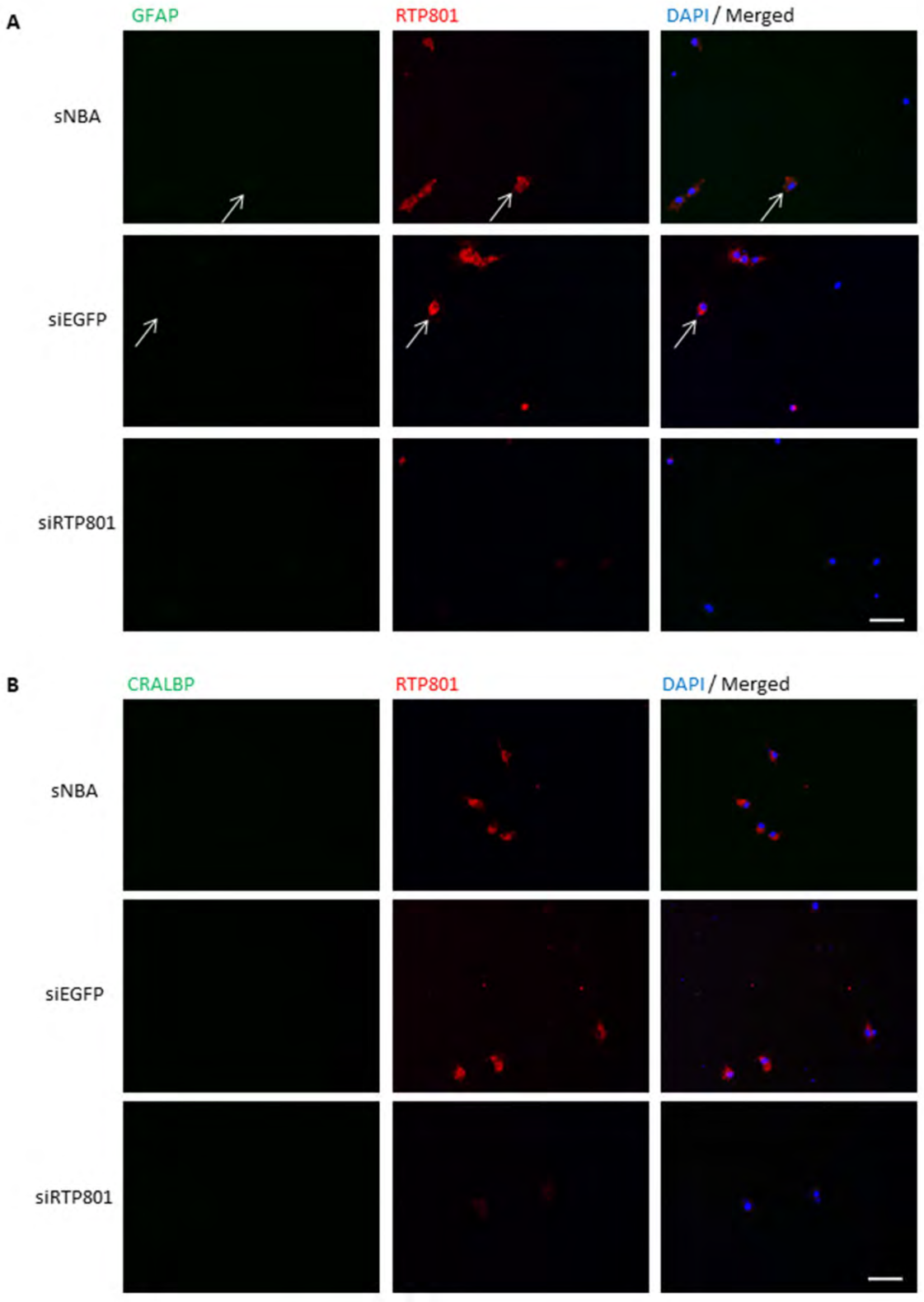


Figure 3.6: Lack of GFAP$^+$ or CRALBP$^+$ activated retinal glia in cultures established from uninjured intact animals. Retinal cultures established from uninjured intact animals immunostained for RTP801 (red), (A) GFAP (green) and (B) CRALBP (green), with DAPI (blue) as a nuclear counterstain, after 3d incubation with sNBA culture medium (top row), siEGFP (middle row) and siRTP801 (bottom row), indicating the presence of RTP801$^+$ cells predominantly in control wells (arrows), but an absence of activated retinal glia (scale bar = 20µm).

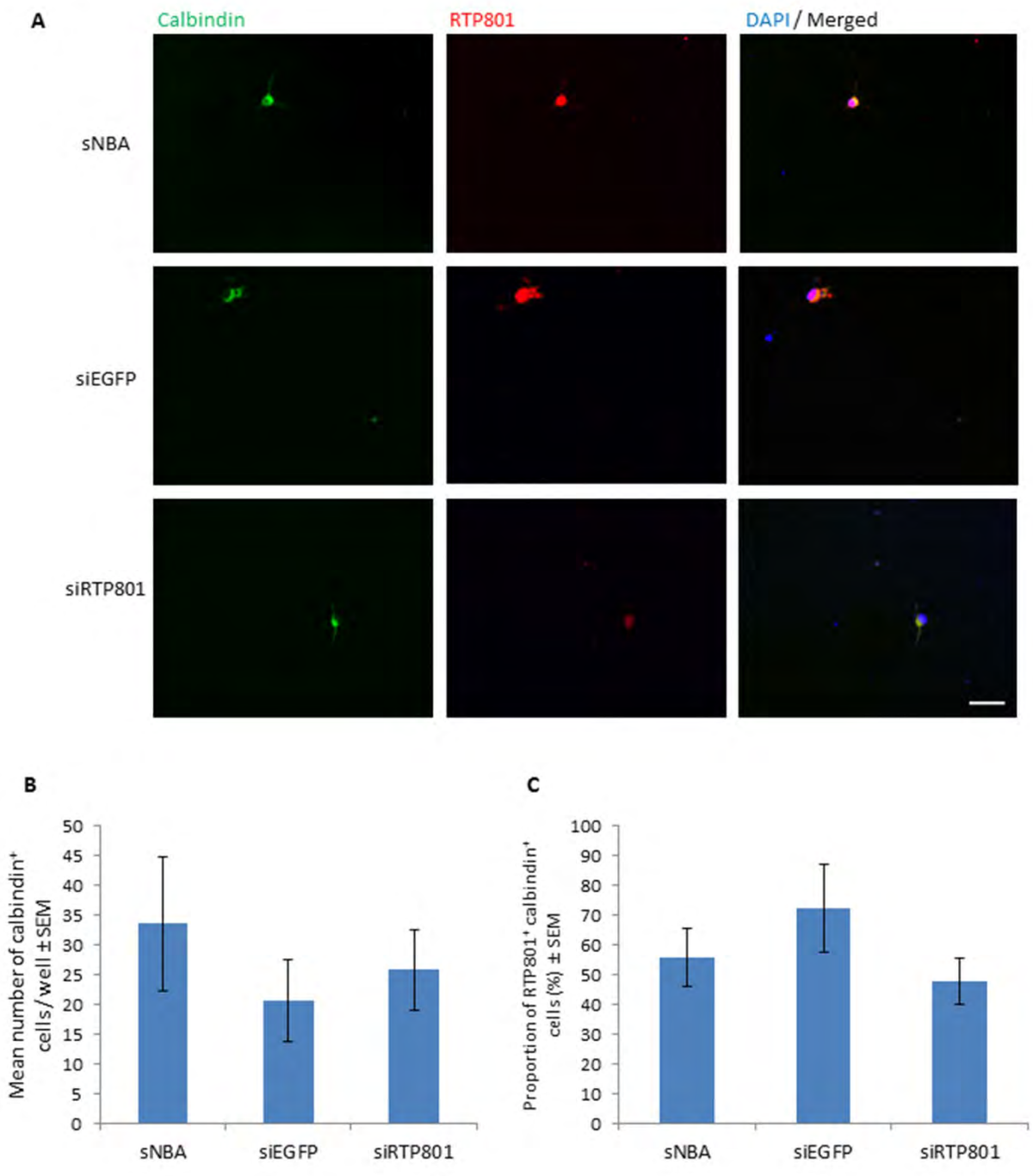


Figure 3.7: RTP801 expression in calbindin$^+$ horizontal cells *in vitro*, and lack of target knock-down by siRTP801. (A) Retinal cultures established from uninjured intact animals immunostained for calbindin (green) and RTP801 (red), with DAPI (blue) as a nuclear counterstain, after 3d incubation with sNBA culture medium (top row), siEGFP (middle row) and siRTP801 (bottom row), indicating RTP801 co-expression with calbindin$^+$ horizontal cells (scale bar = 20µm). (B) Quantification of calbindin$^+$ cells in retinal cultures as described in (A), indicating no significant difference in observed calbindin$^+$ cell number between treatment groups (n=3). (C) Proportion of calbindin$^+$ cells co-expressing RTP801 in cultures as described in (A), indicating a lack of target knock-down by siRTP801 in this cell population (n=3).

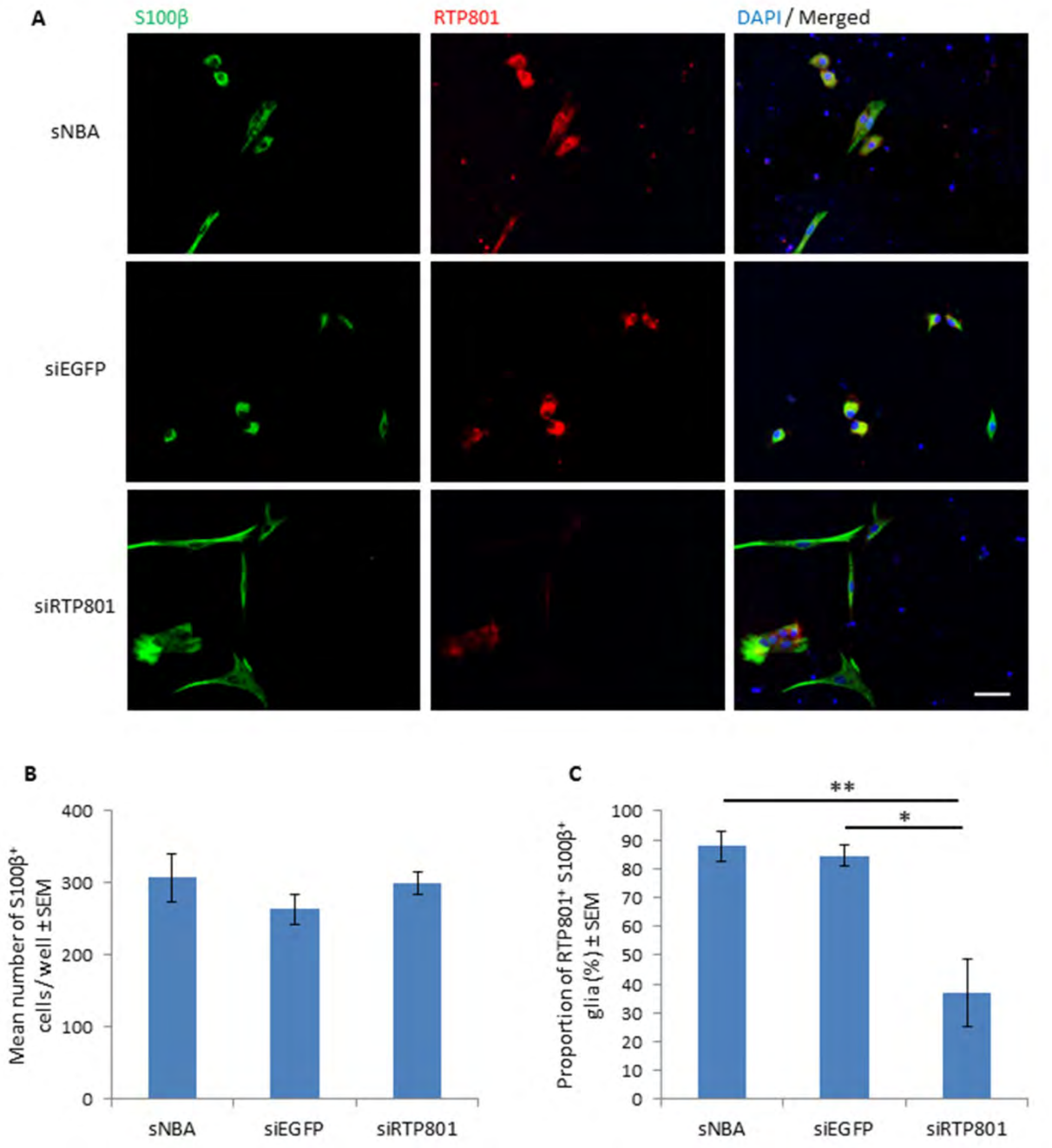


Figure 3.8: RTP801 expression in S100β$^+$ retinal glia *in vitro* and siRTP801-mediated target knock-down. (A) Retinal cultures established from uninjured intact animals immunostained for S100β (green) and RTP801 (red), with DAPI (blue) as a nuclear counterstain, after 3d incubation with sNBA culture medium (top row), siEGFP (middle row) and siRTP801 (bottom row), indicating RTP801 co-expression with S100β$^+$ glia and a reduced RTP801 expression in siRTP801-treated wells (scale bar = 20µm). (B) Quantification of S100β$^+$ cells in retinal cultures as described in (A), indicating no significant difference in observed S100β$^+$ cell number between treatment groups (n=3). (C) Proportion of S100β$^+$ glia expressing RTP801 in cultures as described in (A), indicating siRTP801-mediated target knock-down in this cell population (n=3; *p<0.05, **p<0.01).

3.5.3 Effects of siRTP801 on RGC survival and axon regeneration after ONC *in vivo*

3.5.3.1 siRTP801 promoted RGC survival up to 24d after ONC

A preliminary analysis was undertaken directly comparing RGC survival at 24d after ONC between the siRTP801-treated and the siEGFP control-injected eyes, using the RGC phenotypic marker βIII-tubulin. There was a significantly greater number of βIII-tubulin^{+} RGC in the GCL of siRTP801-treated eyes (17.4 ± 0.4 RGC/250µm GCL) compared to eyes injected with siEGFP (14.1 ± 0.3, $p<0.001$) (Figure 3.9A, B), indicating a RGC neuroprotective effect of siRTP801. This finding was verified in a follow-up analysis using Brn3a, considered a more specific RGC marker which, as a nuclear-expressed factor, is easier to identify and quantify than βIII-tubulin, and accurately correlates RGC survival as well as Fluorogold back-filled retinal whole-mounts (Nadal-Nicolas *et al.*, 2009; Mead *et al.*, 2014). In this evaluation using retinal sections from the same ONC/injected animals, compared to a group of uninjured intact control animals (20.4 ± 0.6 RGC/250µm GCL) there was a significant reduction in Brn3a^{+} RGC survival at 24d after ONC and intravitreal siEGFP (9.2 ± 0.6 RGC, $p<0.001$) (Figure 3.10A, B). Intravitreal treatment with siRTP801 promoted a significant increase in Brn3a^{+} RGC survival (16.9 ± 0.6 RGC, $p<0.001$) compared to those receiving siEGFP (Figure 3.10A, B). In comparison with intact control eyes, treatment with siRTP801 allowed survival of 82% RGC at 24d after ONC, whereas RGC survival after inactive control siEGFP was 45%. These results indicated that targeted siRNA-mediated knock-down of RTP801 was RGC neuroprotective after ONC, and validated similar results obtained in previous evaluations from our laboratory (Table 3.1; Neuregenix, unpublished data). The small quantitative discrepancy in the RGC survival between the βIII-tubulin and Brn3a antibody markers probably reflects the presence of other GCL cells, such as displaced amacrine cells, that are more likely to be immuno-positive for βIII-tubulin than the more RGC specific Brn3a (Mead *et al.*, 2014).

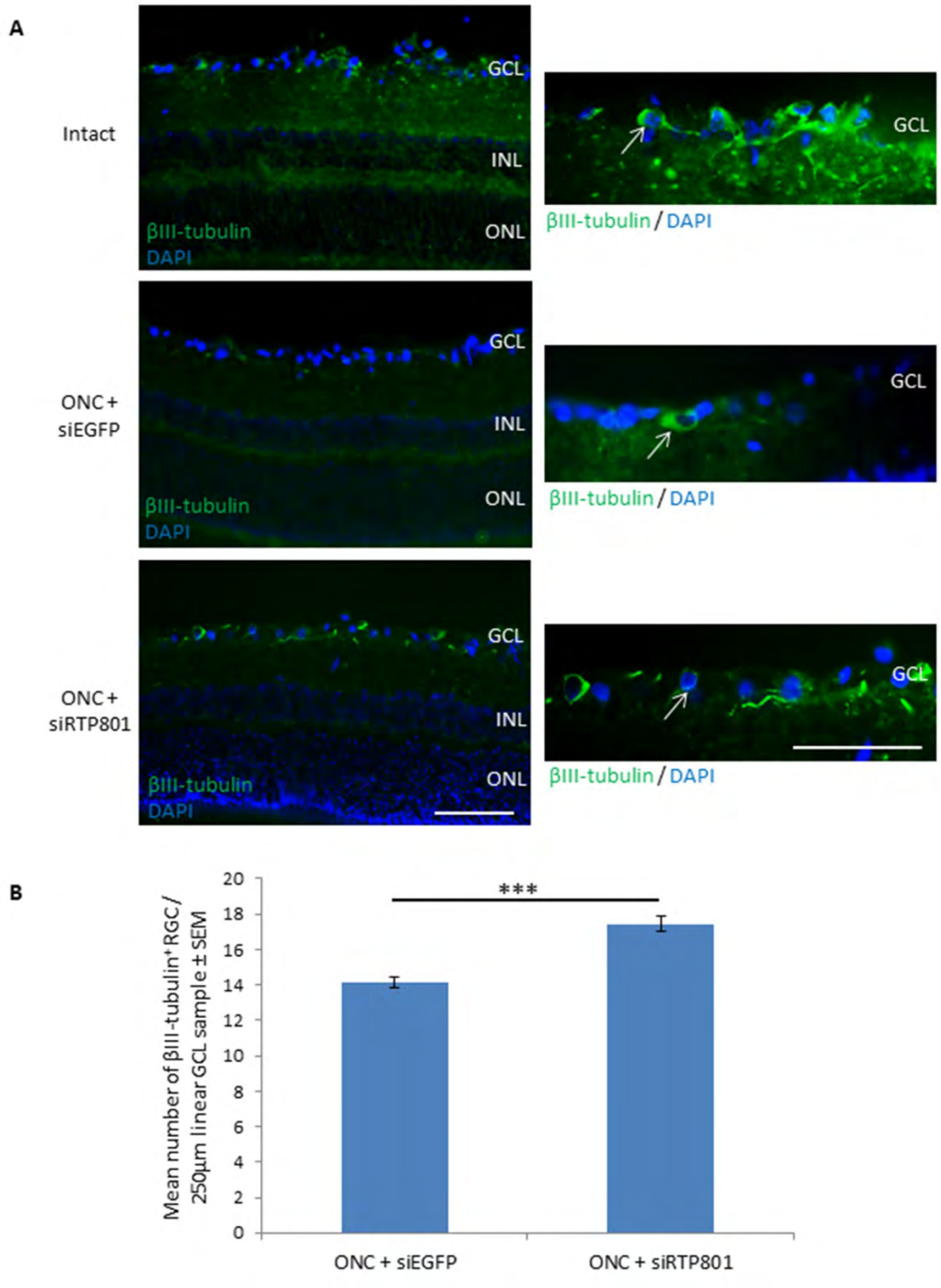


Figure 3.9: βIII-tubulin$^+$ RGC survival after ONC *in vivo*. (A) Retinal sections immunostained for βIII-tubulin (green) with DAPI (blue) as a nuclear counterstain, in intact retinae (top row) and 24d after ONC + siEGFP (middle row) and ONC + siRTP801 (bottom row). Note the reduced expression of βIII-tubulin in the GCL after ONC, which is restored after siRTP801 treatment (scale bar = 100µm). (B) Quantification of surviving βIII-tubulin$^+$ RGC in a 250µm GCL sample in a preliminary analysis, directly comparing treatment with siRTP801 against siEGFP control at 24d after ONC (n=5 retinae/group; ***p<0.001).

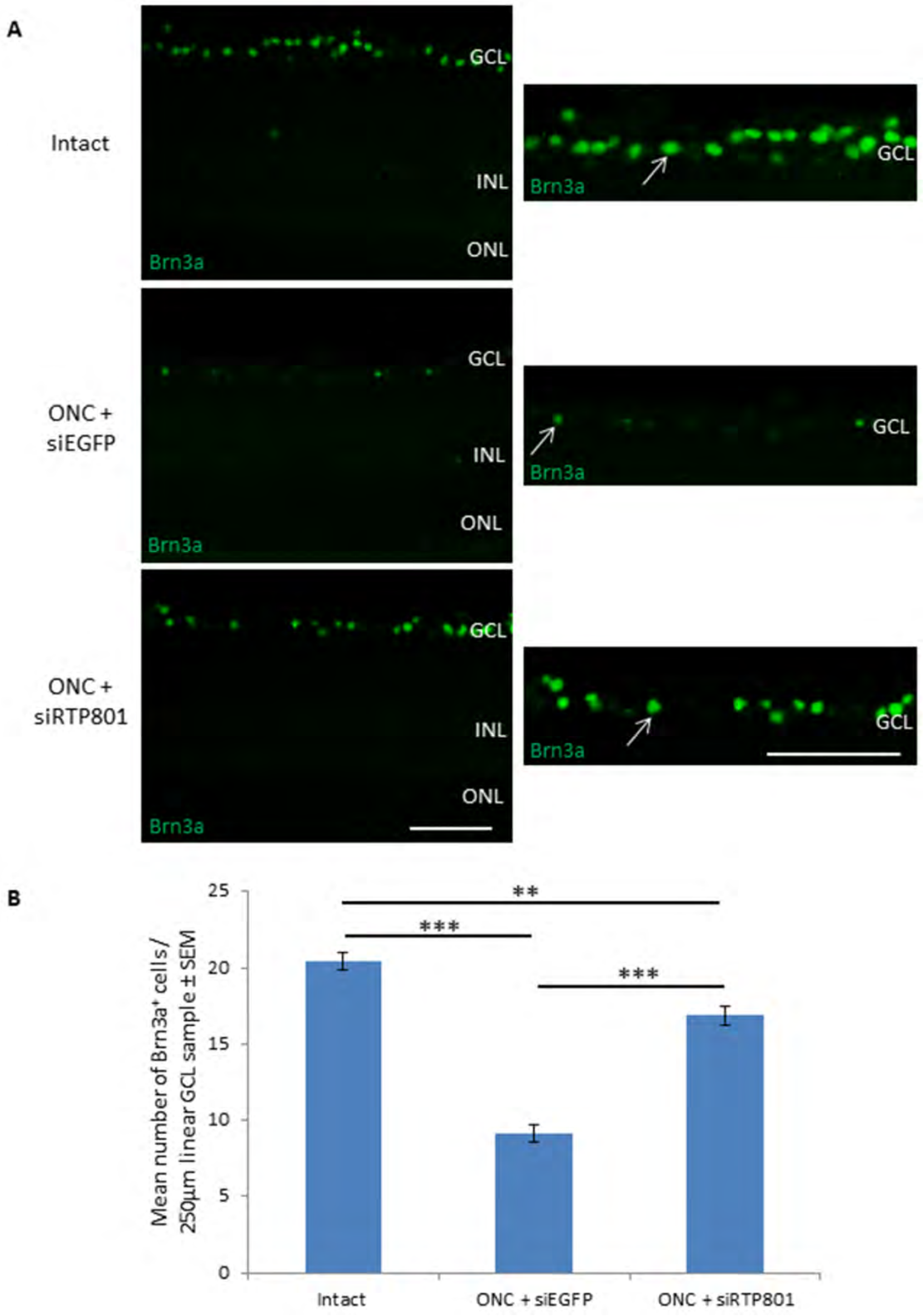


Figure 3.10: Brn3a$^+$ RGC survival after ONC *in vivo*. (A) Retinal sections immunostained for Brn3a (green), in intact retinae (top row) and 24d after ONC + siEGFP (middle row) and ONC + siRTP801 (bottom row). Note the reduced expression of Brn3a in the GCL (arrows) after ONC, which is restored after siRTP801 treatment (scale bar = 100µm). (B) Quantification of surviving Brn3a$^+$ RGC in a 250µm GCL sample in retinal sections from animals described in (A) at 24d after ONC (n=5 retinae/group; **p<0.01, ***p<0.001), indicating significant RGC survival after siRTP801 treatment.

3.5.3.2 siRTP801 promoted longer growth of regenerating RGC axons up to 1200µm beyond the injury site without affecting the initiation of axon sprouting after ONC

After ONC there was no significant difference in the number of $GAP43^+$ RGC axons in the ON at 100µm and 200µm distal to the centre of the ONC site between siRTP801- and siEGFP-injected eyes (Figure 3.11A, B). However, the number of $GAP43^+$ regenerating axons was significantly greater at 400µm ($p=0.024$), 800µm ($p=0.015$) and 1200µm ($p=0.002$) distal to the crush site after treatment with siRTP801 (87.1 ± 21.1, 68.9 ± 11.2, 55.8 ± 11.5 axons/nerve, respectively) compared to siEGFP (44.9 ± 23.0, 28.6 ± 15.8, 15.4 ± 9.9 axons/nerve, respectively) (Figure 3.11A, B), with the difference between treatment and control becoming more pronounced as the distance from the ONC site increased. These results showed that siRTP801 and control siEGFP resulted in initial sprouting of similar numbers of RGC axons about the injury site, but siRTP801 treatment sustained significantly longer growth of $GAP43^+$ regenerating axons along the distal ON segment after ONC. These findings support similar results obtained as part of previous evaluations from our laboratory (Table 3.2; Neuregenix, unpublished data).

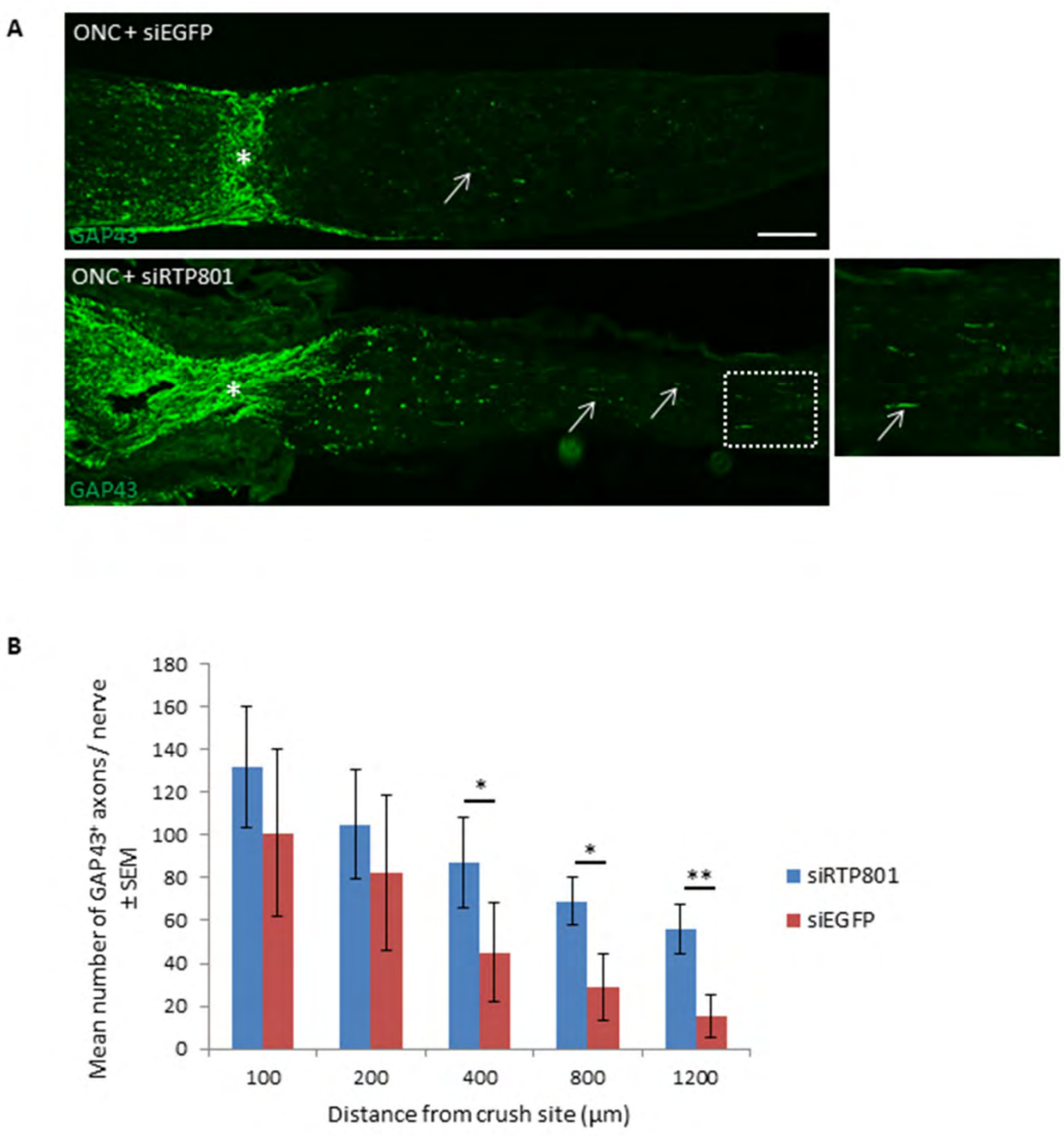


Figure 3.11: Enhanced RGC axon elongation by siRTP801 after ONC without affecting initiation of axon regeneration. (A) Longitudinal ON sections immunostained to demonstrate GAP43^{+} regenerating axons (arrows) after ONC + siEGFP (top panel) and ONC + siRTP801 (lower panel) (scale bar = 200µm). The asterisk demarcates the centre of the ONC sites and the boxed area in the lower panel represents the magnified area. Note the increased number of axons in the proximal ON segment after siRTP801 treatment correlates with enhanced RGC survival. (B) Quantification of GAP43^{+} regenerating axons at 100, 200, 400, 800 and 1200µm beyond the ONC site in siRTP801-treated (blue bars) and siEGFP-treated (red bars) eyes (n=5 nerves/group; *p<0.05, **p<0.01).

3.5.4 Effect of siRTP801 on RGC survival and neurite outgrowth in cultured retinal cells *in vitro*

In order to the confirm the *in vivo* findings, and as the basis for further investigations into putative underlying mechanisms of the RGC neuroprotective and axon elongation effects of siRNA-mediated knock-down of RTP801, experiments were undertaken in cultures prepared from dissociated retinal cells from uninjured adult rats.

3.5.4.1 siRTP801 was RGC neuroprotective in primary retinal cultures from uninjured animals

In primary retinal cultures established from intact adult rat eyes, 3d siRTP801 treatment with 10nM, 20nM and 50nM significantly increased the survival of βIII-tubulin^{+} RGC from 327.7 ± 15.6 RGC/well in untreated (sNBA culture medium alone) controls to 528.7 ± 23.9 RGC, 620.7 ± 15.6 RGC and 533.3 ± 23.3 RGC, respectively ($p<0.001$ at each test concentration) (Figure 3.12A, B). There was no significant difference in RGC survival after incubation of retinal cultures with the siRNA transfection agent Lipofectamine without siRNA (294.3 ± 13.9 RGC), or with siEGFP controls at concentrations of 10nM (264.3 ± 13.9 RGC), 20nM (259.3 ± 23.6 RGC) and 50nM (266.7 ± 22.6 RGC) (Figure 3.12A, B).

3.5.4.2 siRTP801 neither initiated RGC neurite outgrowth nor increased RGC neurite length in primary retinal cultures from uninjured animals

In the same retinal cultures, the proportion of βIII-tubulin^{+} RGC extending at least one neurite in untreated wells was 27.7 ± 3.2%, and no significant difference was observed in wells exposed to Lipofectamine (29.2 ± 2.5%), siEGFP at 10nM (32.5 ± 4.7%), 20nM (29.1± 3.6%) or 50nM (27.5 ± 2.8%), or siRTP801 at 10nM(30.2 ± 7.0%), 20nM (31.2 ± 5.7%) or 50nM (27.7 ± 4.0%) (Figure 3.12C).

The mean length of the longest neurite in RGC in untreated controls was 44.8 ± 4.4µm, and there was no significant difference in neurite lengths in wells exposed to Lipofectamine alone (39.6 ± 3.0µm), siEGFP at 10nM (39.4 ± 2.2µm), 20nM (40.1 ± 1.9µm) or 50nM (43.7 ± 2.6µm), or siRTP801 at 10nM (39.8 ± 1.6µm), 20nM (45.1 ± 2.2µm) or 50nM (51.5 ± 2.9µm) (3.12D). These data indicated that in primary retinal cultures established from eyes of intact uninjured adult rats, containing no activated retinal glia, siRTP801 neither promoted the initiation of RGC neurite sprouting, nor affected the length of RGC neurites.

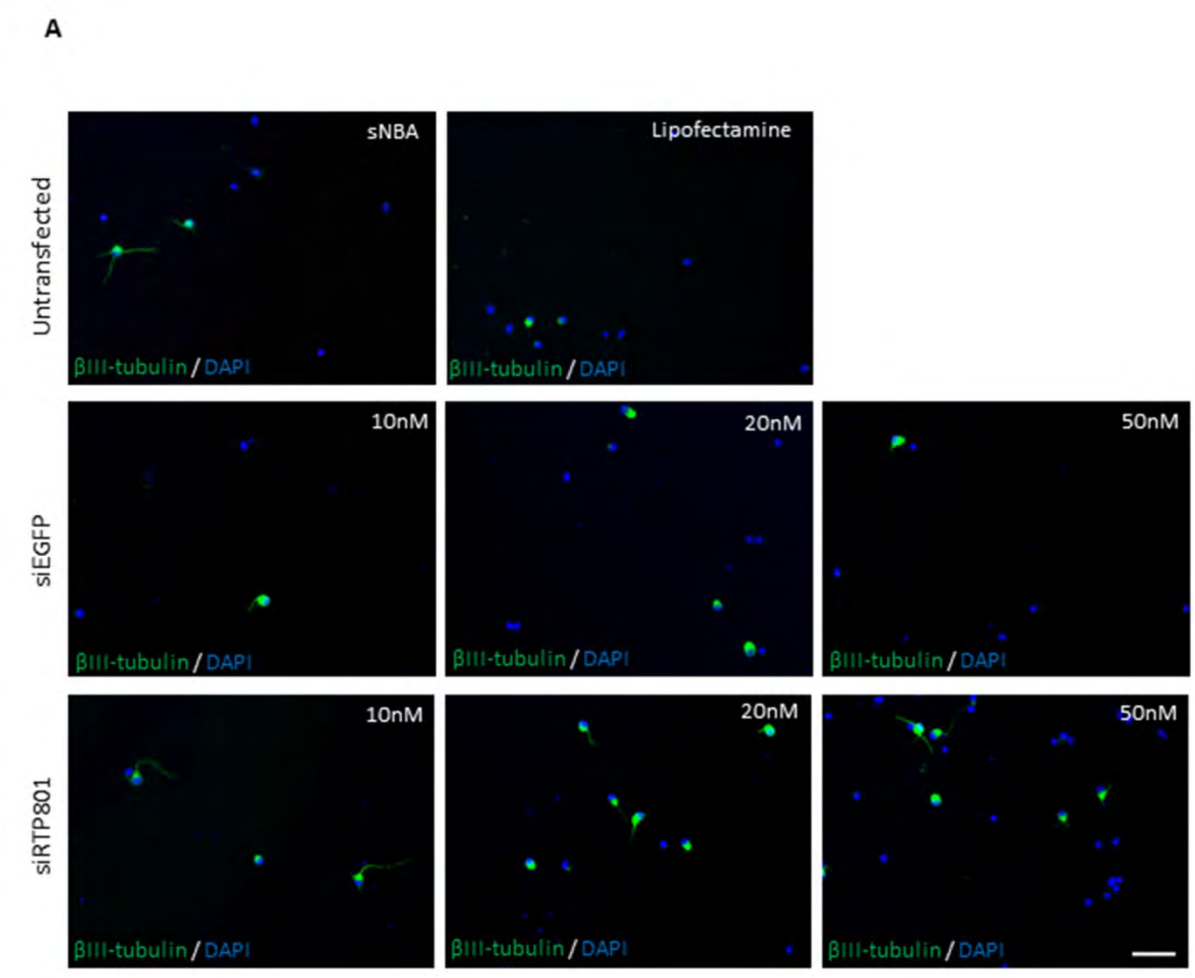


Figure 3.12: RGC survival and neurite outgrowth in cultured retinal cells in the absence of activated retinal glia. (A) Retinal cultures established from intact, uninjured animals, immunostained for βIII-tubulin (green) with DAPI (blue) as a nuclear counterstain, after 3d incubation with sNBA culture medium, Lipofectamine transfection reagent (top row), siEGFP (10nM, 20nM and 50nM, middle row) and siRTP801 (10nM, 20nM and 50nM, bottom row) (scale bar = 20µm). Figure and legend continues on next page.

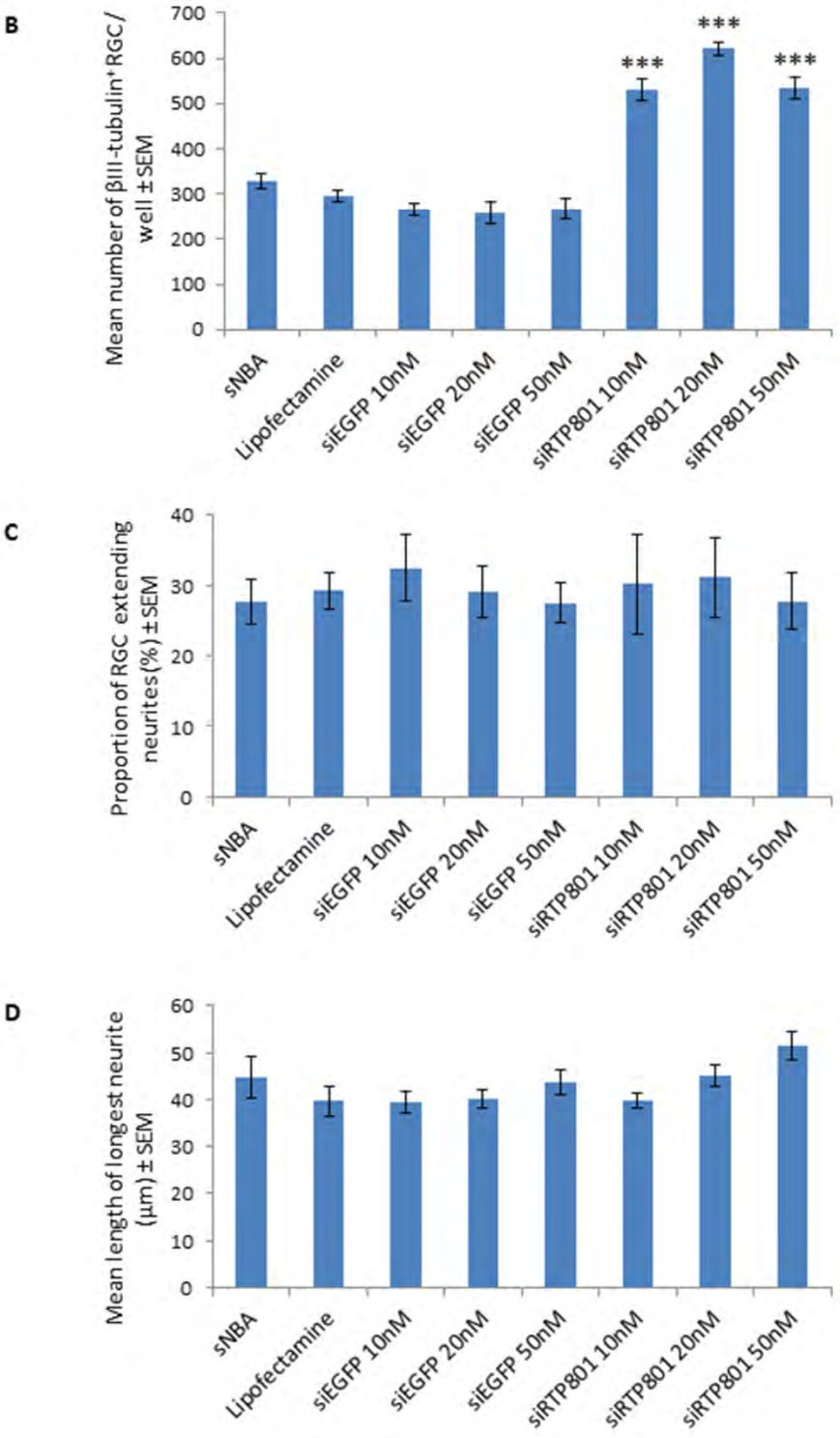


Figure 3.12: RGC survival and neurite outgrowth in cultured retinal cells in the absence of activated retinal glia. Continued from previous page. (B) Quantification of surviving βIII-tubulin$^+$ RGC for cultures described in (A) in the absence of activated retinal glia, indicating a significant RGC neuroprotective effect of siRTP801 (n=3; ***p<0.001 vs sNBA control). (C) Proportion of βIII-tubulin$^+$ RGC extending neurites, and (D) length of longest RGC neurites in cultures described in (A) (n=3). Note that in common with the *in vivo* setting, siRTP801 had no effect on initiation of neurite outgrowth, but in contrast there was also no effect on neurite elongation in these retinal cultures established from intact, uninjured animals.

3.5.5 Summary of results

These results have demonstrated that siRTP801 is a target-specific siRNA, resulting in effective knock-down without the induction of a non-specific pro-inflammatory response. RTP801 expression was low in the retina of uninjured animals *in vivo*, but was significantly up-regulated in cells of the GCL and INL after ONC, and was significantly reduced by siRTP801 treatment. Retinal cultures confirmed that RTP801 activity was evident in RGC, glia and horizontal cells, with significant knock-down in RGC and glia, but not in horizontal cells. Treatment with RTP801 promoted RGC survival after ONC, and had no effect on initiation of RGC axon regeneration but promoted elongation of regenerating axons in the distal ON. Treatment of retinal cultures with siRTP801 *in vitro* enhanced RGC survival in the absence of activated retinal astrocytes/Müller glia, but had no significant effect on either the initiation of neurite outgrowth or the length of neurite growth.

		Intact	ONC + PBS	ONC + siEGFP	ONC + siRTP801
RGC Survival	**Study 1**	21.7 ± 0.3	10.9 ± 0.4	12.1 ± 0.4	17.6 ± 0.4
	Study 2	21.5 ± 0.5	10.9 ± 0.7	14.4 ± 0.9	16.7 ± 0.7

Table 3.1: Effects of siRTP801 on RGC survival after ONC (Quark/Neuregenix). RGC survival in intact uninjured animals and 24d after ONC with either siEGFP or siRTP801. Adult male Wistar rats (n=4/group) underwent bilateral ONC and intravitreal injection of either siRTP801 (20µg) in combination with inactive control siEGFP (20µg, total siRNA 40µg/10µl/eye), control siEGFP alone (40µg/10µl/eye), or PBS at 0d, 8d and 16d post-ONC. Tissues were harvested at 24d for immunohistochemical analysis of βIII-tubulin$^+$ RGC in a 250µm linear region of the GCL as described in Chapter 2. siRTP801 was identified as a suitable candidate for further study. Data kindly provided by Quark Pharmaceuticals and Neuregenix.

			Distance from centre of crush site (µm)				
			100	**200**	**400**	**800**	**1200**
Number of GAP43$^+$ axons beyond crush site	**Study 1**	**siRTP801**	170.5 ± 74.6	215.5 ± 55.2	120.8 ± 44.3	104.5 ± 42.5	62.1 ± 27.3
		siEGFP	176.0 ± 45.4	44.4 ± 26.4	33.7 ± 20.4	14.4 ± 9.7	1.7 ± 1.6
		PBS	109.1 ± 23.4	46.8 ± 16.8	7.5 ± 4.7	6.6 ± 4.2	2.7 ± 2.4
	Study 2	**siRTP801**	177.6 ± 49.3	110.5 ± 31.0	80.2 ± 16.6	47.9 ± 7.1	49.0 ± 12.8
		siEGFP	122.8 ± 28.4	58.9 ± 15.8	19.9 ± 6.9	21.3 ± 5.2	11.8 ± 4.4

Table 3.2: Effects of siRTP801 on axon regeneration after ONC (Quark/Neuregenix). GAP43$^+$ axons observed distal to the ONC site after siRTP801 in previous *in vivo* studies. Adult male Wistar rats (n=4/group) underwent bilateral ONC and intravitreal injection of either siRTP801 (20µg) in combination with inactive control siEGFP (20µg, total siRNA 40µg/10µl/eye) or control siEGFP alone (40µg/10µl/eye) at 0d, 8d and 16 d post-ONC. Tissues were harvested at 24d for immunohistochemical analysis of GAP43$^+$ regenerating axons in longitudinal ON sections as described in Chapter 2. siRTP801 was identified as a suitable candidate for further study. Data kindly provided by Quark Pharmaceuticals and Neuregenix.

3.6 DISCUSSION

In recent years there has been much interest in the mTOR cellular signalling pathway as a determinant of neuronal viability and axon regenerative ability, and consequently, experimental approaches to up-regulate mTOR activity have suggested this pathway as a potentially useful therapeutic target to promote RGC neuroprotection and axon regeneration after ON injury (Park *et al.*, 2010; Park *et al.*, 2008). Results described in this Chapter represent findings from experiments using a clinically translatable siRNA approach, targeting the mTOR negative regulator RTP801. The major findings were that: (1) siRTP801 was target-specific, inducing RTP801 knock-down in cultured retinal cells and after intravitreal injection *in vivo* without induction of a non-specific inflammatory response; (2) RTP801 retinal expression was up-regulated after ONC in RGC, in other cells of the GCL and in the INL, and was significantly reduced by siRTP801; (3) RTP801 was detected in RGC, horizontal cells and glia *in vitro*, with RGC/glial RTP801 activity significantly reduced by siRTP801 treatment; (4) siRTP801 promoted significant RGC neuroprotection after ONC *in vivo* and in culture; (5) siRTP801 had no significant effect on initiation of axon growth after ONC *in vivo*, or on initiation of RGC neurite growth in cultures without activated retinal glia; and (6) siRTP801 promoted elongation of regenerating axons after ONC *in vivo*, but did not significantly affect neurite length in primary retinal cultures from uninjured adult animals in the absence of $GFAP^+$ activated glia.

3.6.1 Specificity and efficacy of siRNA-mediated knock-down of RTP801 and lack of non-specific pro-inflammatory response

Gene silencing with siRNA has emerged as a promising tool for delivery of therapeutic effects, especially for ocular disorders, where intravitreal administration enables high treatment concentrations close to the affected tissues (Guzman-Aranguez *et al.*, 2013). However, unintended

consequences of siRNA, such as off-target effects and the induction of an innate immune response, may confound RGC survival/regeneration studies using siRNA, leading to potentially erroneous conclusions. It was important, therefore, to confirm both the target specificity and lack of immunogenicity in the test siRNA. Using qPCR with specific primers on cDNA prepared from mixed retinal cultures, siRTP801 significantly reduced the expression of RTP801, whereas RTP801 levels were unaffected by either the siRNA transfection reagent Lipofectamine, or the control siEGFP, indicating that the target knock-down was a specific effect of the targeted siRNA. In this setting, RTP801 knock-down was approximately 51% after treatment with siRTP801 at 20nM, the most effective neuroprotective concentration identified in the dose-response assay *in vitro*. Although greater levels of target knock-down have been reported in siRNA studies in neuronal cell lines (Read *et al.*, 2009) or purified cell cultures (Ki *et al.*, 2010), the RTP801 knock-down observed in mixed retinal cultures probably reflects the lack of a significant stress-induced up-regulation in RTP801 expression in retinal cells in the absence of injury such as ONC, and also the presence of large numbers of $RTP801^{-}$ retinal cells, which may dilute the measured knock-down. The knock-down achieved confirms its effect and complements previous results kindly provided by Quark Pharmaceuticals, in which sequence specific RTP801 mRNA cleavage was detected by RLM-RACE, a highly specific technique used to confirm siRNA target knock-down (Lasham *et al.*, 2010). Moreover, the qPCR result obtained compares favourably with other studies using mixed cultures. For example, Suggate *et al.* (2009) reported target mRNA knock-down of approximately 20% in mixed retinal cultures with siRNA against RhoA, and PTEN siRNA achieves approximately 50-60% knock-down in dorsal route ganglion (DRG) cultures (Christie *et al.*, 2010).

The results of experiments using siRTP801 are likely to reflect effects of target-specific knock-down, rather than non-specific effects induced by an inflammatory response, as demonstrated by the lack of induction of expression of the interferon responsive genes IFIT and OAS1 in the retina and choroid

of rat eyes after intravitreal siRTP801 injection (Quark data). In support of this, the mixed retinal cultures used for assessment of RGC survival and neurite outgrowth demonstrated an absence of $GFAP^+$ activated glia, in agreement with previous studies using this paradigm (Suggate *et al.*, 2009; Lorber *et al.*, 2008; Vigneswara *et al.*, 2014), irrespective of whether treated with siRTP801 or controls. Treatment with siRTP801 was therefore unable to directly induce the activation of retinal glia that would be expected in the presence of a significant inflammatory response.

These data regarding siRNA specificity and lack of non-specific pro-inflammatory effect are important as they validate the results of subsequent experiments as being the effects of target knock-down rather than being due to non-specific, off-target effects, such as those reported in other siRNA studies (Aguirre *et al.*, 2013; Forsbach *et al.*, 2008; Kleinman *et al.*, 2008). For example, Kleinman and colleagues demonstrated siRNA-mediated down-regulation of vascular endothelial growth factor (VEGF) and the VEGF receptor (VEGFR1), with accompanying suppression of choroidal neovascularisation, in a sequence-independent fashion in mice: both specific siRNA against VEGFa and VEGFR1, as well as non-specific siRNA had similar effects, attributed to TLR3 activation and the induction of IFN-γ and IL-12 as a class effect of >21 nucleotide siRNA (Kleinman *et al.*, 2008). Furthermore, in a different report, siRNA-mediated inhibition of viral replication *in vivo* was found to be the result of an innate immune response rather than an RNAi-dependent effect, with the negative control siRNA having an unusually low immuno-stimulatory effect (Robbins *et al.*, 2008). Fortunately, RNAi-mediated toxicity and induction of innate immune responses in neuronal cells are sequence dependent, and thus with appropriate siRNA design and profiling it is possible to undertake experiments to investigate the specific effects of siRNA-mediated target knock-down and draw valid and meaningful conclusions (Read *et al.*, 2009; Suggate *et al.*, 2009). The data available for siRTP801 supports its use as a specific, targeted and effective siRNA.

3.6.2 RTP801 expression in the retina, response to injury, and siRTP801-induced knock-down

RTP801 is expressed with low-level constitutive activity in numerous tissues (Shoshani *et al.*, 2002). There was a low basal level of RTP801 immunoreactivity in retinal sections from uninjured animals, and this was predominantly observed in the GCL, where it co-localised both with a small minority of $Brn3a^+$ RGC and a very few $Brn3a^-$ cells (probably amacrine cells or astrocytes). Analysis of retinal sections taken from animals 24d after ONC demonstrated significantly increased RTP801 expression, particularly where it correlated with nearly half of the few remaining $Brn3a^+$ RGC at this stage after injury, suggesting a significant stress reaction as a response to ONC, and probably a precursor to subsequent impending apoptosis, as Brn3a expression is itself maintained in RGC as long as they are alive, irrespective of being injured (Nadal-Nicolas *et al.*, 2012; Sanchez-Migallon *et al.*, 2011). In addition to RGC and other cells in the GCL, $RTP801^+$ cells were evident in the INL after ONC, with some co-localisation with Müller glia. Treatment with siRTP801 significantly reduced RTP801 activity in $Brn3a^+$ RGC, in other cells located in the GCL, and also reduced the intensity of RTP801 immunostaining in the retina as a whole and in the INL, suggesting target knock-down in a number of cell populations in the retina after intravitreal delivery. This supports earlier findings using both a fluorescently-labelled version of siRTP801 and *in situ* hybridisation, which detected siRTP801-specific signal throughout the retina in numerous cell types after intravitreal injection, associated with RTP801 knock-down in retinal tissue in injected eyes (Feinstein *et al.*, 2009).

Further characterisation of the cellular localisation and siRNA-mediated knock-down of RTP801 was enabled by retinal culture studies. In contrast to retinal sections from uninjured animals where RTP801 expression in RGC was very low, the majority of βIII-$tubulin^+$ RGC in mixed primary retinal cultures from uninjured animals were $RTP801^+$, probably reflecting a degree of cellular stress associated with the axotomy and process of establishing the cultures, causing rapid increase in

cellular activity of RTP801. Nonetheless, siRTP801 demonstrated robust knock-down of RTP801 at the 10-50nM concentrations tested. In these cultures, and complementing the *in vivo* observations, RTP801 was also detected in βIII-tubulin$^-$ cells. The RTP801 expression in RGC and other cells was unaffected by incubation with the Lipofectamine transfection reagent, or by siEGFP, but was significantly reduced by siRTP801. As mentioned, there was absence of GFAP$^+$ activated retinal glia, and also a lack CRALBP$^+$ Müller glia in these cultures, suggesting that although the process of establishing these primary retinal cultures exposed cells to sufficient stress to rapidly induce RTP801 expression in RGC and other cells, there was not an observable reactive glial response in this setting. Despite the absence of GFAP$^+$/CRALBP$^+$ glia, RTP801 localisation correlated closely with S100β$^+$, so that it was expressed in retinal glial cells independent of whether they reactive or quiescent (Adami *et al.*, 2001; Zimmer *et al.*, 1995). Again, treatment with siRTP801 significantly reduced RTP801 positivity in this cell population. In addition to βIII-tubulin$^+$ RGC and S100β$^+$ glia, RTP801 was also observed in a small number of calbindin$^+$ horizontal cells, although in contrast to the RGC/glia, siRTP801 did not induce measurable target knock-down in this population of cells. Together, the *in vivo* and *in vitro* observations suggested that RTP801 was up-regulated and sustained for up to 24d after ONC in several retinal cell populations in response to ONC injury and was also expressed in retinal cells *in vitro*, including RGC, glia and horizontal cells, and that siRTP801 effects target knock-down, although likely in a cell-specific fashion. The trigger for increased RTP801 after axotomy is not fully understood, although ON injury increases the production of reactive oxygen species and HIF-1α (Kanamori *et al.*, 2010; Ergorul *et al.*, 2010), which may induce the RTP801 expression observed after ONC, although other factors, such as nutrient deprivation and AMPK, may also contribute (Brugarolas *et al.*, 2004; Ishizuka *et al.*, 2013; Inoki *et al.*, 2003b; DeYoung *et al.*, 2008; Jewell and Guan, 2013). In the absence of RTP801 inhibition this is correlated with reduced RGC survival and lack of a significant axon regenerative response after ONC.

These findings further confirm the specificity of siRTP801 in mediating target knock-down and largely agree with published findings relating to retinal expression of RTP801. For instance, RTP801 activity is described predominantly in the GCL of rodent retinal sections, both in $Brn3a^+$ RGC and in other cells, with some additional detection in cells of the INL and ONL, although mild differences in expression were observed between rat and mouse retinae (del Olmo-Aguado *et al.*, 2013). In a rodent model of retinopathy of prematurity (ROP), very weak RTP801 positivity is observed in all retinal layers in uninjured control animals, consistent with a low basal retinal RTP801 activity, with a dramatic increase throughout the retina in response to establishment of the ROP model, including maximal up-regulation in the INL (Brafman *et al.*, 2004). This ROP model is also associated with reactive oxygen species-induced vaso-obliteration, reactive neovascularisation and INL apoptosis, and therefore the changes in RTP801 expression observed are probably a reflection of the overt pathological model, and not directly comparable to the findings after ONC. RTP801 activity is observed in all retinal layers in a streptozotocin-induced rat diabetic retinopathy model, including INL, ONL, OPL and RPE, although with a particular increase in the ONL, that is rapidly suppressed by PF-04523655, a targeted RTP801 siRNA (Rittenhouse *et al.*, 2014). In the closest comparable study, Morquette *et al.* (2014) reported expression of REDD2 (otherwise known as DDIT4L or RTP801L, sharing 38% homology with RTP801 (Corradetti *et al.*, 2005; Shoshani *et al.*, 2002)) at low levels in $Brn3a^+$ RGC in the GCL of non-injured mouse retinae, along with activity correlating with $calbindin^+$ horizontal cell dendrites. They found a marked increase in RGC REDD2 levels after axotomy, but no detectable change in REDD2 expression in horizontal cell processes after the same injury. Interestingly, they also reported REDD1 (RTP801) GCL expression, albeit with no significant up-regulation of REDD1 after axotomy (Morquette *et al.*, 2014). However, this contrasting finding may be accounted for by several factors: firstly, they used mice rather than rats for their experiments, and as mentioned previously there may be some species-dependent variation in expression (del Olmo-Aguado *et al.*, 2013); secondly, REDD1 was measured in whole retinal homogenates, which may have

affected the sensitivity of RTP801 expression detection; and lastly, expression was measured at 72h, much earlier than the 24d analyses described in this thesis. The pattern/distribution of RTP801 up-regulation in the retina is likely to be context-specific, depending on the nature and time-course of the stress applied. Still, the data indicate that RTP801 is expressed in several retinal cell populations, and is susceptible to siRNA mediated knock-down. It is therefore likely that the observed RGC survival and axon elongation observed with siRTP801 treatment after ONC *in vivo* probably reflects both direct effects in RGC and indirect sequelae from RTP801 suppression in other cells such as glia.

3.6.3 Neuroprotective effect of RTP801 knock-down

At 24d after ONC, treatment with siRTP801 was significantly RGC neuroprotective compared to the control siEGFP. This RGC neuroprotective effect was evident in a preliminary *in vivo* analysis, directly comparing siRTP801 against control, using βIII-tubulin in the GCL as the RGC phenotypic marker. A re-analysis using the more specific RGC marker Brn3a (Mead *et al.*, 2014; Nadal-Nicolas *et al.*, 2009) verified this finding, and was compared with uninjured control tissue. Compared to intact, uninjured animals, ONC with intravitreal siEGFP was associated with a significant reduction in Brn3a$^+$ RGC survival, corresponding to approximately 45% RGC survival, whereas intravitreal injection of siRTP801 resulted in survival of 82% Brn3a$^+$ RGC. This RGC neuroprotective effect of RTP801 knock-down was also observed *in vitro*, with significantly more βIII-tubulin$^+$ RGC observed after treatment with siRTP801 in the 10-50nM treatment range (with optimal neuroprotective effect at 20nM). As mentioned in Chapter 2, βIII-tubulin is preferred *in vitro* as it also enables neurite outgrowth analyses. The pro-survival effect of siRTP801 in culture in the absence of GFAP$^+$ activated glia suggests that the effect is a direct, RGC-intrinsic effect of RTP801 knock-down. The *in vivo* neuroprotection data presented here verify the results of a previous study of siRTP801 after ONC in our laboratory, in which ONC resulted in significant loss of βIII-tubulin$^+$ RGC when combined with

intravitreal delivery of either PBS or siEGFP, but over 80% RGC survival after siRTP801 treatment (Table 3.1), indicating that this is a reliable, repeatable finding.

These observations are also in agreement with several previous reports of neuroprotective effects of RTP801 inhibition both *in vivo* and *in vitro*. RTP801 induction has been reported in neuronal PC12 cells in response to metabolic stress with H_2O_2 and several neurotoxins, and associated with neuron death in cellular models of Parkinson's disease (PD) (Malagelada *et al.*, 2006). Moreover, in the same study, RTP801 expression was up-regulated in substantia nigra neurons in a mouse model of PD, and in dopaminergic neurons of human patients with PD. Significant neuroprotection is induced by shRNA-mediated RTP801 knock-down in PC12 cells and in primary cultured sympathetic neurons after 6-OHDA-induced neurotoxicity (Malagelada *et al.*, 2006). Interestingly, RTP801 expression is not up-regulated in response to some other neuronal stressors, such as tunicamycin exposure or NGF deprivation, despite these factors inducing cell death, and shRTP801 does not afford neuroprotection to these cells. Deprivation of NTF is probably a contributory factor to cell death after ONC (Fischer and Leibinger, 2012), yet is unlikely to account for the rapid initial RTP801 up-regulation, but may contribute to the more sustained RTP801 expression as observed up to 24d after ONC.

In the RGC-5 neuronal cell line (with low basal expression of RTP801), cellular insult with either cobalt chloride ($CoCl_2$) or toxic levels of blue light leads to significant up-regulation of RTP801 immunoreactivity, RTP801 protein and RTP801 mRNA with a concomitant increase in cell death (del Olmo-Aguado *et al.*, 2013). Transfection with siRTP801 reduces both RTP801 expression and the $CoCl_2$-/light-induced cell death, indicating a neuroprotective effect of siRNA-mediated RTP801 knock-down in this neuronal cell population. The RGC-5 cell line was originally thought to be of ganglion cell origin (Krishnamoorthy *et al.*, 2001), but was later identified as a transformed photoreceptor cell line (Krishnamoorthy *et al.*, 2013) and so, whilst not directly translatable in terms of cell population,

these findings still demonstrate the major role that RTP801 has in stress-induced cell death and the neuroprotective sequelae of RTP801 suppression. *In vivo*, Brafman and colleagues established that RTP801 inhibition is neuroprotective in retinal neurons: exposure of newborn mice to hyperoxic conditions (75% O_2) for 5d followed by subsequent return to normoxia induces abnormal retinal vascularisation, associated with up-regulation of RTP801 and induction of apoptosis in the retinal INL (Brafman *et al.*, 2004). In this retinopathy model, cell death is significantly reduced in RTP801 knock-out animals, thus indicating a role for RTP801 in inducing cell death in conditions of relative hypoxia, and demonstrating that RTP801 inhibition is an effective strategy for attenuating neuronal death in the retina. Whilst evidence suggests that RTP801 appears not to be engaged in all paradigms of neuronal death, and RTP801 suppression may not be neuroprotective in all cells or circumstances of neuronal compromise, the enhanced RTP801 expression in the retina after ONC and knock-down by siRTP801 in retinal cells, with associated RGC neuroprotection, largely supports a role for RTP801 in stress-induced neuronal death, including in the retina, and that RTP801 inhibition is a viable RGC neuroprotective strategy.

RTP801 is rapidly up-regulated in response to cellular stress/injury, and acts on the TSC1/2 complex to suppress mTOR signalling (Brugarolas *et al.*, 2004; Corradetti *et al.*, 2005). After axotomy, a reduction in the supply of target/glial-derived NTF, which normally promote mTOR activity *via* receptor-activated PI3K/Akt signalling, is therefore compounded by RTP801 up-regulation, which acts to further suppress mTOR. The siRNA-approach of inhibiting RTP801 to promote mTOR signalling compares favourably with other strategies for RGC neuroprotection, including those aimed at increasing activity of the PI3K/Akt/mTOR pathway. For example, RGC survival of 45% is observed after RGC conditional deletion of the PI3K negative regulator gene *pten* at 14d after ONC in mice (Park *et al.*, 2008), but this rises to 60% survival when PI3K-pathway up-regulation is combined with adjunctive *socs3* deletion and CNTF administration (Sun *et al.*, 2011). It is possible that intraocular

inflammation caused by the injections could account, in part, for the observed neuroprotection with siRTP801, as RGC survival of approximately 45% was seen with the control siEGFP at 24d after ONC. Intraocular inflammation may promote neuroprotection after axotomy (Leibinger *et al.*, 2009), and the siEGFP was not tested for lack of non-specific pro-inflammatory effect, although this non-targeted control siRNA has been used in the same setting previously with similar results, and with no significant difference from intravitreal PBS injection after ONC (Table 3.1). Furthermore, siEGFP transfection of retinal cultures from uninjured animals was not associated with the presence of $GFAP^+$ activated glia; thus, an immunogenic effect from the control siRNA is unlikely to be a major feature. The PI3K/Akt pathway is intricately linked to cell survival signalling complexes. For example, PTEN activity is linked to the induction of neuronal apoptosis (Jayarama *et al.*, 2014; Sedding *et al.*, 2013) and PTEN inhibition rescues cortical neurons from hypoxia-ischemia-induced apoptosis (Zhao *et al.*, 2013), whilst further downstream, mTOR activation inhibits apoptosis (Walker *et al.*, 2013; Pastor *et al.*, 2009), possibly in part by cross-talk with the anti-apoptotic mediators Bcl-2 and Bcl-XL (Zou *et al.*, 2013). RTP801 inhibition after siRTP801 as an approach to protect RGC after axotomy is therefore consistent with other reports linking activity of this pathway to neuronal viability. However, despite the enhanced RGC survival with siRTP801, the level of neuroprotection observed did not reach that seen after inhibition of other targets, such as caspase-2, where RGC survival approaches 100% (Ahmed *et al.*, 2011; Vigneswara *et al.*, 2012), albeit without significant axon regeneration. It was recently reported that M1- and αRGC sub-types survive preferentially (but not exclusively) after ONC (Duan *et al.*, 2015). These ipRGC are βIII-tubulin$^+$ but $Brn3a^-$ (Nadal-Nicolas *et al.*, 2012), which may partly explain the apparent survival disparity between the analyses using these two markers *in vivo*, and suggests that siRTP801 induces RGC survival in different sub-type(s) of RGC, over and above the relatively injury-resistant M1-RGC and αRGC. This is discussed further in Chapter 4. In summary, intravitreal delivery of siRTP801 promotes favourable RGC neuroprotection, probably

by direct modulation of RGC-intrinsic mTOR signalling, and may therefore be a useful component of future treatment strategies to prevent visual loss after ON injury.

3.6.4 Axon regeneration/elongation after RTP801 knock-down

In addition to RGC neuroprotection, the *in vivo* findings suggested that RTP801 knock-down promoted axon regeneration, in terms of supporting the elongation of sprouting axons rather than the initiation of axogenesis after ONC. There was, however, a marked disparity between the potent RGC neuroprotective effect and the relatively modest effect on axon regeneration. In a typical rodent ON containing approximately 100,000 RGC axons (Joos *et al.*, 2010), the number of regenerating axons observed represents a regenerative response of fewer than 0.1% RGC. In addition, there was also a marked contradiction between the *in vivo* response, with enhanced axon elongation, and the effect of siRTP801 *in vitro*, where neither RGC neurite outgrowth initiation nor elongation of sprouting neurites was enhanced by siRTP801. This suggests that, in contrast to the presumed direct RGC-intrinsic effect of siRTP801 on RGC survival, the enhanced axon growth seen after ONC was dependent on external factors that were not present in the retinal culture model, such as $GFAP^+$ glia-derived NTF. RTP801 expression in cells other than RGC, such as glia, and knock-down by siRTP801 lends support to the notion that indirect effects on RGC result from modulation of mTOR activity in other cells. This is explored in more detail in Chapter 4.

Whilst there are no directly comparable studies evaluating axon/neurite growth after RTP801 inhibition, the *in vivo* results complement the existing literature implicating the PI3K/Akt/mTOR pathway as a mediator of axon regeneration in several models of CNS injury (Park *et al.*, 2010; Park *et al.*, 2008; Christie *et al.*, 2010; Liu *et al.*, 2010a). Axon regeneration into the distal ON after ONC is reported in up to 10% of surviving RGC after *pten* gene deletion, associated with maintenance of

mTOR activity (Park *et al.*, 2008). RTP801 modulates the PI3K/Akt/mTOR signalling pathway at a more downstream level than PTEN, by acting on the TSC1/2 complex to suppress mTOR activity (Brugarolas *et al.*, 2004; Corradetti *et al.*, 2005). A more muted axon regenerative response is observed after ONC in *tsc* deleted animals compared to *pten* deletion (Park *et al.*, 2008), possibly reflecting differential signalling through GSK3β, which is associated with axon growth in a PI3K-dependent fashion but is regulated upstream of TSC (Park *et al.*, 2010; Saijilafu *et al.*, 2013; Seira and Del Rio, 2014). Thus, the downstream level of signalling pathway manipulation may contribute to the degree of axon growth and may partly account for the relatively weak regenerative effect of siRTP801 compared to other reports modulating the same signalling pathway. In addition, siRNA treatment does not completely abrogate RTP801 expression, achieving approximately 50-70% reduction in the qPCR/immunocytochemistry analyses, and thus the effects cannot be directly compared with the more complete target suppression achieved by conditional gene deletion and imply that residual RTP801 activity may be sufficient to limit axon elongation. Indeed, a very recent report has observed a lesser degree of RGC axon regeneration after viral vector-mediated short hairpin RNA (shRNA) against PTEN compared to previous PTEN knock-out data, likely due to incomplete gene silencing from RNAi (Yungher *et al.*, 2015), thus implying that deeper suppression of RTP801 than that observed with siRNA used in the present studies might enable superior results. Moreover, axon regeneration after *pten* deletion is restricted to predominantly the αRGC sub-type, which is preferentially resistant to apoptosis after ONC (Duan *et al.*, 2015). The predominant weighting of RTP801 knock-down in favour of survival compared to axon growth may reflect survival of RGC classes in which a regenerative response is not possible, with mTOR-related protein synthesis maintaining neuronal viability and contributing to growth of axons in regeneration-permissive RGC that have initiated regeneration in response to other triggers.

Elsewhere in the nervous system, deletion of *pten* enhances both compensatory sprouting and regenerative growth of adult CST neurons after SC injury (Liu *et al.*, 2010a), which was recently associated with motor functional recovery (Danilov and Steward, 2015). CST regeneration after SC injury has also been reported after inhibition of PTEN *via* shRNA-mediated knock-down (Zukor *et al.*, 2013) and using PTEN peptide antagonists (Ohtake *et al.*, 2014). In contrast to RGC, where basal mTOR signalling is further down-regulated by injury (Park *et al.*, 2008), mTOR activity is reportedly activated in DRG soma following a conditioning injury, where it is associated with enhanced axon growth, and constitutive mTOR activation by *tsc* deletion promotes longer DRG peripheral axon regeneration (Abe *et al.*, 2010). However, although PTEN inhibition also increases both the number and length of regenerating PN axons after transection injury (Christie *et al.*, 2010; Singh *et al.*, 2014), the latter finding was independent of mTORC1 (Christie *et al.*, 2010), suggesting that the pro-regenerative effects of suppressing PTEN are not simply a reflection of mTOR up-regulation. The PI3K signalling pathway that is modulated by PTEN upstream and RTP801 further downstream, amongst other factors, has connections to multiple cellular signalling cascades, and it is therefore highly likely that a balance of activity between pathways determines the neuronal response to injury.

After ONC *in vivo*, siRTP801 promoted axonal elongation up to 1200µm beyond the injury site, but had no significant effect on short distance axonal sprouting up to 100-200µm, suggesting a distinction between the initiation of axon growth after ON injury and the elongation of regenerating axons. This disparity between induction of axon growth and elongation of axon growth is not unique to the effects of siRTP801 after ONC, and reflects a requirement for additional factors to fully optimise RGC axon regeneration. Indeed, the axon regenerative effect of mTOR activation by *pten* deletion is greatly enhanced when combined with intraocular inflammation (induced by intravitreal injection of zymosan) and a cAMP analogue (Kurimoto *et al.*, 2010), and may lead to some target re-innervation and the functional restitution of certain visually dependent behaviours (de Lima *et al.*,

2012). It was recently demonstrated that mTOR was dispensable for compensatory sprouting of CST axons after injury (Lee *et al.*, 2014), and mTOR activity has been implicated as an important factor in the maintenance the axon growth state in response to inflammatory stimulation (Leibinger *et al.*, 2012), whilst the initiation of the axogenic programme may be dependent on separate, although complementary, pathways such as CNTF/LIF-mediated JAK-STAT activity (Muller *et al.*, 2007; Leibinger *et al.*, 2009; Vigneswara *et al.*, 2014; Fischer and Leibinger, 2012; Leibinger *et al.*, 2012; Cui *et al.*, 1999). Consistently, CNTF induces neurite outgrowth in other CNS neurons independently of mTOR, and combined activation of PI3K/Akt/mTOR signalling by *pten* deletion with an additional inflammatory stimulus or with neutralisation of the JAK-STAT pathway negative regulator SOCS3, enables significantly greater numbers of axons to regenerate than observed in this study or after *pten* deletion alone (Sun *et al.*, 2011; de Lima *et al.*, 2012; Kurimoto *et al.*, 2010). Available evidence therefore suggests that maintaining or enhancing mTOR activity has a major role in neuronal survival and the maintenance of growth in regenerating axons, probably by enhancing protein synthesis to provide the metabolic substrates required for survival and growth. Axon elongation requires the manufacture of neuronal cytoplasm and membranes, and thus enhanced PI3K/Akt/mTOR activity may be the basis of increases neuronal synthetic capacity to provide the lipid and protein building blocks required for axon elongation (Goldberg, 2003). Protein translation in axon growth is not limited to the cell soma, and the localisation of ribosomes/mRNA to axons has highlighted the fact that intra-axonal synthesis also plays an important role (Goldberg, 2003; Zheng *et al.*, 2001; Gallant, 2000), and mTOR activity has been reported in determining local axon/dendritic translational capacity (Tsokas *et al.*, 2005; Obara and Hunt, 2014). Moreover, mTOR is thought to regulate neuronal cytoskeleton re-organisation and motility, which are key elements of axon elongation, and may particularly reflect mTORC2-dependent activity on the actin cytoskeleton *via* PKC (Liu *et al.*, 2010b; Angliker and Ruegg, 2013). RTP801 was recently found as a rate-limiting factor for myelination (Noseda *et al.*, 2013), and mTOR positively regulates initiation and extent of myelination

in the spinal cord (Wahl *et al.*, 2014). Therefore, in addition to influencing the RGC viability and elongation of axons, mTOR activity enhanced by RTP801 inhibition may also positively influence myelination in support of regenerating ON axons.

In summary, work described in this chapter provides evidence that siRTP801 is a specific and reliable siRNA, inducing target knock-down in several retinal cell types in the absence of a non-specific inflammatory response. Low level basal RTP801 expression is evident in the retina of uninjured animals, but is significantly up-regulated in RGC and other cells after ON injury. Treatment with siRTP801 is RGC neuroprotective both after ONC *in vivo* and in cultured retinal cells from uninjured animals, suggesting a direct effect on RGC, and enhances elongation but not initiation of regenerating axons after ONC, findings largely in agreement with published studies. The absence of a neurite elongation effect in the culture model, combined with RTP801 activity and modulation in several retinal cell populations, suggests that the pro-growth phenotype in RGC *in vivo* reflects a contribution from indirect, extrinsic factors. Moreover siRTP801 has no demonstrable effect on the initiation of axon regeneration after ONC *in vivo* or neurite outgrowth *in vitro*, indicating that independent mechanisms underlie these facets of RGC axon regeneration. Subsequent work, described in Chapters 4 and 5, aims to investigate some of the potential cellular mechanisms responsible for siRTP801-induced RGC survival and axon growth.

CHAPTER 4

INVESTIGATING THE CONTRIBUTION OF mTOR SIGNALLING AND GLIAL-DEPENDENT FACTORS TO RGC SURVIVAL AND AXON/NEURITE GROWTH AFTER RTP801 KNOCK-DOWN

Elements of work presented in this Chapter have been published in:

Morgan-Warren PJ, O'Neill J, De Cogan F, Spivak K, Ashush H, Kalinski H, Ahmed Z, Berry B, Feinstein E, Scott RAH, Logan A. siRNA mediated knockdown of the mTOR inhibitor RTP801 promotes retinal ganglion cell survival and axon elongation by direct and indirect mechanisms. *Invest Ophthalmol Vis Sci.* 2016 (in press). DOI:10.1167/iovs.15-17511

4.1 INTRODUCTION / RATIONALE

It has been demonstrated that RTP801 is up-regulated in the retina after ONC injury, and that treatment with siRTP801 suppresses the expression of RTP801, and is associated with both enhanced RGC survival and axon elongation after ONC *in vivo*. The central function of RTP801 is to down-regulate mTOR activity in response to cellular stress, *via* the TSC1/2 complex (Brugarolas *et al.*, 2004; Canal *et al.*, 2014; Corradetti *et al.*, 2005), and thus it is likely that the observed increase in RGC survival and axon elongation after RTP801 knock-down reflects mTOR-dependent effects. Similarly, the neuroprotective and axon regenerative effect of *pten* gene deletion after ONC is attributed to mTOR activity for two main reasons: (1) maintenance of retinal expression of the mTOR substrate pS6, indicating prevention of an injury-induced down-regulation of mTOR activity; and (2) a dramatic reduction in the effects of *pten* deletion in the presence of Rapamycin. Specifically, rather than reflecting the activity of 'mTOR', which as described previously encompasses two complexes with different Rapamycin sensitivity and different substrates (Perluigi *et al.*, 2015), these two factors (pS6 activity and Rapamycin sensitivity) implicate mTORC1 as a candidate for mediating neuronal survival and axon growth.

Importantly, the findings of experiments described in Chapter 3 revealed some contrast between the *in vivo* and *in vitro* paradigms. Whilst siRNA-mediated knock-down of RTP801 was RGC neuroprotective both after ONC *in vivo* and in primary retinal cultures from uninjured animals, the enhanced elongation of regenerating RGC axons observed after ONC with siRTP801 treatment was not replicated in the culture model. Moreover, siRTP801 did not affect the initiation of axon/neurite growth in either setting. These results suggested that neuroprotection was afforded by a direct, RGC intrinsic mechanism, whereas the axon elongation effect of RTP801 knock-down required the presence of additional factors present *in vivo* but not in the culture model, a notion supported by

detection of RTP801 in glia and knock-down after siRTP801 treatment. As mTOR activity in the CNS is not restricted to neurons (Perluigi *et al.*, 2015; Codeluppi *et al.*, 2009; Li *et al.*, 2015), it is likely that the modulation of mTOR activity in glia would contribute to neuronal viability and growth, and the contribution of retinal glial-derived factors to neuroprotection and axon growth is increasingly recognised (Ahmed *et al.*, 2010; Fischer and Leibinger, 2012; Lewis and Kucenas, 2014; Lorber *et al.*, 2009a; Lorber *et al.*, 2012; Muller *et al.*, 2007; Vigneswara *et al.*, 2014; Toy and Namgung, 2013).

The purpose of experiments described in this Chapter was to investigate mechanisms underlying the RGC neuroprotective and axon elongation effects of siRTP801, by evaluating the contributions of mTORC1 signalling after RTP801 knock-down and the role of activated retinal glia in mediating potential indirect effects on axon/neurite growth.

4.2 HYPOTHESES

- RGC survival and axon growth effects of siRTP801 are mediated *via* increased mTORC1 activity.
- The presence of activated retinal glia is required to mediate the axon growth effects of siRTP801 *via* the enhanced production of NTF.

4.3 AIMS

The specific aims of experiments described in this Chapter were to:

1. Characterise the effects of siRTP801 on RGC expression of the mTORC1 substrate pS6 after ONC *in vivo* and in cultured retinal cells;

2. Investigate the effects of siRTP801 on the activation of retinal glia after ONC *in vivo*;
3. Investigate the effects of siRTP801 on RGC survival and neurite outgrowth in the presence of activated retinal glia;
4. Evaluate the contribution of mTORC1 activity to the RGC neuroprotective and axon/neurite growth effects of siRTP801;
5. Evaluate the contribution of activated-glial-derived NTF and Trk-dependent signalling to the RGC neuroprotective and axon/neurite growth effects of siRTP801.

4.4 EXPERIMENTAL DESIGN

Details of specific experimental techniques and methodologies are described in Chapter 2.

4.4.1 Characterisation of RGC expression of pS6 and the effects of siRTP801 *in vivo*

The characterisation of RGC expression of the mTORC1 substrate pS6 was undertaken on retinal sections from the same animals used for assessment of RGC survival and axon regeneration, as described in Chapters 2 and 3. In brief, bilateral ONC was performed, followed immediately by intravitreal injection of siEGFP to one eye and siRTP801 to the fellow eye, and repeated 8d and 16d after ONC, with ocular tissue processed for retinal sections after 24d. Assessment of RGC pS6 expression was undertaken by immunohistochemistry on sections from these two treatment conditions, and also on retinal sections obtained from eyes of intact, uninjured animals (n=5 eyes/group).

4.4.2 Characterisation of RGC expression of pS6 and the effects of siRTP801 *in vitro*

Primary retinal cultures were established from uninjured adult rats as described previously (Section 2.4.1). Cultured retinal cells were incubated for 3d with sNBA culture medium alone, siEGFP (20nM) or siRTP801 (20nM) and immunocytochemistry was subsequently undertaken for detection of βIII-tubulin and pS6. The proportion of $pS6^{+}$ RGC from the total βIII-$tubulin^{+}$ RGC was calculated (2-3 wells/condition, from n=3 independent animals) and compared between groups. A further set of cultures were established from animals subjected to ONC injury 5d before (without any intravitreal injections) and subsequently incubated in the same three treatment conditions (2-3 wells/condition from n=3 replicate animals).

4.4.3 Assessment of the effects of siRTP801 on activation of retinal glia after ONC *in vivo*

Comparison of retinal glial activation was undertaken between treatment groups using retinal sections from the same animals as described previously (Chapter 3), including uninjured intact animals, plus those 28d after ONC + siEGFP and ONC + siRTP801. Immunohistochemistry was undertaken on these sections for the glial markers GFAP and S100β, with comparison between these conditions as described in Section 2.3.7.3.

4.4.4 Assessment of the effects of siRTP801 on activation of retinal glia *in vitro*, on RGC survival and neurite outgrowth in the presence of activated retinal glia, and the contribution of mTORC1- and Trk-dependent signalling

For the assessment of siRTP801 in the presence of activated retinal glia, primary retinal cultures were established from animals 5d after having undergone ONC *in vivo*. Cultures were prepared with the

same treatment conditions as described previously: incubated either with sNBA culture medium alone, siEGFP (20nM) or siRTP801 (20nM). These cultures were used for immunocytochemical assessment of the presence of $GFAP^+$ cells, $CRALBP^+$ cells and $S100\beta^+$ cells, and the proportion of these cell populations co-expressing RTP801. The assessment of RGC survival and neurite outgrowth (initiation and elongation) was undertaken with these glial-activated cultures in the same fashion as described in Chapter 3 in the absence of activated glia. For each treatment condition, further wells were incubated with the mTORC1 inhibitor Rapamycin or the Trk-receptor antagonist K252a (Section 2.4.3). All *in vitro* experiments were undertaken using 2-3 wells/condition from n=3 independent animals.

4.4.5 Assessment of the effects of siRTP801 on the production of retinal glial-derived NTF

Conditioned medium was collected from culture wells established both in the absence of activated glia (cultures prepared from intact, uninjured animals) and in the presence of activated glia (5d after prior ONC *in vivo*) for each of the three treatment conditions of sNBA culture medium alone, siEGFP and siRTP801, therefore a total of six conditions. Samples of medium were used for ELISA in accordance with the specific NTF ELISA protocols as described in Chapter 2 (Section 2.7.2), investigating the presence in culture medium of the following NTF: BDNF, NGF, NT-3, CNTF, GDNF, and PEDF, using medium from n=3 independent animals.

4.5 RESULTS

4.5.1 Effect of siRTP801 on RGC mTORC1 activity

4.5.1.1 Injury-induced reduction in RGC pS6 expression was prevented by siRTP801

The expression of pS6 was evident in the GCL of uninjured, intact animals, although was limited to a minority of Brn3a$^+$ RGC (15.4 ± 1.7% RGC, Figure 4.1). After ONC and intravitreal delivery of control siEGFP, there was a significant reduction in pS6 expression, co-localising to only 5.9 ± 0.5% surviving RGC ($p<0.01$) at 24d post ONC. Treatment with siRTP801 was associated with pS6 expression in 13.7 ± 1.4% RGC at the same time-point after ONC, significantly greater than the ONC + siEGFP group ($p<0.01$), but not significantly different from intact control animals (Figure 4.1). Thus, the expression of pS6, a marker of mTORC1 activity, was reduced by ONC injury and maintained at pre-injury levels by siRTP801 treatment.

4.5.1.2 siRTP801 increased RGC expression of pS6 in retinal cultures established from uninjured adult rats

In primary mixed retinal cultures established from uninjured adult rats, the expression of pS6 was observed in 23.1 ± 1.7% βIII-tubulin$^+$ RGC in sNBA culture medium control wells, with no significant difference after transfection with control siEGFP (24.4 ± 1.7%) (Figure 4.2). There was a small, but statistically significant, increase in the proportion of βIII-tubulin$^+$ RGC expressing pS6 after treatment with 20nM siRTP801 (31.9% ± 1.4%, $p<0.05$), suggesting that siRNA-mediated knock-down of RTP801 increased mTORC1 activity in RGC in these cultures (Figure 4.2).

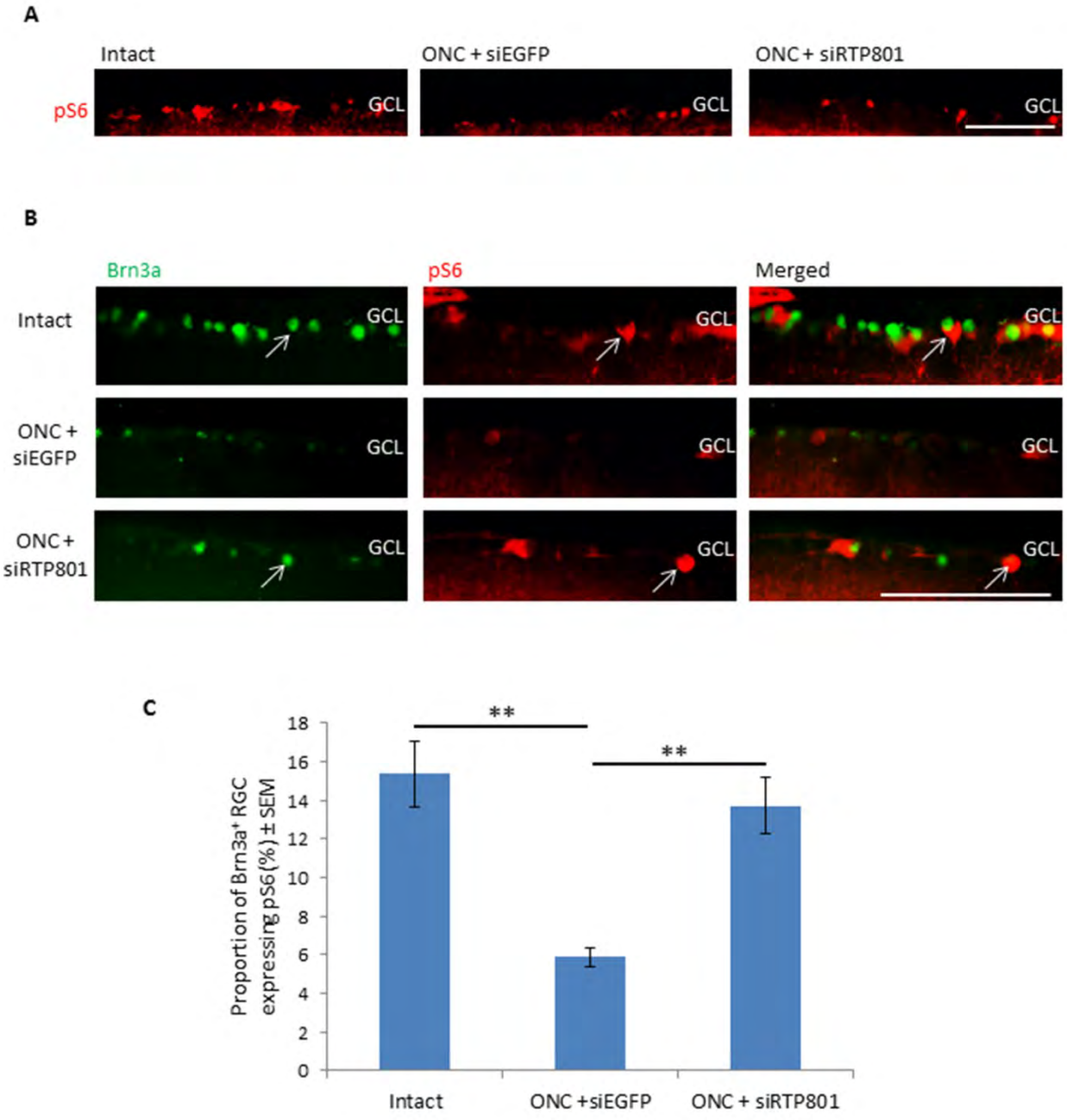


Figure 4.1: Maintenance of RGC expression of mTORC1 substrate pS6 after ONC *in vivo*. (A) Sections of the retinal GCL immunostained for pS6 in uninjured intact animals (left), and after ONC + siEGFP (middle) and ONC + siRTP801 (right) (scale bar = 100µm). (B) Higher magnification sections of retinal sections from groups described in (A), immunostained for Brn3a (green) and pS6 (red), demonstrating $pS6^+$ RGC (arrows) (scale bar = 100µm). (C) Quantification of pS6 expression in $Brn3a^+$ RGC in retinal sections of groups described in (A), demonstrating low level constitutive pS6 expression, injury-induced pS6 down-regulation, and maintenance of RGC pS6 expression after siRTP801 treatment (n=5 retinae/group; **p<0.01).

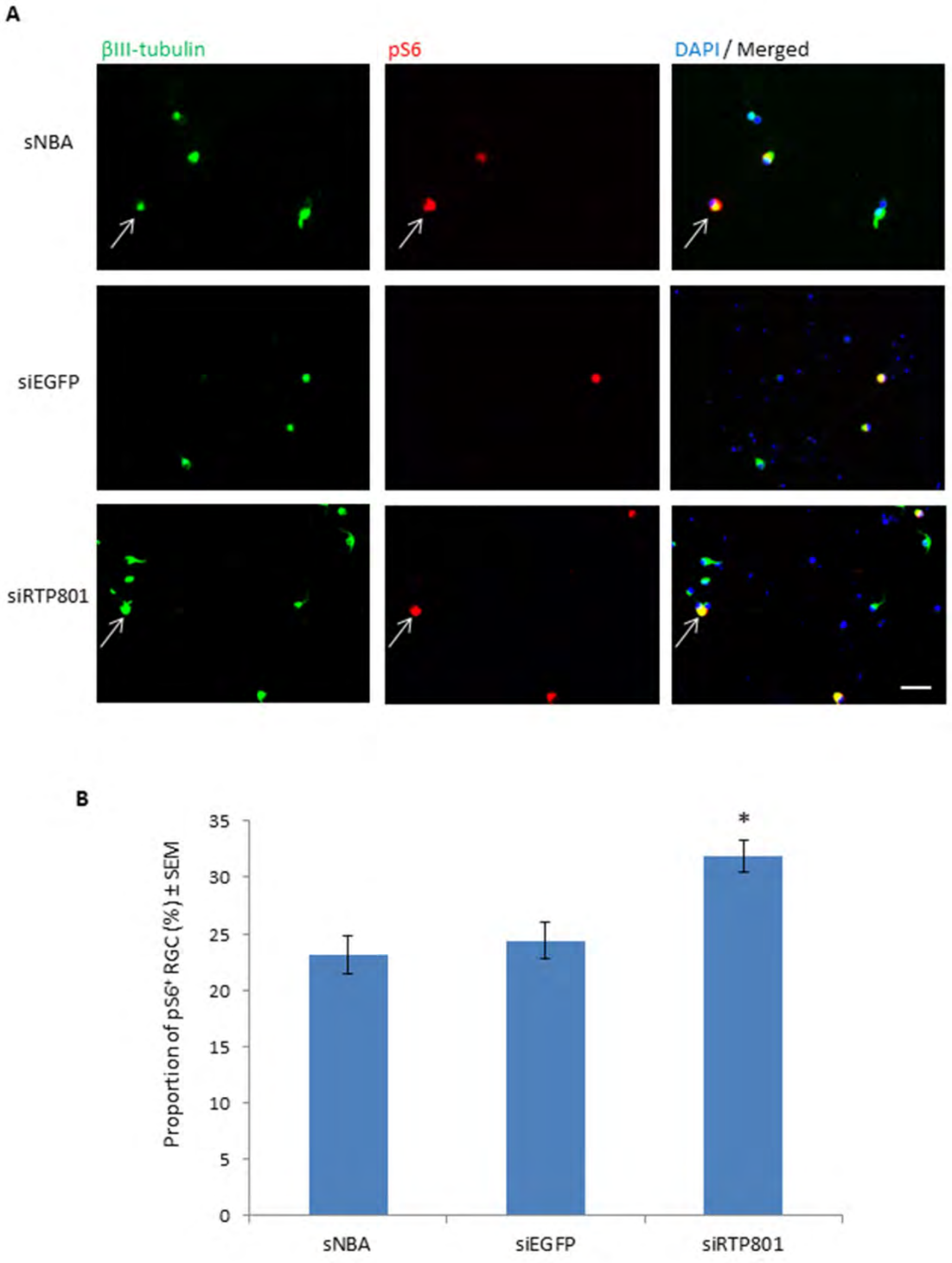


Figure 4.2: Effect of siRTP801 on RGC pS6 expression in retinal cultures established from uninjured animals. (A) Retinal cultures established from intact, uninjured animals, immunostained for βIII-tubulin (green) and pS6 (red), with DAPI (blue) as a nuclear counterstain, after 3 d incubation with sNBA culture medium alone (top row), siEGFP (middle row) and siRTP801 (bottom row), demonstrating the expression of pS6 in a population of RGC (arrows) (scale bar = 20µm). (B) Proportion of $pS6^{+}$ RGC for the treatment conditions described in (A), indicating increased pS6 expression after siRTP801 treatment (n=3; *$p<0.05$ *vs* sNBA control).

4.5.1.3 Expression of pS6 was reduced in cultured RGC after ONC injury, but maintained after siRTP801 treatment

Compared to retinal cultures prepared from uninjured animals in the presence of sNBA culture medium alone, as described above (Section 4.5.1.2), detection of pS6 in RGC was significantly reduced in retinal cultures established from animals 5d after ONC injury and incubated with either sNBA (9.2 ± 3.1% RGC, $p<0.05$) or siEGFP (6.7 ± 2.7% RGC, $p<0.05$) (Figure 4.3). However, transfection with siRTP801 in these cultures from post-ONC injured animals demonstrated pS6 positivity in 23.5 ± 3.9% RGC, approximately the same proportion as observed in the cultures from uninjured animals prepared sNBA culture medium (Figure 4.3). These data correlate with the *in vivo* findings, indicating that RGC activity of pS6 was suppressed after ONC, and that this injury-induced reduction of pS6 was prevented by siRTP801 treatment, reflecting the maintenance of mTORC1 activity despite injury.

4.5.1.4 RGC pS6 activity was not mandatory for neurite outgrowth, and pS6 was detected in non-RGC retinal cells

The sprouting of RGC neurites was not limited to $pS6^+$ RGC, as this mTORC1 substrate was observed in 51.1 ± 9.8% neurite-bearing RGC in cultures prepared from post-ONC animals incubated with sNBA culture medium alone (Figure 4.4A, B). Similarly, there was no significant difference after transfection with either siEGFP (41.0 ± 5.8%) or siRTP801 (52.1 ± 4.8%) (Figure 4.4A, B), suggesting that despite the maintenance of mTORC1 activity by siRTP801, pS6 positivity (reflecting mTORC1 activity) was not obligatory for initiation of neurite outgrowth. In addition to RGC, pS6 was also observed in a small population of βIII-tubulin$^-$ cells, suggesting the activity of mTORC1 in other cells, such as glia (Figures 4.3A and 4.4C). The number of $pS6^+$ βIII-tubulin$^-$ cells in these cultures was 58.8 ± 9.7 and 54.2 ± 10.9

in sNBA and siEGFP control wells, respectively, and increased to 95.2 ± 11.2 in siRTP801-treated wells (Figure 4.4D), although the increase after siRTP801 did not reach statistical significance.

Together, these *in vivo* and *in vitro* data indicated that mTORC1 activity, as estimated by quantification of pS6 detection, was present in a minority of RGC in uninjured adult animals and that an injury-induced suppression in mTORC1 activity was prevented by treatment with siRTP801. However, the *in vitro* findings suggested that pS6 activity was not obligatory for RGC neurite outgrowth, and that pS6 was modulated in cells other than RGC. Thus, in support of findings from experiments described in Chapter 3, RGC-extrinsic factors are likely to contribute to the induction of axon/neurite growth, and mTORC1-independent mechanisms are involved.

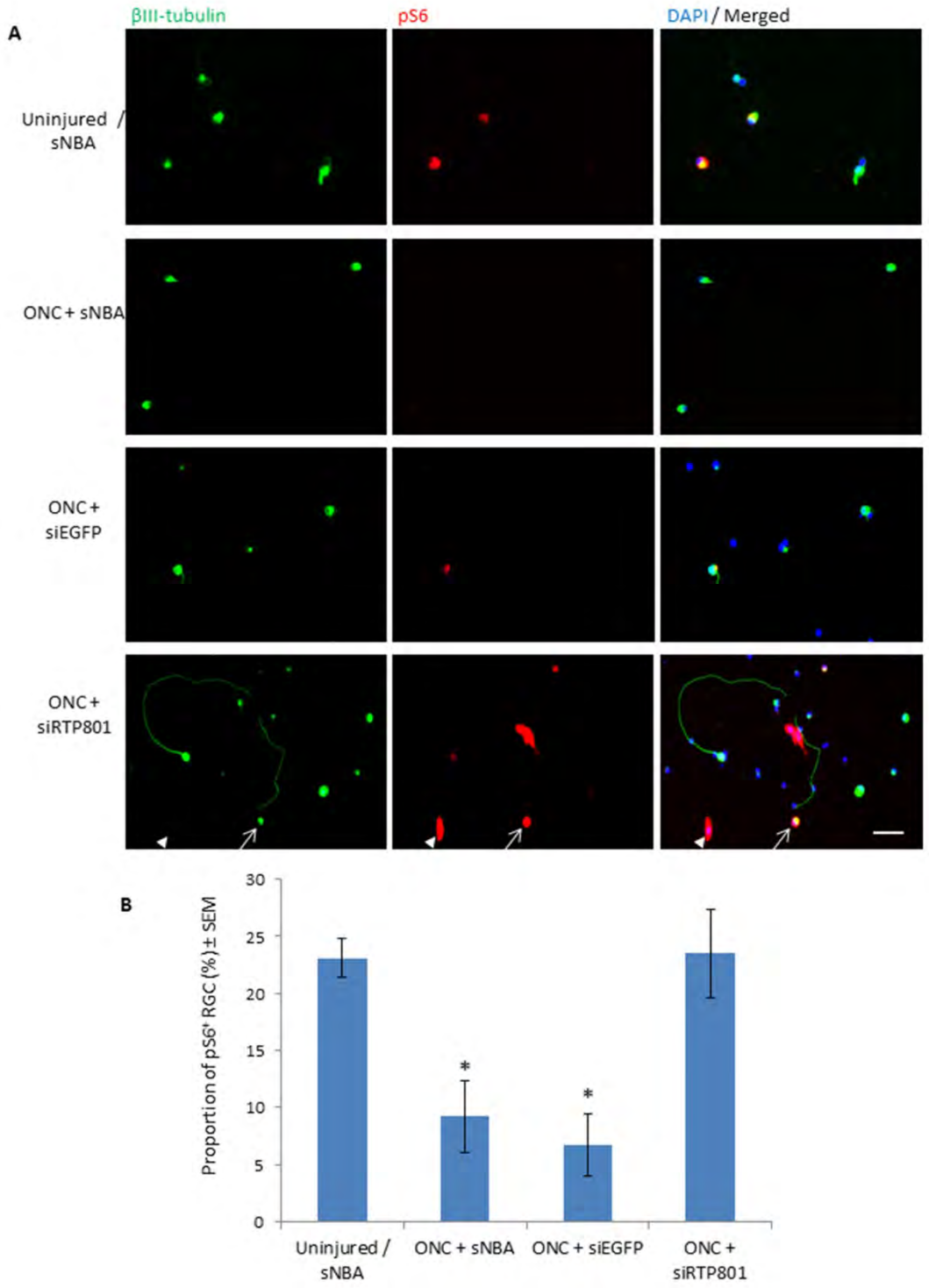


Figure 4.3: Maintenance of RGC pS6 expression after injury *in vitro.* (A) Retinal cultures established from intact, uninjured animals (top row, as per Figure 4.2 A), and cultures established 5d after prior ONC injury and incubated with sNBA culture medium alone (2nd row), siEGFP (3rd row) and siRTP801 (bottom row), immunostained for βIII-tubulin (green) and pS6 (red), with DAPI (blue) as a nuclear counterstain, demonstrating reduced RGC pS6 expression after injury, but maintained at approximately uninjured levels after siRTP801 treatment (arrows). Note the expression of pS6 in some βIII-tubulin$^-$ cells also (arrowhead) (scale bar = 20µm). (B) Proportion of pS6$^+$ RGC for the treatment conditions described in (A), indicating the prevention of injury-induced RGC pS6 down-regulation after siRTP801 treatment (n=3; *p<0.05 *vs* sNBA control).

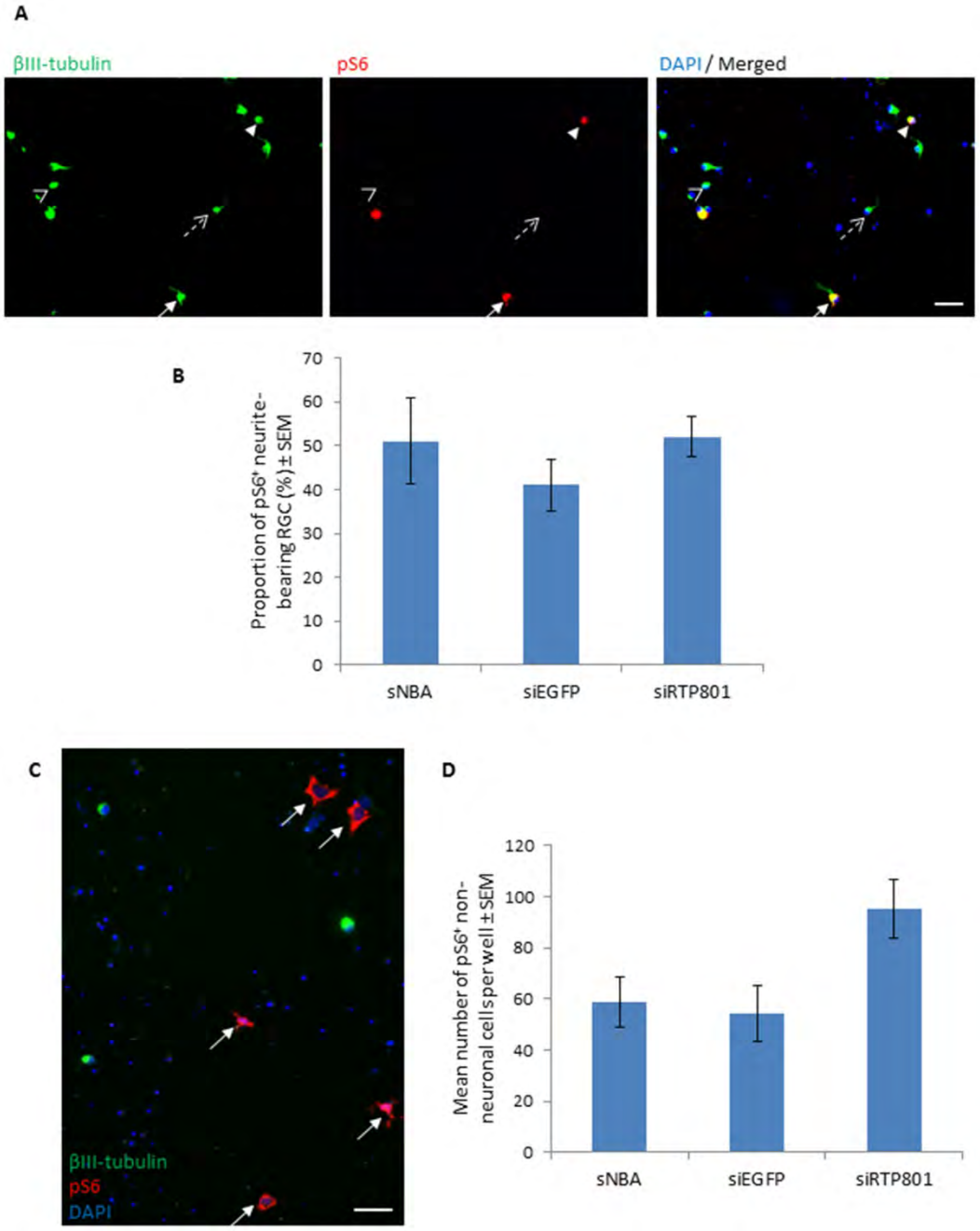


Figure 4.4: Expression of pS6 does not correlate with RGC neurite outgrowth, and is present in non-neuronal cells. (A) Retinal cultures established 5d after prior ONC injury and treated with siRTP801, immunostained for βIII-tubulin (green) and pS6 (red), with DAPI (blue) as a nuclear counterstain, indicating that pS6 expression was not restricted to neurite-bearing RGC (closed arrow = $pS6^+$ RGC with neurite, dashed open arrow = $pS6^-$ RGC with neurite, closed arrowhead = $pS6^+$ RGC without neurite, open arrowhead = $pS6^-$ RGC without neurite) (scale bar = 20µm). (B) Proportion of neurite-bearing RGC expressing pS6 in sNBA/siEGFP controls and after siRTP801 treatment (n=3). (C) Retinal cultures established 5d after prior ONC injury and treated with siRTP801, immunostained for βIII-tubulin (green) and pS6 (red), with DAPI (blue) as a nuclear counterstain, indicating that pS6 is expressed in a heterogeneous population of βIII-$tubulin^-$ cells *in vitro* (arrows) (scale bar = 20µm). (D) Quantification of $pS6^+$ non-neuronal cells in retinal cultures in sNBA/siEGFP controls and after siRTP801 treatment (n=3; the difference between groups was not statistically significant on ANOVA).

4.5.2 Effect of siRTP801 on retinal glial activity

4.5.2.1 Retinal glial activation after ONC in vivo *was potentiated by siRTP801 without affecting retinal glial proliferation*

In the retina there was subdued $GFAP^+$ astrocyte immunoreactivity in the NFL, and $GFAP^+$ reactive Müller glial processes were absent from the IPL in intact, uninjured animals (Figure 4.5A, B). After ONC, $GFAP^+$ immunoreactivity increased in the NFL, and $GFAP^+$ reactive Müller glial processes traversed the IPL (Figure 4.5A, B). The number of $GFAP^+$ Müller glial processes in the IPL was significantly increased at 24d after ONC in retinae treated with siRTP801 (14.9 ± 0.7 processes/250µm) compared to siEGFP (10.2 ± 0.5, $p<0.001$) after the same injury (Figure 4.5A, B). The number of $S100\beta^+$ Müller glial somata in the INL was unchanged after ONC in siEGFP controls (16.6 ± 0.4 processes/250µm) and siRTP801-treated retinae (17.3 ± 0.4) compared to intact retinae (16.7 ± 0.5) (Figure 4.5C, D). These data suggested that siRTP801 enhanced the activation of $GFAP^+$ glia after ONC injury, without significantly increasing Müller glial proliferation *in vivo*.

4.5.2.2 Activated $GFAP^+$ retinal glia were present in vitro *after prior ONC, and RTP801 expression in activated glia was knocked-down by siRTP801*

Whilst absent from primary retinal cultures established from intact animals (Chapter 3), $GFAP^+$ retinal glia were observed in cultures at 5d after prior ONC *in vivo*, reflecting astrocyte/Müller glial activation in response to injury, although there was no significant difference in $GFAP^+$ cell number between sNBA controls (518.6 ± 42.6 cells/well), siEGFP controls (537.0 ± 26.1 cells) and siRTP801-transfected wells (568.1 ± 24.1 cells) after 3d in culture (Figure 4.6A, B). The proportion of $GFAP^+$ glia expressing RTP801 in these cultures was significantly reduced after siRTP801 treatment (40.2 ± 5.4%)

compared to sNBA control wells (81.2 ± 3.9%, p<0.001), whereas siEGFP (84.4 ± 4.3%) did not affect RTP801 expression in these glia (Figure 4.6A, C). In addition to $GFAP^+$ glia, these cultures established 5d after prior ONC also demonstrated the presence of $CRALBP^+$ Müller glia, and there was no significant difference in the number of $CRALBP^+$ cells between sNBA controls (314.2 ± 21.9 cells/well), siEGFP controls (328.2 ± 24.1 cells) and siRTP801-transfected wells (339.0 ± 19.0 cells) after 3d in culture (Figure 4.7A, B). RTP801 was seen in 77.6 ± 4.8% $CRALBP^+$ glia in sNBA control wells, 76.0 ± 4.7% in siEGFP control wells, and 44.0 ± 4.9% in siRTP801 wells (p<0.001 *vs* sNBA) (Figure 4.7A, C). As in retinal cultures prepared from uninjured animals, the cultures prepared after ONC included $S100\beta^+$ glia, although there was no significant difference in $S100\beta^+$ glial number between the treatment groups (Figure 4.8A, B). Whereas siEGFP did not affect the proportion of $RTP801^+/S100\beta^+$ glia (82.2 ± 4.4%), compared to sNBA controls (84.4 ± 3.9%) the frequency of RTP801 expressing cells was significantly reduced by siRTP801 (38.2 ± 5.3%, p<0.001) (Figure 4.8A, C).

Thus, whilst siRTP801 was unable to directly induce activation of retinal glia (Chapter 3), these *in vivo* and *in vitro* findings suggested that siRTP801 potentiated ONC-induced reactive gliosis after ONC *in vivo*, and knocked-down RTP801 in reactive glia *in vitro*, although did not induce proliferation of these glial cells. Together, these data indicated a likely role for indirect, glial-dependent factors in the siRTP801-induced RGC survival and axon regeneration after ONC *in vivo*.

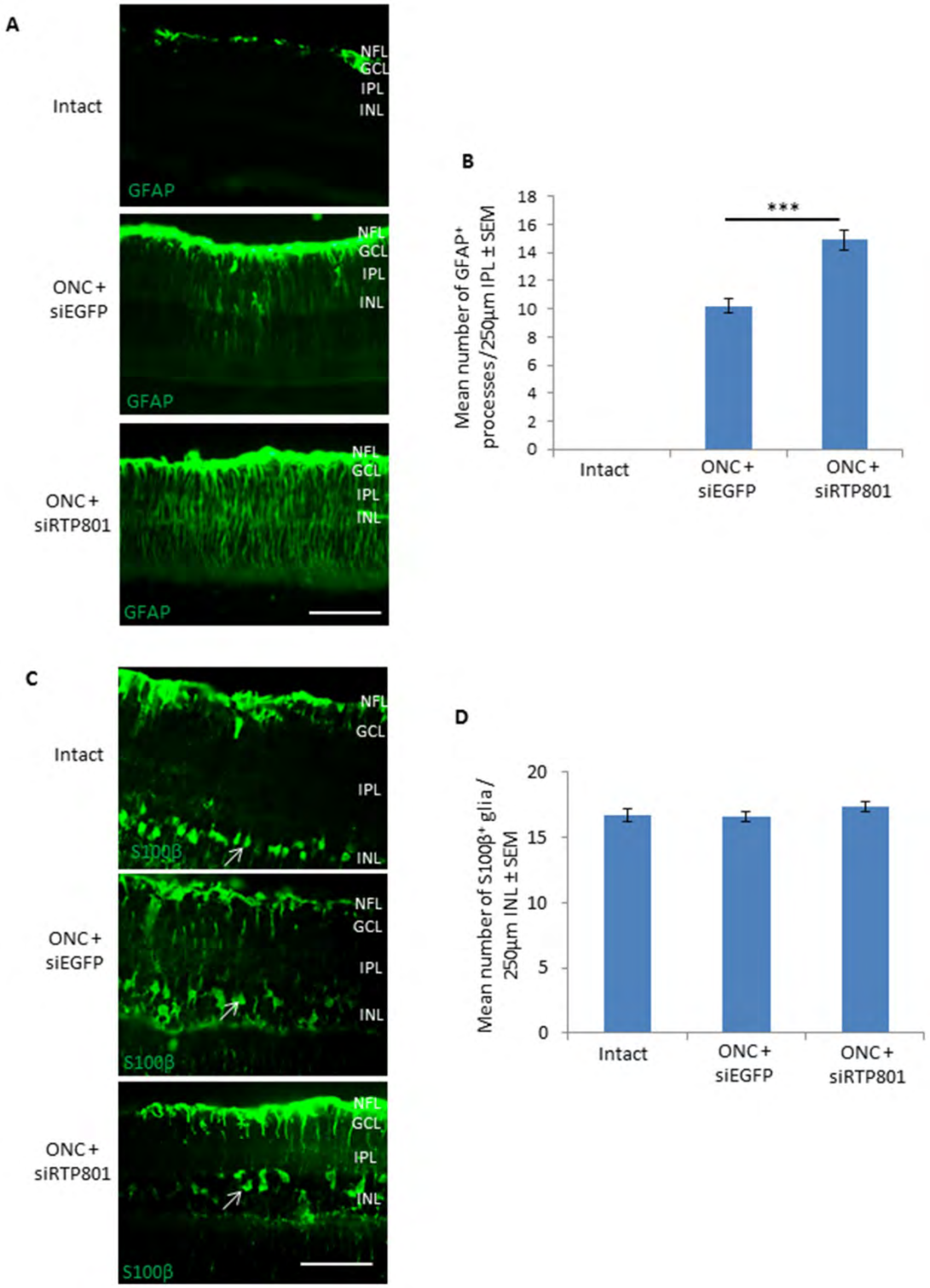


Figure 4.5: Retinal astrocyte/Müller glial response after ONC *in vivo*. (A) Immunostained retinal sections showing GFAP$^+$ glia in intact uninjured retinae and in sections after ONC + siEGFP and ONC + siRTP801 (scale bar = 100µm). (B) Quantification of GFAP$^+$ Müller glial processes in a 250µm linear sample of IPL for groups described in (A) (n=5 retinae/group; ***p<0.001), demonstrating potentiated GFAP$^+$ glial activation after siRTP801 treatment. (C) Immunostained retinal sections showing S100β$^+$ Müller glia for the same conditions as described in (A) (arrows indicate Müller glial somata; scale bar = 100µm). (D) Quantification of S100β$^+$ Müller glial somata in a 250µm linear sample of INL for groups described in (A), demonstrating lack of glial proliferation after siRTP801 treatment (n=5 retinae/group).

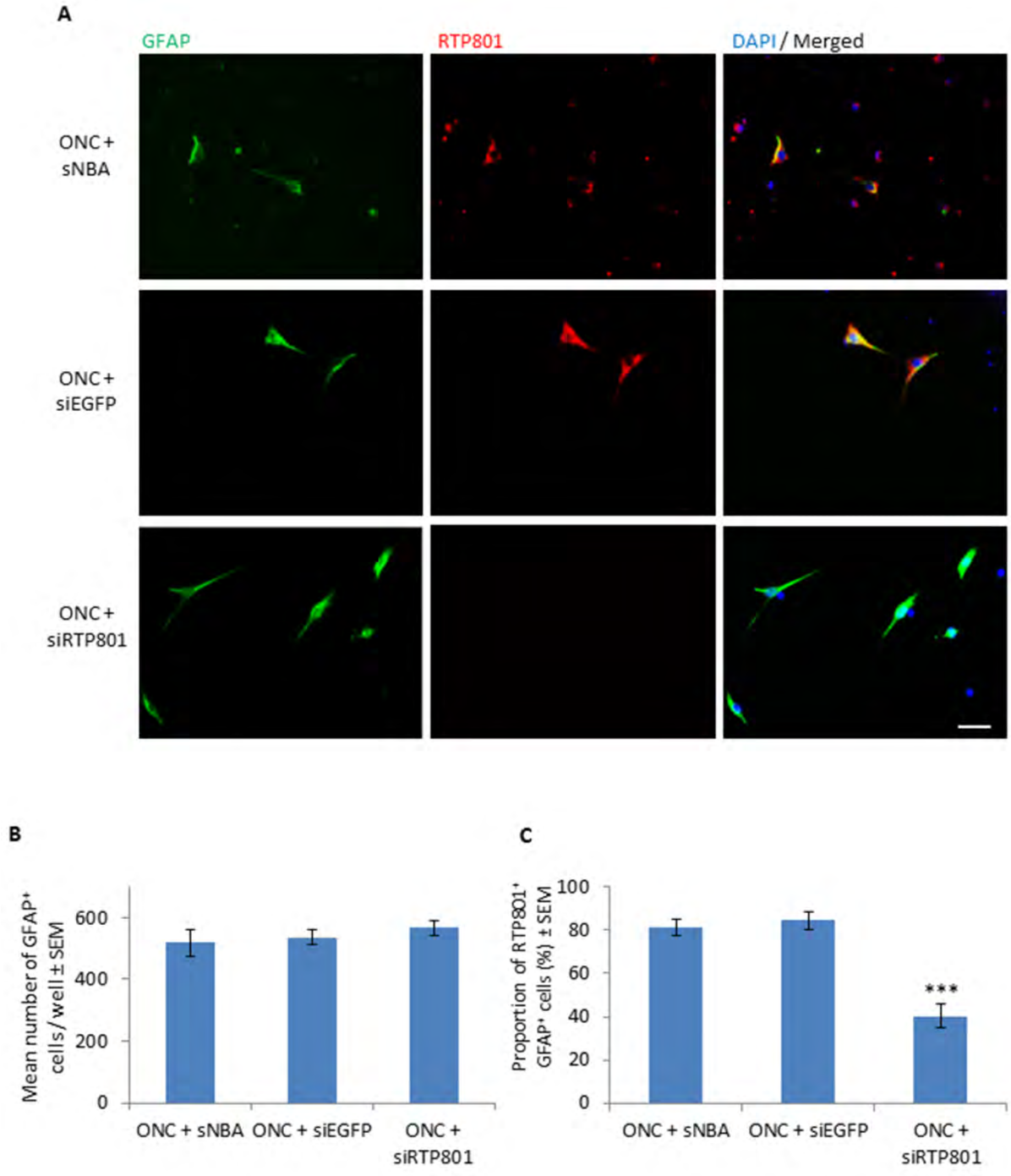


Figure 4.6: GFAP$^+$ activated retinal glia and RTP801 knock-down in activated glia in retinal cultures established 5d after ONC. (A) GFAP (green) and RTP801 (red) immunostaining of cultured retinal cells, with DAPI (blue) as a nuclear counterstain, established 5d after prior ONC *in vivo* and treated with sNBA culture medium alone (top row), siEGFP (middle row) and siRTP801 (bottom row), indicating presence of GFAP$^+$ glia and expression of RTP801, which is reduced after siRTP801 treatment (scale bar = 20µm). (B) Quantification of GFAP$^+$ cells in glial-activated retinal cultures for conditions described in (A), indicating no significant effect of siRTP801 on GFAP$^+$ glial proliferation (n=3). (C) Proportion of GFAP$^+$ glia expressing RTP801 after siRTP801 treatment compared to controls, indicating RTP801 knock-down in GFAP$^+$ activated glia (n=3; ***p<0.001 *vs* sNBA control).

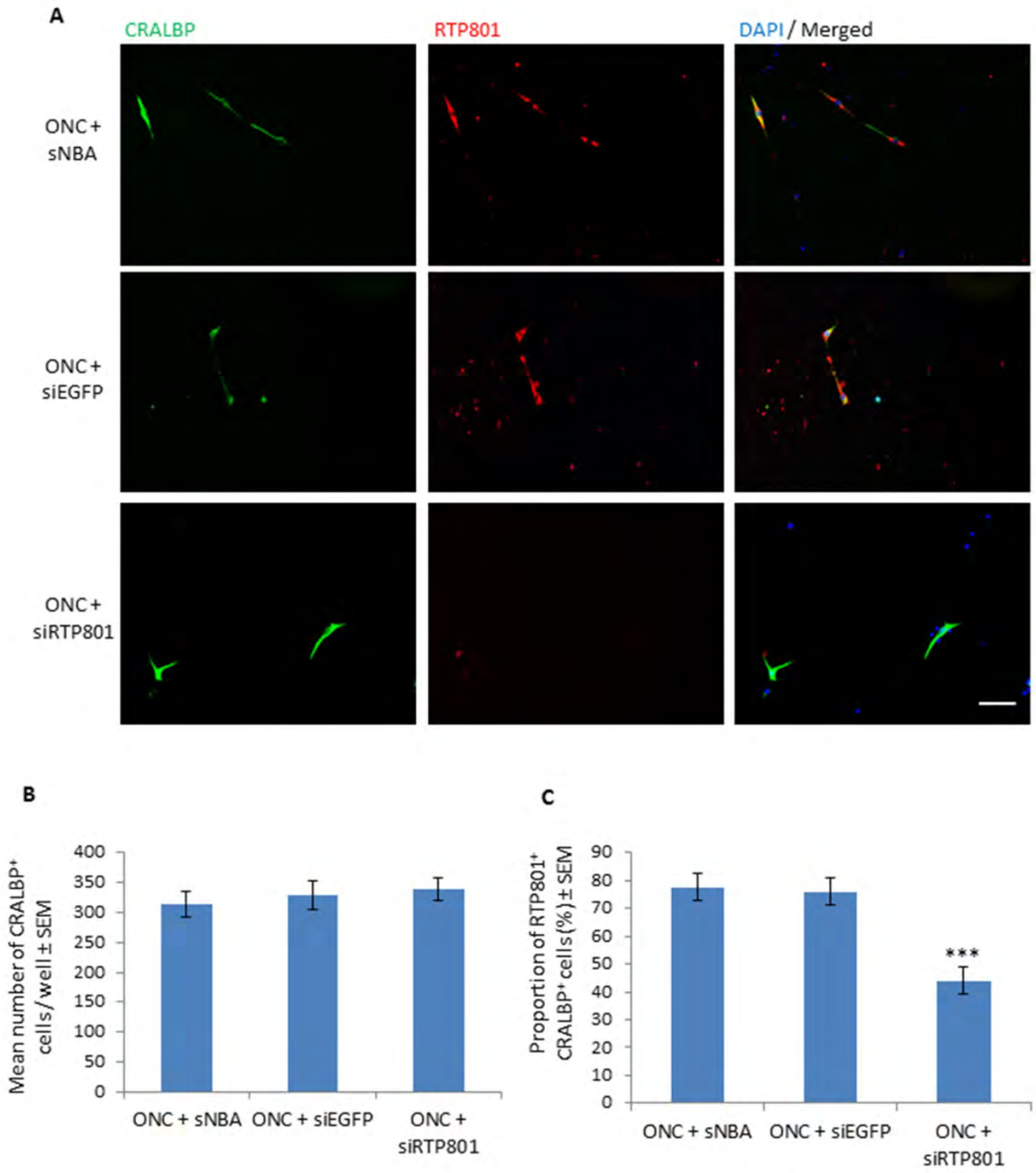


Figure 4.7: CRALBP$^+$ activated retinal glia and RTP801 knock-down in activated glia in retinal cultures established 5d after ONC. (A) CRALBP (green) and RTP801 (red) immunostaining of cultured retinal cells, with DAPI (blue) as a nuclear counterstain, established 5d after prior ONC *in vivo* and treated with sNBA culture medium alone (top row), siEGFP (middle row) and siRTP801 (bottom row), indicating presence of CRALBP$^+$ glia and expression of RTP801, which is reduced after siRTP801 treatment (scale bar = 20µm). (B) Quantification of CRALBP$^+$ cells in glial-activated retinal cultures for conditions described in (A), indicating no significant effect of siRTP801 on CRALBP$^+$ glial proliferation (n=3). (C) Proportion of CRALBP$^+$ glia expressing RTP801 after siRTP801 treatment compared to controls, indicating RTP801 knock-down in CRALBP$^+$ activated glia (n=3; ***p<0.001 *vs* sNBA control).

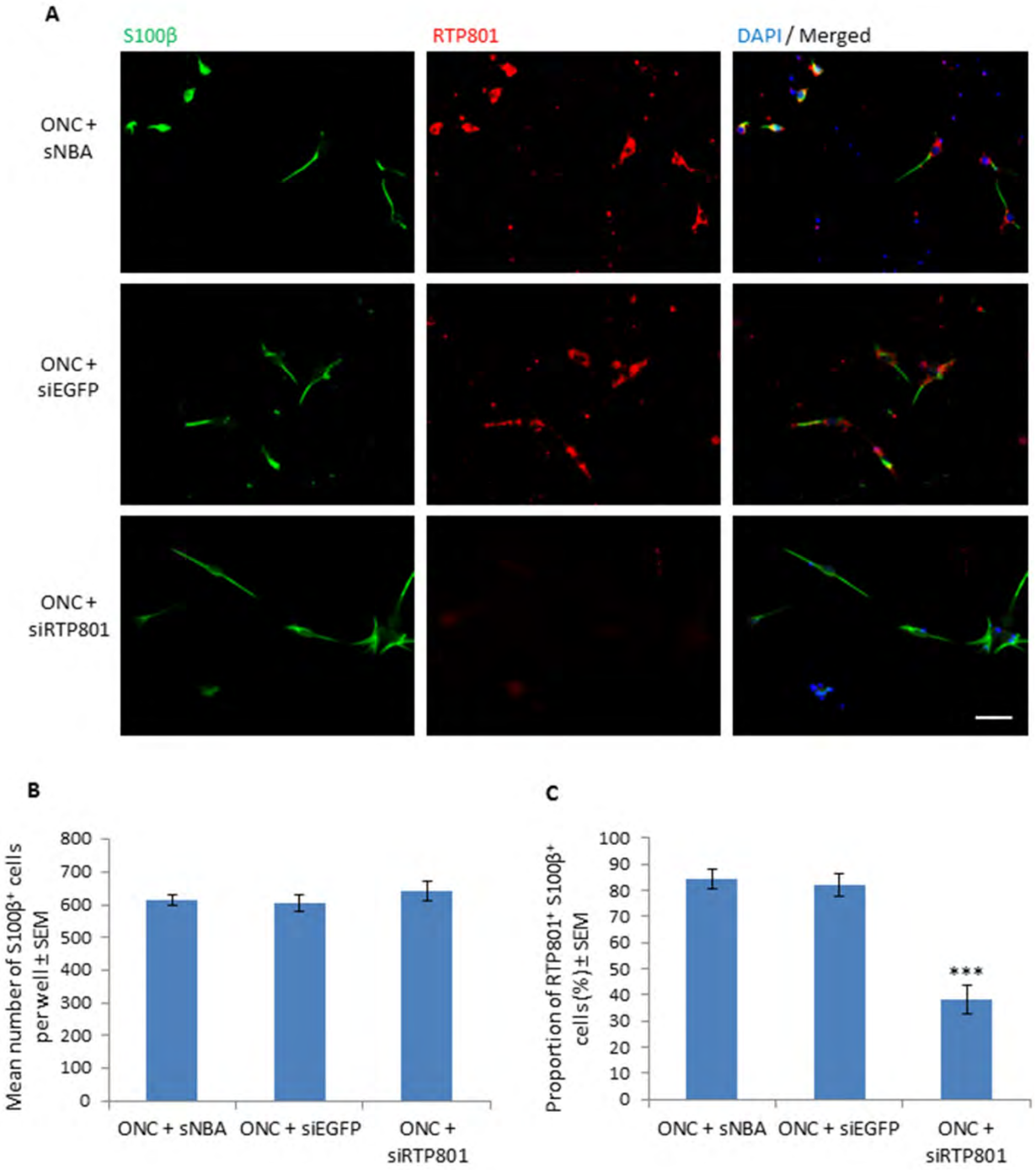


Figure 4.8: S100β$^+$ retinal glia and RTP801 knock-down in activated glia in retinal cultures established 5d after ONC. (A) S100β (green) and RTP801 (red) immunostaining of cultured retinal cells, with DAPI (blue) as a nuclear counterstain, established 5d after prior ONC *in vivo* and treated with sNBA culture medium alone (top row), siEGFP (middle row) and siRTP801 (bottom row), indicating presence of S100β$^+$ glia and expression of RTP801, which is reduced after siRTP801 treatment (scale bar = 20µm). (B) Quantification of S100β$^+$ cells in glial-activated retinal cultures for conditions described in (A), indicating no significant effect of siRTP801 on S100β$^+$ glial proliferation (n=3). (C) Proportion of S100β$^+$ glia expressing RTP801 after siRTP801 treatment compared to controls, indicating RTP801 knock-down in S100β$^+$ glia (n=3; ***p<0.001 *vs* sNBA control).

4.5.3 Effect of siRTP801 on RGC survival and neurite outgrowth in the presence of activated glia, and the role of mTORC1- and Trk-dependent signalling

4.5.3.1 siRTP801 promoted RGC survival and neurite elongation in the presence of activated retinal glia in vitro*, without affecting neurite growth initiation*

In the presence of activated retinal glia *in vitro*, the number of surviving βIII-tubulin^{+} RGC significantly increased from 299.5 ± 27.9 and 264.7 ± 28.9 in sNBA and siEGFP control wells, respectively, to 605.3 ± 31.3 cells after siRTP801 treatment ($p<0.001$) (Figure 4.9A, B). These data are comparable to that seen in cultures established from intact eyes (Chapter 3), indicating both that significant RGC death had not yet occurred after ONC in these cultures, and also that the presence of activated retinal glia in culture did not affect the pro-survival effect of siRTP801. There was no statistically significant difference in the proportion of neurite-bearing RGC between siRTP801-treated wells (37.2 ± 4.9%) and sNBA- (26.8 ± 5.2%) and siEGFP-treated (24.8 ± 5.5%) controls (Figure 4.9A, C), comparable to observations in the absence of activated retinal glia. However, the mean length of longest neurite extending from RGC was 36 ± 8μm and 34 ± 6μm for sNBA and siEGFP controls, respectively, and significantly longer (78 ± 12μm, $p<0.05$) after siRTP801 treatment (Figure 4.9A, D). Thus, in the presence of activated retinal glia *in vitro*, siRTP801 promoted both RGC survival and neurite elongation, but not neurite growth initiation.

4.5.3.2 The contribution of mTORC1-dependent signalling to siRTP801-induced RGC neuroprotection and neurite elongation in vitro

The RGC neuroprotective effect of siRTP801 was significantly reduced in the presence of the mTORC1 inhibitor Rapamycin (452.0 ± 36.1 cells/well, $p<0.05$), but not abolished, indicating both mTORC1-

dependent and mTORC1-independent mechanisms contributing to the RGC pro-survival effect of siRTP801 (4.10A, B). Rapamycin did not reduce the number of βIII-tubulin^{+} RGC in sNBA or siEGFP control wells, indicating that Rapamycin was not directly RGC neurotoxic in this model (Figure 4.10A, B). Rapamycin also had no significant effect on RGC neuritogenesis (Figure 4.10A, C), but did reduce mean neurite length in siRTP801-treated wells (54 ± 6μm), although the latter result did not reach reach statistical significance (Figure 4.10D), suggesting that siRTP801-induced neurite elongation was predominantly mTORC1-independent.

4.5.3.3 The contribution of Trk-dependent signalling to siRTP801-induced RGC neuroprotection and neurite elongation in vitro

In the presence of the Trk receptor antagonist K252a, the siRTP801-induced RGC survival effect was significantly reduced (387.0 ± 38.2 cells/well; $p<0.01$), indicating an important role for Trk receptor downstream signalling pathways in mediating RGC neuroprotection (Figure 4.10A, B). K252a was not associated with significant RGC death in sNBA and siEGFP control wells (Figure 4.10B), and had no significant effect on the initiation of RGC neurite outgrowth (Figure 4.10C). However, the siRTP801-induced neurite elongation effect was abolished in the presence of K252a (32 ± 4μm; $p<0.01$ *vs* siRTP801 in the absence of K252a), indicating an essential role for Trk-dependent signalling, rather than mTOR activity *per se* for promoting the growth of longer neurites after RTP801 knock-down in the presence of activated retinal glia (Figure 4.10A, D).

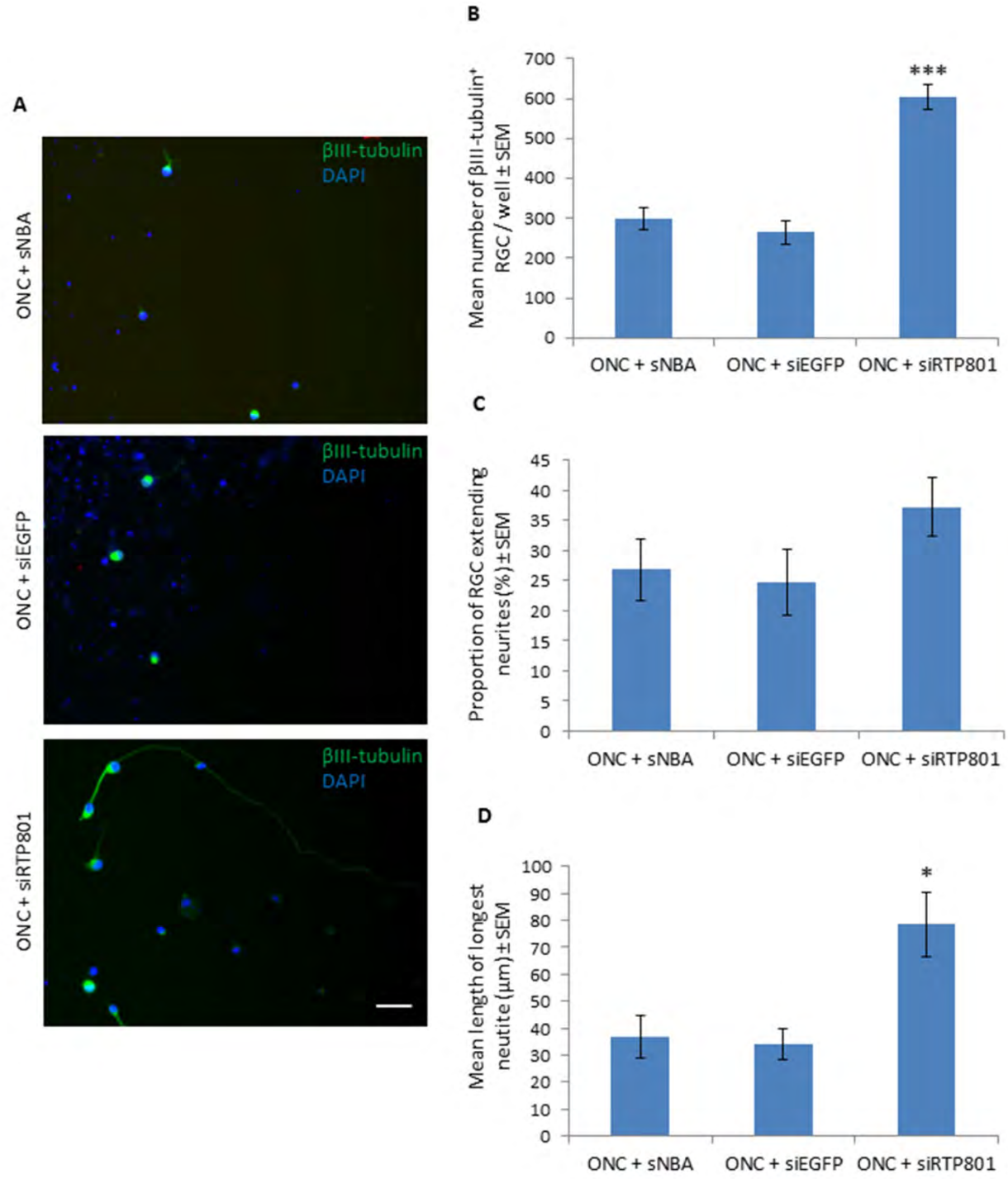


Figure 4.9: RGC survival and neurite outgrowth in cultured retinal cells in the presence of activated retinal glia. (A) βIII-tubulin (green) immunostained retinal cultures established 5d after prior ONC *in vivo* to activate retinal glia, and treated with sNBA alone, siEGFP and siRTP801. DAPI (blue) was used as a nuclear counterstain (scale bar = 20µm). Quantification of (B) surviving βIII-tubulin^{+} RGC, (C) proportion of RGC extending neurites, and (D) length of longest RGC neurites for treatment conditions described in (A). Note that in glial-activated cultures siRTP801 promoted RGC survival, had no significant effect on neurite initiation, but increased RGC neurite elongation compared to controls (n=3; *p<0.05, ***p<0.001).

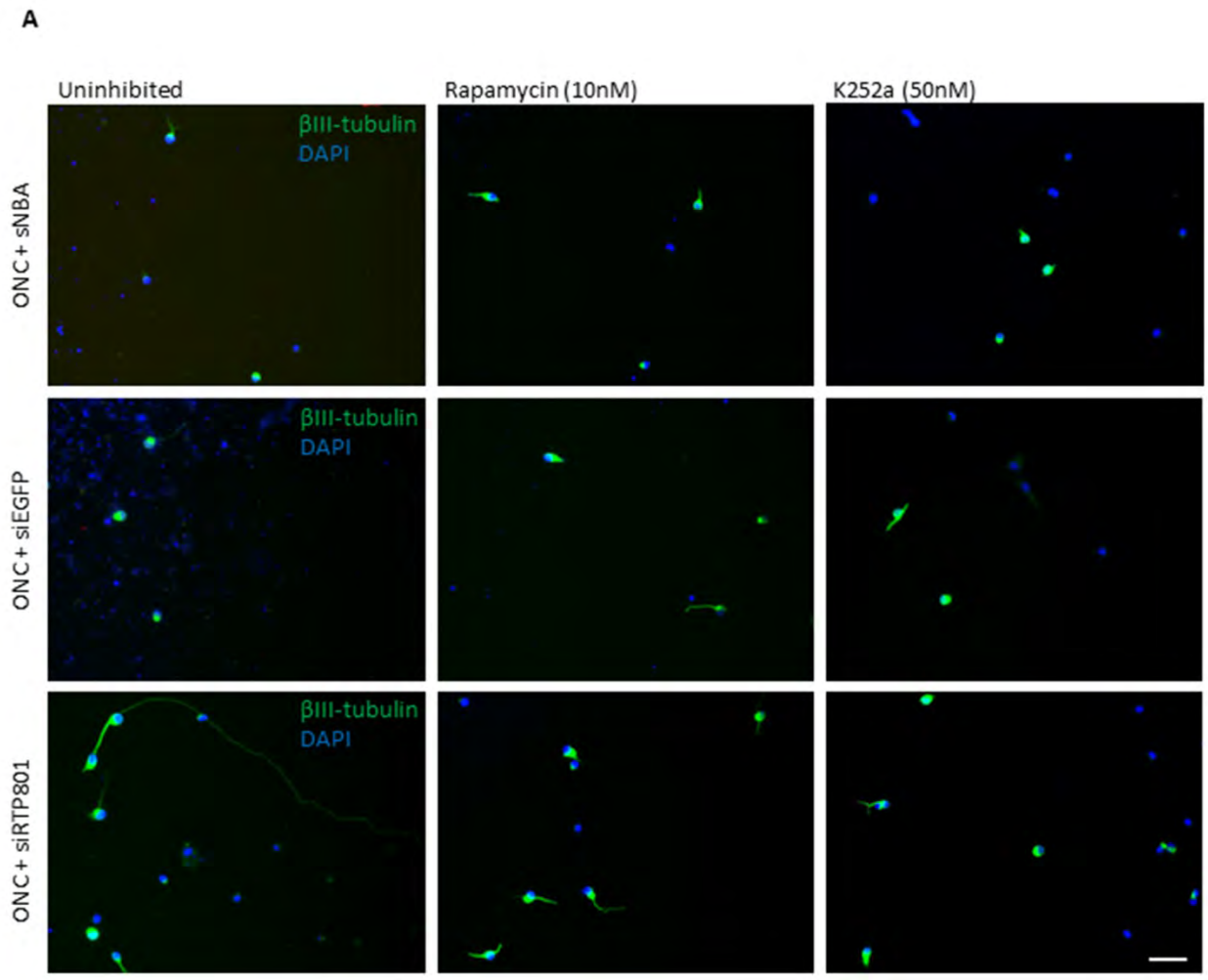


Figure 4.10: Effects of mTORC1 inhibitor Rapamycin and pan-Trk receptor antagonist K252a on RGC survival and neurite outgrowth in glial-activated retinal cultures. (A) βIII-tubulin (green) immunostained retinal cultures, established 5d after prior ONC *in vivo* to activate retinal glia and treated with sNBA alone, siEGFP and siRTP801 in the absence of inhibitors (left column, as per Figure 4.9A) and in the presence of the mTORC1 inhibitor Rapamycin (10nM; middle column) or the pan-Trk receptor antagonist K252a (50nM; right column). DAPI (blue) was used as a nuclear counterstain (scale bar = 20µm). Quantification of (B) surviving βIII-tubulin$^+$ RGC, (C) proportion of RGC extending neurites, and (D) length of longest RGC neurites for treatment conditions described in (A). The blue bars represent uninhibited cultures as per Figure 4.9B-D. Note that the siRTP801-induced RGC survival and neurite elongation effects are partially reduced but not abolished by Rapamycin, but completely suppressed by K252a (n=3; *p<0.05, **p<0.01, ***p<0.001). Figure continues on the next page.

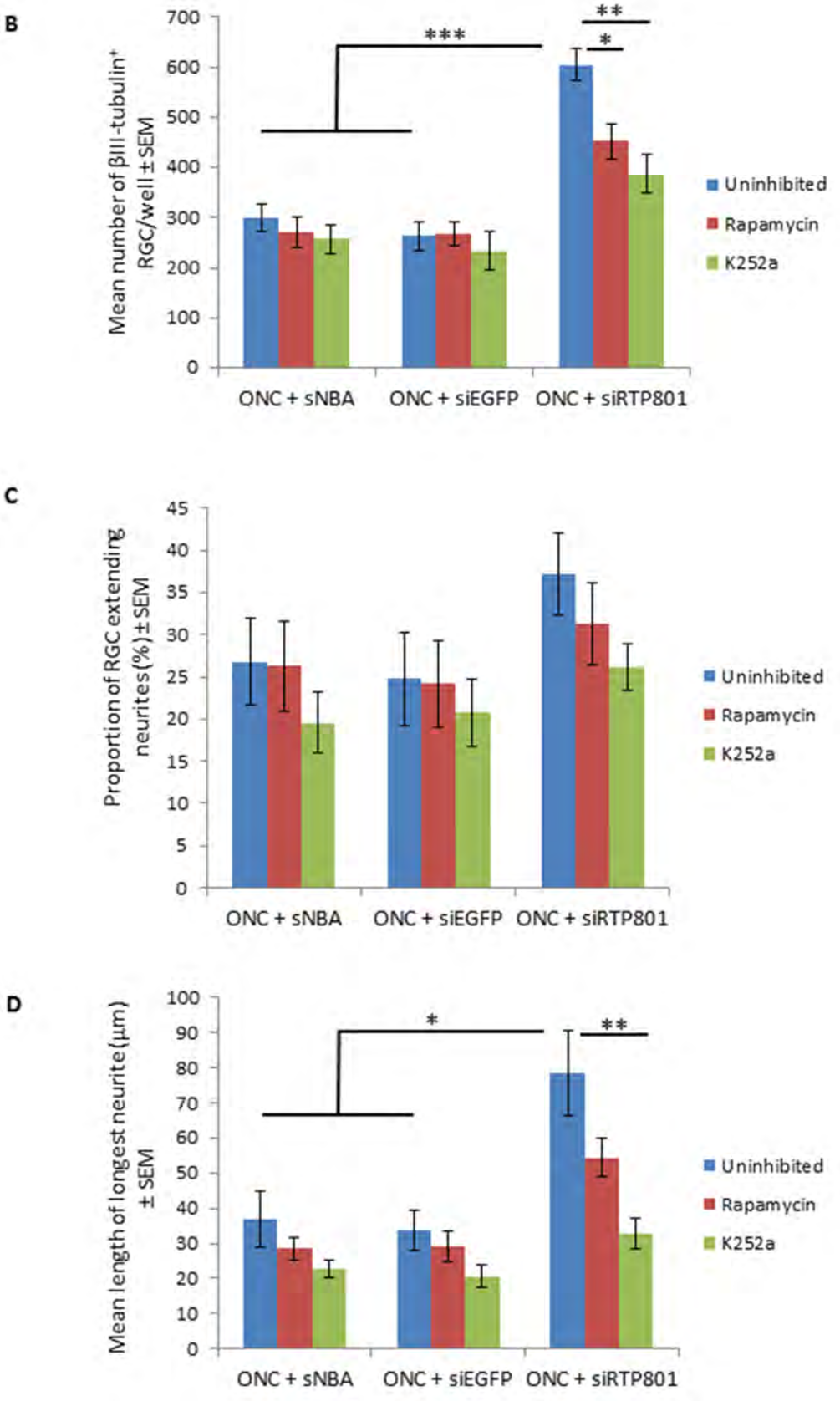


Figure 4.10: Effects of mTORC1 inhibitor Rapamycin and pan-Trk receptor antagonist K252a on RGC survival and neurite outgrowth in glial-activated retinal cultures. Continued from previous page.

4.5.4 Effect of siRTP801 on the production of NTF *in vitro*

4.5.4.1 Effect of siRTP801 on the production of neurotrophins and other NTF in the absence and presence of activated retinal glia

In medium from retinal cultures established from uninjured animals, in which activated retinal glia were absent, titres of the neurotrophins BDNF, NGF and NT3, and GDNF were very low or undetectable (Figure 4.11A, B, C, E; blue bars), irrespective of whether incubated with sNBA, siEGFP or siRTP801. CNTF was detected in medium from these cultures in the absence of activated retinal glia, although the titres were not significantly different between treatment groups (Figure 4.11D; blue bars). After activation of retinal glia by prior ONC *in vivo*, titres of BDNF, NGF, NT-3, CNTF and GDNF were all increased relative to the cultures in the absence of activated retinal glia (Figure 4.11A-E; red bars). Compared to sNBA and siEGFP, treatment with siRTP801 resulted in significantly higher detected titres of BDNF ($p<0.001$), NGF ($p<0.001$), NT-3 ($p<0.05$) and CNTF ($p<0.01$) in the presence of activated glia (Figure 4.11A-D), although detected levels of GDNF were not further increased by siRTP801 (Figure 4.11E). These data suggested that activation of retinal glia by ONC led to increased production and release of NTF, and provided further evidence that although siRTP801 was unable to directly activate retinal glia, addition of siRTP801 to cultures comprising already activated glia resulted in the potentiation of the secretory phenotype of the activated glia, i.e. in significantly increased production of NTF.

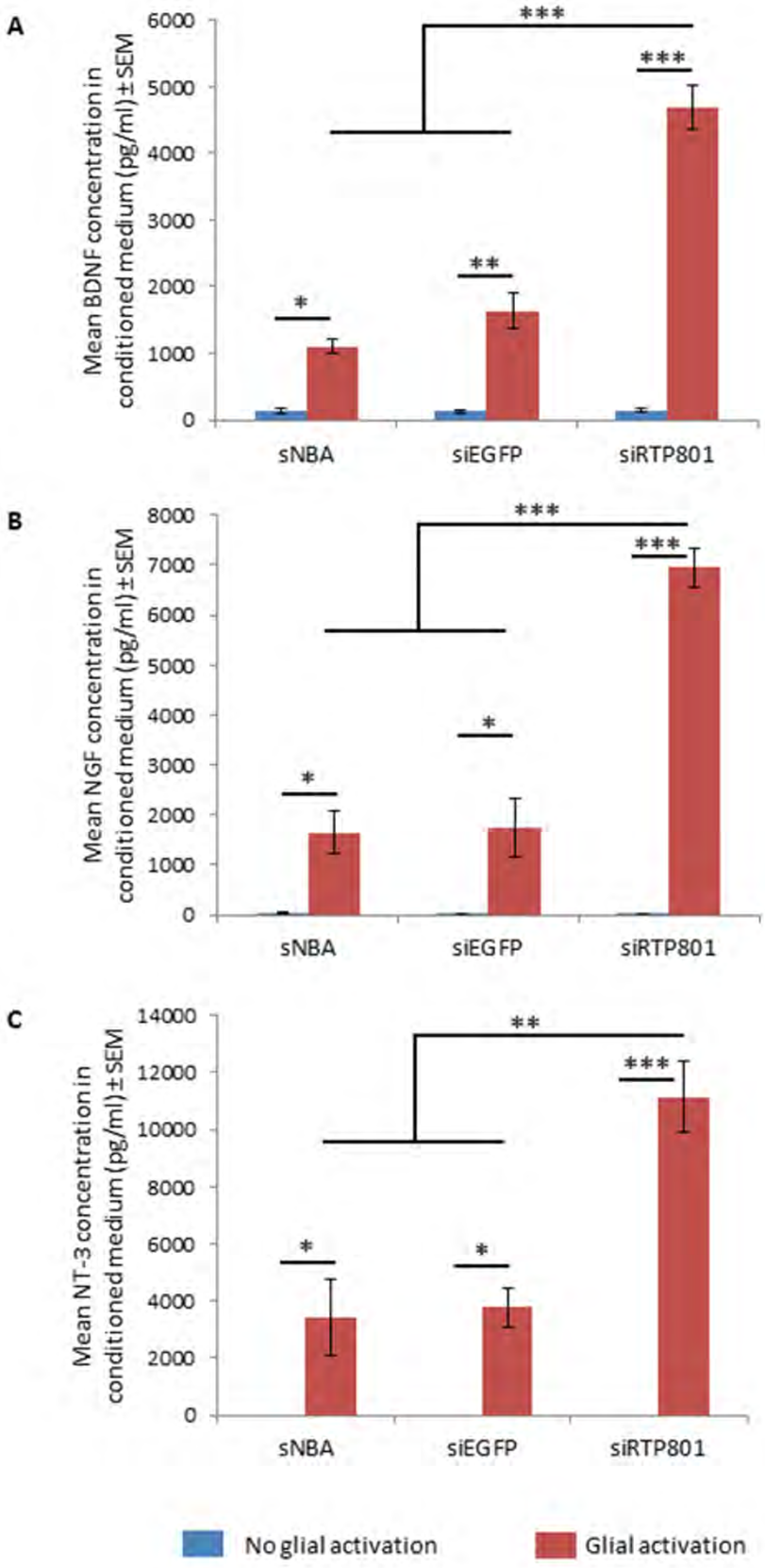


Figure 4.11: Effects of siRTP801 treatment on NTF titres in the absence and presence of activated retinal glia. Figure continues with the full legend on the next page.

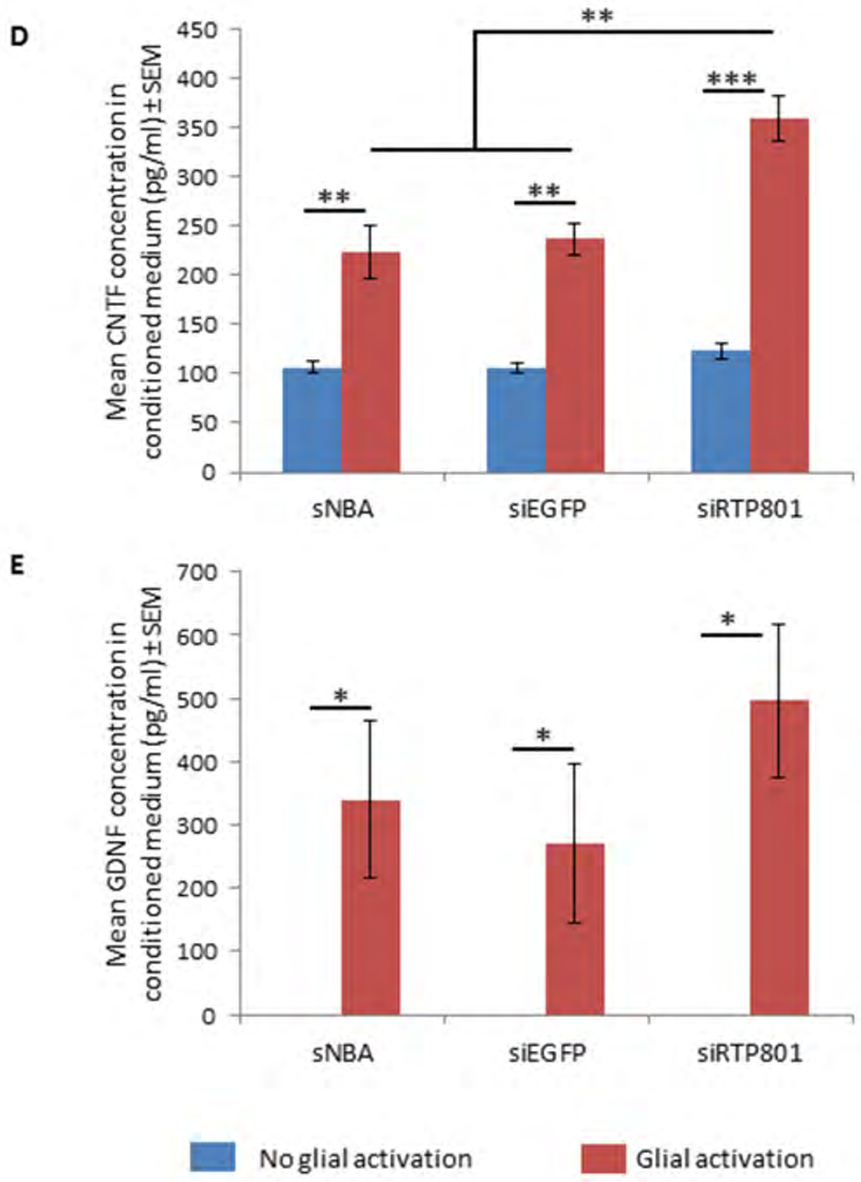


Figure 4.11: Effects of siRTP801 treatment on NTF titres in the absence and presence of activated retinal glia. Titres of (A) BDNF, (B) NGF, (C) NT-3, (D) CNTF, and (E) GDNF in conditioned culture medium, measured by ELISA on samples obtained from primary retinal cultures incubated with sNBA culture medium alone, siEGFP and siRTP801 in the absence (blue bars) and presence (red bars) of activated retinal glia. Note the increased titres of all measured NTF in cultures established after glial activation by prior ONC *in vivo*, and potentiation of secretion of BDNF, NGF, NT-3, and CNTF by siRTP801 treatment (n=3; *p<0.05, **p<0.01, ***p<0.001).

4.5.4.2 Neurotrophic factor production both from RGC and glia

In retinal cultures established from animals 5d after prior ONC to activate retinal glia, immunocytochemical detection of phenotypic antibodies for the neurotrophins BDNF (Figure 4.12A) and NT-3 (Figure 4.12B) indicated expression of these NTF both in βIII-tubulin^{+} RGC and in βIII-tubulin^{-} cells, presumed to be glia. Unfortunately, insufficient wells were available for quantitative analysis of cell-type-specific NTF expression. Nonetheless, these qualitative results indicate that both autocrine and paracrine effects are likely to contribute to NTF-dependent RGC survival and neurite outgrowth.

4.5.5 Summary of results

These results have demonstrated that siRTP801 prevented injury-induced down-regulation of pS6 in retinal cells *in vivo* and *in vitro*, indicating the maintenance of mTORC1 activity. Retinal cultures established 5d after prior ONC *in vivo* were associated with the presence of activated retinal glia, in which RTP801 activity was observed and shown to be susceptible to siRNA-mediated knock-down. In the presence of activated retinal glia, siRTP801 was both RGC neuroprotective and promoted neurite elongation, without affecting neurite initiation, findings which replicate the *in vivo* paradigm described in Chapter 3. The neuroprotective and axon elongation effects of siRTP801 had contributions from mTORC1-dependent signalling, but were predominantly mTORC1-independent. RTP801 knock-down promoted ONC-induced retinal glial-activation and potentiated the release of NTF, signalling of which *via* Trk-receptors was necessary for the mediation of siRTP801-induced RGC survival and neurite elongation.

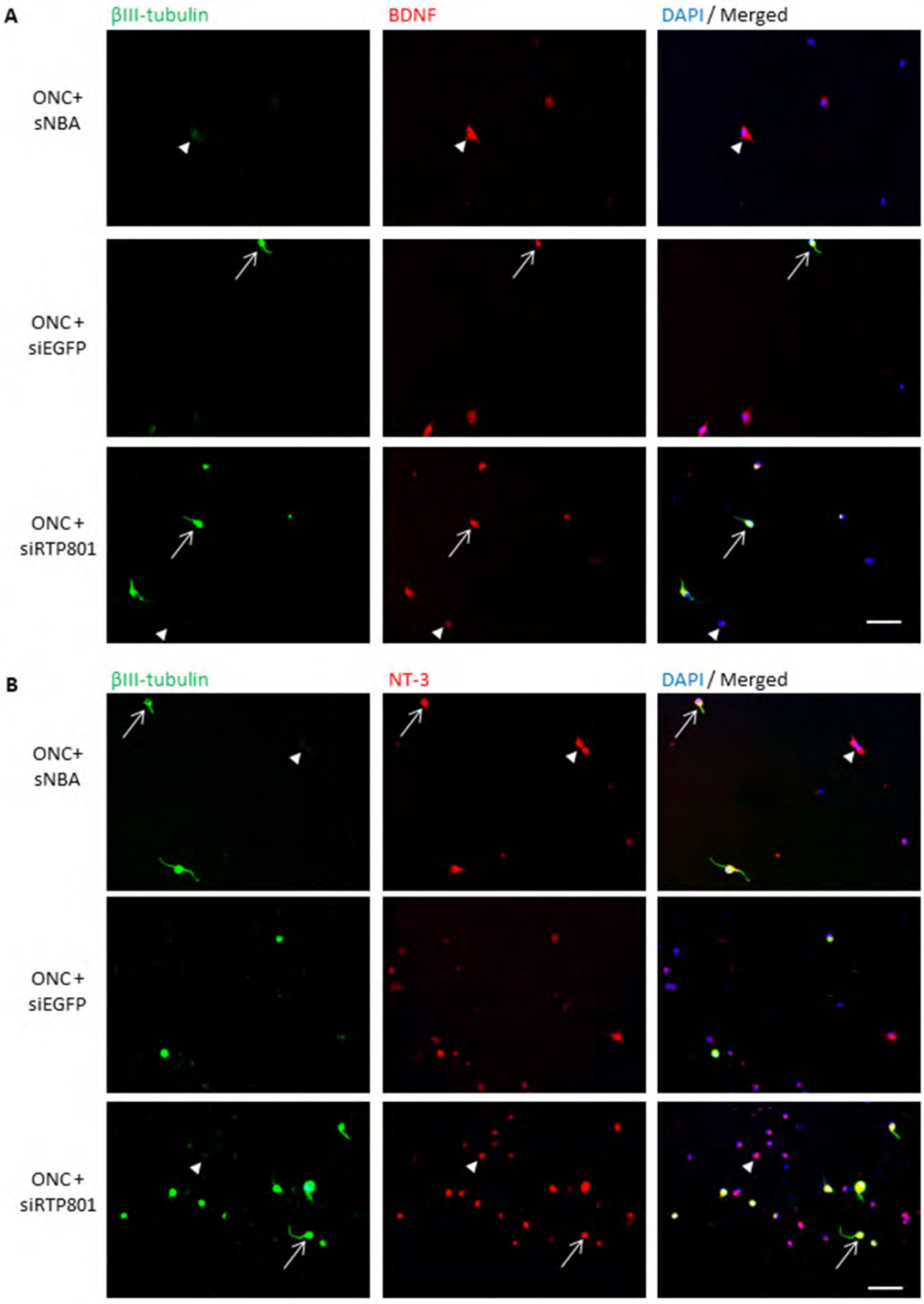


Figure 4.12: NTF detection in RGC and non-neuronal cells in glial-activated retinal cultures. (A) Retinal cultures established after prior glial activation by ONC *in vivo*, and incubated with sNBA culture medium alone (top row), siEGFP (middle row) and siRTP801 (bottom row), immunostained for βIII-tubulin (green) and BDNF (red), with DAPI (blue) as a nuclear counterstain, indicating BDNF positivity in both RGC (arrows) and non-neuronal cells (arrowheads) (scale bar = 20µm). (B) Retinal cultures established after prior glial activation by ONC *in vivo*, and incubated with sNBA culture medium alone (top row), siEGFP (middle row) and siRTP801 (bottom row), immunostained for βIII-tubulin (green) and NT-3 (red), with DAPI (blue) as a nuclear counterstain, indicating NT-3 positivity in both RGC (arrows) and non-neuronal cells (arrowheads) (scale bar = 20µm).

4.6 DISCUSSION

There is increasing evidence that the PI3K/Akt/mTOR signalling pathway plays a major role in neuronal viability and capacity for axon regeneration. Whilst siRNA-mediated knock-down of the mTOR negative regulator RTP801 promoted RGC survival and axon elongation after ONC injury *in vivo*, as described in Chapter 3, translation of experimental results into the development of potential novel therapeutics requires a thorough understanding of underlying cellular mechanisms. The aims of experiments described in this Chapter were to investigate the effects of siRTP801 on mTORC1 activity and on retinal glial activation in relation to the mechanism of promoting RGC survival and axon/neurite growth. The main findings were that: (1) expression of pS6, a correlate of mTORC1 activity, occurred in a minority of RGC in intact retinae *in vivo*, with siRTP801 treatment preventing an injury-induced down-regulation in pS6; (2) siRTP801 led to an increase in $pS6^{+}$ RGC in cultures obtained from uninjured animals and prevented injury-induced down-regulation of RGC pS6 *in vitro*; (3) RGC expression of pS6 was not obligatory for neurite outgrowth; (4) pS6 was not limited to RGC; (5) siRTP801 potentiated the activation of retinal glia after ONC *in vivo* without inducing Müller glial proliferation; (6) RTP801 activity was detected in activated retinal glia in cultures established after prior ONC, and knocked-down by siRTP801 treatment; (7) in the presence of activated retinal glia *in vitro*, siRTP801 was RGC neuroprotective and promoted growth of longer neurites, without affecting initiation of neurite growth; (8) siRTP801-induced RGC survival and neurite elongation were mediated by both mTORC1-dependent and independent mechanisms; (9) siRTP801-induced RGC survival and neurite elongation were mediated by Trk-dependent signalling; and (10) activation of retinal glia led to increased production of NTF, an effect which was potentiated by siRTP801 treatment.

4.6.1 The role of mTOR activity in siRTP801-mediated RGC survival and axon/neurite growth

In contrast to the retinal culture experiments described in Chapter 3, in which $GFAP^+$ activated glia were absent, retinal cultures established 5d after prior ONC *in vivo* contained $GFAP^+$ cells, consistent with previous reports (Ahmed *et al.*, 2010; Vigneswara *et al.*, 2014; Lorber *et al.*, 2012; Lorber *et al.*, 2008), and also $CRALBP^+$ glia, indicating the presence of activated retinal astrocytes and Müller glia and therefore may be considered more representative of the *in vivo* condition after ONC injury. Treatment with siRTP801 in these cultures knocked-down RTP801 expression in activated glia, indicating both that RTP801 is present in these cells (and presumably modulating mTOR activity) and that siRTP801 transfected these glia sufficient to induce target knock-down. Thus, the effects of siRTP801 on RGC survival and neurite growth were unlikely to be entirely due to RTP801 knock-down in RGC alone, but occurred with a contribution from mTOR activity in glia also. In this glial-activated *in vitro* setting, siRTP801 treatment replicated the RGC survival effect, suggesting that siRTP801 was RGC neuroprotective irrespective of the presence of activated glia, indicative of a direct effect of the siRNA on RGC, but was also associated with the growth of longer RGC neurites, mirroring the *in vivo* observation of axon elongation and providing strong evidence that additional factors were present in the glial-activated cultures that enabled more sustained neurite growth.

RTP801 is induced by cellular stress, including after ONC, and primarily acts to reduce mTOR signalling (Brugarolas *et al.*, 2004; Corradetti *et al.*, 2005). As siRTP801 effectively knocked-down RTP801 expression in the retina, and was associated with RGC survival and axon/neurite elongation both *in vivo* and *in vitro*, it was hypothesised that the neuroprotection and axon growth promotion afforded by siRTP801 were mediated by enhanced mTOR activity. In order to quantify mTOR activity, pS6 is one of the most commonly measured functional read-outs (Ikenoue *et al.*, 2009; Park *et al.*, 2008; Morquette *et al.*, 2014), reflecting the action of mTORC1 on p70 ribosomal S6 kinase (p70S6K)

leading to increased phosphorylation of ribosomal S6 protein, which in turn up-regulates mRNA translation (Jefferies *et al.*, 1997) (see Figure 1.7). Commonly reported to correlate with 'mTOR' activity, expression of pS6 is more specifically associated with mTORC1 activity. To assess the contribution of mTORC1 activity to the effects of siRTP801, two approaches were used: (1) RGC pS6 expression was measured both *in vivo* and *in vitro* by immunofluorescence; and (2) Rapamycin was used *in vitro* to block mTORC1 activity.

Detection of pS6 was limited to a minority of RGC, both in retinal sections (approximately 15%) and in cultures (approximately 23%) from uninjured animals, indicating a low, but constitutive mTORC1 activity in the retina. There was a significant reduction in $pS6^{+}$ RGC after ONC, and in RGC in cultures established 5d after ONC, reflecting a well-described injury-induced suppression of mTORC1 activity (Park *et al.*, 2008; Smith *et al.*, 2009). Treatment with siRTP801 prevented the reduction in RGC pS6 expression both after ONC and in the culture paradigm. Furthermore, in retinal cultures established from uninjured animals, siRTP801 resulted in a small, but statistically significant increase in $pS6^{+}$ RGC. These findings, together with the ONC-induced RTP801 up-regulation that was reduced by siRTP801 (as described in Chapter 3), indicated that RTP801 activity contributed to the reduced pS6 expression observed after injury, and that siRTP801 acted to overcome this down-regulation and maintain mTORC1 activity. However, the RGC survival and axon/neurite elongation effects of siRTP801 cannot be entirely attributed to mTORC1 activity, since although Rapamycin abolished pS6 expression, as reported previously (Leibinger *et al.*, 2012; Heskamp *et al.*, 2013; Park *et al.*, 2008), it only partially attenuated the siRTP801 neuroprotective effect. Also, neurite elongation was predominantly mTORC1-independent and the initiation of neurite outgrowth was unaffected by either siRTP801 treatment, or mTORC1 blockade with Rapamycin. These findings are consistent with several previous reports on the role of mTORC1 in RGC survival and axon growth. For example, Park and colleagues showed that pS6 levels in RGC were development-dependent, reducing from almost 50% in early

post-natal mice to a constitutive level of 8-10% at adulthood, with a further down-regulation after injury (Park *et al.*, 2008; Smith *et al.*, 2009). Also, Leibinger *et al.* (2012) reported pS6 to be localised to approximately 14% of RGC in intact animals, and pS6 expression *in vitro* correlates with approximately 10-20% RGC in the absence of treatments/inhibitors (Heskamp *et al.*, 2013). Thus, there is a low but detectable constitutive level of pS6 in RGC, representing basal mTORC1 activity, in keeping with both the *in vivo* and *in vitro* data presented here. The down-regulation of this mTORC1 activity after injury was prevented by siRTP801 treatment, similar to that seen after *pten* deletion to maintain PI3K pathway signalling after ONC (Park *et al.*, 2008), and after inflammatory stimulation (Leibinger *et al.*, 2012). In addition, a reduction in the proportion of $pS6^{+}$ RGC after axotomy is reversed by siRNA-mediated knock-down of Redd2, a complex structurally and functionally similar to RTP801 (Morquette *et al.*, 2014).

The maintenance of 8-10% of $pS6^{+}$ RGC after ONC in *pten* deleted animals correlates closely with the proportion of surviving RGC that regenerate axons beyond the ONC site, and moreover, around 88% of regenerating axons in that model are $pS6^{+}$ (Park *et al.*, 2008). In addition, expression of pS6 is up-regulated in DRG neurons after injury, associated with enhanced peripheral sensory axon regeneration (Abe *et al.*, 2010), and thus mTORC1 has been implicated as an important factor in determining axon regenerative ability, both in the retina and elsewhere in the CNS (Park *et al.*, 2010; Park *et al.*, 2008; Liu *et al.*, 2010a). However, despite siRTP801 maintaining pS6 levels *in vitro*, RGC neurite growth was observed both in $pS6^{+}$ and $pS6^{-}$ RGC, indicating that RGC mTORC1 activity was not mandatory for neuritogenesis. Both initiation and elongation of neurite growth were predominantly independent of mTORC1, a finding which is, in part, consistent with previous observations that some axon regeneration is recorded in $pS6^{-}$ RGC after *pten* deletion, and that Rapamycin does not completely abolish axon regeneration after *pten* deletion (Park *et al.*, 2008). Moreover, accelerated neurite growth in the PNS after PTEN inhibition is unaltered by Rapamycin

(Christie *et al.*, 2010). The precise role of mTORC1 in mediating RGC survival and axon growth is yet to be fully elucidated, as there is further conflicting evidence from other studies. The granulocyte-macrophage colony stimulating factor (GM-CSF) chemokine reportedly enhances both RGC survival and neurite growth in an mTORC1-dependent fashion (Legacy *et al.*, 2013), and the axon growth promoting effect of the chemotactic cytokine CXCL12 is abolished by Rapamycin (Heskamp *et al.*, 2013), indicating a vital role for mTORC1 in these circumstances. By contrast, induction of an intraocular inflammatory response by lens injury or intravitreal Pam3Cys promotes RGC survival and induces neurite outgrowth, effects which are unaffected by Rapamycin, and CNTF-induced neurite growth initiation is similarly mTORC1-independent (Leibinger *et al.*, 2012). As mentioned previously, compensatory sprouting of CST axons after injury was recently shown to be unaffected by Rapamycin (Lee *et al.*, 2014), although maintenance of RGC axons in a regenerative state after inflammatory stimulation is Rapamycin sensitive (Leibinger *et al.*, 2012), as is the enhanced dendrite elongation induced by siRedd2 (Morquette *et al.*, 2014). Thus, the role of mTORC1 in RGC survival is likely to be context-specific, with further evidence required to understand this more completely. It is probable that initiation of axon/neurite growth is mTORC1-independent, possibly *via* gp130 receptor-dependent, CNTF/LIF/IL-6-mediated JAK-STAT signalling (Leibinger *et al.*, 2009; Fischer and Leibinger, 2012; Muller *et al.*, 2007; Vigneswara *et al.*, 2014), but under certain cellular conditions mTORC1 contributes to maintaining axonal growth, albeit with inputs from mTORC1-independent mechanisms in other conditions. Indeed, in apoptosis-resistant RGC over-expressing Bcl-2, inhibition of PI3K or MAPK individually partially block axon outgrowth, whereas inhibition of both of these complexes together is necessary to abrogate axon elongation altogether (Goldberg, 2003; Goldberg *et al.*, 2002a), thus reflecting multiple contributing pathways and complexes. RGC pS6 expression was not mandatory for RGC neurite outgrowth, but pS6 was observed in around 50% of neurite-bearing RGC, which was notably higher than the measured proportion of pS6 expression in the total (neurite- and non-neurite-bearing) RGC population as a whole, and suggested an increased likelihood of neurite

growth in RGC with detectable mTORC1 activity. Strikingly, the mTORC1 component Raptor is concentrated in the αRGC sub-type, indicating a higher constitutive level of mTORC1, and these ipRGC selectively express the phosphoprotein osteopontin, which is able to positively regulate mTOR activity (Duan *et al.*, 2015). Although the experiments described in this thesis have not investigated particular RGC classes, the enhanced neurite elongation induced by siRTP801 may reflect increased mTORC1 activity in this RGC subset, and mTORC1-independent mechanisms in other RGC.

An added complexity in relation to the role of mTORC1 in contributing to RGC survival and axon/neurite growth is that phosphorylation of S6 also occurs in response to mTORC1-independent pathways, such as ERK/MAPK, PKA (Roux *et al.*, 2007; Pende *et al.*, 2004), PDK1, and cell division control protein 2 (cdc2) (Weng *et al.*, 1998; Saitoh *et al.*, 2002). Additionally, a recent genome-wide screen identified nearly 600 functionally diverse genes with regulatory effects on S6 phosphorylation (Papageorgiou *et al.*, 2015). Therefore, pS6 may not be as sensitive or specific a correlate of mTORC1 activity as previously thought, and reported outcomes for mTOR pathway manipulations may, at least in part, actually reflect effects of mTORC1/4E-BP1-specific activity. The role of the mTORC1 substrate 4E-BP1 has rarely been considered in terms of mTOR-dependent neuronal survival and axon growth, but a recent study has attempted to provide clarity (Yang *et al.*, 2014). Activation of mTORC1 leads to phosphorylation (inhibition) of 4E-BP1, releasing it from the eIF4E complex and thereby allowing the latter to initiate protein translation (Gingras *et al.*, 1998; Hay and Sonenberg, 2004). In an ONC model, constitutive activation of S6 kinase (thus increasing pS6 expression) results in enhanced RGC survival and axon regeneration, whereas 4E-BP1 knock-out leads to a small increase in RGC survival, but is insufficient to promote axon regeneration (Yang *et al.*, 2014). Interestingly, 4E-BP1 inhibition appears necessary for *pten* deletion-induced RGC axon regeneration, indicating that mTORC1-mediated effects on axon regeneration are not limited to the pS6 output, and highlighting the complexity of mTORC1-related translational control in RGC survival and axon growth.

Treatment with siRTP801 prevented injury-induced down-regulation of mTORC1 activity, and Rapamycin sensitive mTORC1 activity appeared to contribute to, but was not obligatory for the neuroprotection and axon/neurite growth elicited by siRTP801. Combined with the observations from other studies, discussed above, this finding implicates alternative intracellular signalling pathways; among them, the relatively Rapamycin insensitive mTORC2 is a primary candidate (Maiese *et al.*, 2013; Ma and Blenis, 2009). The activity of mTORC2 is down-stream of RTP801/TSC1/2 (Figure 1.7) and is likely, therefore, to be potentiated by RTP801 inhibition and contribute to the neuroprotection/axon growth by siRTP801 in the presence of the mTORC1 inhibitor Rapamycin. The mTORC2 complex influences cellular processes either through the downstream substrate PKCα, which is associated with actin dynamics and may influence axonal growth cone activity (Ma and Blenis, 2009; Angliker and Ruegg, 2013), or by feedback phosphorylation and activation of Akt, which in turn regulates the activity of other growth and cell survival mediators such as GSK3β and components of mitochondrial apoptosis machinery (Park *et al.*, 2010; Jacinto *et al.*, 2006; Tang *et al.*, 2014). RTP801 knock-out in the PNS is associated with increased phosphorylation of Akt at residue 473, consistent with Akt activation downstream of RTP801 inhibition through the mTORC2 feedback loop (Jacinto *et al.*, 2006). Whilst not widely studied in the context of RGC survival, mTORC2 activity *in vitro* is implicated in cellular survival mechanisms, *via* inhibition of caspase-mediated apoptosis, through other anti-apoptotic proteins like Annexin A5, Mortalin and Cofilin-1, and through Akt-mediated suppression of FoxO (Tang *et al.*, 2014; Zhang *et al.*, 2011). Indeed, the seemingly paradoxical reports of neuroprotection after treatment with Rapamycin can be explained by the fact that Rapamycin inhibits only mTORC1 and not mTORC2, enabling the latter to influence cell survival, and also that Rapamycin treatment blocks translation of RTP801 (Malagelada *et al.*, 2010). In terms of axon growth, mTORC2-mediated activation of Akt influences the activity of GSK3β, which negatively regulates axon growth cone assembly and is inactivated by Akt (Zhou and Snider, 2005b). Several reports provide evidence that GSK3β inhibition is associated with enhanced neuronal growth

(investigated further in Chapter 5) (Dill *et al.*, 2008; Liz *et al.*, 2014; Seira and Del Rio, 2014). Thus, in addition to the maintenance of mTORC1 signalling after ONC, siRTP801-mediated mTORC2 signalling provides a plausible explanation for a major contributory role in enhancing RGC survival and neurite extension.

4.6.2 The role of activated retinal glia in siRTP801-mediated RGC survival and axon/neurite growth

Previous studies investigating the role of the PI3K/Akt/mTOR signalling axis on neuronal survival and axon regeneration have focused on RGC responses alone, rather than on the contribution of glial-derived factors, although it is possible that the surgical manipulations undertaken to induce conditional gene deletion before ONC, for example, result in altered glial activity and may therefore contribute to reported outcomes despite neuron-specific gene targeting (Park *et al.*, 2008; Smith *et al.*, 2009; Sun *et al.*, 2011). Retinal glial activation has a major influence on axon regeneration, and is likely to be a significant factor that underpins the differential regenerative ability between the PNS and CNS (Brosius Lutz and Barres, 2014). Activation of retinal glia, including astrocytes and Müller glia, is associated with the production and release of neurotrophins and other pro-regenerative and inflammatory cytokines, which modulate the injury response through autocrine and paracrine mechanisms (Ahmed *et al.*, 2010; Vigneswara *et al.*, 2014; Lorber *et al.*, 2009a; Lorber *et al.*, 2012; Fischer and Leibinger, 2012; Harada *et al.*, 2002; Taylor *et al.*, 2003; Seki *et al.*, 2005; Pernet and Schwab, 2014). Development of therapies for RGC neuroprotection and/or axon regeneration must, therefore, acknowledge the glial response and associated cellular signalling.

RTP801 was detected in retinal glia, with knock-down evident after siRTP801 treatment, and the associated enhanced pS6 activity was not limited to RGC. This is consistent with other reports of

mTOR activity in glia, such as in reactive astrocytes after spinal cord injury (Codeluppi *et al.*, 2009), in retinal INL Müller glia after N-methyl-D-Aspartate (NDMA) treatment (Ichikawa *et al.*, 2014), and in retinal glia in culture after GM-CSF stimulation where it is associated with enhanced RGC neurite growth (Legacy *et al.*, 2013). Modulation of mTORC1 activity in glia by siRTP801, together with enhanced RGC neurite elongation by siRT801 in the presence of activated retinal glia, and the observation that siRTP801 potentiated retinal astrocyte/Müller glial activation is compatible with a key role for activated glia in mediating RGC survival and axon growth after ON injury. These data support some previous reports demonstrating the importance of reactive gliosis in promoting RGC axon growth, albeit with some paradigm-specific differences in the underlying cellular signalling mechanisms. For example, Müller glial activation after ONC is enhanced by lens injury or PN graft (Lorber *et al.*, 2008), intravitreal zymosan-induced retinal inflammation (Ahmed *et al.*, 2010) and translimbal diode-laser photocoagulation-induced glaucoma (Lorber *et al.*, 2012), all of which are associated with promotion of RGC axon regeneration after ONC. In retinal cultures prepared from rats subjected to lens injury or PN graft *in vivo*, more significant elongation of neurite growth in the latter is associated with an increase in the number of $GFAP^+$ activated glia (Lorber *et al.*, 2008), in contrast to the present results, which indicated potentiated glial activation by siRTP801 in the absence of glial proliferation either *in vivo* or *in vitro*. The combination of ONC with laser-induced experimental glaucoma results in a greater number of $GFAP^+$ activated glia in retinal cultures compared to cultures after ONC alone, correlated with both enhanced neurite lengths and a significant increase in the proportion of neurite-bearing RGC, effects which are abolished in the presence of the selective astrocyte/Müller glial toxin α-Aminoadipic acid (Lorber *et al.*, 2012). Furthermore, the transfer of conditioned culture medium from experimental-glaucomatous rats to retinal cultures from uninjured animals reproduces the neurite growth effects, thus providing evidence for the $GFAP^+$ glia producing soluble factor(s) that act on RGC and promote neurite growth (Lorber *et al.*, 2012). However, unlike the present observation that siRTP801-induced RGC survival

and neurite elongation were blocked by the pan Trk-inhibitor K252a, the neurite growth response to the induced-glaucoma paradigm is unaffected by both K252a or the gp130 receptor blocker MAB228, thereby both ruling out neurotrophins or CNTF/LIF/IL-6 as the mediators of the glial-derived growth response in the latter model (Lorber *et al.*, 2012), and also highlighting different factors contributing to axon growth in different experimental settings. Activated retinal glia also produce several other factors, including FGF, GDNF and ApoE, which may be contributory growth factors in some contexts (Logan *et al.*, 2006; Koeberle and Ball, 1998; Lorber *et al.*, 2009a). Differences between siRTP801 effects on the glial response and other reports, including siRTP801-induced glial activation without proliferation and Trk-sensitive neurite elongation, is probably explained by injury-specific, model-specific and temporal differences in the glial response and its modulation. Indeed, a recent analysis of changes in gene expression associated with reactive gliosis after ONC identified over 1300 differentially expressed genes within 1d of ON injury, including those associated with immune regulation and inflammation, cell-cycle determinants and tissue re-modelling factors, with varying temporal and spatial profiles (Qu and Jakobs, 2013), highlighting the complexity of the glial reaction to injury and multiple opportunities to inflect the response.

The present *in vivo* observation of potentiated glial activation in the absence of glial proliferation after siRTP801 treatment was supported *in vitro*. Although being unable to induce glial activation directly in cultures derived from intact eyes (lack of $GFAP^+$ glia despite siRTP801 treatment), addition of siRTP801 to cultures comprising already activated glia resulted in the potentiation of the secretory phenotype of the activated glia, with enhanced NTF titres, particularly the neurotrophins BDNF, NGF and NT-3, although a small potentiation in CNTF titres was also observed. GDNF was detected in culture medium from animals only after glial activation, reflecting increased production of this factor, but siRTP801 did not affect the measured titres. This suggests a degree of specificity in the siRTP801-mediated potentiation of NTF production rather than merely a global cellular increase in protein

synthesis associated with up-regulated mTOR activity. Of note, pigment epithelium derived factor (PEDF), a potent RGC neuroprotective and axogenic NTF glycoprotein (Vigneswara *et al.*, 2013), was not detected in culture medium from either uninjured animals or after glial activation by ONC, irrespective of siRTP801 or control treatment.

Both the RGC neuroprotective effect and the RGC neurite elongation effect of siRTP801 were significantly reduced by K252a, indicating major role for Trk-dependent signalling in mediating these effects. Insofar as the RGC neuroprotective effect of siRTP801 is likely to be a direct effect on RGC intrinsic signalling (as the effect is independent of the presence of $GFAP^+$ glia), the results imply a Trk-dependent autocrine mechanism, which is supported by the observation of BDNF and NT-3 expression both in glia and in RGC themselves, as previously described for these neurotrophins along with NGF (Douglas *et al.*, 2009). The survival effect was not abolished by K252a, indicating additional, non-Trk-mediated contributions. The gp130-ligand CNTF, potentiated by siRTP801, is RGC neuroprotective *in vivo* and *in vitro* (Zhang *et al.*, 2005; Heskamp *et al.*, 2013; Leaver *et al.*, 2006), and close links between the JAK-STAT and PI3K- and ERK/MAPK signalling pathways suggests that this may contribute to the RGC survival. GDNF, a member of the TGF-β superfamily, also protects RGC against axotomy-induced apoptosis, utilising its own receptor complex to up-regulate the MAPK pathway (Koeberle and Ball, 1998; Worby *et al.*, 1996). The RGC neurite length enhancement of siRTP801 in the presence of activated glia was abolished by K252a which, combined with the potentiated production of Trk-ligand neurotrophins, strongly indicated glial-derived neurotrophins as the mediators of an indirect, paracrine mechanism for neurite elongation in this model. Individual Trk receptor sub-types exhibit different affinity for neurotrophins; TrkA is specific for NGF, TrkB binds BDNF and NT-4/5, and TrkC predominantly binds NT-3 (Barbacid, 1995; Barbacid, 1994). K252a is a potent blocker of all Trk-subtypes (Tapley *et al.*, 1992), and has been widely utilised at the concentration used here (50nM) to investigate the role of NTF in mediating biological functions,

including on RGC survival and neurite growth (Mead *et al.*, 2013; Douglas *et al.*, 2009; Lorber *et al.*, 2002). However, despite potent pan-Trk blockade, K252a probably also influences a variety of kinases (Morotti *et al.*, 2002; Martin *et al.*, 2011), and so some caution should be placed on attributing effects of this inhibitor solely on Trk-dependent signalling.

The experimental findings from the glial-activated cultures are consistent with a model in which activated-glial-derived NTF act upon RGC to increase the neurite growth capacity, with RTP801 knock-down subsequently promoting production both of additional glial-derived factors and also RGC-derived factors to act in paracrine and autocrine fashion, respectively, to maintain RGC survival and promote elongation of neurites which have sprouted. In this setting, Trk antagonism may prevent RGC becoming 'primed' to further enhance NTF in response to RTP801 inhibition or to respond to exogenous NTF.

The results indicated that siRTP801 treatment enhanced neurotrophin production and that Trk-mediated signalling contributed both to RGC survival and was necessary for neurite elongation. However, neurotrophin titres recorded were lower than those previously reported with other neurite-growth promoting treatments, such as the EGFR antagonist AG1478, which may partly account for the less dramatic neurite outgrowth seen in the present study compared to EGFR blockade (Douglas *et al.*, 2009). With the glial-dependent production of multiple different factors, and the synergistic nature of NTF combinations on neuronal survival and growth (Logan *et al.*, 2006; Logan *et al.*, 1994; Douglas *et al.*, 2009), the balance of NTF production/signalling with their different characteristics is likely to vary between experimental models. For example, BDNF protects over 95% RGC from ONC-induced apoptosis at 7d after injury, although the effect of a single injection is short lived and has no significant axogenic potency (Ahmed *et al.*, 2011; Parrilla-Reverter *et al.*, 2009; Pernet and Di Polo, 2006), although it may have a more pronounced effect on axon growth when

applied directly to axons rather than to neuronal somata (Park *et al.*, 2014). NGF is both produced and utilised by RGC and retinal glia, acting in local autocrine and paracrine fashion to effect neuronal survival and axon outgrowth (Roberti *et al.*, 2014), NT-3 promotes neurite growth and axon regeneration, and both have synergistic effect when combined (Logan *et al.*, 2006). However, survival and growth-enhancing NTF do not signal exclusively through Trk-receptors, or *via* the PI3K/Akt/mTOR cascade. The low affinity neurotrophin receptor $p75^{NTR}$ also mediates neurotrophin signalling, utilising the ERK-MAPK and PI3K pathways (Koeberle and Ball, 2002), and the pro-regenerative cytokines CNTF/LIF/IL-6 act on gp130 receptors to activate JAK-STAT signalling, as mentioned (Muller *et al.*, 2007; Muller *et al.*, 2009). CNTF and NT-4 are RGC neuroprotective for a short period after ON injury, with over 90% survival in the first week (Parrilla-Reverter *et al.*, 2009), but are unable to sustain this effect in the absence of repeated injection (Vigneswara *et al.*, 2013; Parrilla-Reverter *et al.*, 2009; Weise *et al.*, 2000; Zhang *et al.*, 2005), although sustained CNTF release has a longer lasting axon regenerative effect (Leaver *et al.*, 2006). Interestingly, the presence of activated glia in retinal cultures was an absolute requirement for the neurite elongating effect of siRTP801, suggesting that despite activated glia promoting NTF production, axon growth may be limited by the downstream inactivation of mTOR by RTP801 in control wells. Inhibition of RTP801 therefore appears both to potentiate glial NTF production, and to disinhibit the RGC growth response to enable longer neurite extension, and it is possible that the latter effect is RGC sub-type dependent, as discussed earlier. These findings, in relation to the published literature, reinforce the complexity of cellular signalling in relation to neuronal survival/axon growth responses, and the opportunity for pathway cross-talk and feedback regulation.

In summary, siRTP801-dependent potentiation of PI3K pathway signalling in RGC *via* paracrine secretion of NTF from activated retinal glia combined with siRTP801-mediated activation of both

mTORC1 and mTORC2 in RGC themselves may be responsible for the observed increased survival and longer axon/neurite growth seen after siRTP801 treatment both *in vitro* and *in vivo*.

CHAPTER 5

EVALUATION OF THE EFFECTS OF GSK3β INHIBITION ON RGC SURVIVAL AND AXON/NEURITE GROWTH

5.1 INTRODUCTION / RATIONALE

Experiments described in Chapters 3 and 4 demonstrated that suppression of the cellular-stress-induced factor RTP801 with a translatable siRNA enabled significant RGC survival and axon elongation after ON injury. Complementary retinal culture studies indicated potential underlying cellular mechanisms, including the importance of glial-derived NTF in promoting axon/neurite elongation and the contribution of mTORC1-independent cellular signalling to both RGC survival and neurite growth. Moreover, siRTP801 had no significant effect on axonal sprouting/neurite initiation, indicating a role for other factors in mediating this aspect of axon regeneration. Other laboratory approaches that aim to up-regulate activity of the PI3K/Akt/mTOR pathway to promote neuronal survival and axon regeneration have consistently found that combinatorial approaches yield superior results (Sun *et al.*, 2011; Kurimoto *et al.*, 2010; de Lima *et al.*, 2012), and that the kinase GSK3β may play a pivotal role in mediating axon growth (Park *et al.*, 2010; Park *et al.*, 2008; Hur and Zhou, 2010; Seira and Del Rio, 2014).

Like mTOR, the GSK3 proteins are serine/threonine kinases. Although both α- and β- isoforms exist, sharing 85-95% homology (Ali *et al.*, 2001), GSK3β is the major isoform expressed in the CNS (Rui *et al.*, 2013). GSK3β is linked to numerous cellular pathways, including PI3K/Akt signalling (Figure 1.11 and Figure 5.1), and consequently implicated as a key regulator of a host of neurodevelopmental processes, including neurogenesis, neuronal migration and polarisation, and axon growth and guidance (Hur and Zhou, 2010). Unusually, GSK3β has a high constitutive activity and is inactivated by upstream factors. For example, Trk-mediated activation of the PI3K/Akt pathway leads to Akt-dependent phosphorylation of the amino-terminal serine residue (Ser9) with subsequent functional inactivation (Hur and Zhou, 2010; Cross *et al.*, 1995; Zhou and Snider, 2005b). Thus, activation of the PI3K pathway acts both to up-regulate mTORC1/2 and suppress GSK3β activity (Figure 1.11 and 5.1).

Activation of GSK3β through a separate phosphorylation site (Tyr216) has also been described but the significance of this is not completely understood (Hur and Zhou, 2010; Liz *et al.*, 2014). Major functions of GSK3β include regulation of the cellular threshold for apoptosis in response to internal and external factors (Beurel and Jope, 2006), and also the activity of axonal growth cones through modulation of both the phosphorylation state of several proteins associated with polymerisation of the microtubular cytoskeleton, and the regulation of local somatic and axonal protein synthesis (Seira and Del Rio, 2014). Several of the CNS axon growth inhibitory factors are thought to mediate growth cone collapse *via* GSK3β activity: the repulsive axonal guidance factors semaphorins Sema3A and Sema6C promote GSK3β-dependent axonal growth cone collapse (Seira and Del Rio, 2014; Burgaya *et al.*, 2006; Hida *et al.*, 2012); CSPGs are thought to invoke axon growth inhibition by receptor-mediated suppression of Akt and consequent reduction of GSK3β-Ser9 phosphorylation, thereby enhancing GSK3β activity (Seira and Del Rio, 2014; Dill *et al.*, 2008). Myelin associated inhibitors such as Nogo, OMgp and MAG, acting through the Nogo-receptor complex, are also associated with increased GSK3β activity (Seira and Del Rio, 2014; Dill *et al.*, 2008; Shen *et al.*, 2011; Wang *et al.*, 2011). Suppression of GSK3β by Ser9 phosphorylation or the addition of GSK3β inhibitors may render regenerating axonal growth cones blind to external inhibitory factors and enable disinhibited growth.

Although not previously described in relation to RGC axon regeneration after injury, several reports in other neuronal paradigms indicate that inhibition of GSK3β is required for both the inception of initial axogenesis and axon elongation (Seira and Del Rio, 2014; Zhou *et al.*, 2004; Dill *et al.*, 2008; Garrido *et al.*, 2007). However, there is some controversy in the area, particularly whether Ser9 phosphorylated GSK3β (pGSK3β) truly represents inactivation of the kinase, and also whether this step is pro-growth or growth-repressive (Hur and Zhou, 2010; Seira and Del Rio, 2014; Gobrecht *et al.*, 2014; Liz *et al.*, 2014). Furthermore, changes in the activity of GSK3β may not always correlate

with the Ser9 phosphorylation status, and so the latter is not necessarily a reliable indicator of GSK3β activity (McManus *et al.*, 2005; Gobrecht *et al.*, 2014; Hur and Zhou, 2010). The controversy probably reflects the multiple substrates of GSK3β which determine axonal growth cone responses, including CRMP2, MAP1b, APC and Smad1, amongst others (Hur and Zhou, 2010; Saijilafu *et al.*, 2013), and it is therefore perhaps more physiologically relevant to analyse changes in the phosphorylation status of known GSK3β substrates to understand the role of GSK3β in a particular setting. A schematic overview of GSK3β signalling and diverse range of substrates is presented in Figure 5.1.

Activation/up-regulation of mTORC1/2 activity in response to siRTP801 occurs downstream of Akt in the PI3K signalling pathway, and therefore bypasses the GSK3β inhibition that occurs after NTF/Trk-mediated activation of PI3K pathway stimulation or after *pten* knock-out, for example (Figure 1.11). However, as mentioned in Chapter 4, the feedback connection from mTORC2 to Akt (Jacinto *et al.*, 2006) offers a possible mechanism for siRTP801-modulation of GSK3β activity, which may contribute to the limited axon growth seen after RTP801 knock-down. Also, the elevation of endogenous glial-derived NTF levels after RTP801 knock-down would activate the PI3K pathway after Trk activation, with associated downstream transmission to both up-regulate mTORC1/2 and down-regulate GSK3β signals. While inhibition of mTOR does not alter the activation of state GSK3β, inhibition of GSK3β reportedly promotes mTOR activity in cultured DRG neurons (Manns *et al.*, 2012; Hur and Zhou, 2010), presumably by releasing the TSC complex from direct GSK3β-dependent activation (Figure 1.11 and 5.1) (Inoki *et al.*, 2006). Thus, suppression of GSK3β activity may enhance RGC survival and disinhibit RGC axon growth by modulation of growth cone regulators through multiple potential substrates. However, siRTP801-induced mTORC1/2 activity may be partly suppressed by a GSK3β intrinsic 'brake', and so additional inhibition of GSK3β may potentiate siRTP801-induced mTORC1/2 activity by reducing TSC activity. There is, therefore, a clear rationale for aiming to suppress GSK3β activity as a targeted manipulation to promote RGC neuroprotection and disinhibited axon growth,

but perhaps more promisingly as a combined approach together with siRTP801 to facilitate the optimal signalling conditions for robust RGC survival and axon growth after ON injury.

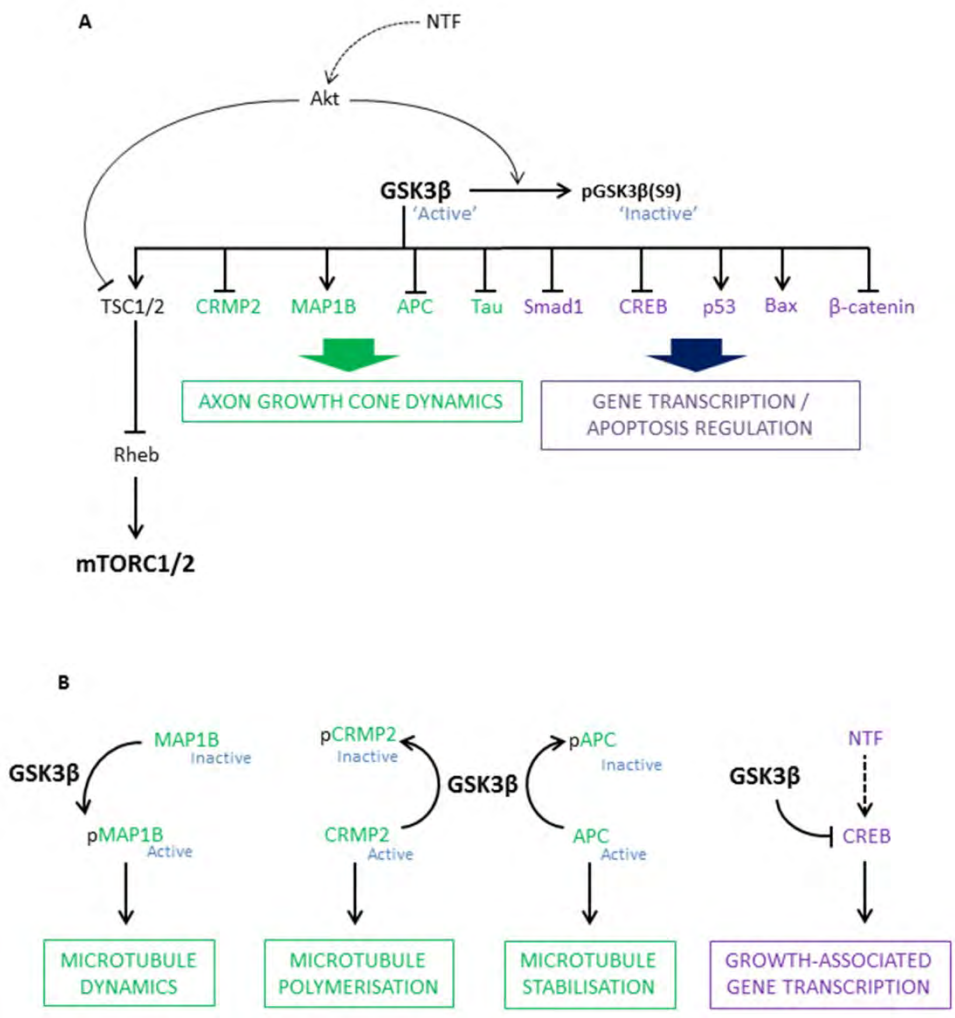


Figure 5.1: Regulation and substrates of GSK3β activity. (A) Schematic representation of GSK3β regulation and substrates. NTF act to up-regulate PI3K pathway signalling, leading to Akt-dependent inhibitory phosphorylation of GSK3β on Ser9. There is some controversy whether this step truly represents inactivation of GSK3β, and GSK3β can also be activated and inactivated *via* other mechanisms (see text). Multiple downstream substrates of GSK3β exist, which may either be activated or inactivated by GSK3β-dependent phosphorylation. The range of GSK3β substrates shown is not exhaustive. Activity of GSK3β substrates enables regulation of apoptosis, gene transcription and axon growth cone dynamics. Note that GSK3β promotes activity of TSC1/2, an upstream negative regulator of mTORC1/2 activity, which itself is inhibited by Akt when the PI3K pathway is activated. GSK3β therefore functions as an intrinsic 'brake' to mTORC1/2. See also Figures 1.7 and 1.11. (B) Differential regulation of GSK3β substrates in axon growth. GSK3β-dependent phosphorylation may lead to activation of some substrates (e.g. MAP1B) and inhibition of others (e.g. CRMP2, APC and CREB), to enable fine co-ordination of axonal growth responses. Adapted from Hur and Zhou (2010).

The purpose of the experiments described in this Chapter was to investigate the RGC neuroprotective and axon/neurite regeneration effects of GSK3β inhibition, to ascertain possible underlying cellular signalling mechanisms, and evaluate whether a synergistic effect would be achieved with combined knock-down of RTP801 and GSK3β.

5.2 HYPOTHESES

- Inhibition of GSK3β promotes RGC survival and axon growth
- Combined siRNA-mediated knock-down of both RTP801 and GSK3β potentiates siRTP801-induced RGC survival and axon regeneration

5.3 AIMS

The specific aims of the experiments described in this Chapter were to:

1. Investigate the effects of the GSK3β pharmacological inhibitor Chir99021 on RGC survival and neurite outgrowth in dissociated primary adult rat retinal cultures;
2. Confirm the target specificity and knock-down effects of siGSK3β on retinal cells *in vitro*;
3. Investigate the effects of siGSK3β on RGC survival and neurite outgrowth in the presence and absence of activated retinal glia *in vitro*;
4. Investigate the effects of intravitreal siGSK3β on RGC survival, axon regeneration and retinal glial activation after ONC *in vivo*;
5. Evaluate the potential cellular signalling mechanisms underlying the RGC survival and axon growth effects of GSK3β inhibition;

6. Investigate the effects of combined siRNA-mediated knockdown of RTP801 and GSK3β on RGC survival and axon regeneration *in vitro* and after ONC *in vivo*.

5.4 EXPERIMENTAL DESIGN

Details of specific experimental techniques, materials and methodologies are described in Chapter 2.

5.4.1 Assessment of the effects of Chir99021 on RGC survival, neurite outgrowth and GSK3β expression *in vitro*

The potent and highly selective GSK3β inhibitor Chir99021 (see Section 2.4.3.3) was assessed for its effects on RGC survival and neurite outgrowth *in vitro*, as a prelude to subsequent *in vivo* and *in vitro* studies using a GSK3β targeted siRNA (siGSK3β). Primary retinal cultures were established from uninjured adult rat eyes as described previously (Section 2.4.1). Typically used at 3μM in culture (Ye *et al.*, 2012; Gouti *et al.*, 2014), a dose-response assay was undertaken using the following concentrations of Chir99021: 0.03μM (30nM), 0.3μM (300nM), 3μM, 30μM and 300μM, together with untreated sNBA/vehicle control cultures. Culture wells (up to 3 wells/condition, n=6 independent animals) were incubated with treatments for 3d and subsequently evaluated for βIII-tubulin^{+} RGC survival and neurite outgrowth (initiation and elongation) as described earlier (Section 2.6), plus the cellular localisation of GSK3β using immunocytochemistry.

5.4.2 Assessment of the effects of siGSK3β on RGC survival, neurite outgrowth and GSK3β expression *in vitro*

The siGSK3β was initially tested in retinal cultures established from uninjured rats, using the standard technique and protocol described earlier (Section 2.4.1). A dose-response assay was undertaken to identify the optimum concentration for use in later experiments using the following treatment conditions: sNBA culture medium alone; Lipofectamine transfection reagent; siEGFP at 10nM, 20nM, 50nM, 100nM and 200nM; and siGSK3β at 10nM, 20nM, 50nM, 100nM and 200nM, with up to 3 wells/condition, n=4 independent animals. Cultures were incubated for 3d and subsequently analysed for βIII-tubulin^{+} RGC survival, neurite outgrowth initiation and elongation and RGC cellular immunocytochemical localisation of GSK3β.

5.4.3 Confirmation of siRNA specificity and target knock-down with qPCR

RNA was obtained from mixed retinal cultures incubated with sNBA culture medium alone (untreated), and from cultures treated with siGSK3β, siEGFP and Lipofectamine, as described previously (Section 2.8.2), with n=5 independently treated culture wells/condition. Specificity of the GSK3β primer was confirmed by running a qPCR reaction with cDNA from an untreated sample in duplicate, and undertaking melt-curve analysis to detect a single amplicon. GSK3β knock-down was evaluated by measuring GSK3β mRNA expression, as a fold-change relative to the housekeeping gene GAPDH, in samples from the different treatment conditions.

5.4.4 *In vivo* assessment of the effects of siGSK3β on RGC survival, axon regeneration and retinal glial activation, and of combination siRNA treatment with siGSK3β and siRTP801 on RGC survival and axon regeneration after ONC

Adult rats underwent bilateral ONC (Section 2.3.3), immediately followed by intravitreal injections and again 8d and 16 after ONC, in a total of 12 animals (24 eyes). Treatment groups consisted of ONC + PBS (n=6 eyes), ONC + siEGFP (n=6 eyes), ONC + siGSK3β (n=6 eyes) and ONC + siGSK3β/siRTP801 (n=6 eyes). Similar to the *in vivo* studies described in Chapter 3, ON sections from these rats were prepared after 24d and analysed for the presence of $GAP43^{+}$ regenerating axons. Assessment of RGC survival and retinal glial activation was undertaken using retinal sections from each of these treatment conditions, and from eyes of intact uninjured animals (n=5 eyes). Analysis was first undertaken to compare the effects of siGSK3β on RGC survival, axon regeneration and glial activation compared to control conditions (intact [not for axon regeneration], ONC + PBS and ONC + siEGFP). Subsequent analysis was undertaken to evaluate the effects of the combined siRNA treatment on RGC survival and axon regeneration compared with the other groups, incorporating the data of the siRTP801 alone group as described in Chapter 3.

5.4.5 *In vitro* assessment of the effects of siGSK3β on RGC survival and neurite outgrowth in the presence of activated retinal glia and the evaluation of the underlying cellular signalling mechanisms

For the investigation of the effects of siGSK3β in the presence of activated retinal glia, primary retinal cultures were established from animals 5d after ONC *in vivo*. Cultures were treated with sNBA alone, siEGFP (50nM) and siGSK3β (50nM), each in the presence and absence of the mTORC1 inhibitor Rapamycin, and used for the assessment of RGC survival and neurite outgrowth initiation and

elongation. Further glial-activated cultures were prepared to evaluate underlying cellular signalling mechanisms, with comparisons made between sNBA, siEGFP and siGSK3β treatment conditions for the RGC expression of Ser9 phospho-GSK3β ('pGSK3β'), phospho-CRMP2 (pCRMP2), phospho-Smad1 (pSmad1) and phospho-MAP1B (pMAP1B).

To investigate whether GSK3β inhibition enabled RGC to overcome the effects of CNS myelin-derived neurite growth inhibition, a series of retinal glial-activated cultures were prepared with the subsequent addition of 25μM Nogo-P4 peptide, a potent axon growth inhibitory ligand causing growth cone collapse (Wang and Zhu, 2008; Geoffroy and Zheng, 2014). In the presence of the Nogo-P4 peptide, the following treatment conditions were evaluated for effects on RGC neurite outgrowth initiation and elongation: sNBA culture medium; Lipofectamine transfection reagent, siEGFP (50nM), siGSK3β (50nM), Chir99021 (300nM) and CNTF (positive control). All these *in vitro* experiments were undertaken using up to 3 wells/condition and were repeated with at least 3 independent animals.

5.4.6 Assessment of combined siRNA treatment with siGSK3β and siRTP801 on RGC survival and axon/neurite growth

To investigate the potential for a combinatorial siRNA approach to yield potentially superior regenerative results, a combination of siRTP801 and siGSK3β was tested both *in vitro* and *in vivo*. The use of combined siRTP801/siGSK3β as a treatment group for assessment of RGC survival and axon regeneration after ONC *in vivo* was described in Section 5.4.4 above.

For the *in vitro* assessment, glial-activated retinal cultures were established from animals 5d after ONC, and prepared with the following treatment conditions: sNBA culture medium alone, siGSK3β (50nM) + siRTP801 (20nM) (utilising the optimum concentration of each siRNA established from

studies using each individual siRNA alone [Sections 3.5.4 and 5.5.5-6]), and siEGFP (70nM, to give an equivalent total siRNA concentration to the test combination). RGC survival, neurite outgrowth (initiation and elongation) and RGC localisation of RTP801 and GSK3β were evaluated. Due to potential RGC toxicity with high concentration of siRNA (see Results, Section 5.5.11), further glial-activated cultures were treated with a combination of 25nM siGSK3β + 25nM siRTP801, with siEGFP (50nM) and sNBA as control groups. All these *in vitro* experiments were undertaken using up to 3 wells/condition and were repeated with at least 3 independent animals.

5.5 RESULTS

5.5.1 Effects of GSK3β inhibition using the pharmacological inhibitor Chir99021 on RGC survival, neurite outgrowth and RGC expression of GSK3β in the absence of activated retinal glia *in vitro*

5.5.1.1 Chir99021 was RGC neuroprotective in a concentration-dependent manner in retinal cultures in the absence of activated retinal glia

The effect of GSK3β inhibition on RGC survival and neurite outgrowth was first assessed with the pharmacological inhibitor Chir99021 in a dose-response assay *in vitro* (Figure 5.2). In primary adult rat retinal cultures in the absence of activated glia, there was no significant difference in RGC survival between the untreated control cultures (316.6 ± 22.2 RGC/well) and Chir99021 at a concentration of 30nM (412.8 ± 51.1) (Figure 5.2B). However, there was a significant increase in RGC survival after treatment with Chir99021 at concentrations of 300nM (512.1 ± 52.4; $p<0.05$) and 3μm (544.4 ± 79.9; $p<0.01$), indicating a neuroprotective effect at these concentrations. Higher concentrations of Chir99021 (30μM and 300μM) exhibited RGC toxicity, with survival reduced after treatment with 30μM and abolished after 300μM Chir99021. These data indicated that GSK3β inhibition with the

pharmacological inhibitor Chir99021 was RGC neuroprotective *in vitro* at concentrations 300nM and 3μM (3000nM) in the absence of activated retinal glia, implicating a role for GSK3β activity in determining RGC survival. Cellular toxicity was seen with higher concentrations of Chir99021.

5.5.1.2 Chir99021 promoted RGC neurite initiation but did not affect neurite length in retinal cultures in the absence of activated retinal glia

The frequency of neurite bearing RGC was significantly ($p<0.05$) increased from 10.7 ± 1.5% in untreated control wells to 18.9 ± 1.9% and 18.1 ± 2.2% after treatment with Chir99021 at concentrations of 30nM and 300nM, respectively (Figure 5.2C). Treatment with 3μM and 30μM did not significantly affect the proportion of neurite-bearing RGC compared to untreated controls. In these primary retinal cultures in the absence of activated retinal glia, Chir99021 did not significantly affect the mean length of RGC neurites compared to untreated controls (Figure 5.2D). These data suggested that GSK3β inhibition with Chir99021 promoted the initiation of neurite outgrowth, thus implicating GSK3β activity as a suppressor of neurite outgrowth initiation in this model. GSK3β activity was not associated with effects on RGC neurite elongation in this culture model on a growth-permissive laminin substrate in the absence of activated retinal glia.

5.5.1.3 Chir99021 did not affect RGC localisation of GSK3β in vitro

Immunocytochemical localisation of GSK3β was detected in all RGC in these cultures, indicating that GSK3β activity was constitutive (Figure 5.2E). The observation that neurites sprouted from GSK3β$^+$ RGC demonstrated that GSK3β was not an absolute inhibitor of neurite outgrowth. Treatment with Chir99021 did not affect the cellular detection of GSK3β in RGC, suggesting that the pro-survival and neurite outgrowth initiation effects of this particular inhibitor reflect an alteration in the level of

downstream GSK3β activity rather, consistent with a mechanism of action as a competitive inhibitor of GSK3β (Meijer *et al.*, 2004).

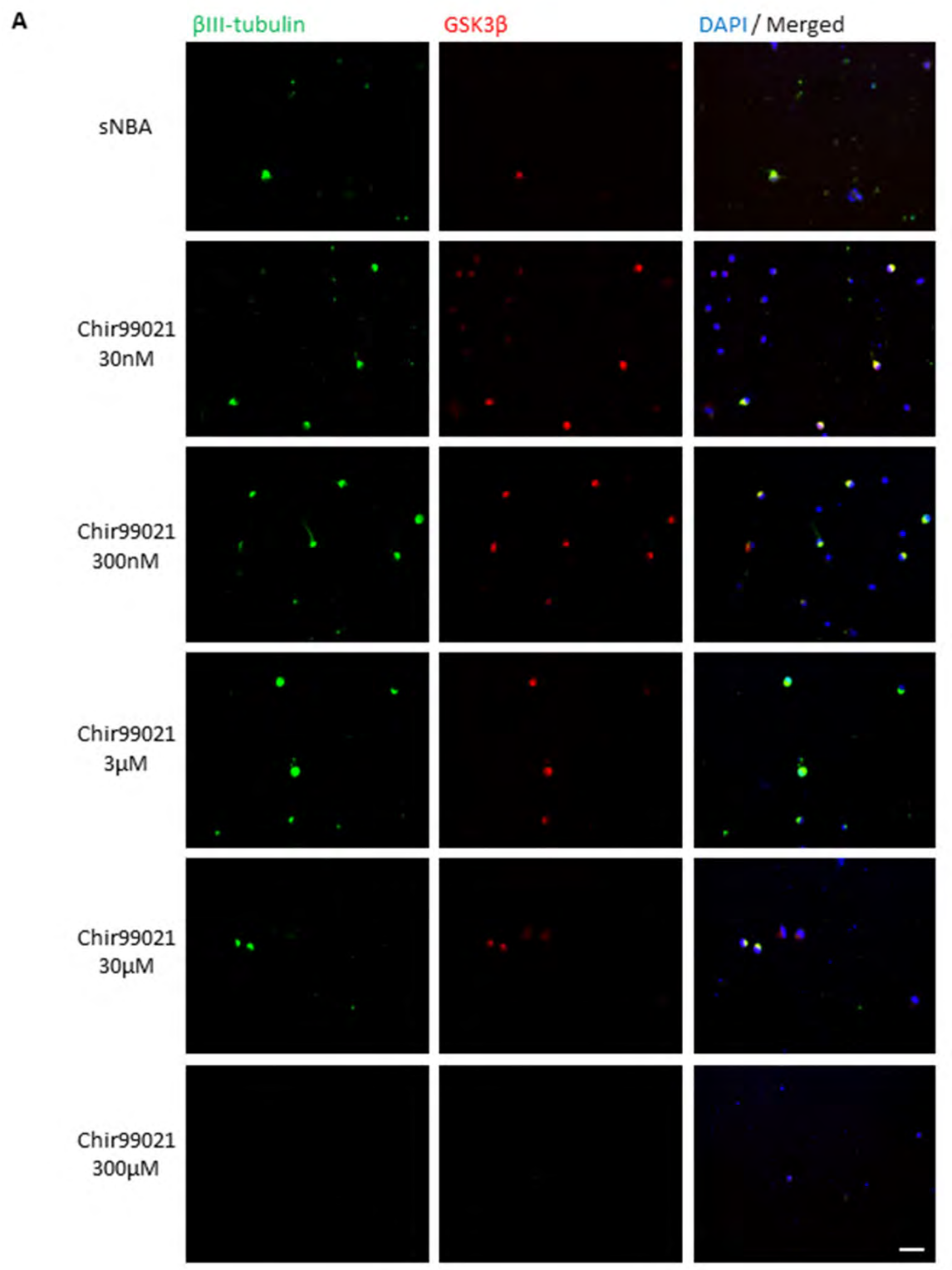


Figure 5.2: Effects of GSK3β inhibitor Chir99021 on RGC survival and neurite outgrowth in cultured retinal cells in the absence of activated retinal glia. Figure continues with full legend on the next page.

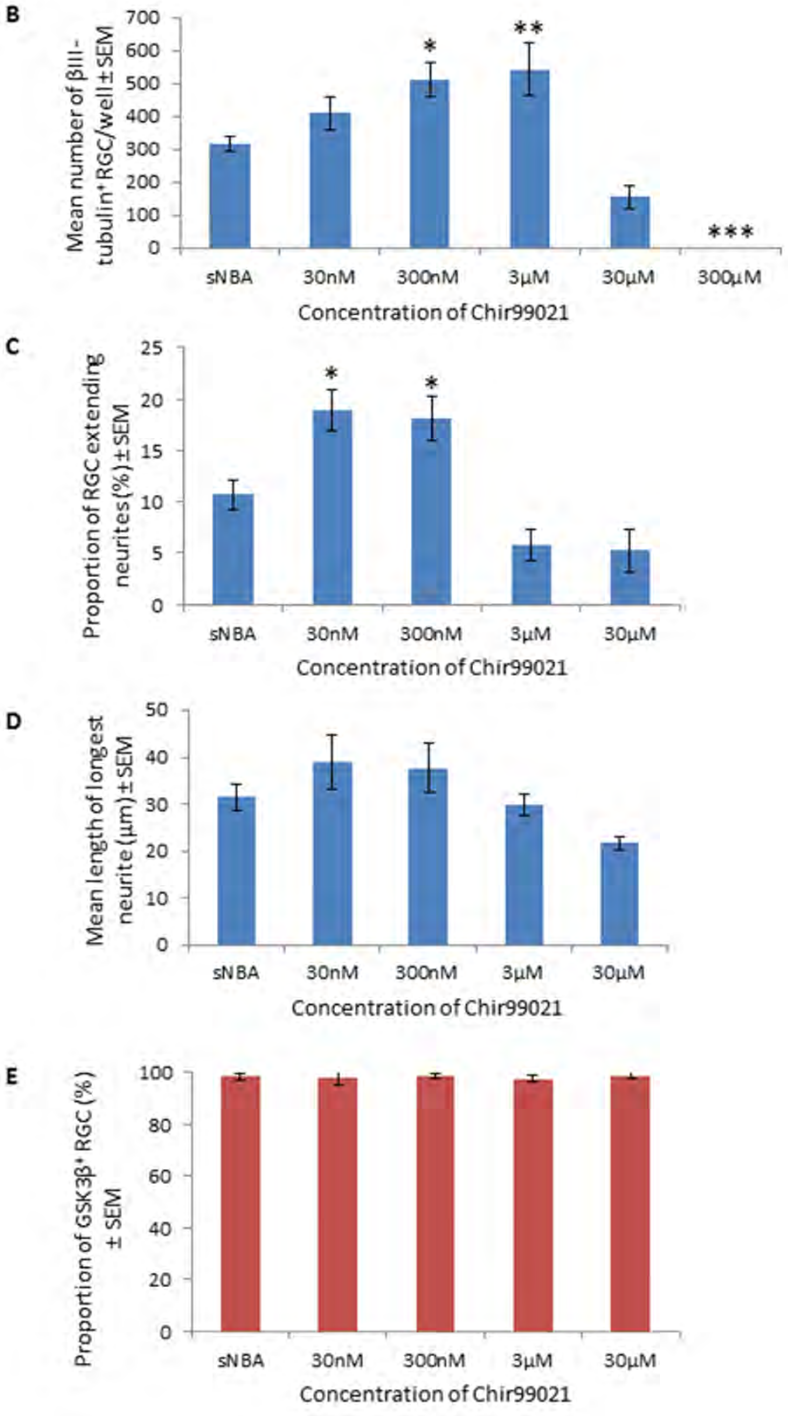


Figure 5.2: Effects of GSK3β inhibitor Chir99021 on RGC survival and neurite outgrowth in cultured retinal cells in the absence of activated retinal glia. (A) Retinal cultures established from intact, uninjured animals, immunostained for βIII-tubulin (green) and GSK3β (red), with DAPI (blue) as a nuclear counterstain, after 3d incubation with sNBA culture medium and the GSK3β inhibitor Chir99021 at concentrations of 30nM, 300nM, 3μM, 30μM and 300μM (scale bar = 20μm). (B) Quantification of surviving βIII-tubulin$^+$ RGC for cultures described in (A), in the absence of activated retinal glia. (C) Proportion of βIII-tubulin$^+$ RGC extending neurites, and (D) length of longest RGC neurite in cultures described in (A). (E) Proportion of βIII-tubulin$^+$ RGC demonstrating GSK3β positivity after treatment of retinal cultures with Chir99021 (n=6; *p<0.05, **p<0.01, ***p<0.001 *vs* sNBA control).

5.5.2 Effects of siGSK3β on RGC expression of GSK3β and knock-down *in vitro*

Constitutive activity of GSK3β was observed by immunocytochemistry in RGC in all untreated control wells, confirming the observation from control wells in the Chir99021 study described previously (Figure 5.3A, B). GSK3β was also detected in 100% RGC in the presence of Lipofectamine and siEGFP at concentrations of 10nm, 20nM, 50nM, 100nM, and 200nM, demonstrating no GSK3β knock-down in these controls. The frequency of $GSK3\beta^{+}$ RGC was significantly reduced after transfection with siGSK3β at concentrations of 10nM (67.3 ± 3.4%; $p<0.001$), 20nM (54.0 ± 4.7%; $p<0.001$), 50nM (49.0 ± 5.3%; $p<0.001$), 100nM (74.0 ± 3.3%, $p<0.001$) and 200nM (82.5 ± 4.4%, $p<0.05$), indicating optimal knock-down of GSK3β protein at 50nM, corresponding to 51% knock-down.

5.5.3 Effects of siGSK3β on RGC survival and neurite outgrowth in the absence of activated retinal glia *in vitro*

5.5.3.1 siGSK3β was RGC neuroprotective in primary retinal cultures

Compared to sNBA control cultures (403.0 ± 27.2 RGC/well), RGC survival was significantly increased after treatment with siGSK3β at concentrations of 10nM (651.6 ± 47.8; $p<0.001$), 20nM (580.0 ± 40.6; $p<0.01$) and 50nM (773.6 ± 35.3; $p<0.001$), but there was no significant RGC survival effect at siGSK3β concentrations of 100nM (353.8 ± 316), and there was a reduction in RGC survival after treatment with 200nM siGSK3β (145.4 ± 198) (Figure 5.3C). There was no significant difference compared to untreated cultures when incubated with Lipofectamine (345.8 ± 398), and siEGFP at concentrations of 10nM (385.5 ± 29.2), 20nM (333.4 ± 45.6), 50nM (374.0 ± 21.3) and 100nM (243.1 ± 15.6), but a reduction in RGC survival was observed after incubation with 200nM siEGFP (134.0 ± 12.9). These data showed that treatment with siGSK3β promoted RGC survival *in vitro* in the absence

of activated glia, at an optimal neuroprotective concentration of 50nM and suggested that higher concentrations of siRNA were RGC toxic, independent of whether treatment or control siRNA was used. Furthermore, these findings confirmed data obtained with the small-molecule inhibitor Chir99021, indicating that active GSK3β suppresses RGC survival.

5.5.3.2 siGSK3β promoted RGC neurite growth initiation in the absence of activated retinal glia in vitro

The proportion of βIII-tubulin^{+} RGC extending at least one neurite was 18.6 ± 1.9% in untreated control cultures in the absence of GFAP^{+} glia and no significant difference was observed in the presence of Lipofectamine (14.0 ± 2.5%) (Figure 5.3D). While there was an increase in neurite-bearing RGC after treatment with siGSK3β at concentrations of 10nM (21.9 ± 4.9%) and 20nM (25.9 ± 5.7%), these results did not reach statistical significance. However, treatment with 50nM siGSK3β promoted a significant increase in the proportion of neurite-bearing RGC (34.3 ± 2.1%; $p<0.01$), but no significant difference from control after treatment with 100nM (17.0 ± 2.5%) or 200nM (8.6 ± 1.6) siGSK3β, or with siEGFP at concentrations of 10nM (11.1 ± 1.0%), 20nM (15.8 ± 1.6%), 50nM (13.1 ± 2.6%) and 100nM (8.9 ± 2.3%). There was a significant reduction in RGC bearing neurites after 200nM siEGFP (4.0 ± 0.8%; $p<0.01$). These data indicated that siGSK3β promoted the initiation of neurite outgrowth in RGC *in vitro* in the absence of activated glia, with an optimal concentration of 50nM, confirming the results obtained with Chir99021 that GSK3 has a role in inhibiting neurite outgrowth initiation. The neurite-growth promoting effect of siGSK3β was abolished/inhibited at higher siRNA concentrations.

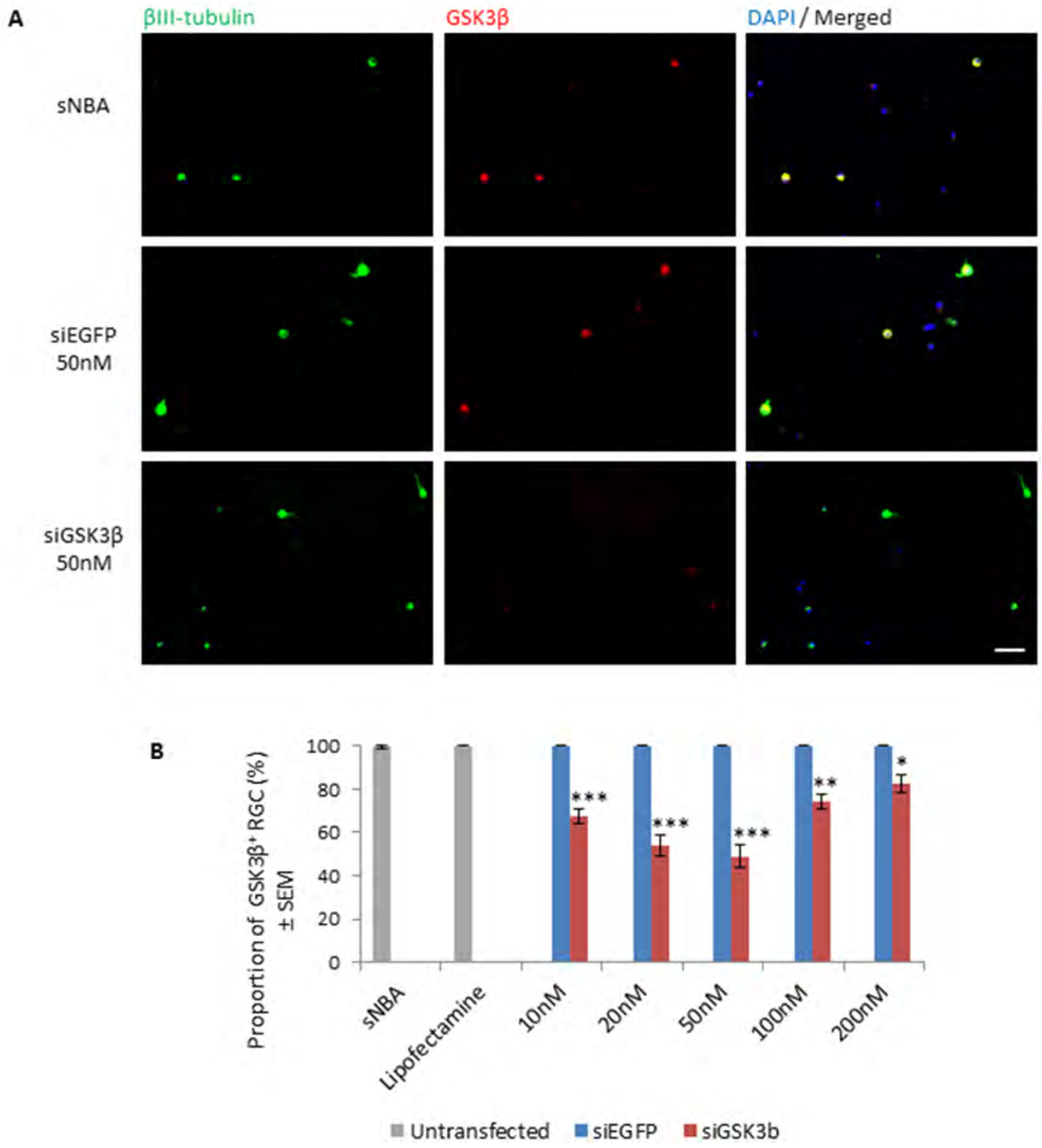


Figure 5.3: Effects of siGSK3β on cellular localisation of GSK3β, RGC survival and neurite outgrowth in cultured retinal cells in the absence of activated retinal glia. (A) Retinal cultures established from intact, uninjured animals, immunostained for βIII-tubulin (green) and GSK3β (red), with DAPI (blue) as a nuclear counterstain, after 3d incubation with sNBA culture medium (top row), 50nM siEGFP (middle row) and 50nM siGSK3β (bottom row) (scale bar = 20μm). (B) Proportion of βIII-tubulin$^+$ RGC demonstrating GSK3β positivity after 3d incubation with sNBA culture medium, Lipofectamine, siEGFP (10nM, 20nM, 50nM, 100nM and 200nM) and siGSK3β (10nM, 20nM, 50nM, 100nM and 200nM). Quantification of (C) βIII-tubulin$^+$ RGC survival, (D) proportion of RGC bearing neurites, and (E) length of longest RGC neurite in retinal cultures for the treatment groups described in (B)(n=4; *p<0.05, **p<0.01, ***p<0.001 *vs* sNBA control). Figure continues on next page.

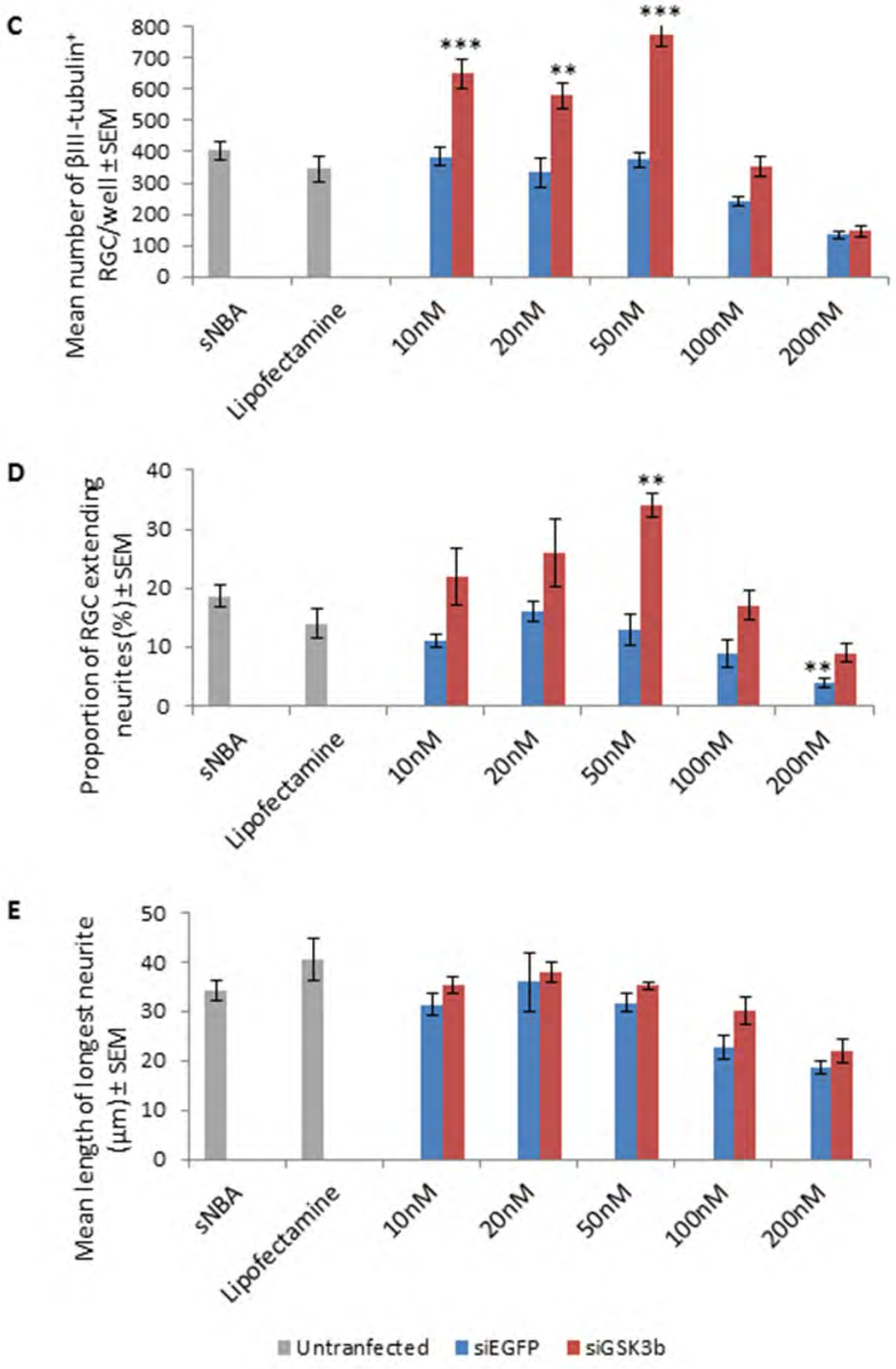


Figure 5.3: Effects of siGSK3β on cellular localisation of GSK3β, RGC survival and neurite outgrowth in cultured retinal cells in the absence of activated retinal glia. Continued from previous page.

5.5.3.3 siGSK3β did not affect RGC neurite elongation in the absence of activated retinal glia in vitro

The mean length of the longest RGC neurite in untreated control cultures was 34 ± 2µm (Figure 5.3E). There was no significant difference in neurite length after incubation with either Lipofectamine (40 ± 4µm), siEGFP at concentrations of 10nM (31 ± 2µm), 20nM (36 ± 6µm) and 50nm (31 ± 2µm), or treatment with siGSK3β at concentrations of 10nM (35 ± 2µm), 20nM (38 ± 2µm), 50nM (35 ± 1µm) and 100nM (30 ± 2µm). The mean length of longest RGC neurite was reduced by siEGFP 100nM (23 ± 3µm) and 200nM (18 ± 1µm) and after treatment with siGSK3β at 200nM (22 ± 2µm). Treatment of retinal cultures with siGSK3β therefore did not promote RGC neurite elongation on laminin substrate *in vitro*, and high concentrations of siRNA appeared to inhibit neurite elongation. Again, these data confirmed the findings of GSK3β inhibition by Chir99021, suggesting that GSK3β activity has no effect on neurite outgrowth elongation in this model in the absence of activated retinal glia.

5.5.4 Confirmation of siRNA-mediated knock-down of GSK3β mRNA in retinal cells

The specificity of the GSK3β primer used for qPCR was confirmed by the presence of a single peak on the melt curve (Figure 5.4A), indicating a single amplified product and the absence of non-specific amplification products, primer-dimers or contaminates. Compared to retinal cells incubated in sNBA culture medium alone, there was no significant change in GSK3β mRNA levels (fold-change compared to GAPDH reference gene) after either sham transfection with Lipofectamine or after transfection with control siEGFP (Figure 5.4B). However, transfection of primary retinal cultures with 50nM siGSK3β resulted in a significant ($p<0.05$) reduction of GSK3β mRNA levels, with a fold-change of 0.41 ± 0.11, corresponding to knock-down of 59%.

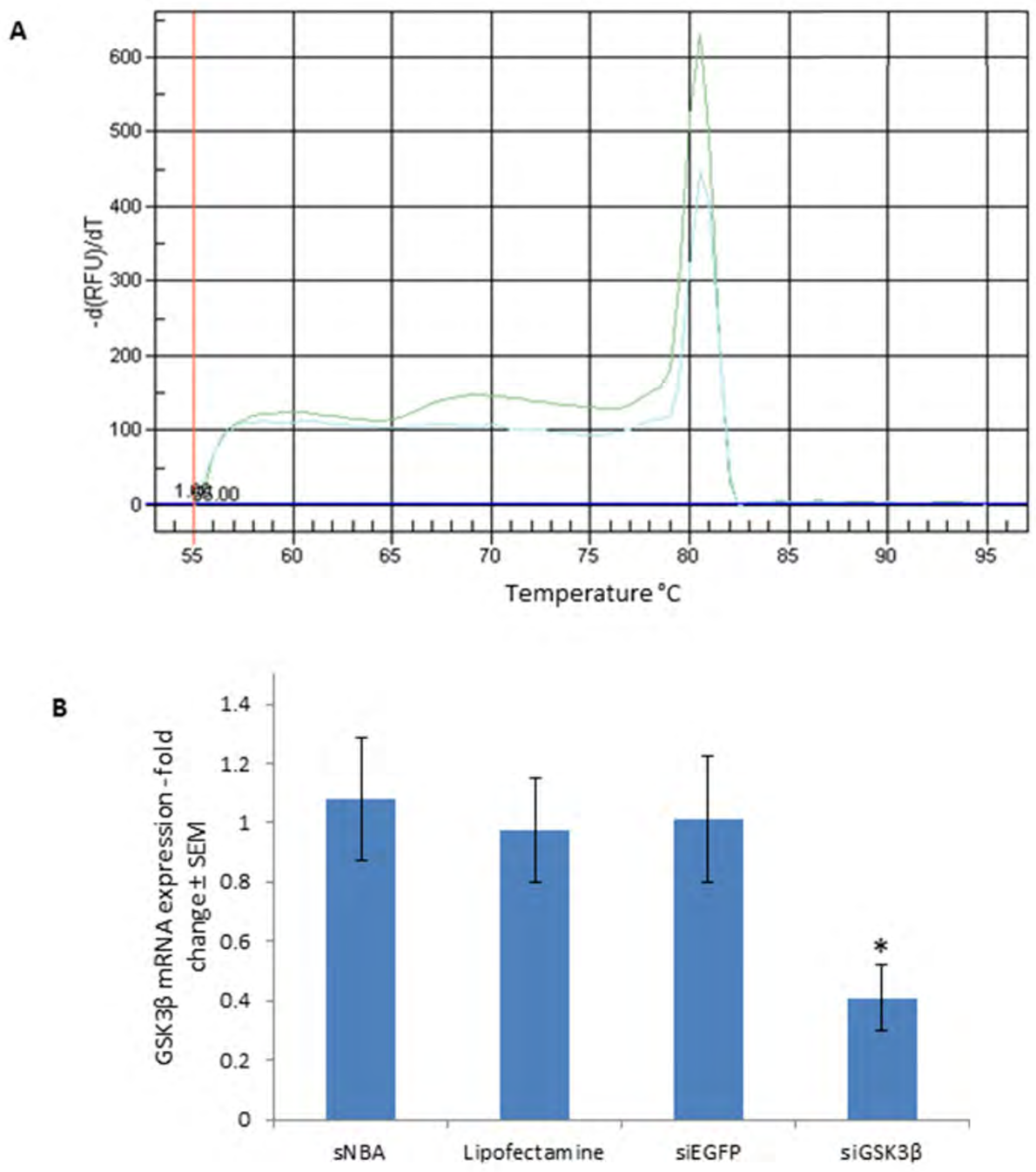


Figure 5.4: Target specificity and knock-down efficacy of siGSK3β. (A) Melt curve analysis of qPCR reaction using GSK3β-specific primers on cDNA samples obtained from retinal cultures of uninjured adult rats. A single peak in the melt curve indicates a single PCR amplicon and the absence of non-specific amplification, confirming the specificity of the GSK3β primers. (B) GSK3β mRNA expression in cultured retinal cells (as a fold-change relative to the house-keeping gene GAPDH) after treatment with sNBA culture medium alone, Lipofectamine transfection reagent, control siEGFP (50nM) and siGSK3β (50nM), indicating target knock-down by siGSK3β (n=5; *$p<0.05$ *vs* sNBA control).

5.5.5 Effects of siGSK3β on RGC survival and axon regeneration 24d after ONC *in vivo*

5.5.5.1 siGSK3β was RGC neuroprotective 24d after ONC

The number of $Brn3^+$ RGC in retinal sections obtained from uninjured (intact) rats was 19.9 ± 0.2 RGC/250µm GCL (Figure 5.5). RGC survival was significantly reduced ($p<0.001$) 24d after ONC and intravitreal delivery of either PBS (10.4 ± 0.6 RGC) or siEGFP (10.9 ± 0.5 RGC), corresponding to RGC survival of 52.1% and 54.8%, respectively. There was no statistically significant difference in RGC survival between PBS and siEGFP control groups. In eyes treated with intravitreal siGSK3β after ONC, the number of surviving $Brn3^+$ RGC was 13.9 ± 0.7, significantly higher ($p<0.01$) than both PBS treated and siEGFP treated eyes, but significantly lower ($p<0.001$) compared to uninjured control retinae. Treatment with siGSK3β promoted 69.4% RGC survival compared to uninjured controls, and represented an increase in RGC survival of 33% and 27% compared to PBS and siEGFP controls, respectively. These data indicated GSK3β activity limits RGC survival after ONC and that intravitreal delivery of siGSK3β promoted modest, but significant, RGC neuroprotection 24d after ONC.

5.5.5.2 siGSK3β promoted elongation of regenerating RGC axons beyond the injury site without affecting initiation of axon sprouting at 24d after ONC

At 24d after ONC, there was no significant difference in the number of $GAP43^+$ axons regenerating beyond the ONC site into the distal ON after intravitreal injection of either PBS, siEGFP or siGSK3β at 100µm (52.8 ± 26.4, 45.7 ± 11.8 and 61.3 ± 9.0 axons/nerve, respectively, $p=0.792$), 200µm (35.1 ± 12.9, 31.1 ± 11.8 and 43.2 ± 7.9 axons/nerve, respectively, $p=0.626$) or 400µm (8.2 ± 5.1, 16.9 ± 5.1 and 25.9 ± 8.3 axons/nerve, respectively, $p=0.214$) (Figure 5.6). However, compared to PBS and siEGFP injected eyes, there was a statistically significant increase in the number of $GAP43^+$

regenerating axons in siGSK3β treated eyes at 800μm (10.8 ± 2.9, 5.5 ± 4.5 and 25.2 ± 7.1 axons/nerve, respectively; $p<0.05$) and 1200μm (1.7 ± 1.7, 4.9 ± 3.1 and 21.8 ± 5.5 axons/nerve, respectively, $p<0.05$) beyond the ONC site. These data suggested that siGSK3β had little effect on the number of RGC sprouting axons into the distal ON, but promoted elongation of regenerating axons compared to PBS and siEGFP controls after ONC beyond 800μm into the distal ON. In this model, therefore, GSK3β activity did not affect initial RGC axogenesis, but was a limiting factor in axon elongation.

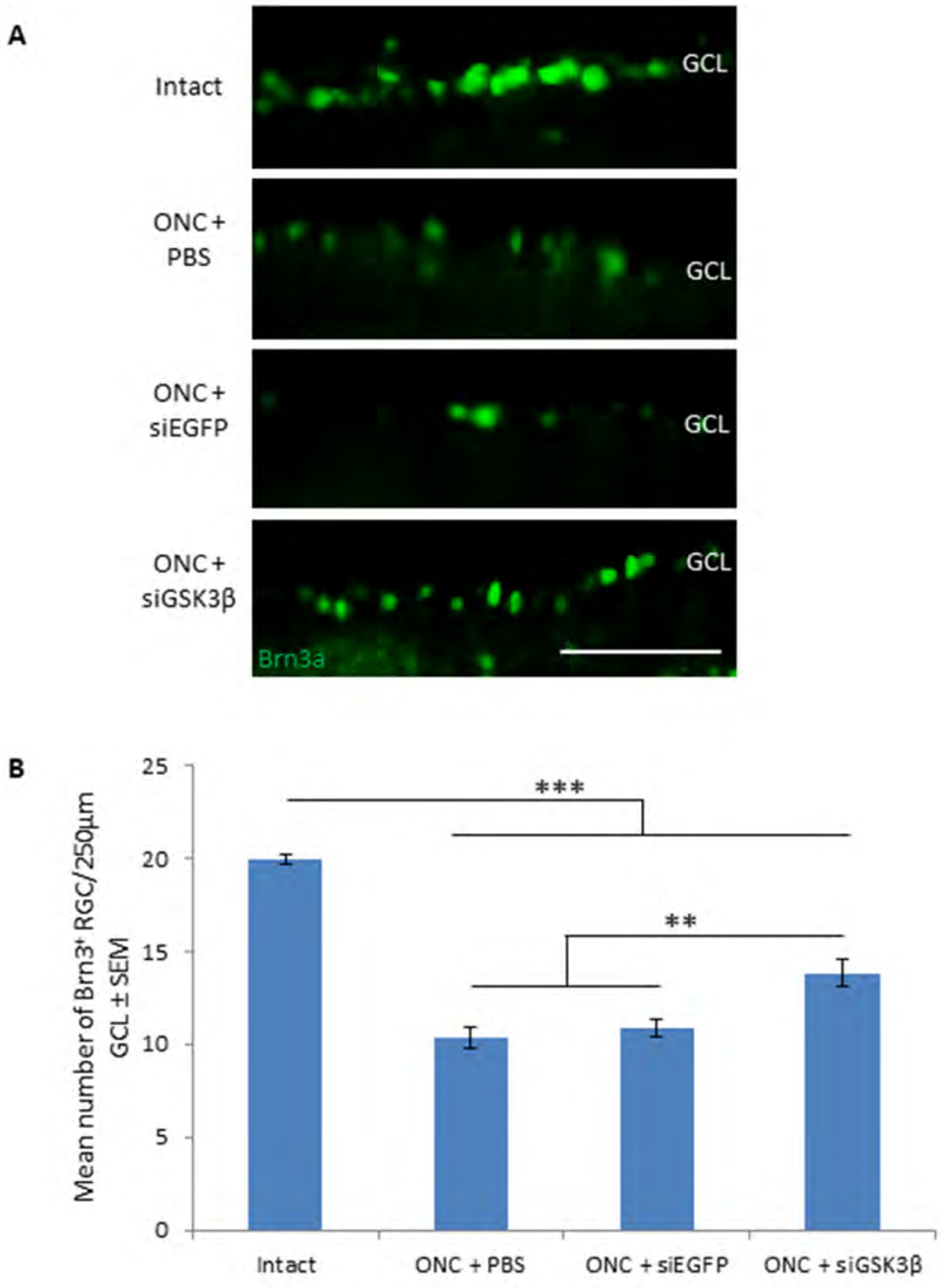


Figure 5.5: Brn3a$^+$ RGC survival after ONC *in vivo.* (A) Retinal sections immunostained for Brn3a (green) in intact retinae (top row) and 24d after ONC + PBS (2nd row), ONC + siEGFP (3rd row) and ONC + siGSK3β (bottom row) (scale bar = 100µm). Note the reduced expression of Brn3a in the retinal GCL after ONC which is improved with treatment with siGSK3β. (B) Quantification of surviving Brn3$^+$ RGC in a 250µm GCL sample in retinal sections from animals described in (A) at 24d after ONC, indicating enhanced RGC survival after siGSK3β treatment (n=6 retinae/group [n=5 for intacts]; **p<0.01, ***p<0.001).

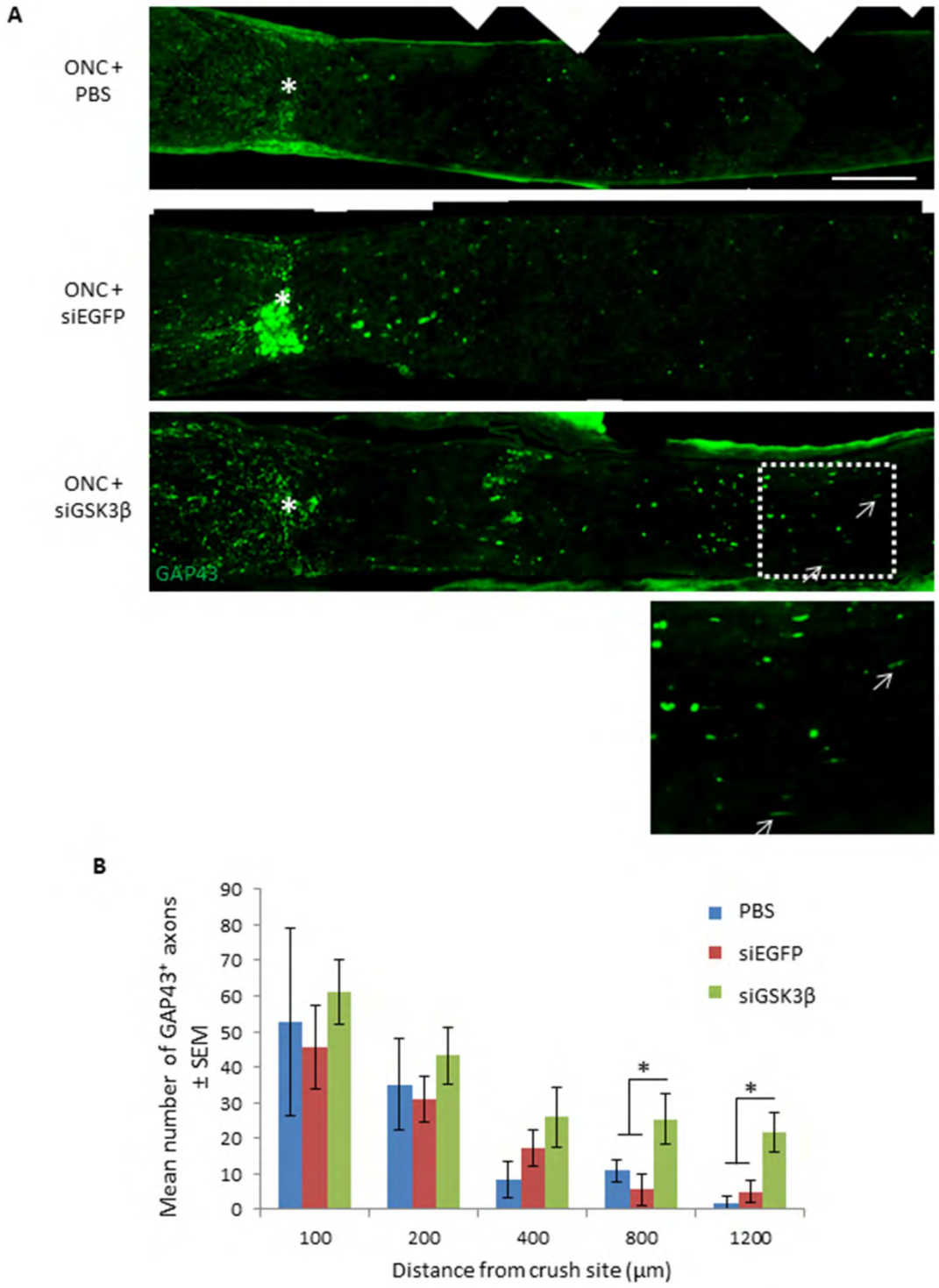


Figure 5.6: Enhanced RGC axon elongation by siGSK3β without affecting initiation of axon regeneration after ONC *in vivo*. (A) Longitudinal ON sections immunostained to demonstrate GAP43^{+} regenerating axons (arrows) after ONC + PBS (top panel), ONC + siEGFP (middle panel) and ONC + siGSK3β (bottom panel) (scale bar = 200µm). The asterisk demarcates the ON site and the boxed area in the lower panel represents the magnified area. (B) Quantification of GAP43^{+} regenerating axons 100, 200, 400, 800 and 1200µm beyond the ONC site in eyes after intravitreal injection of PBS (blue bars), siEGFP (red bars) and siGSK3β (green bars) (n=6 nerves/group; *p<0.05).

5.5.6 Effects of siGSK3β on RGC survival, neurite outgrowth and mTORC1 activity in the presence of activated retinal glia *in vitro*

To investigate the possible mechanisms underlying the effects of siGSK3β observed in the initial retinal cell culture studies, further experiments were undertaken in cultures prepared from animals 5d after ONC, when the retinal glial response is underway. In contrast to primary retinal cultures prepared from uninjured animals, $GFAP^+$ glia were observed after ONC, indicating the presence of activated astrocytes and Müller glia (as described in Section 4.5.2.2). This allowed investigation of a glial contribution to the siRNA effects, and therefore to the effects of GSK3β activity in the presence of activated retinal glia. In addition, the mTORC1 inhibitor Rapamycin was used to investigate whether the effects of siGSK3β on RGC survival and neurite growth were dependent upon mTORC1 signalling.

5.5.6.1 siGSK3β was RGC neuroprotective in the presence of activated retinal glia in vitro, *and the effects were dependent upon mTORC1 signalling*

In glial-activated cultures, there was no significant difference in RGC survival between wells prepared with culture medium alone (357.3 ± 19.3 RGC/well) and wells transfected with control siEGFP (288.9 ± 12.3), with RGC survival in these control wells comparable to levels described previously in the controls wells in the absence of activated retinal glia (Section 5.5.3), and to the control wells used in the presence of activated retinal glia for the evaluation of siRTP801 (Chapter 4) (Figure 5.7A, B). Treatment with 50nM siGSK3β significantly increased ($p<0.01$) RGC survival (523.7 ± 19) compared to controls, indicating that siGSK3β was RGC neuroprotective both in the presence and absence of $GFAP^+$ glia, and therefore reflected a direct effect of GSK3β on RGC viability. The presence of Rapamycin, an mTORC1 inhibitor, did not significantly reduce RGC survival in culture medium or

siEGFP control wells. This was consistent with earlier observations (Chapter 4), and confirmed both that mTORC1 activity was not obligatory for constitutive RGC survival, and that Rapamycin was not RGC toxic in this culture model. However, the presence of Rapamycin significantly reduced ($p<0.01$) the RGC neuroprotection induced by siGSK3β (392.2 ± 2.6 RGC/well) to a level not significantly different from baseline RGC survival in controls, suggesting that the RGC neuroprotective effect of siGSK3β was dependent upon mTORC1 signalling, and consistent with GSK3β activity suppressing mTORC1-dependent cell survival signalling.

5.5.6.2 siGSK3β increased RGC neurite outgrowth initiation in the presence of activated retinal glia in vitro*, independent of mTORC1 signalling*

In glial-activated cultures, the proportion of neurite-bearing RGC was 24.2 ± 3.3% in sNBA control wells, levels that were not significantly different after transfection with control siEGFP (18.4 ± 1.4%) (Figure 5.7C). However, treatment with siGSK3β significantly increased ($p<0.05$) the frequency of neurite-bearing RGC to 35.2 ± 3.0%, indicating that siGSK3β had an effect on promoting the initiation of neurite outgrowth in this culture model. Rapamycin did not significantly alter the proportion of neurite-bearing RGC, either in control wells or after siGSK3β treatment. These data indicated that RGC neurite initiation was mTORC1-independent, and that GSK3β has a role in suppressing neurite outgrowth through an mTORC1-independent mechanism.

5.5.6.3 siGSK3β promoted RGC neurite elongation in the presence of activated retinal glia in vitro*, independent of mTORC1 signalling*

The mean length of the longest RGC neurite was 55 ± 2µm in wells incubated with culture medium alone, and 50 ± 1µm after transfection with siEGFP (Figure 5.7D). In contrast to retinal cultures

prepared in the absence of $GFAP^+$ glia, in this setting transfection with siGSK3β resulted in significantly longer neurites (92 ± 2µm; $p<0.05$), suggesting that siRNA-mediated GSK3β knock-down promoted neurite elongation only in the presence of $GFAP^+$ retinal glia. Rapamycin did not significantly affect the elongation of RGC neurites, either in control wells or after siGSK3β treatment, indicating that mTORC1 activity was not responsible for the elongation of sprouting RGC neurites, and siGSK3β-mediated promotion of neurite elongation in the presence of $GFAP^+$ glia was mTORC1-independent.

5.5.6.4 siGSK3β did not affect RGC expression of pS6 in the presence of activated retinal glia in vitro

To investigate the effect of siGSK3β on mTORC1 signalling in RGC, retinal cultures (prepared as described above) were immunostained for the mTORC1 substrate pS6. There was no significant difference in the number of $pS6^+$ RGC between wells incubated with culture medium alone (15.8 ± 2.8%), or after transfection with siEGFP (14.3 ± 1.0%), or siGSK3β (16.4 ± 1.9%). Exposure to Rapamycin abolished the expression of pS6 in both RGC and βIII-$tubulin^-$ cells (Figure 5.7A, E), irrespective of all other treatments applied. These data indicated that siGSK3β did not affect mTORC1-signalling through the pS6 substrate in RGC. However, the earlier observation that siGSK3β-induced RGC neuroprotection was mTORC1-dependent suggested that the neuroprotective effect was mediated *via* mTORC1-dependent non-pS6 substrate(s), such as 4E-BP1.

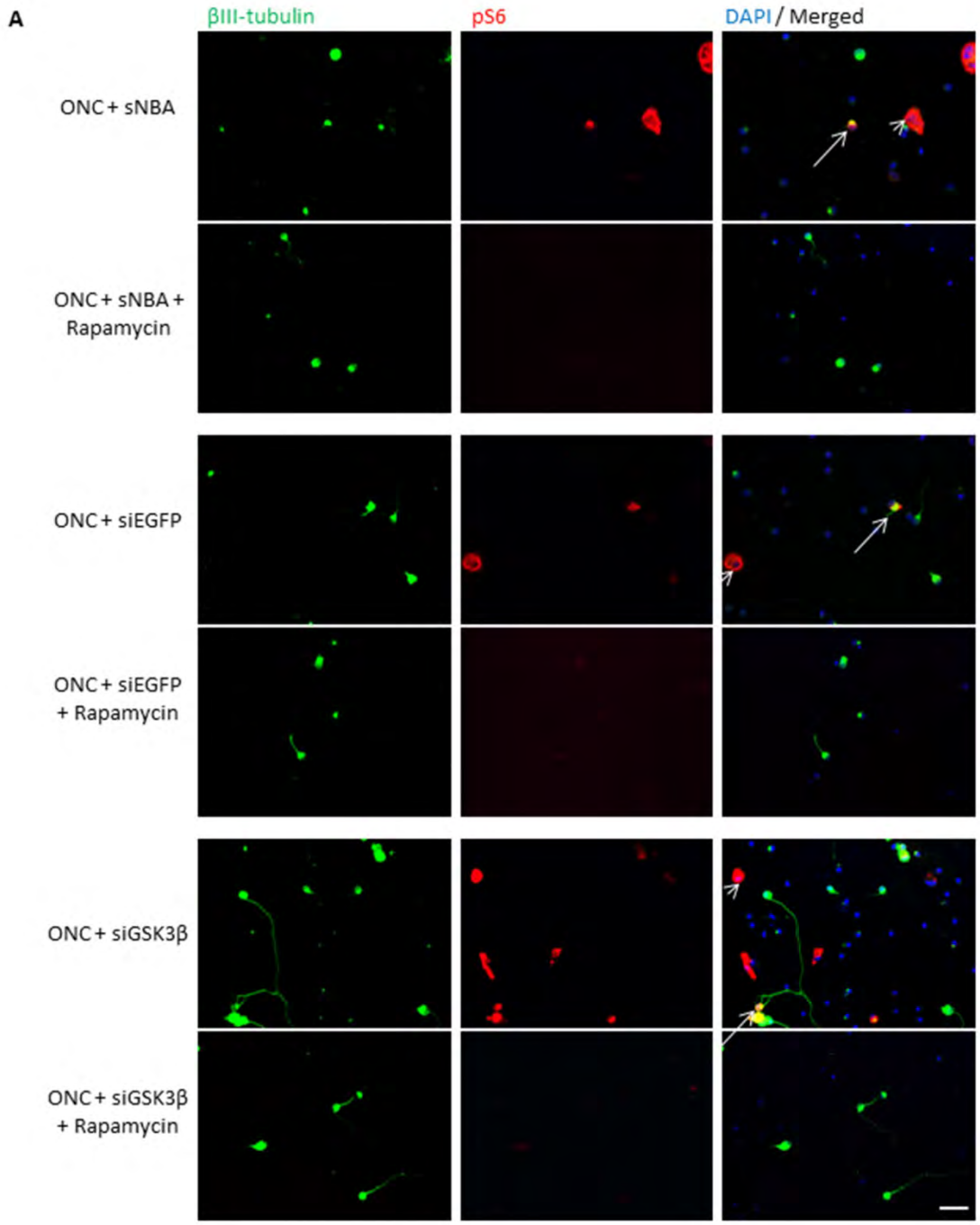


Figure 5.7: Effects of siGSK3β on RGC survival, neurite outgrowth and mTORC1 activity in the presence of activated retinal glia *in vitro*. (A) Retinal cultures established 5d after ONC *in vivo* to activate retinal glia, treated for 3d with sNBA, siEGFP and siGSK3β in the presence and absence of the mTORC1 inhibitor Rapamycin and immunostained for βIII-tubulin (green) and pS6 (red), with DAPI (blue) as a nuclear counterstain. Note that pS6 is detected both in βIII-tubulin^{+} RGC (long arrows) and βIII-tubulin^{-} cells (short arrows) and the abolition of pS6 immunostaining in the presence of Rapamycin (scale bar = 20μm). Quantification of (B) surviving βIII-tubulin^{+} RGC, (C) proportion of RGC bearing neurites, and (D) length of longest RGC neurite for conditions described in (A). (E) Proportion of βIII-tubulin^{+} RGC exhibiting pS6 positivity, indicating abolition of pS6 expression in the presence of Rapamycin, but no significant effect of siGSK3β on the proportion of pS6^{+} RGC (n=3; *p<0.05, **p<0.01, *p<0.001). Figure continues on the next page.

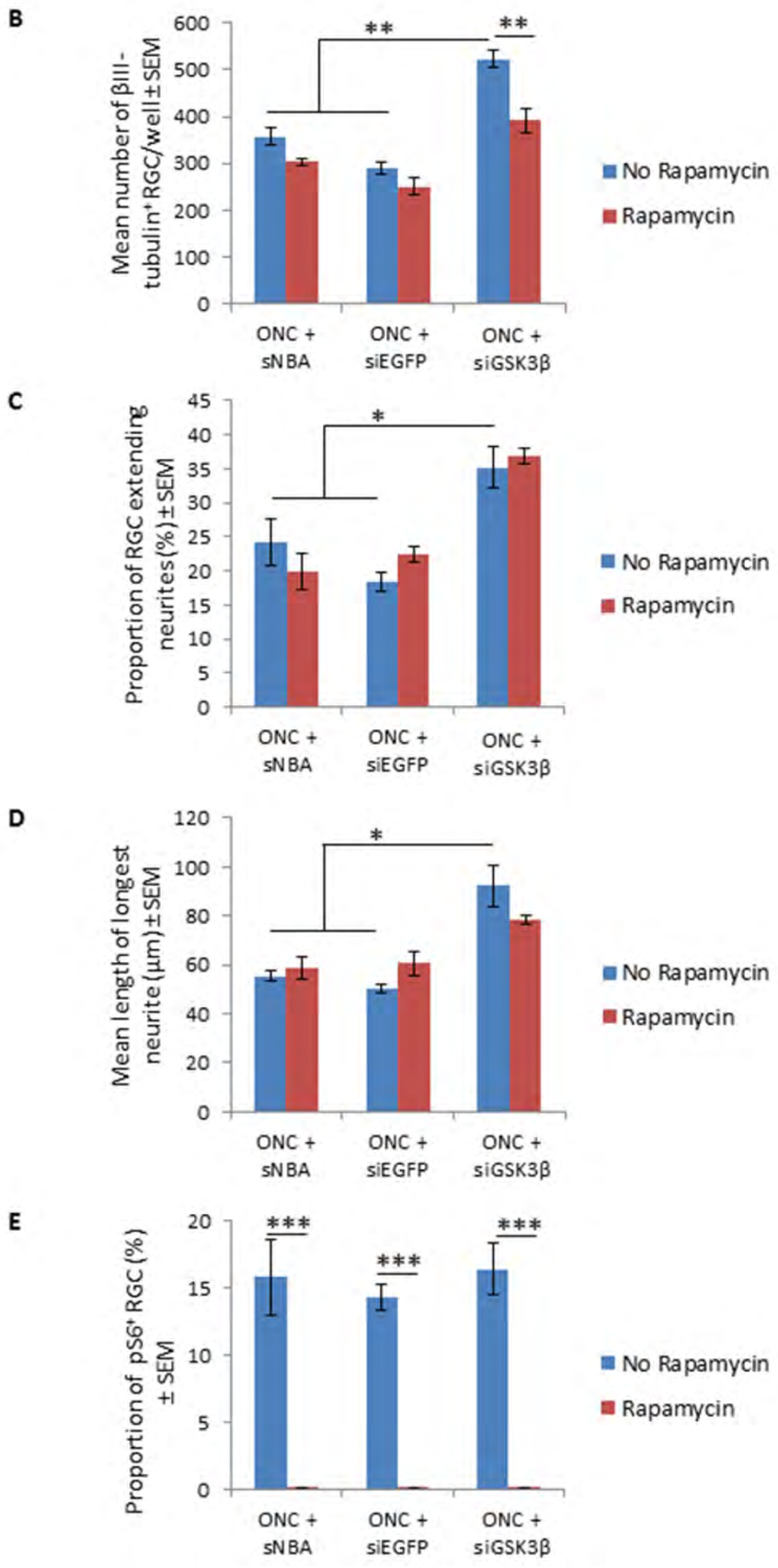


Figure 5.7: Effects of siGSK3β on RGC survival, neurite outgrowth and mTORC1 activity in the presence of activated retinal glia *in vitro*. Continued from previous page.

5.5.7 Cellular localisation of GSK3β was limited to RGC and not present in activated retinal glia

Unlike the retinal cellular expression of RTP801, which was evident in both neuronal and non-neuronal cells (Chapter 3), the immunofluorescent detection of GSK3β was limited to RGC and not observed in glia. In retinal sections, GSK3β expression correlated closely with the RGC phenotypic marker Brn3a (Figure 5.8A), without significant detectable immunostaining of other retinal layers. This was confirmed in culture, with the complete absence of detectable GSK3β co-immunostaining in $GFAP^+$ glia both in siGSK3β-transfected and control wells (Figure 5.8B). The restriction of GSK3β expression to RGC and its absence in glia suggested that the RGC survival and neurite growth effects of GSK3β knock-down reflected RGC-specific responses rather than indirect effects from modulation of GSK3β activity in non-RGC retinal cells.

5.5.8 siGSK3β did not affect reactive gliosis after ONC *in vivo*

As demonstrated in Chapter 4, there was minimal GFAP expression in retinal sections obtained from intact animals, with an absence of $GFAP^+$ Müller glial processes traversing the IPL (Figure 5.9), but retinal $GFAP^+$ expression was increased after ONC. While there was a significant increase in the number of $GFAP^+$ Müller glial processes in the IPL after ONC, consistent with earlier observations (Chapter 4), there was no significant difference in Müller glial activation between eyes injected with PBS (10.7 ± 1.0 processes/250μm IPL), siEGFP (12.4 ± 0.7) or siGSK3β (12.5 ± 0.6). Thus, in contrast to siRTP801, siGSK3β had no significant effect on reactive gliosis after ONC. Together with the absence of GSK3β in glia, as described above, these findings strongly suggested that effects of siGSK3β on RGC viability and axon/neurite growth reflected RGC intrinsic responses rather than modulation of glia. However, these data remained consistent with the possibility that glial-derived factors may influence RGC when GSK3β activity is suppressed.

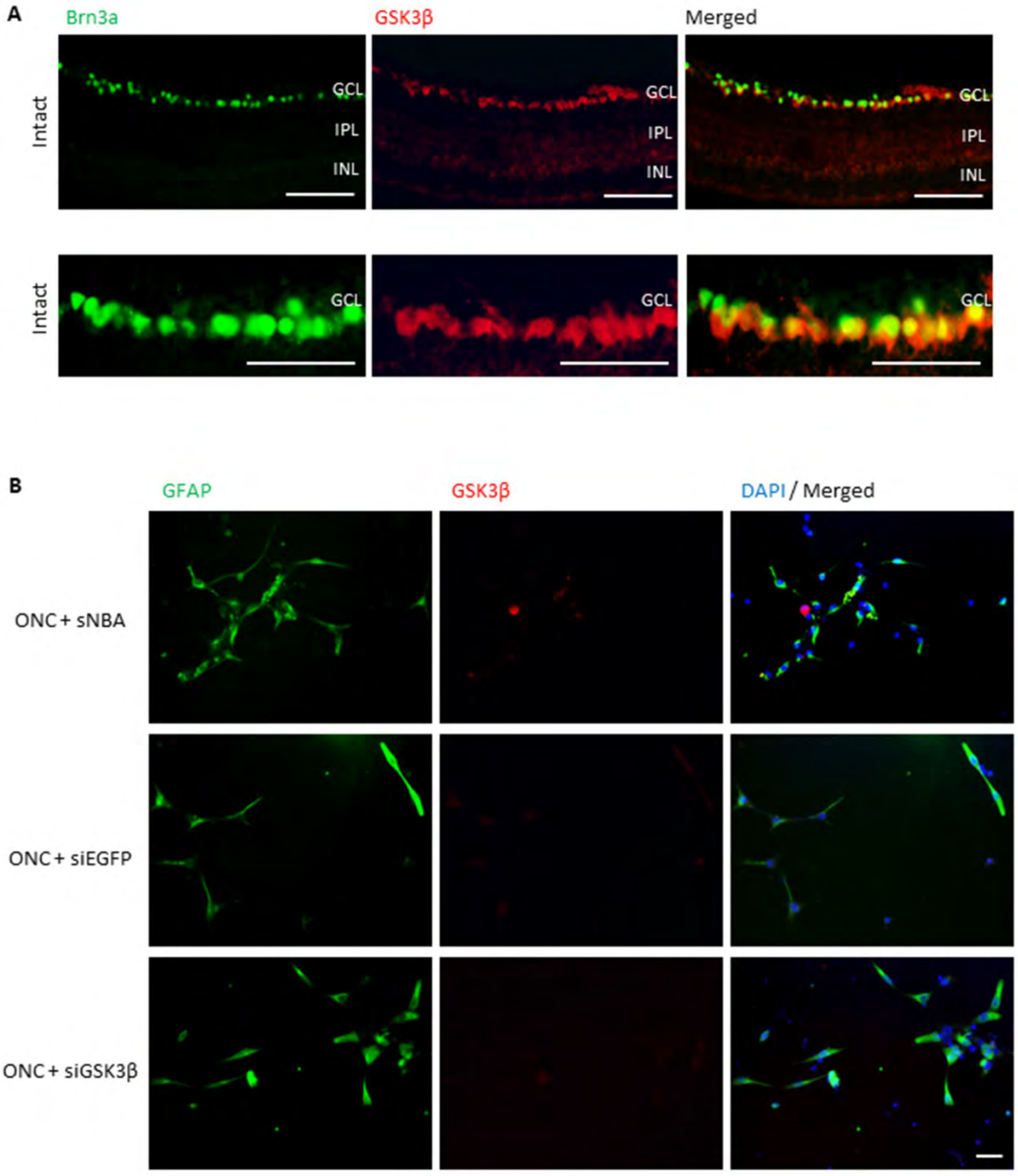


Figure 5.8: Cellular localisation of GSK3β was limited to RGC with no detectable expression in glia. (A) Retinal sections from uninjured adult rats immunostained for Brn3a (green) and GSK3β (red), demonstrating that constitutive expression of GSK3β was limited to the GCL, where it localised to $Brn3a^{+}$ RGC (higher magnification GCL sections in lower panel) (scale bar = 100µm). (B) Retinal cultures established 5d after ONC *in vivo* to activate retinal glia, treated for 3d with sNBA, siEGFP and siGSK3β and immunostained for GFAP (green) and GSK3β (red) with DAPI (blue) as a nuclear counterstain, demonstrating lack of GSK3β detection in activated retinal glia (scale bar = 20µm).

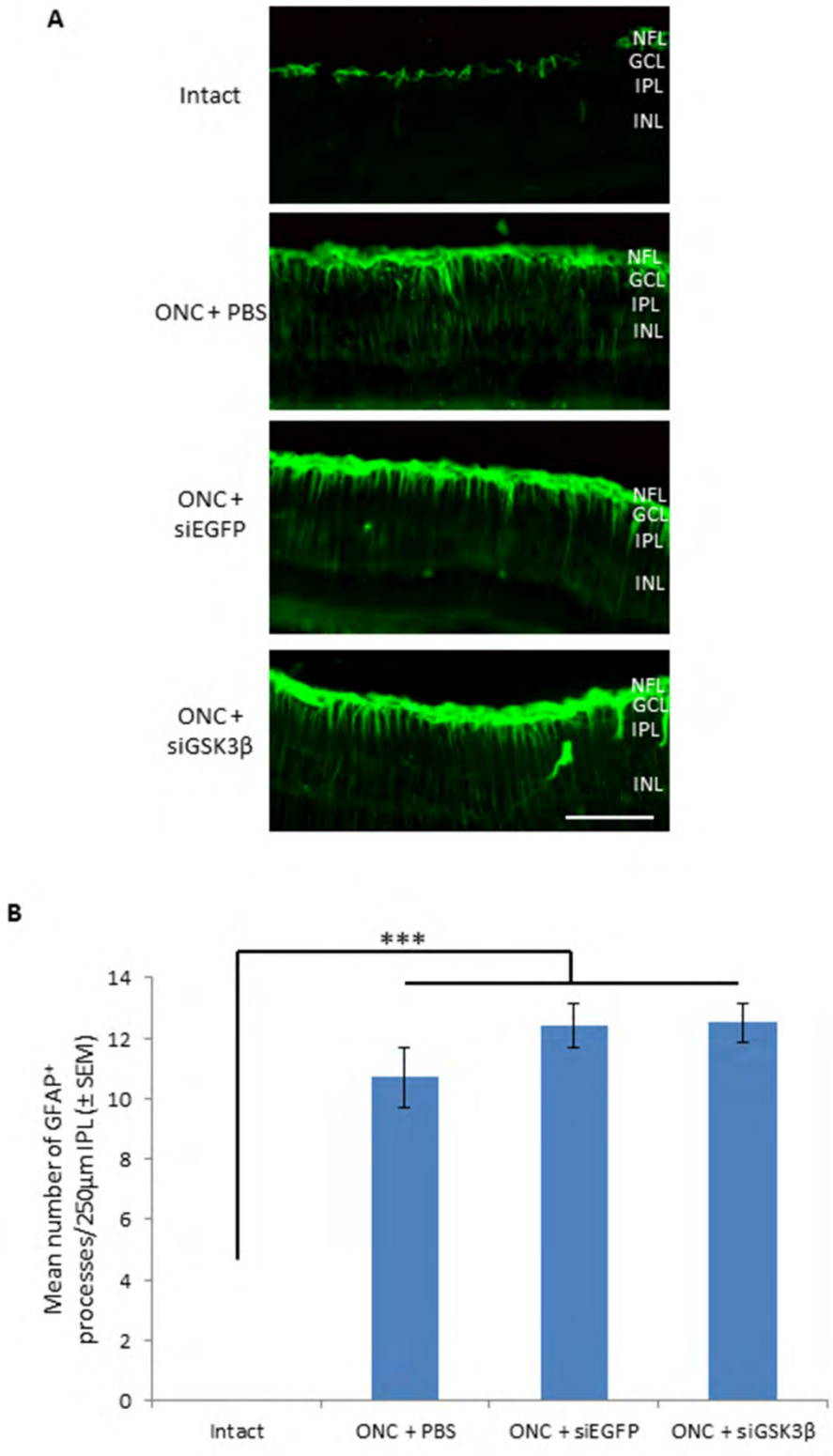


Figure 5.9: Effect of siGSK3β on retinal astrocyte/Müller glial response after ONC *in vivo*. (A) Immunostained retinal sections showing GFAP$^+$ glia in sections of intact uninjured retinae and after ONC + PBS, ONC + siEGFP and ONC + siGSK3β (scale bar = 100µm). (B) Quantification of GFAP$^+$ Müller glial processes in a 250µm linear sample of IPL for groups described in (A), demonstrating no significant effect of siGSK3β treatment on the GFAP$^+$ Müller glial response after ONC (n=6 retinae/group [n=5 for intacts]; ***p<0.001 *vs* intact control).

5.5.9 Effects of siGSK3β on downstream substrates of GSK3β

To investigate the possible underlying signalling mechanisms associated with enhanced RGC survival and neurite growth after siGSK3β, the glial-activated culture paradigm was used to evaluate the RGC immunocytochemical detection of possible correlates of GSK3β activity, including pGSK3β, pCRMP2, pSmad1 and pMAP1B.

5.5.9.1 Effects of siGSK3β on RGC cellular expression of pGSK3β

Detection of pGSK3β (Ser9) was observed in a minority of RGC in sNBA (9.3 ± 3.2%) and siEGFP (13.4 ± 2.1%) control wells of glial-activated cultures and, while the proportion of $pGSK3\beta^{+}$ RGC after siGSK3β treatment was increased to 19.9 ± 2.3%, this did not reach statistical significance (p=0.06 *vs* sNBA control wells) (Figure 5.10).

5.5.9.2 Effects of siGSK3β on RGC cellular expression of pCRMP2

Immunocytochemical staining for pCRMP2 demonstrated positivity in 100% RGC in sNBA and siEGFP control wells, indicating constitutive RGC expression of pCRMP2 (Figure 5.11), and this was not affected by siGSK3β, indicating that the RGC survival and neurite growth promoting effects of siGSK3β were independent of pCRMP2.

5.5.9.3 Effects of siGSK3β on RGC cellular expression of pSmad1

Immunocytochemical staining for pSmad1 demonstrated positivity in 92.0 ± 1.7% and 91.3 ± 0.9% RGC in sNBA and siEGFP control wells, respectively, but there was no significant difference in RGC

pSmad1 detection after treatment with siGSK3β (92.4 ± 1.3%) (Figure 5.12), indicating that the RGC survival and neurite growth promoting effects of siGSK3β were independent of pSmad1.

5.5.9.4 Effects of siGSK3β on RGC cellular expression of pMAP1B

Immunocytochemical staining for pMAP1B demonstrated positivity in 40.8 ± 4.5% and 42.0 ± 4.8% RGC in sNBA and siEGFP control wells, respectively, and the small decrease in pMAP1B expression recorded after siGSK3β treatment (31.8 ± 3.6%) was not statistically significant (Figure 5.13), indicating that pMAP1B expression was not a major contributing factor to the RGC survival and neurite growth promoting effects of siGSK3β.

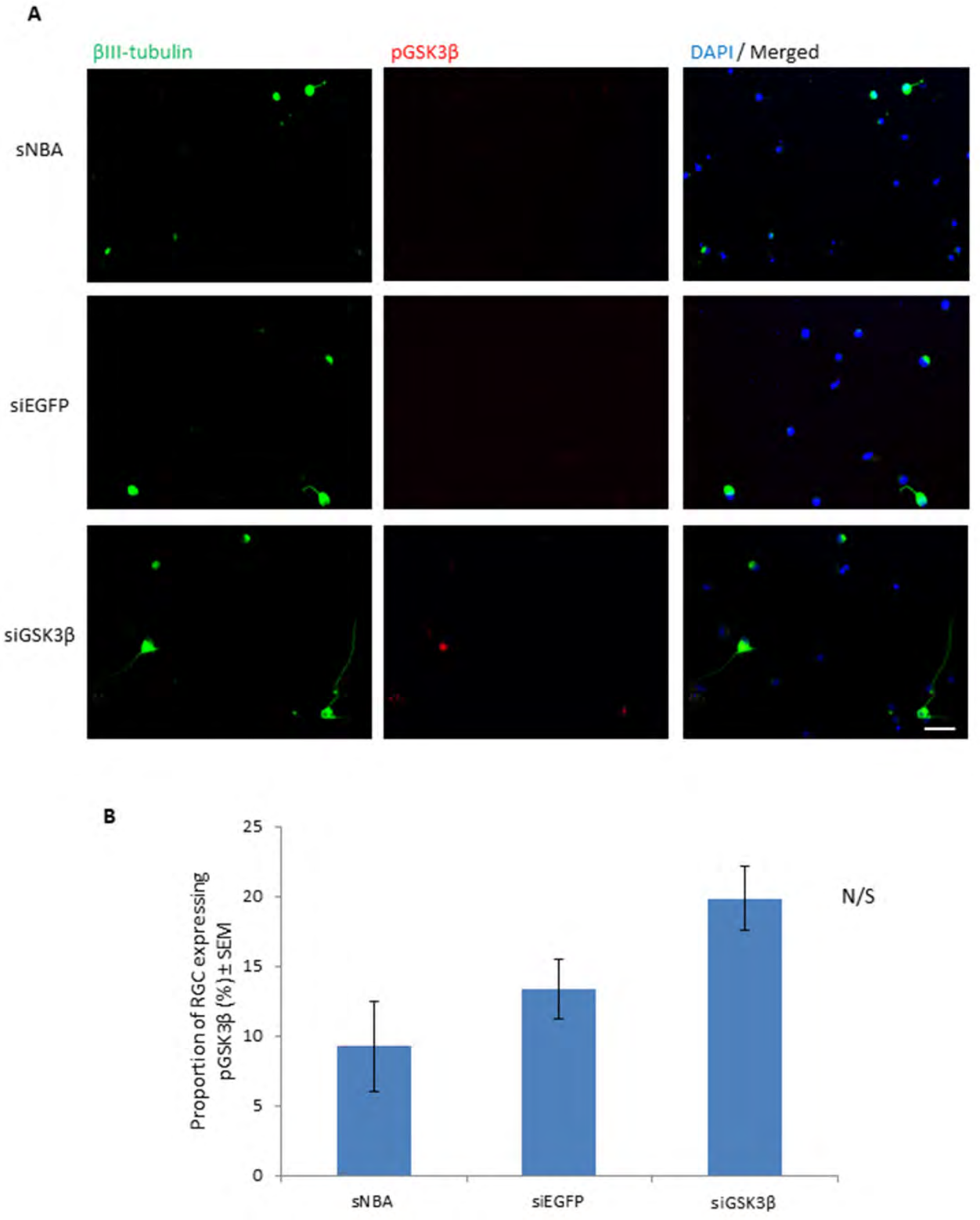


Figure 5.10: Effect of siGSK3β on RGC cellular localisation of pGSK3β. (A) Glial-activated retinal cultures incubated for 3d with sNBA (top row), siEGFP (middle row) and siGSK3β (bottom row) and immunostained for βIII-tubulin (green) and pGSK3β (red), with DAPI (blue) as a nuclear counterstain (scale bar = 20μm). (B) Proportion of βIII-tubulin^{+} RGC demonstrating pGSK3β positivity for cultures described in (A) (n=3). The difference between groups was not statistically significant (ANOVA).

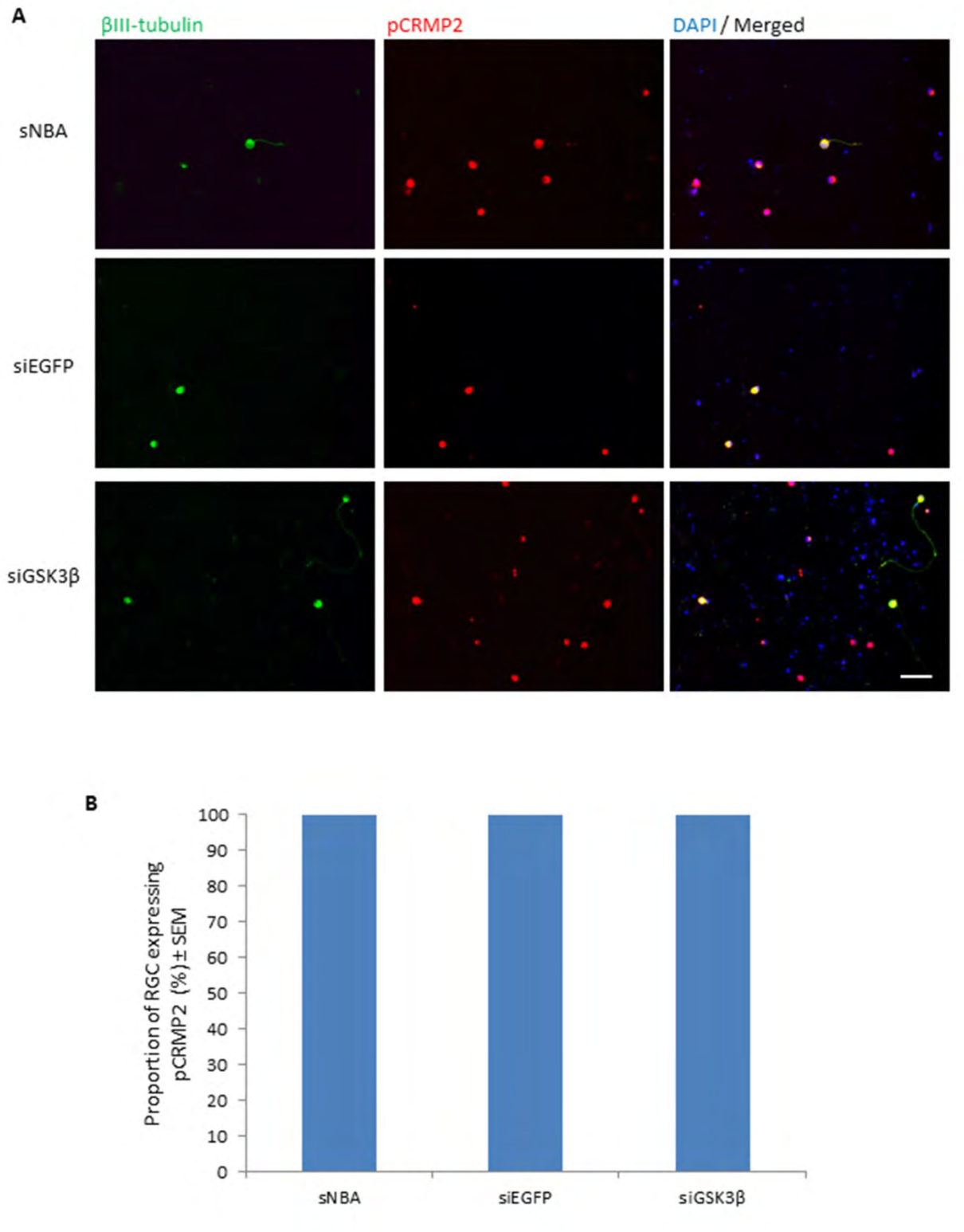


Figure 5.11: Effect of siGSK3β on RGC cellular localisation of pCRMP2. (A) Glial-activated retinal cultures incubated for 3d with sNBA (top row), siEGFP (middle row) and siGSK3β (bottom row) and immunostained for βIII-tubulin (green) and pCRMP2 (red), with DAPI (blue) as a nuclear counterstain (scale bar = 20μm). (B) Proportion of βIII-tubulin^{+} RGC demonstrating pCRMP2 positivity for cultures described in (A), indicating that pCRMP2 was detected in all RGC, irrespective of incubation with siGSK3β or controls (n=3).

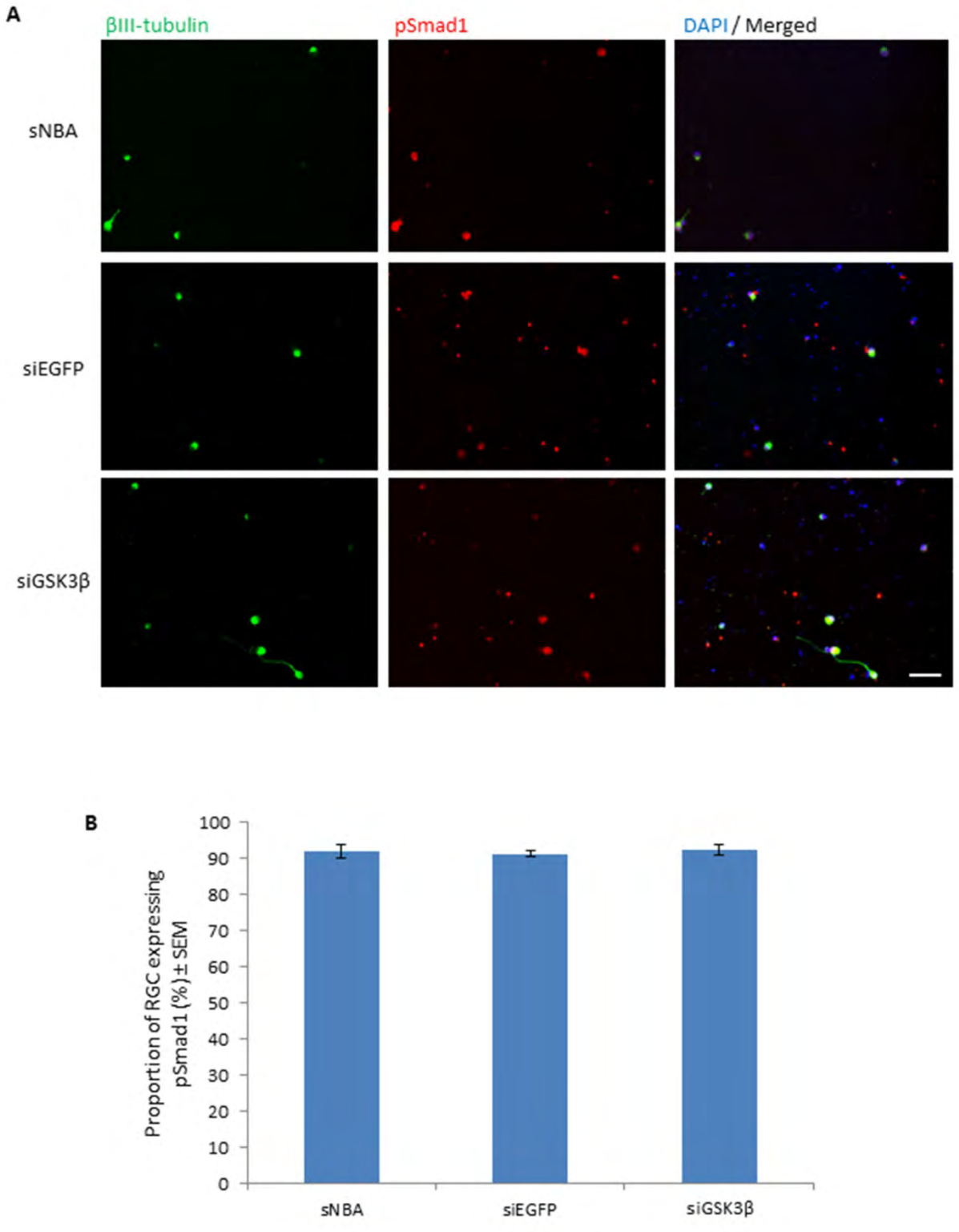


Figure 5.12: Effect of siGSK3β on RGC cellular localisation of pSmad1. (A) Glial-activated retinal cultures incubated for 3d with sNBA (top row), siEGFP (middle row) and siGSK3β (bottom row) and immunostained for βIII-tubulin (green) and pSmad1 (red), with DAPI (blue) as a nuclear counterstain (scale bar = 20μm). (B) Proportion of βIII-tubulin^{+} RGC demonstrating pSmad1 positivity for cultures described in (A) (n=3). There was no statistically significant difference between groups (ANOVA).

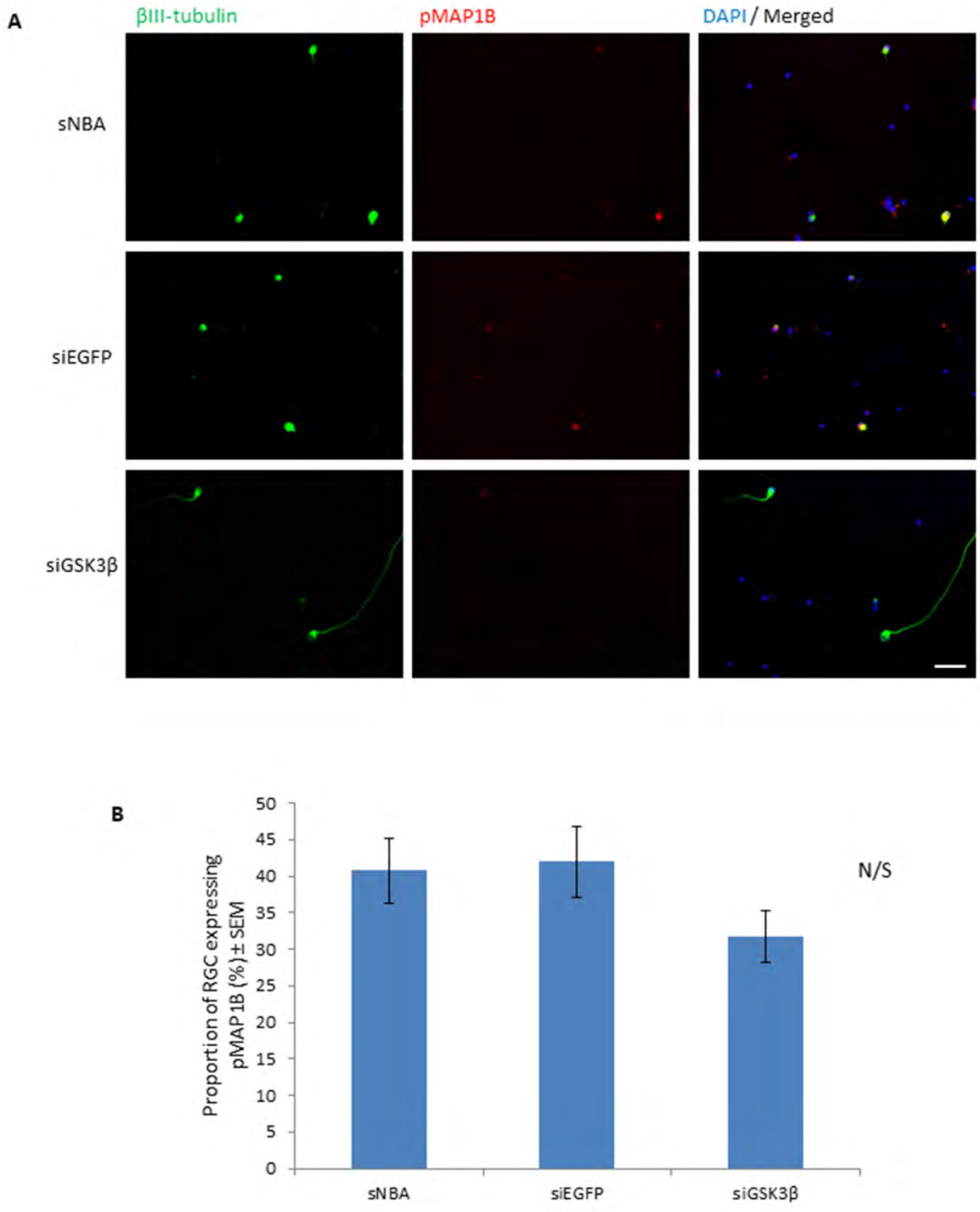


Figure 5.13: Effect of siGSK3β on RGC cellular localisation of pMAP1B. (A) Glial-activated retinal cultures incubated for 3d with sNBA (top row), siEGFP (middle row) and siGSK3β (bottom row) and immunostained for βIII-tubulin (green) and pMAP1B (red), with DAPI (blue) as a nuclear counterstain (scale bar = 20µm). (B) Proportion of βIII-tubulin^{+} RGC demonstrating pMAP1B positivity for cultures described in (A) (n=3). The difference between groups was not statistically significant (ANOVA).

5.5.10 Effects of GSK3β inhibition on overcoming Nogo inhibitory peptide *in vitro*

5.5.10.1 GSK3β inhibition overcame the inhibitory effect of Nogo on RGC neurite outgrowth initiation in vitro

In retinal cultures in the presence of activated glia, the proportion of neurite-bearing RGC (24.2 ± 3.3%, as per section 5.5.6.2) was reduced in the presence of 25μM Nogo-P4 peptide to 12.8 ± 2.0%, 12.1 ± 3.7% and 10.2 ± 3.3% in wells incubated with sNBA, Lipofectamine and siEGFP, respectively (Figure 5.14A, B), indicating suppression of neurite outgrowth initiation by Nogo-P4 peptide. However, despite the presence of this growth inhibitor, treatment with siGSK3β resulted in a significant increase in the proportion of neurite-bearing RGC (28.4 ± 2.3%; $p<0.05$ *vs* each of the three control conditions) to a level similar to that seen in the absence of Nogo-P4, and was replicated by treatment with the pharmacological GSK3β inhibitor Chir99021 (300nM; 34.2 ± 3.5%). Neither GSK3β inhibitor promoted neurite outgrowth to the same degree as the CNTF positive control (40.9 ± 4.8%).

5.5.10.2 GSK3β inhibition overcame the inhibitory effect of Nogo on RGC neurite elongation in vitro

Nogo-P4 peptide similarly suppressed the elongation of RGC neurites, with the mean length of longest RGC neurite in the glial-activated cultures reduced from 55.5 ± 2.3μm (as per Section 5.5.6.3) to 28.8 ± 3.6μm, 23.0 ± 2.8μm and 25.3 ± 2.6μm after incubation with sNBA, Lipofectamine solution and siEGFP controls, respectively (Figure 5.14A, C). Treatment with siGSK3β restored neurite length to 57.8 ± 5.7μm ($p<0.01$ *vs* each of the three control conditions), and a similar effect was seen with Chir99021 (65.4 ± 4.8μm), although less than with CNTF (75.3 ± 7.3μm). Together, these data

confirmed the growth-inhibitory effect of Nogo-P4, even in the presence of activated retinal glia, and indicated that GSK3β inhibition, both by siRNA and pharmacological inhibition, enabled RGC to overcome the Nogo-dependent inhibition of neurite outgrowth initiation and elongation. Thus, the modest but significant RGC axon elongation effect observed after siGSK3β treatment in the ONC model *in vivo* may be explained by the rendering of regenerating RGC axon growth cones insensitive to the effects of CNS myelin-derived inhibitory ligands.

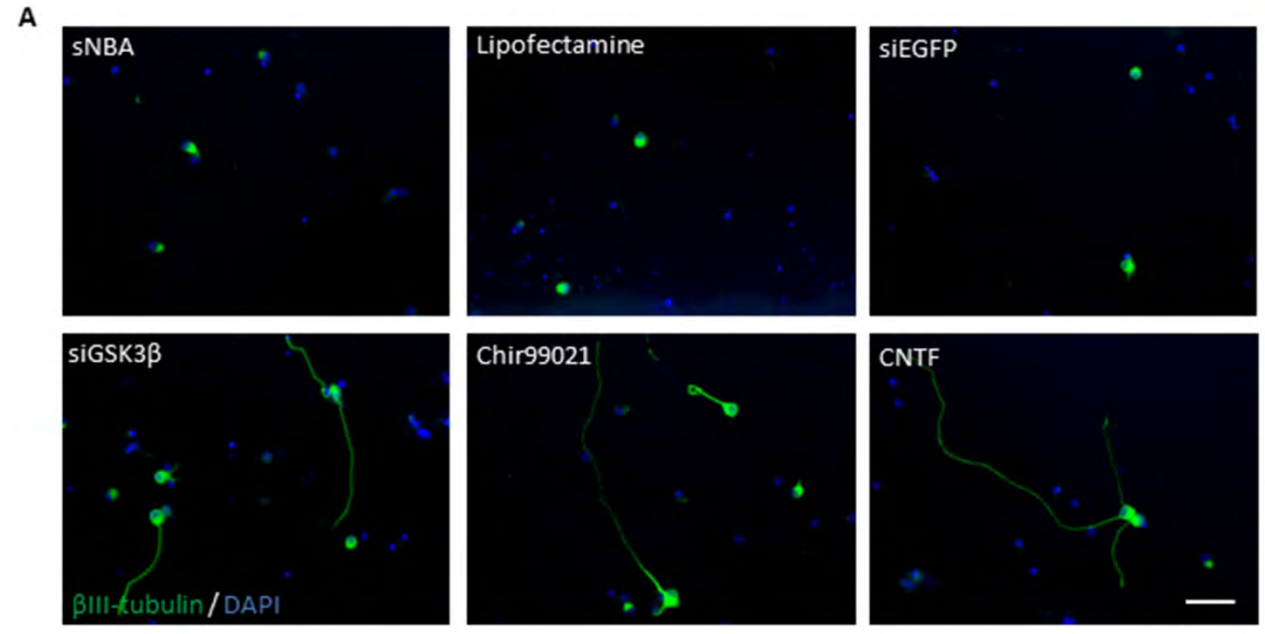


Figure 5.14: Effect of GSK3β inhibition on overcoming Nogo growth-inhibitory peptide in cultured retinal cells. (A) Glial-activated retinal cultures incubated for 3d with sNBA, Lipofectamine, siEGFP, siGSK3β, Chir99021 and CNTF (positive control) in the presence of Nogo-P4 growth-inhibitory peptide, and immunostained for βIII-tubulin (green) with DAPI (blue) as a nuclear counterstain (scale bar = 20μm). Figure and legend continues on the next page.

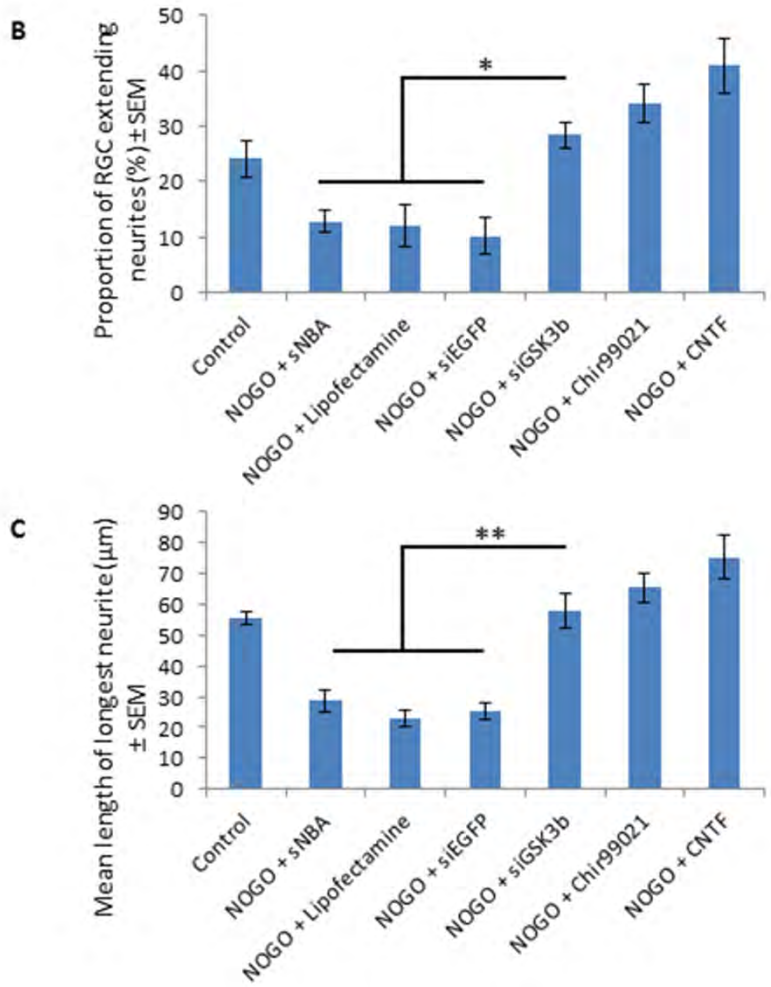


Figure 5.14: Effect of GSK3β inhibition on overcoming Nogo growth-inhibitory peptide in cultured retinal cells. Continued from previous page. Quantification of (B) proportion of βIII-tubulin^{+} RGC bearing neurites, and (C) length of longest RGC neurite for the cultures described in (A) and after incubation with sNBA culture medium in the absence of Nogo ('Control' bar), demonstrating that Nogo-dependent reduction in RGC neurite growth initiation and neurite elongation were counteracted by GSK3β inhibition with siGSK3β and Chir99021 (n=3; *p<0.05, **p<0.01).

5.5.11 Effects of combined siGSK3β/siRTP801 on RGC survival, neurite outgrowth and target knock-down in the presence of activated retinal glia *in vitro*

5.5.11.1 Combined siGSK3β (50nM) + siRTP801 (20nM) did not induce dual target knock-down, nor promoted RGC survival or neurite outgrowth in vitro

To evaluate the effects of combined siRNA treatment on RGC survival and neurite growth, experiments were undertaken using the optimal concentration of each siRNA, as determined from earlier *in vitro* studies. Consequently, a combined approach using 50nM siGSK3β + 20nM siRTP801, was predicted to produce the most favourable results. This combination of siRNA did not promote RGC survival when compared with either sNBA culture medium alone or 70nM siEGFP (Figure 5.15A). Furthermore, combined siGSK3β + siRTP801 had no significant effect on the proportion of neurite-bearing RGC (Figure 5.15B), nor on the length of RGC neurites (Figure 5.15C). This combination siRNA treatment reduced the frequency of $GSK3\beta^{+}$ RGC to 58.5 ± 9.9%, indicating GSK3β knock-down compared to controls, although there was no significant effect on $RTP801^{+}$ RGC, indicating a relative lack of RTP801 knock-down (Figure 5.15D). These data suggested that a combination of 50nM siGSK3β + 20nM siRTP801 enabled knock-down of GSK3β only (i.e. only the most concentrated siRNA in the combination was effective), probably due to competition for the RISC (Tanudji *et al.*, 2010). Moreover, despite 50nM siGSK3β promoting RGC survival and enhanced neurite growth when transfected in the absence of another siRNA (Sections 5.5.6.1-5.5.6.3), when used in combination with 20nM siRTP801 the pro-survival and neurite growth effects were abolished. This may reflect a degree of RGC toxicity/growth-inhibitory effect in the presence of a higher total siRNA load.

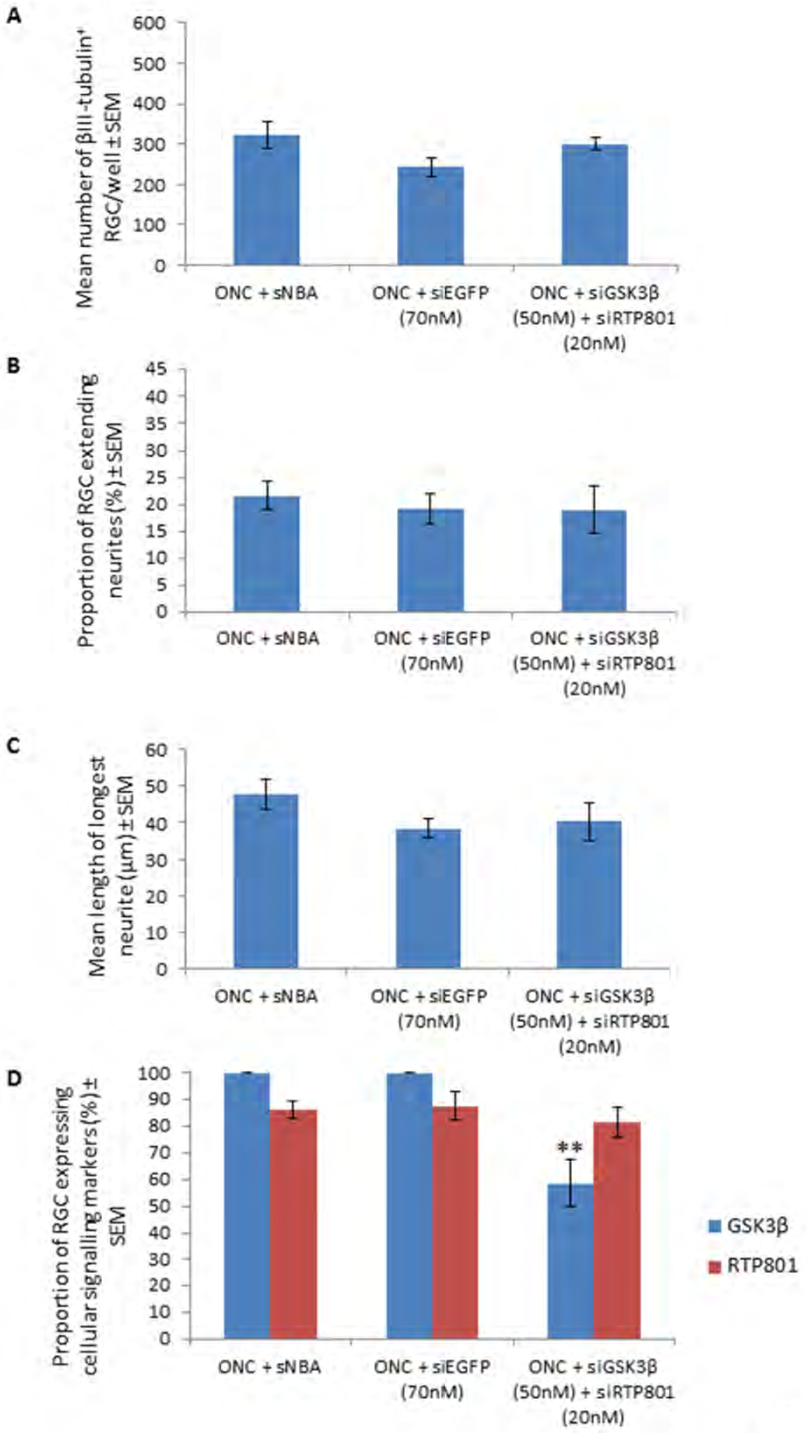


Figure 5.15: Effects of combined siGSK3β (50nM) and siRTP801 (20nM) RGC survival, neurite outgrowth and target knock-down in cultured retinal cells. Quantification of (A) βIII-tubulin$^+$ RGC survival, (B) proportion of βIII-tubulin$^+$ RGC bearing neurites, (C) length of longest RGC neurite, and (D) proportion of βIII-tubulin$^+$ RGC demonstrating positivity for GSK3β (blue bars) and RTP801 (red bars), in glial-activated retinal cultures incubated for 3d with sNBA, siEGFP (70nM) and combination siGSK3β (50nM)/siRTP801 (20nM) (n=3). Note that target knock-down was only achieved for the more concentrated siGSK3β (**p<0.01), and in contrast to the individual siRNA components alone (demonstrated in Figures 4.9 and 5.7), the combination siRNA treatment did not improve RGC survival or neurite outgrowth parameters compared to controls.

5.5.11.2 Combined siGSK3β (25nM) + siRTP801 (25nM) enabled dual target knock-down, was RGC neuroprotective and promoted neurite outgrowth initiation and elongation in vitro

In order to prevent competition between the two siRNA in the combination, and to avoid a potentially toxic effect of higher total siRNA load, further experiments were undertaken using a combination of 25nM siGSK3β + 25nM siRTP801 (Figure 5.16). Compared to incubation with sNBA alone (321.1±32.3 RGC/well) and transfection with 50nM siEGFP (273.5 ± 22.5 RGC), the combination of 25nM siGSK3β + 25nM siRTP801 promoted significantly more RGC survival (525.1 ± 39.7; $p<0.01$), albeit without an additive survival response (Figure 5.16C). Furthermore, this siRNA combination increased both the proportion of neurite-bearing RGC (33.5 ± 2.7%, compared to 21.6 ± 2.7% and 22.1 ± 2.9% for culture medium alone and siEGFP controls, respectively; $p<0.05$) (Figure 5.16D) and the mean length of longest neurite growth (79 ± 9µm, compared to 48 ± 4µm and 54 ± 7µm for the same controls as described; $p<0.05$) (Figure 5.16E). There was no evidence of an additive or synergistic effect of this siRNA combination on neurite outgrowth. Immunocytochemical evaluation of RGC expression of the siRNA target proteins demonstrated that the combined 25nM siGSK3β + 25nM siRTP801 enabled significant knock-down of both targets. GSK3β detection in RGC was reduced from 100% in control wells to 59.2 ± 5.6%, representing 40.8% knock-down, and RGC detection of RTP801 was reduced from 86.4 ± 3.2% and 91.6 ± 4.3% in culture medium and siEGFP controls, respectively, to 60.1 ± 4.3%, representing knock-down of 30.4 – 34.4% (Figure 5.16F). These data indicated that combined treatment with 25nM each of siGSK3β and siRTP801 enabled a degree of knock-down of both targets, resulting in enhanced RGC survival, neurite outgrowth initiation and neurite elongation compared to controls.

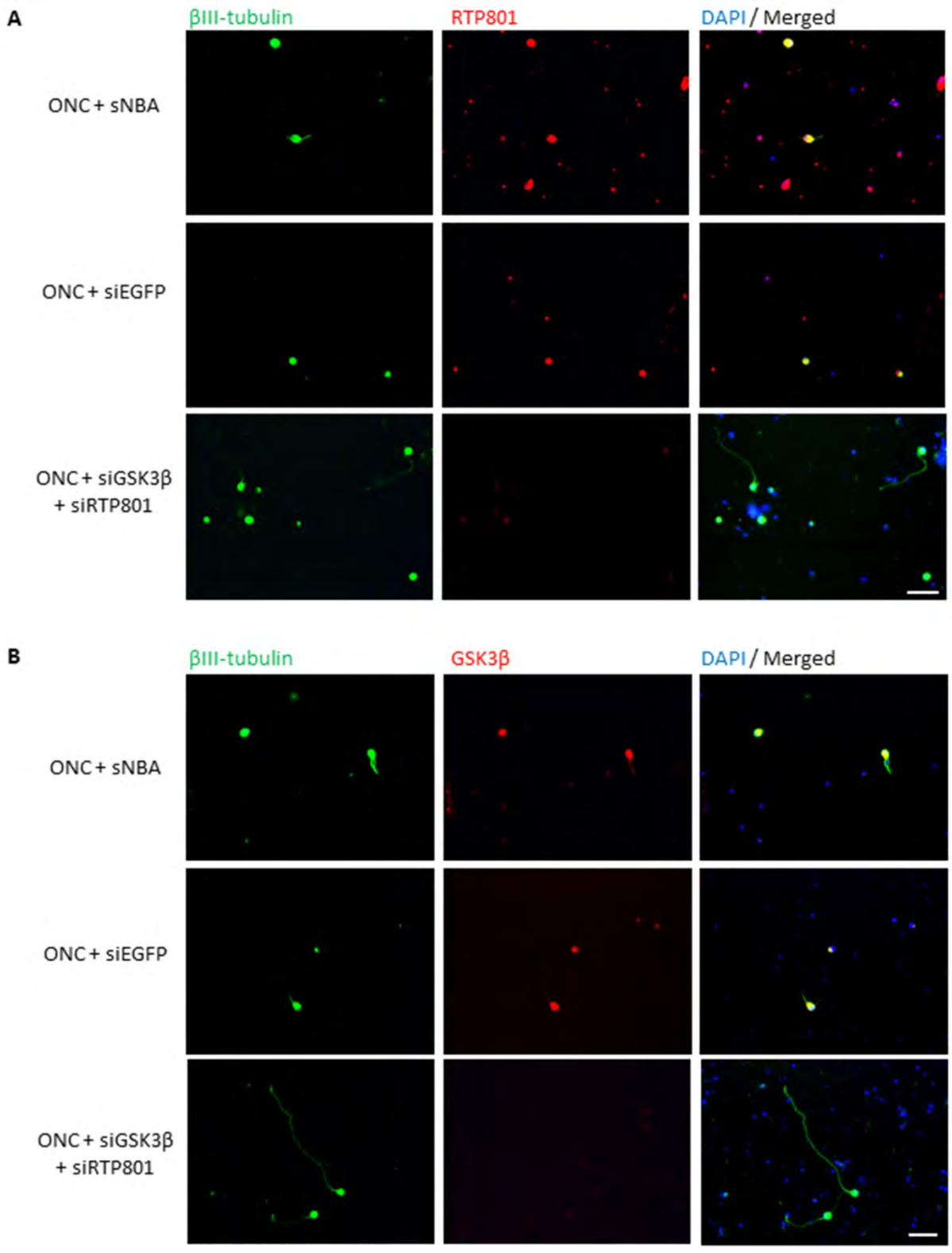


Figure 5.16: Effects of combined siGSK3β (25nM) and siRTP801 (25nM) RGC survival, neurite outgrowth and target knock-down in cultured retinal cells. (A, B) Glial activated retinal cultures incubated for 3d with sNBA, siEGFP (50nM) and combination siGSK3β (25nM)/siRTP801 (25nM) were immunostained for βIII-tubulin (green) and RTP801 (A; red) and GSK3β (B; red), with DAPI (blue) as a nuclear counterstain (scale bar = 20µm). Figure and legend continues on the next page.

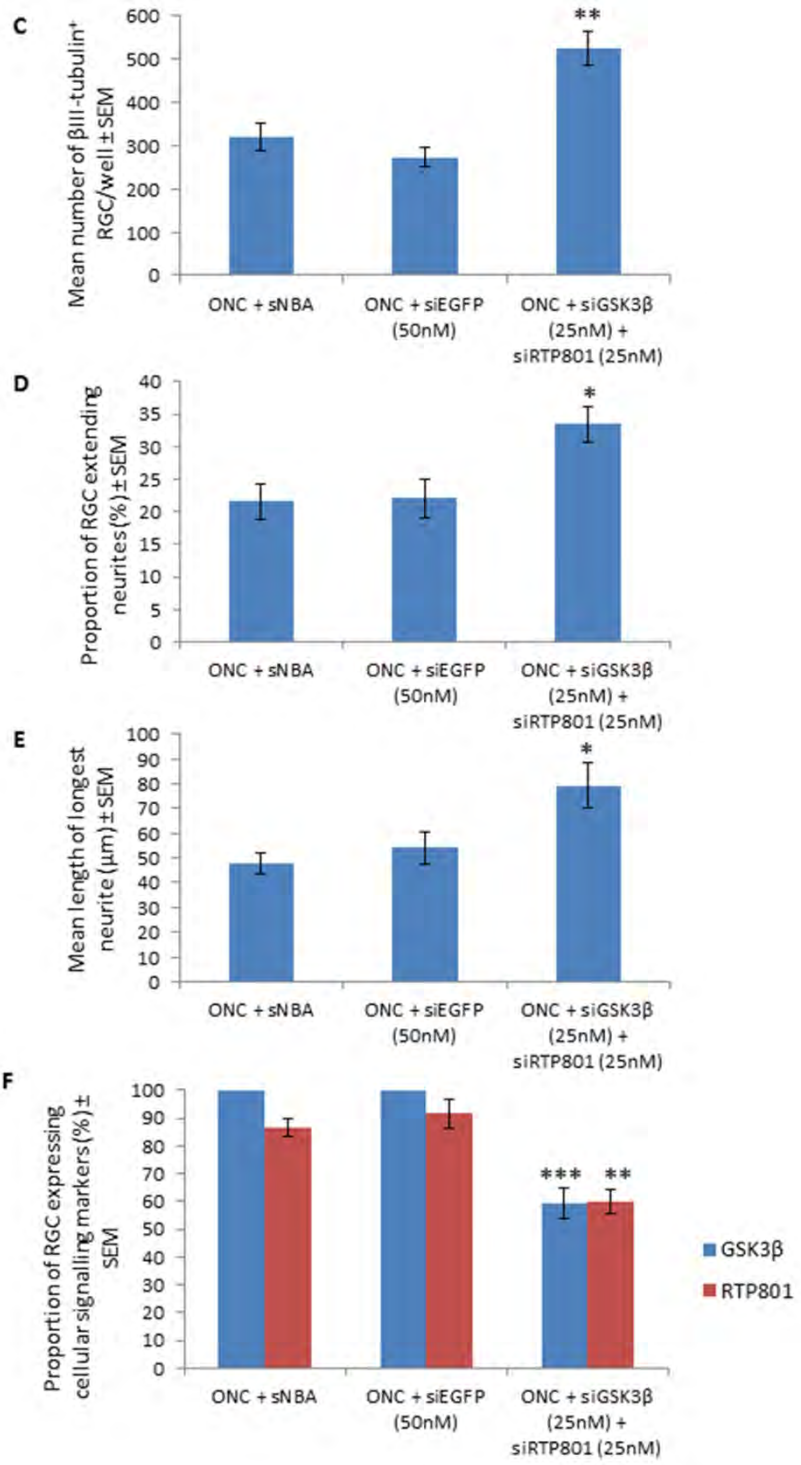


Figure 5.16: Effects of combined siGSK3β (25nM) and siRTP801 (25nM) RGC survival, neurite outgrowth and target knock-down in cultured retinal cells. Continued from the previous page. Quantification of (C) βIII-tubulin$^+$ RGC survival, (D) proportion of βIII-tubulin$^+$ RGC bearing neurites, (E) length of longest RGC neurite, and (F) proportion of βIII-tubulin$^+$ RGC demonstrating positivity for GSK3β (blue bars) and RTP801 (red bars), in cultures described in (A) and (B). Note that in contrast to the 50nM/20nM combination, this 25nM/25nM siGSK3β/siRTP801 combination promoted dual target knock-down in RGC as well as RGC survival, neurite outgrowth initiation and elongation compared to controls (n=3; *p<0.05, *p<0.01, *p<0.001 *vs* sNBA control).

5.5.12 Effects of combined siGSK3β/siRTP801 on RGC survival and axon regeneration after ONC *in vivo*

5.5.12.1 Effects of combined siGSK3β/siRTP801 treatment on RGC survival after ONC in vivo

The effects of siGSK3β on RGC survival after ONC *in vivo* have been described in Section 5.5.5.1 (Figure 5.5). At 24d after ONC, intravitreal treatment with a combination of both siGSK3b + siRTP801 resulted in $Brn3a^+$ RGC survival of 16.0±0.5 RGC/250µm GCL which, while enabling significantly greater RGC neuroprotection than either PBS or siEGFP after ONC ($p<0.01$), was not significantly different from either of the component siRNAs when administered as single agent therapies, and survival was still significantly below the level of uninjured intact animals (Figure 5.17).

5.5.12.2 Effects of combined siGSK3β/siRTP801 treatment on axon regeneration after ONC in vivo

The effects of siGSK3β on RGC axon regeneration after ONC *in vivo* have been described in Section 5.5.5.2 (Figure 5.6) and effects of siRTP801 are described in Chapter 3. Whereas both siRTP801 and siGSK3β as individual agents did not promote significant axon sprouting adjacent to the lesion site in the distal ON, the combination treatment resulted in a significant increase in the number of $GAP43^+$ regenerating axons compared to PBS, siEGFP and siGSK3β treatments at 100µm (179.5 ± 23.9 axons; $p<0.05$), 200µm (154.3 ± 16.7 axons; $p<0.05$), 400µm (126.8 ± 11.6 axons; $p<0.01$), 800µm (109.2 ± 9.4 axons; $p<0.001$) and 1200µm (81.0 ± 8.1 axons; $p<0.001$) distal to the ONC site (Figure 5.18). There were more $GAP43^+$ regenerating RGC axons than after siRTP801 treatment alone at each of the distances along the ON, although the differences only reached statistical significance at 800µm ($p<0.05$). These results suggested that the combination of siGSK3β + siRTP801 was superior to

siGSK3β alone as an axogenic intervention after ONC, promoting both axon sprouting and longer distance axon regeneration and that, while siRTP801 was probably the major axon-growth-promoting component of the combination treatment, there was a trend toward an additive regenerative effect, particularly beyond 800µm from the ONC site.

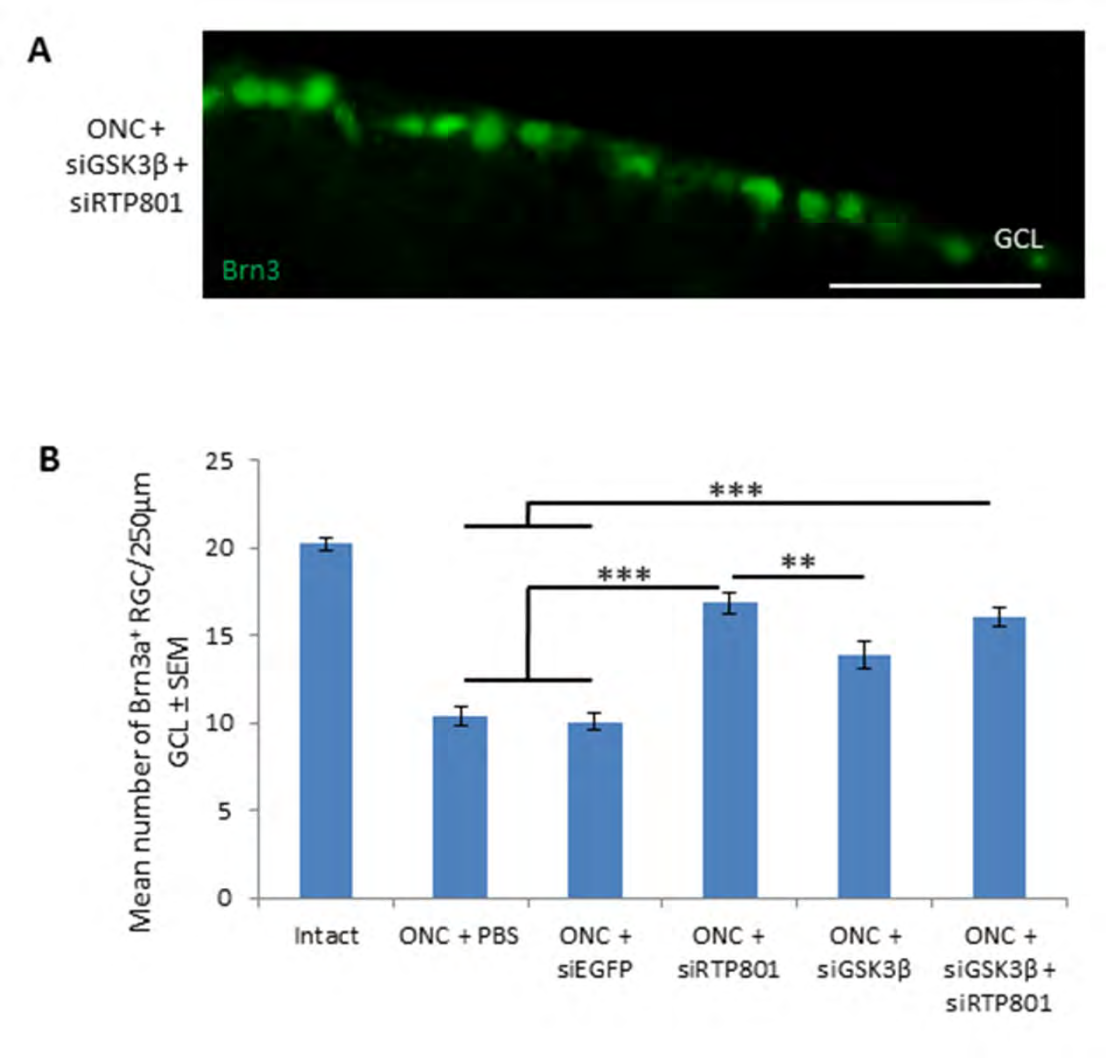


Figure 5.17: Effect of combined siGSK3β/siRTP801 treatment on Brn3a$^+$ RGC survival after ONC *in vivo.* (A) Section of the retinal GCL immunostained for Brn3a (green) 24d after ONC + siGSK3β/siRTP801 combined treatment (scale bar = 100µm). (B) Quantification of surviving Brn3a$^+$ RGC in a 250µm GCL sample in sections from intact, uninjured retinae and 24d after ONC + PBS, ONC + siEGFP, ONC + siGSK3β (data from Figure 5.5) and ONC + siRTP801 (data from Chapter 3), indicating enhanced RGC survival after siGSK3β/siRTP801 combination treatment compared to PBS- and siEGFP-injected control eyes, but no additional neuroprotective effect compared to either component siRNA (n=6 retinae/group [n=5 for intacts and siRTP801]; **p<0.01, ***p<0.001).

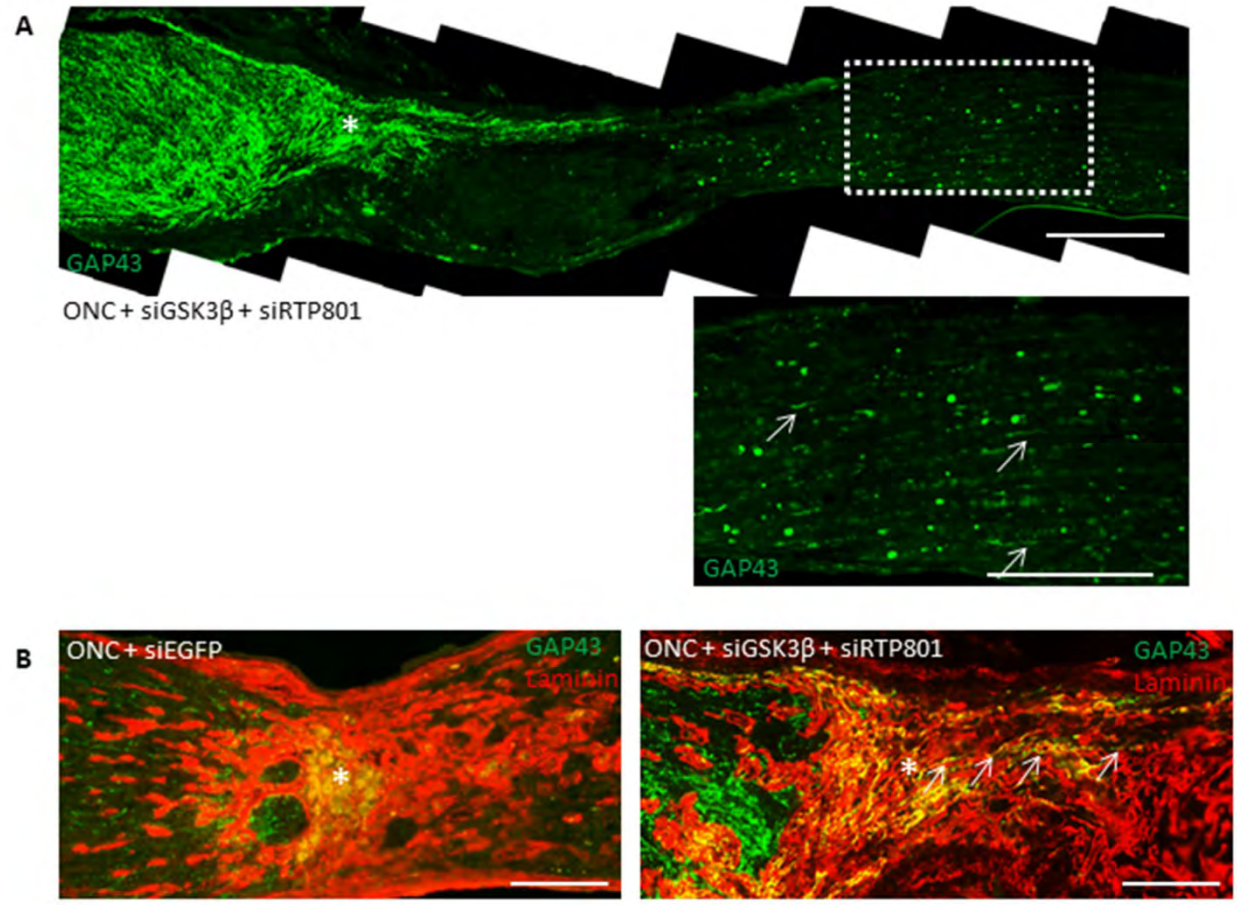


Figure 5.18: Effect of combined siGSK3β/siRTP801 treatment on GAP43$^+$ axon regeneration after ONC *in vivo.* (A) Longitudinal ON section immunostained to demonstrate GAP43$^+$ regenerating axons (arrows) 24d after ONC + siGSK3β/siRTP801 combined treatment (scale bar = 200µm). The asterisk demarcates the ON site and the boxed area represents the magnified area below. (B) High magnification of longitudinal ON sections immunostained for GAP43 (green) and laminin (red) 24d after ONC + siEGFP (left panel) and ONC + siGSK3β/siRTP801 combined treatment (right panel), demonstrating presence of laminin$^+$ scar tissue at the ONC site (*) and GAP43$^+$ axons regenerating through the scar after combined siRNA treatment (arrows) (scale bar = 100µm). Figure and legend continues on the next page.

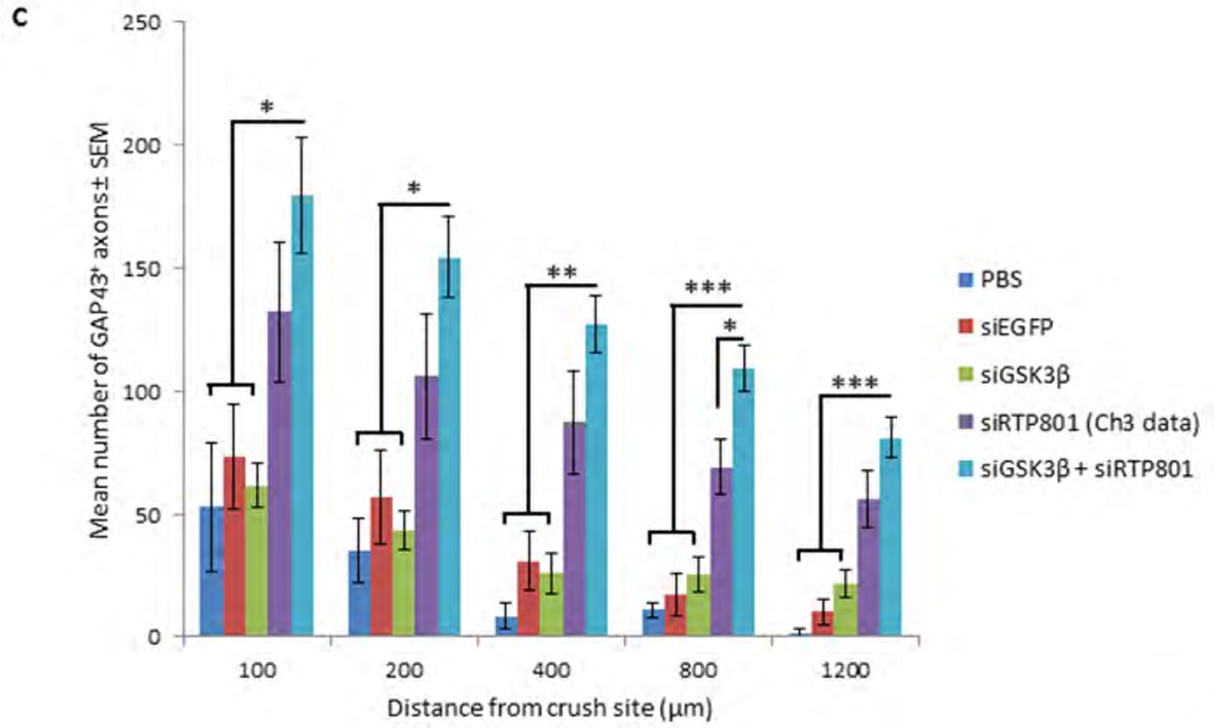


Figure 5.18: Effect of combined siGSK3β/siRTP801 treatment on GAP43$^+$ axon regeneration after ONC *in vivo*. Continued from previous page. (C) Quantification of GAP43$^+$ regenerating axons 100, 200, 400, 800 and 1200µm beyond the ONC site after intravitreal injection of PBS (blue bars), siEGFP (red bars), siGSK3β (green bars), siRTP801 (purple bars; data from Chapter 3) and combination siGSK3β/siRTP801 (light blue bars). Note the increased number of GAP43$^+$ regenerating axons after combination siRNA treatment at each of the measured distances in the distal ON (n=6 nerves/group [n=5 for siRTP801]; *p<0.05, **p<0.01, ***p<0.001).

5.5.13 Summary of results

These results demonstrated that GSK3β inhibition was directly RGC neuroprotective both *in vitro* and after ONC *in vivo*. GSK3β inhibition promoted initiation of neurite outgrowth *in vitro* and promoted neurite elongation, the latter only in the presence of activated retinal glia. After ONC, siGSK3β did not affect initial axon sprouting but supported elongation of GAP43$^+$ regenerating axons in the distal ON. The RGC neuroprotective effect of siGSK3β was mTORC1 dependent, probably mediated *via* the

mTORC1 substrate 4E-BP1, but the neurite growth effects were mTORC1 independent. siGSK3β did not affect the reactive glial response after ONC. The RGC neuroprotective and neurite growth promoting effects of siGSK3β were not associated with significant changes in RGC positivity for pGSK3β, pCRMP2, pSmad1 or pMAP1B, but inhibition of GSK3β reversed the neurite outgrowth inhibitory effects of Nogo-P4 peptide. Combined treatment with siRTP801 + siGSK3β was RGC neuroprotective *in vitro* and *in vivo*, and promoted neurite outgrowth initiation and elongation *in vitro*, without additive effect compared to the individual components alone. The combination siRNA treatment resulted in enhanced axon regeneration at 100-1200μm in the distal ON after ONC compared to each of the individual component siRNA treatments.

5.6 DISCUSSION

Closely linked to PI3K signalling, GSK3β is considered an important regulator of many cellular processes, including neuronal viability, cytoskeletal integrity and axonal growth cone dynamics (Hur and Zhou, 2010; Seira and Del Rio, 2014). With its site of action upstream of the RTP801-mTORC1/2 interactions, it was hypothesised that suppression of GSK3β activity would be associated with enhanced RGC survival and axon/neurite growth and that, in combination with siRTP801, GSK3β inhibition would further optimise the balance of cellular signalling to potentiate these neurotrophic effects compared to either manipulation alone. The major findings were that: (1) suppression of GSK3β with the pharmacological inhibitor Chir99021 and a targeted siRNA was RGC neuroprotective and promoted initiation of neurite outgrowth, but did not affect neurite elongation in the absence of activated retinal glia *in vitro*; (2) in the presence of activated retinal glia *in vitro*, siGSK3β also enhanced neurite elongation; (3) the neuroprotective effect of siGSK3β was mTORC1-dependent, but the neurite outgrowth effects were mTORC1-independent; (4) siGSK3β was RGC neuroprotective and promoted limited but significant axon elongation after ONC *in vivo*; (5) siGSK3β did not significantly

affect the retinal glial response to injury; (6) siGSK3β did not significantly affect the RGC levels of pGSK3β, pCRMP2, pSmad1, or pMAP1B *in vitro*; (7) GSK3β inhibition with either siGSK3β or Chir99021 counteracted the RGC neurite outgrowth-inhibitory effects of the CNS myelin-derived inhibitory ligand Nogo; (8) combined treatment with siGSK3β + siRTP801 was RGC neuroprotective and promoted both neurite outgrowth initiation and elongation in the presence of activated retinal glia *in vitro*, although without additive or synergistic effects; (9) combined treatment with siGSK3β + siRTP801 was RGC neuroprotective after ONC *in vivo*, although without additive or synergistic effects compared to either treatment alone; and (10) combined treatment with siGSK3β + siRTP801 enhanced the number and length of regenerating axons compared to either treatment alone, with siRTP801 as the major contributor to the axon regenerative effect.

5.6.1 GSK3β and neuroprotection

A major finding was that GSK3β inhibition was RGC neuroprotective after treatment with Chir99021 *in vitro*, siGSK3β *in vitro* and after ONC *in vivo*. The RGC neuroprotection effect of Chir99021 *in vitro* in the absence of activated glia was concentration-dependent, albeit with a toxic effect at the highest concentrations, which may reflect that deep GSK3β suppression itself induced neuronal death, but more likely that a general toxic effect was induced by the pharmacological agent at higher concentration, due to more global 'off-target' kinase inhibition (Eldar-Finkelman and Martinez, 2011). Treatment with siGSK3β was also RGC neuroprotective, with the dose-response assay performed in the absence of activated retinal glia indicating that a siRNA concentration of 50nM was the optimum for RGC neuroprotection, corresponding to approximately 50% knock-down. Higher concentrations of targeted siRNA were associated with less GSK3β knock-down and reduced RGC survival compared to untransfected controls, and equivalent RGC survival to control siRNA, suggesting a neurotoxic effect of the greater siRNA load, rather than a result of more complete

inhibition of GSK3β. At 24d after ONC *in vivo*, intravitreal siGSK3β had a modest, but significant RGC neuroprotective effect, with almost 70% RGC survival compared to only 50-55% in controls. The presence of activated retinal glia did not enhance the pro-survival effect of siGSK3β *in vitro* which, coupled with the lack of a demonstrable effect of siGSK3β on the retinal glial response to injury, suggested that GSK3β knock-down had a direct, intrinsic effect on RGC to enhance survival in this model, as seen with siRTP801 (Chapters 3 & 4). The neuroprotective effect of siGSK3β was significantly reduced in the presence of Rapamycin, indicating that siGSK3β induced RGC survival predominantly *via* an mTORC1-dependent mechanism. Furthermore, the finding that siGSK3β did not significantly alter the proportion of $pS6^+$ RGC implicated the other mTORC1-dependent substrate, 4E-BP1, as the major underlying mediator of the effects on RGC survival.

Phosphorylation of 4E-BP1 by mTORC1 releases the inhibitory effect of the former on protein translation, and thus enables protein synthesis to proceed (Gingras *et al.*, 1998) (Figure 1.7). The notion that GSK3β inhibition may contribute to RGC survival through this pathway supports a recent report demonstrating a modest but significant increase in RGC survival after ONC in 4E-BP knock-out mice (Yang *et al.*, 2014), and is consistent with a model in which, in the absence of any other stimulation of the PI3K/Akt/mTOR pathway (e.g. by NTF), suppression of GSK3β is sufficient to upregulate mTORC1 signalling (probably by reducing GSK3β action on TSC1/2, see Figures 1.7 and 5.1). However, enhanced mTORC1 activity after GSK3β inhibition might be expected to increase activity of both mTORC1 substrates, although an increase in $pS6^+$ RGC was not found. Possible explanations could include the weighting of mTORC1 output toward 4E-BP1 rather than pS6 after GSK3β inhibition, or there may be a direct link between GSK3β and 4E-BP1, as recently demonstrated in a cancer cell line (Shin *et al.*, 2014). Considering ipRGC sub-types and the preferential survival tendency of αRGC, which account for the majority of $pS6^+$ RGC (Duan *et al.*, 2015), the enhanced RGC

survival induced by GSK3β inhibition may reflect survival of a different non-ipRGC sub-type responsive to alterations in 4E-BP1 activity, or other GSK3β substrates.

Despite a paucity of comparable studies to evaluate the role of GSK3β signalling in relation to RGC survival, there is a large body of evidence linking GSK to a regulatory role in cell death, including the induction of caspase-3 activation (King *et al.*, 2001), activation of the pro-apoptotic p53 tumour suppressor gene (Turenne and Price, 2001) and Bax (Somervaille *et al.*, 2001). Using an *in vitro* model, Loberg *et al.* (2002) demonstrated that hypoxia-induced cell death was associated with a decrease in (activated) pAkt and ('inactivated') pGSK3β, an increase in overall GSK3β kinase activity, and that incubation with two specific GSK3β inhibitors reduced both the hypoxia-induced apoptosis and the induction of caspases-3 and -9. Although undertaken using non-neuronal (Cos-7) cells *in vitro*, and not considering possible downstream mTOR effects, the Loberg *et al*. study implicates GSK3β as an important mediator of cellular stress-induced cell death, and is consistent with the neuroprotective response of RGC to GSK3β inhibition with Chir99021 and siGSK3β *in vitro* and with siGSK3β after ONC *in vivo*. Lithium is known to be a potent GSK3β inhibitor, acting primarily *via* the PI3K/Akt pathway to increase 'inhibitory' GSK3β-S9 phosphorylation and decrease GSK3β-T216 'activation' phosphorylation (Mills *et al.*, 2011). Treatment with lithium protects against several neuronal insults (Nonaka *et al.*, 1998; Cimarosti *et al.*, 2001), including axotomy in RGC (Wu *et al.*, 2014), although some of these findings are circumstantial, rather than directly attributing the effect to GSK3β inhibition, and may reflect enhanced mTOR activity downstream of Akt or effects of lithium on other kinases and phosphatases (Kirshenboim *et al.*, 2004; Zhen *et al.*, 2002).

It is reported that GSK3β activity alone is sufficient to induce apoptosis, including in the nervous system, where genetic overexpression of GSK3β is associated with apoptosis in the PC12 neuronal cell line, plus primary cortical neurons and sympathetic neurons (Pap and Cooper, 1998; Hetman *et*

al., 2000; Crowder and Freeman, 2000). While these studies certainly imply a role for GSK3β as an inducer of neuronal apoptosis, it is likely that genetic over-expression of GSK3β increases its activity to a level significantly higher than that attained after cellular stress-induced GSK3β activity, and thus may influence a different set of substrates than would normally be modulated by changes in endogenous GSK3β levels, and therefore not reflect pathophysiological conditions. Transfection with targeted GSK3β siRNA is robustly neuroprotective against glutamate-induced NMDA-receptor-mediated toxicity in cerebral cortical neurons (Liang and Chuang, 2007; Chuang *et al.*, 2011) and shGSK3β suppresses the up-regulation of pro-apoptotic Drp1 in the retina in response to raised IOP (Wu *et al.*, 2013). Thus, GSK3β is heavily implicated as a key mediator of cell death and the current RGC neuroprotective effects of GSK3β suppression are in keeping with previous studies, including in the CNS.

Other studies investigating the role of GSK in cellular viability have yielded conflicting and often paradoxical results, with some reports suggesting GSK3β inhibits apoptosis, and some indicating the opposite, although a recent review has endeavoured to rationalise the evidence and suggests that the effects of GSK3β in regulating cell death and survival may depend upon whether the intrinsic or extrinsic pathway of apoptosis is the primary trigger (Beurel and Jope, 2006). The intrinsic apoptosis pathway is initiated in response to a diverse range of cellular stressors including growth factor restriction, oxidative stress, and DNA damage, amongst others, and is exacerbated by the activity of GSK3β (Beurel and Jope, 2006; Jacobs *et al.*, 2012). The intrinsic pathway results in mitochondrial failure *via* the pro-apoptotic Bax, which undergoes a conformational change in response to cellular insults and subsequent translocation from the cytosol to mitochondrial membranes to release apoptotic proteins such as cytochrome C (Beurel and Jope, 2006; Armstrong, 2006). In addition to acting as a key regulator of mitochondrial function after cell stressors, GSK3β also modulates other apoptotic proteins and regulators of cellular structure, including: (1) stabilisation of the tumour

suppressor transcription factor p53 after DNA damage to induce apoptosis; (2) phosphorylation of the pro-survival transcription factor β-catenin to induce its degradation; (3) inhibition of the cell-stress-induced neuroprotective heat shock factor-1; (4) modulation of the transcription factors Myc and nuclear factor-κB (NF-κB) to promote apoptosis; and (5) destabilisation of microtubule-associated proteins (Beurel and Jope, 2006), although the latter may play a larger role in regulating axon growth than neuronal survival (see later).

Interestingly, in addition to the evidence that GSK3β is a key pro-apoptotic regulator, supporting a role for GSK3β inhibition in neuroprotection, some studies indicate that GSK3β activity protects against cell death under certain conditions. For example, activation of the extrinsic pathway of apoptosis by TNFα is potentiated by GSK3β knock-out or treatment with the GSK3β inhibitor lithium in non-neuronal paradigms (Hoeflich *et al.*, 2000; Schwabe and Brenner, 2002). The protective effect of GSK3β has been linked to other 'death receptors', such as Fas in mature hippocampal neurons (Song *et al.*, 2004; Beurel and Jope, 2006). It is increasingly clear that GSK3β does not simply have a role in either promoting or inhibiting apoptosis, but rather has opposite effects on the intrinsic and extrinsic apoptotic pathways, promoting the former but inhibiting the latter, and thus this dual-regulatory model places GSK3β as an exquisitely sensitive nodal point for integrating cell signals and setting the threshold for cell viability. In healthy cells, it is likely that the balance of cellular inputs maintains GSK3β activity within a tolerable range that favours an anti-apoptotic signal whereas, in conditions of cellular stress such as axonal injury, deprivation of NTF, hypoxia or oxidative stress, the balance of GSK3β substrate activity is altered to enable intrinsic pathway-activated apoptosis to proceed (Beurel and Jope, 2006).

In summary, the present results indicated that GSK3β inhibition was RGC neuroprotective, both *in vitro*, where the effect was robust, and also after ONC *in vivo*, where the effect was significant, yet

limited, probably reflecting the presence of multiple other signalling complexes including glial- and scar-derived factors. The *in vitro* data supports the notion that GSK3β activity directly contributes to cell death after injury, possibly by suppressing downstream mTORC1 activity, and that knock-down of GSK3β enhances RGC viability, at least in part by disinhibiting the mTORC1/4E-BP1 axis.

5.6.2 GSK3β and axon regeneration

In addition to regulating neuronal survival and the threshold for apoptosis in response to different stimuli, GSK3β is considered a key factor in the co-ordination of axon growth by altering the phosphorylation state of multiple substrates associated with microtubule dynamics, as a mediator of growth cone collapse induced by CNS myelin- and scar-derived factors, and as a transcriptional regulator of growth-associated factors (Seira and Del Rio, 2014; Hur and Zhou, 2010) (Figure 5.1).

In terms of neurite growth *in vitro*, both Chir99021 and siGSK3β had similar effects in culture in the absence of activated retinal glia, inducing more RGC to sprout neurites, but without a significant effect on neurite elongation. As with the neuroprotection effects discussed above, the neurite growth-inducing effects of GSK3β suppression were abolished at higher concentrations of both agents which, in the case of Chir99021, may reflect a growth inhibitory effect or off-target effects on other kinases at higher concentrations. In the case of the siGSK3β, where increasing siRNA concentration above 50nM was not associated with greater target knock-down, it was likely to reflect neurotoxicity of the greater siRNA load (Read *et al.*, 2009; Suggate *et al.*, 2009). In retinal cultures in the presence of activated retinal glia (5d after ONC *in vivo*), siGSK3β had the additional effect of promoting the growth of longer RGC neurites. Thus, GSK3β inhibition appeared to have a direct intrinsic RGC effect on the initial sprouting of neurites *in vitro*, and in the presence of activated retinal glia also enabled longer neurite outgrowth. Immunofluorescent detection of GSK3β was

limited to neurons with no detectable localisation in glia, either *in vivo* or *in vitro*, and siGSK3β did not significantly affect the glial response to ONC (in contrast to siRTP801, as discussed in Chapter 4). This suggested that the siGSK3β-induced neurite elongation was due to 'priming' of RGC by glial-derived NTF, acting to up-regulate PI3K/Akt signalling, thereby rendering them more responsive to subsequent further GSK3β suppression and enabling neurite extension with stabilised axonal growth cones, rather than as a result of glial modulation by siGSK3β. However, the *in vivo* findings did not mirror the culture studies. After ONC, siGSK3β did not have a significant positive effect on the number of $GAP43^{+}$ regenerating axons sprouting beyond the ONC site into the distal ON compared to controls, yet significantly increased the number of regenerating axons more distally (800-1200μm) beyond the ONC site, suggesting that GSK3β suppression promoted axonal elongation rather than the initiation of axon regeneration after injury. The apparent disparity of axon/neurite growth initiation after siGSK3β *in vitro* and *in vivo* (enhanced in the former, no effect in the latter) is likely to reflect the presence of multiple cell types and factors present in the injured retina and ON that are incompletely represented in the culture model. GSK3β is associated with the transcriptional control of axon growth *via* regulation of transcription factors such as NFAT, CREB and β-catenin (Hur and Zhou, 2010). *In vitro*, GSK3β down-regulation may increase the transcription of growth-related genes sufficient to induce neurite outgrowth, enhanced and maintained by glial-derived NTF, which are known to influence gene transcription in part *via* CREB (Lonze and Ginty, 2002; Lonze *et al.*, 2002). After ONC, modulation of growth-related gene transcription may be insufficient to induce significant axon regenerative sprouting after siGSK3β treatment in the absence of additional growth stimulation. Moreover, although GSK3β inhibition may act partly to overcome Nogo-dependent growth inhibition (see later), the inhibitory milieu after ONC is more complex, with siGSK3β-treated RGC unable to overcome external inhibition and mount a significant regenerative sprouting response but being more effective at supporting the extension of axons initiated by other factors, such as glial-derived NTF, as suggested by the culture studies.

Several previous studies have implicated modulation of GSK3β activity in axonal regeneration after injury, although there is very little evidence relating to RGC and there is some controversy in the literature as to the precise roles and mechanisms underlying GSK3β effects on axon growth. In keeping with the finding that both Chir99021 and siGSK3β promoted initiation of neurite outgrowth in culture in the absence of glial factors *in vitro*, Dill *et al.* (2008) demonstrated that two different GSK3β inhibitors enhanced the proportion of cultured DRG neurons with axons and also axon length, suggesting a degree of enhancement of inherent axon growth capacity, attributed to the transcriptional up-regulation of growth-associated genes (Zhou and Snider, 2006). As mentioned, elongation of neurite growth by siGSK3β was only evident in the presence of activated retinal glia, indicating that GSK3β inhibition may have a role in mediating axonal growth in response to glial-derived factors. It has been shown that the neurotrophin NGF mediates DRG axon growth *via* GSK3β inhibition localised to the tip of the growing axon (Zhou *et al.*, 2004). In response to NGF, levels of 'inactive' pGSK3β are concentrated at the growing axon tip in a PI3K-dependent manner, and significantly shorter axon growth is observed in the presence of mutant GSK3β that is unable to be phosphorylated on Ser9, suggesting that activation of the NGF-PI3K-Akt axis, with subsequent GSK3β inhibition, was required for axon growth (Zhou *et al.*, 2004). This mechanism provides a possible explanation for the siGSK3β-induced neurite elongation only observed in the presence of activated glia and the axon elongation effect seen *in vivo*, relying on glial-derived NTF activating PI3K-Akt signalling, with siGSK3β further reducing GSK3β activity to stabilise growth cones and enable neurite/axon extension to progress. In the absence of glial-derived NTF, suppression of baseline GSK3β activity may be sufficient to initiate axon growth *in vitro* on a permissive laminin substrate, but insufficient to maintain extension of axonal growth without NTF driving further PI3K-dependent signalling and inducing regulated intramembranous proteolysis (RIP) of the $p75^{NTR}$ to disinhibit axon growth (Ahmed *et al.*, 2005; Ahmed *et al.*, 2006; Berry *et al.*, 2008). Moreover, GSK3β down-regulation may contribute to the mTORC1-independent neurite growth after siRTP801 (*via* mTORC2-

Akt feedback, as discussed in Chapter 4). Inactivation of GSK3β also promotes axonal growth after PN injury (Saijilafu *et al.*, 2013; Su *et al.*, 2014), and underlies DRG axon regeneration in the injured spinal cord after a conditioning lesion (Liz *et al.*, 2014).

5.6.3 Mechanisms of siGSK3β-induced axon growth

The difficulty of ascribing a precise role for GSK3β in axon regeneration probably reflects the diverse range of GSK3β substrates. The *in vitro* experiments described in this Chapter were designed to investigate possible mechanisms underlying the RGC axon growth effects seen after GSK3β knock-down. Unlike the direct RGC neuroprotective effect of siGSK3β, which was primarily mTORC1-dependent, both the RGC neurite outgrowth initiation and elongation induced by siGSK3β in the presence of activated retinal glia were unaffected by Rapamycin, indicating that they were mTORC1-independent. Treatment of retinal cultures with siGSK3β led to a small increase in RGC expressing pGSK3β(Ser9), considered to be the 'inactive' form after phosphorylation by Akt, although the increase did not reach statistical significance. Furthermore, levels of pCRMP2, pSmad1 and pMAP1B were not significantly affected by siGSK3β treatment, indicating that these substrates were not contributors to siGSK3β-induced neurite growth.

Activation of PI3K/Akt signalling regulates GSK3β activity, through Akt mediated Ser9 phosphorylation of GSK3β leading to subsequent inactivation (Cross *et al.*, 1995). However, in rodents carrying mutated GSK3β that cannot be phosphorylated, animals develop normally into adulthood without an overt CNS phenotype (McManus *et al.*, 2005), suggesting that this Akt-induced phosphorylation step is not the sole determinant or indicator of GSK3β activity. Moreover, GSK3β activity is facilitated by Tyr216 phosphorylation, although regulation through this mechanism is thought to be independent of external stimuli and to occur by auto-phosphorylation or post-

translational modification (Hur and Zhou, 2010; Hughes *et al.*, 1993). Studies investigating the role of GSK3β in axonal regeneration have attempted to shed light on mechanisms by measuring levels of known GSK3β substrates. In a recent study, a marked increase in pGSK3β(Ser9) and concomitant decrease in pCRMP2 were reported after sciatic nerve transection, and GSK3β inhibitors were able to rescue axon growth repression induced by a PI3K-inhibitor (Saijilafu *et al.*, 2013). The PN regenerative effect was attributed to regulation of the transcription factor Smad1 through a mechanism distinct from the well-described Smad1 regulation by bone morphogenic protein (Saijilafu *et al.*, 2013; Ueki and Reh, 2012; Zhong and Zou, 2014). In contrast, the RGC neurite growth promoted here by siGSK3β treatment was not associated with changes in RGC expression either of pCRMP2 or pSmad1, indicating different downstream substrates between the two different experimental paradigms. Using a conditioning PN lesion DRG model, Liz and colleagues reported an increase in pAkt and pGSK3β(Ser9) and a concomitant decrease in pGSK3β(Tyr216) in DRG neurons, corresponding to an overall decrease in GSK3β activity (Liz *et al.*, 2014). The enhanced DRG axonal growth in the conditioning lesion paradigm was associated with increased growth cone microtubule dynamics and correlated more closely with a decrease in pGSK3β(Tyr216) than increased pGSK3β(Ser9) suggesting that, although overall reduced GSK3β activity promoted axonal regeneration, the degree of Akt-dependent Ser9-phosphorylation was not a critical factor. Consistent with findings in the PNS (Saijilafu *et al.*, 2013), a reduction in pCRMP2 is associated with the enhanced neurite growth in DRG neurons after a conditioning lesion (Liz *et al.*, 2014). Unphosphorylated CRMP2 promotes microtubule assembly in axonal growth cones, contributing to axonal elongation, an effect which is reduced by GSK3β-dependent phosphorylation (Figure 5.1B) (Yoshimura *et al.*, 2005). Inactivation of GSK3β, with consequent reduction of pCRMP2, appears to be a major mechanism in DRG axonal regeneration studies (Liz *et al.*, 2014), but the evidence from experiments in this Chapter suggests that this is not the case in the RGC model.

In contrast to CRMP2, which is phosphorylated and inactivated by GSK3β in a RhoA/ROCK-dependent manner (Mimura *et al.*, 2006), microtubule associated protein 1B (MAP1B) is activated in response to GSK3β-dependent phosphorylation, leading to polymerisation of axonal growth cone microtubules and growth cone advancement (Figure 5.1B) (Hur and Zhou, 2010; Trivedi *et al.*, 2005). Indeed, this GSK3β substrate is a possible factor underpinning reports that GSK3β activity promotes axonal growth (Goold *et al.*, 1999; Trivedi *et al.*, 2005; Owen and Gordon-Weeks, 2003), which appears contradictory to the plethora of evidence supporting the assertion that GSK3β inhibition supports axon regeneration. Inhibition of GSK3β would therefore be expected to lead to reduced pMAP1B, with a consequent reduction in axonal growth, and this has been demonstrated with pharmacological inhibition of GSK3β in embryonic chick sensory neurons (Owen and Gordon-Weeks, 2003). After treatment of retinal cultures with siGSK3β, there was no significant decrease in the proportion of RGC expressing pMAP1B, indicating that alterations in pMAP1B are not the major substrate for siGSK3β-induced neurite growth in RGC. Consistently, enhanced axonal regeneration after spinal cord injury in GSK3β deleted neurons in adult rodents was also found to be independent of MAP1B activity (Liz *et al.*, 2014), thus the importance of MAP1B as a GSK3β substrate in axon growth may be more relevant in initial axonal polarisation and growth in embryonic development rather than regenerative growth in the adult CNS after injury. Nonetheless, this reinforces the complexities of GSK3β actions on its multiple substrates for regulating axon growth and the difficulty in comparing results between very different experimental paradigms.

The activity of GSK3β and subsequent modulation of microtubule dynamics is thought to contribute to axonal growth collapse in response to CNS myelin-derived and scar-derived inhibitory factors, activity of which may contribute to regenerative failure of RGC axons in the ON after injury (Eickholt *et al.*, 2002; Tan *et al.*, 2011). To investigate whether GSK3β suppression would enable RGC axons to counteract the presence of an extrinsic inhibitory ligand, retinal culture studies were undertaken in

the presence of Nogo-P4 inhibitory peptide, the active inhibitory segment of NogoA protein (Wang and Zhu, 2008; GrandPre *et al.*, 2000). This inhibitory peptide was used as an example axon growth inhibitor as a crude representation of the myelin inhibitory environment present *in vivo*, rather than using CNS myelin extract, as the latter contains a diverse array of inhibitory ligands, making interpretation of results potentially problematic. Nogo-P4 peptide is soluble, making it easy to use in culture studies, and at 25μM effectively inhibits RGC neurite outgrowth without compromising RGC survival (J O'Neill, University of Birmingham, unpublished data). In the presence of the Nogo peptide, there was a significant reduction in the proportion of neurite-bearing RGC and the mean length of longest RGC neurite in control wells incubated with sNBA culture medium, Lipofectamine transfection reagent or siEGFP, indicating that Nogo suppressed both neurite growth inhibition and elongation, whereas GSK3β knock-down counteracted this effect, increasing both the proportion of neurite-bearing RGC and the mean length of neurites to levels similar to that seen in the absence of Nogo inhibitory peptide. This result was replicated by GSK3β inhibition with Chir99021. These findings suggested that, in addition to enhancing the intrinsic growth potential of RGC, GSK3β suppression also counteracted Nogo-dependent growth inhibition. Nogo is just one of several myelin- and scar-derived factors that are ligands for the Nogo receptor complex, causing activation of RhoA/ROCK signalling and growth cone collapse (Fujita and Yamashita, 2014). Downstream of RhoA/ROCK, inactivation of the GSK3β substrate CRMP2 by phosphorylation inhibits microtubule polymerisation, resulting in axon/neurite growth inhibition (Fujita and Yamashita, 2014; Mimura *et al.*, 2006; Fukata *et al.*, 2002). However, as mentioned above, siGSK3β did not alter RGC expression of pCRMP2, indicating involvement of other substrates in this setting. Although not previously reported, the observation that GSK3β suppression counteracted Nogo-induced RGC neurite growth inhibition is in keeping with the report of Dill *et al.* (2008), who found that MAG and CSPG activated GSK3β signals in PC12 and cerebellar granule cell neurons, and was associated with attenuated numbers and shorter neurites in cultured DRG neurons, effects that were similarly reversed with two

different GSK3β inhibitors. Furthermore, Nogo protein reduces neurite outgrowth in a N2a neuronal cell line, associated with GSK3β activation, and treatment with either a GSK3β inhibitor or shRNA-mediated GSK3β knock-down reverses this effect (Shen *et al.*, 2011).

Notably, the neurite sprouting effect of GSK3β inhibition *in vitro* and the reversal of Nogo-dependent inhibition of neuritogenesis was not mirrored by enhanced RGC axon sprouting after ONC *in vivo*, where siGSK3β did not enhance short-distance axonal regeneration. This may be due to the presence of multiple extrinsic axon growth inhibitors *in vivo*, such as MAG, OMgp and CSPG, which do not modify GSK3β activity, despite siGSK3β and Chir99021 being able to overcome the specific effects of Nogo peptide. In contrast to the present findings, Alabed *et al.* (2010) found that GSK3β over-expression attenuated myelin-dependent axon growth inhibition *via* a mechanism involving interaction between CRMP4 and RhoA, suggesting that different factors may be in play against different inhibitory substrates. Moreover, it was also reported that GSK3β inhibitors attenuated neurite outgrowth in cultured DRG neurons, and had no additional growth promotion or repressive effects in the presence of CNS myelin. However, the specific pharmacological inhibitors used may have had off-target effects on other kinases, and the neurite growth assay was undertaken after an overnight incubation, which may not have allowed sufficient time for true effects to be fully evident (Alabed *et al.*, 2010).

The apparent contrast in evidence for GSK3β roles in mediating the effects of axonal growth inhibitors and in influencing neurite growth in culture and axonal regeneration after injury *in vivo* probably relates to the degree of GSK3β inhibition, temporal aspects of GSK3β activity, relative activation/inhibition of the diverse range of GSK3β substrates, and the neuronal cell-type and injury paradigm. Indeed, GSK3β knock-down after siGSK3β treatment was approximately 50%, indicating that some effective GSK3β activity was probably still present. Consistent with this, GSK3β

heterozygous knock-out mice exhibit approximately 50% GSK3β kinase activity, associated with enhanced axonal regeneration through the glial scar in a spinal cord injury model (Liz *et al.*, 2014). Although the culture studies with siGSK3β suggested that the effects of GSK3β in RGC were not closely associated with changes in pGSK3β(Ser9), pCRMP2, pSmad1 or pMAP1B, there are multiple other substrates which may be correlated, such as APC, CLASP, Tau, CREB and others (Figure 5.1A) (Hur *et al.*, 2011; Hur and Zhou, 2010). It has been suggested that, to ensure efficient axon growth, GSK3β activity should be modulated such that one set of substrates is specifically preserved whereas activity toward other substrates is specifically suppressed (Figure 5.1B), dependent on whether they have been 'primed' by an additional phosphorylation event (Hur and Zhou, 2010), which may vary depending on cellular localisation (e.g. soma *vs* axon) and stages of development.

In summary, the present findings demonstrate that GSK3β is an important regulator of RGC neurite growth and axonal regeneration. Inhibition of GSK3β, by pharmacological inhibition or siRNA-mediated knock-down, promoted intrinsic RGC growth ability *in vitro*, enhancing the neurite sprouting of axotomised RGC, and also promoted the growth of longer neurites in the presence of activated retinal glia. Axon regeneration after ONC *in vivo* was supported by siGSK3β, which may in part be due to attenuation of the effects of inhibitory CNS myelin and nascent-scar-derived growth inhibitors.

5.6.4 Combined siRNA approach for RGC neuroprotection and axon regeneration

Given the RGC neuroprotective and axon growth promoting effects of siRTP801 (Chapters 3 & 4), and the potential for disinhibited axon growth after GSK3β suppression in the literature, supported by both *in vitro* and *in vivo* data (this Chapter), it was hypothesised that a combinatorial approach using both siRTP801 and siGSK3β would optimise cellular signalling to enhance RGC survival and axon

regeneration. Combining the optimum *in vitro* concentration of each individual siRNA (20nM siRTP801, 50nM siGSK3β) conferred no beneficial effect on either RGC survival or neurite outgrowth (initiation or elongation) and target knock-down was limited to approximately 40% reduction of RGC GSK3β expression but no detectable reduction in $RTP801^{+}$ RGC. This suggested that despite a degree of GSK3β knock-down, the high total siRNA load of the combination treatment counteracted any RGC neuroprotective or neurite growth-promoting effect. This probably reflected toxicity associated with higher concentration of siRNA, as observed previously (Read *et al.*, 2009; Suggate *et al.*, 2009), rather than a true inhibitory effect of combined RTP801 and GSK3β suppression as there was no significant knock-down of RTP801 and only reduced target knock-down of GSK3β. Differential target knock-down with the 20nM/50nM combination was most likely a result of competition for, and saturation of, the RNA-induced silencing complex (RISC), the cellular machinery that induces mRNA degradation by siRNA (Tanudji *et al.*, 2010). Also, RISC saturation may itself be associated with cellular toxicity (Grimm *et al.*, 2010; Bader *et al.*, 2010). As a compromise to try and confirm dual target knock-down whilst limiting competition between the two siRNA and avoiding potentially toxic effects of high-dose siRNA, the combination was revised to 25nM each of siRTP801 and siGSK3β, corresponding to a total siRNA load of 50nM. In glial-activated cultures, the revised combination of siRNA resulted in approximately equal dual target knock-down, RGC neuroprotection, and increased neurite-bearing RGC and the length of RGC neurites over untreated controls. However, there were no additive or synergistic effects of the combined siRTP801/siGSK3β knock-down, as neither RGC survival nor neurite outgrowth parameters were promoted beyond that obtained by each individual siRNA treatment alone. It is possible that in this setting, the RGC survival and neurite elongation effects were optimally stimulated by RTP801 knock-down, with GSK3β suppression *via* the mTORC2-Akt feedback loop, suggesting that GSK3β activity was not limiting the effects of RTP801 knock-down and therefore the addition of siGSK3β did not significantly further suppress GSK3β to induce additional effects. However, in contrast to siRTP801 alone, but consistent with siGSK3β alone, this combination

was associated with enhanced RGC neuritogenesis compared to the sNBA/siEGFP controls, thereby demonstrating that GSK3β inhibition was promoting RGC neurite sprouting.

After ONC, combined siRNA treatment with both siRTP801 and siGSK3β *in vivo* was RGC neuroprotective, although survival was not significantly different from either siRTP801 or siGSK3β alone, indicating the lack of an additive effect on neuronal viability after injury. The maximal RGC survival effect observed was with siRTP801 alone (Chapter 3 data), which had a small but statistically significant advantage over siGSK3β treatment alone, but was not significantly different from the combined treatment, implying that with the combination treatment *in vivo* RTP801 knock-down was the major neuroprotective component, with no further beneficial effect afforded by additional GSK3β knock-down. The siGSK3β was sufficient to enable a degree of RGC neuroprotection after ONC, but was unnecessary in the presence of RTP801 knock-down, indicating that GSK3β activity was not a limiting factor for the siRTP801 neuroprotective effect, which may reflect a degree of GSK3β suppression already occurring *via* the mTORC2-Akt axis.

In contrast to RGC survival after ONC, where the combination siRNA treatment conferred no significant survival advantage over either of the individual component siRNAs, the siRTP801/siGSK3β combination was associated with significantly more $GAP43^{+}$ regenerating axons than PBS and siEGFP controls and also the siGSK3β component alone at each measurement point in the distal ON. There were also more regenerating axons than seen in the siRTP801 treated eyes, although this only reached statistical significance at 800µm. Despite neither of the component siRNAs significantly enhancing short distance axonal sprouting, the combined treatment did have a significant effect, suggesting that RGC axon growth induction was promoted in the presence of both RTP801 and GSK3β knock-down. GSK3β knock-down alone did not fully stimulate axonal growth, nor significantly overcome the array of extrinsic axonal growth inhibitory ligands such as Nogo, MAG, OMgp and CSPG

after ONC *in vivo* in the absence of mTOR-mediated protein synthesis or potentiated glial-derived NTF, but was sufficient to support longer growth of some regenerating axons. RTP801 knock-down alone was also insufficient to induce much axonal growth, whereas the combination did enable more robust axon growth initiation and elongation. The results implied that siRTP801 was the major component underlying the effects of the combination on axon regeneration, and that the siGSK3β component contributed to the potentiation of this effect. The finding that GSK3β inhibition acted in part to overcome the growth inhibitory effects of Nogo suggests that a key aspect of the enhanced axon regeneration supported by siGSK3β may be stabilisation of axonal growth cones, rendering regenerating axons relatively insensitive to external growth inhibitors. The *in vivo* results are consistent with a very recent study demonstrating that CST neuronal regeneration induced by *pten* deletion was further enhanced by additional deletion of Nogo (Geoffroy *et al.*, 2015), as well as previous studies indicating that inactivation of RhoA/ROCK growth-inhibitory signalling enables limited regenerative growth, but enhanced by other measures to promote growth capacity (Lehmann *et al.*, 1999; Bertrand *et al.*, 2005; Fischer *et al.*, 2004a; Fischer *et al.*, 2004b; Ahmed *et al.*, 2009). The findings are in keeping with a model of mTORC1/2 activity enabling RGC survival after axotomy and determining responsiveness to additional factors. After ONC, untreated RGC down-regulate mTOR activity and are very sensitive to extrinsic growth inhibitory factors associated with CNS myelin and the nascent glial scar. Treatment with siRTP801 after ONC enhances RGC protein synthesis capability and, coupled with the potentiated glial-derived NTF, promotes limited RGC axon regeneration, but with residual GSK3β activity acting as a 'brake' to the regenerative effect (without altering the survival threshold). Further suppression of GSK3β with the addition of siGSK3β reduces both the inhibitory action of TSC on mTORC1/2 activity and modulates axonal growth cone dynamics to enable potentiated axon regeneration.

In summary, despite involving elements of the same signalling pathway, the combined siRNA-mediated knock-down of RTP801 and GSK3β modulated the balance of signalling so that RGC survival was no greater than either of the individual siRTP801 or siGSK3β components alone, but both axon sprouting and axon elongation were beneficially enhanced. This provides evidence that a combined siRNA approach may yield superior results than a single treatment.

CHAPTER 6

SUMMARY, GENERAL DISCUSSION, FUTURE DIRECTIONS AND CONCLUSIONS

Elements of work presented in this Chapter have been published in:

Morgan-Warren PJ, Berry M, Ahmed Z, Scott RAH, Logan A. Exploiting mTOR signaling: a novel translatable treatment strategy for traumatic optic neuropathy? *Invest Ophthalmol Vis Sci.* 2013; 54: 6903-6916

The inability of CNS neurons to regenerate is a major limitation to the functional recovery of patients who have suffered CNS injury. In the context of TON after ocular/head injury, RGC apoptosis and axon regenerative failure are associated with poor visual prognosis for which there is a lack of effective therapeutic options. Recent laboratory studies and genetic techniques have shed light on the cellular mechanisms underpinning CNS neuronal death and axon regenerative failure after injury, and the PI3K/Akt/mTOR pathway has been implicated as a key regulator (Park *et al.*, 2010; Park *et al.*, 2008). Experiments to manipulate cell signalling pathways, such as up-regulation of mTOR signalling, demonstrate that neuroprotection and limited axon regeneration are indeed possible in the adult CNS, offering hope for the development of novel treatments. The aim of the experiments described in this thesis was to use a clinically translatable siRNA approach to target key regulatory points of the PI3K/Akt/mTOR pathway, including knock-down of the mTOR negative regulator RTP801 and the neuronal apoptosis/axon growth cone modulator GSK3β, in order to promote RGC survival and axon regeneration and to evaluate this strategy as the basis for the development of a novel therapy for TON.

6.1 CONSIDERATION OF PROJECT HYPOTHESES

The overall project hypothesis was that siRNA-mediated knock-down of key regulatory targets in the PI3K/mTOR pathway promotes mTOR activity to enhance RGC survival and axon regeneration after TON.

6.1.1 Hypothesis 1: siRNA-mediated knock-down of the stress-induced mTOR negative regulator RTP801 promotes RGC survival and axon regeneration in a rat model of TON

Work presented in Chapter 3 confirmed that siRTP801 was a target-specific siRNA, resulting in effective knock-down of RTP801 without inducing a non-specific inflammatory response, thus validating the fidelity of subsequent experiments to be attributable to RTP801 knock-down. There was a low constitutive expression of RTP801 in the retina of uninjured rats *in vivo*, consistent with previous studies (Brafman *et al.*, 2004; del Olmo-Aguado *et al.*, 2013; Feinstein *et al.*, 2009; Lee *et al.*, 2012; Rittenhouse *et al.*, 2014), that was shown to be up-regulated after ONC and associated with RGC loss and a failure of axon regeneration. Treatment with siRTP801 knocked-down expression of RTP801 in RGC and glia, and resulted in enhanced RGC survival both *in vivo* and *in vitro*. RTP801 knock-down had no significant effect on initiation of RGC axon/neurite regeneration, but enhanced the elongation of $GAP43^{+}$ regenerating axons in the distal ON after injury *in vivo* without affecting neurite elongation in the absence of activated retinal glia in a culture model. Thus, RTP801 was implicated as a stress-induced factor that modulated RGC responses to ONC, and the results showed that siRTP801 was RGC neuroprotective in a direct neuron-intrinsic manner, supporting previous reports of mTOR as an important determinant of neuronal viability (Malagelada *et al.*, 2008; Malagelada *et al.*, 2011; del Olmo-Aguado *et al.*, 2013; Park *et al.*, 2010; Park *et al.*, 2008). Furthermore, the findings demonstrated that siRTP801 facilitated the extension of RGC axons that were induced into the regenerative state by external factors, consistent with previous studies attributing mTOR activity as an important regulator of axonal extension (Lee *et al.*, 2014; Leibinger *et al.*, 2012).

6.1.2 Hypothesis 2: RGC survival and axon growth effects are mediated *via* increased mTORC1 activity

The observed RGC survival and enhanced axon elongation after siRTP801 treatment *in vivo* were consistent with the notion that maintenance or up-regulation of mTOR activity was a key mechanism underlying RGC responses to injury. Most previous studies on the role of mTOR signalling have specifically focussed on mTORC1, using pS6 as a functional read-out and the mTORC1-specific inhibitor Rapamycin to attribute phenotypic effects to 'mTOR' (Park *et al.*, 2008). Experiments in Chapter 4 showed that RGC expression of pS6 was reduced after ONC, consistent with an injury-induced suppression of mTORC1 activity (Park *et al.*, 2008), and that siRTP801 counteracted this. Therefore, at least part of the RGC survival and axon elongation effects of siRTP801 was attributable to maintenance of mTORC1 activity after injury, probably mediated through the synthesis of proteins necessary for neuronal survival and axon growth. However, rather than simply reflecting mTORC1 activity, the effects of siRTP801 were also shown to have mTORC1-indendent components, as expression of pS6 was not an absolute requirement for RGC neurite outgrowth. Also, the RGC neuroprotective effect of siRTP801 was reduced, but not abolished by Rapamycin, which also did not significantly reduce the effect of siRTP801 on neurite elongation in the presence of activated retinal glia. Accordingly, although siRTP801 resulted in the maintenance of mTORC1 activity, it was apparent that mTORC1-independent mechanism(s) were also contributing, with the Rapamycin-resistant mTORC2 a likely candidate, possibly *via* feedback activation of Akt and modulation of GSK3β (Maiese, 2014; Ikenoue *et al.*, 2009; Tang *et al.*, 2014; Jacinto *et al.*, 2006; Park *et al.*, 2010).

6.1.3 Hypothesis 3: The presence of activated retinal glia is required to mediate the axon growth effects of siRTP801, *via* the enhanced production of NTF

RGC neuroprotection afforded by siRTP801 was robust and presumed to be a direct effect on RGC themselves, but the apparent disparity in axon elongation between the *in vivo* ONC model and the retinal culture experiments in Chapter 3 (in which activated retinal glia were absent) suggested a role for additional, indirect effects on axon growth in response to RTP801 knock-down. Activity of mTOR has previously been demonstrated in numerous retinal cell types, and the expression of RTP801 in glia and of siRTP801-dependent knock-down of the protein in these cells implicated activated retinal glia as a major influence on siRTP801-stimulated axonal growth. Treatment with siRTP801 resulted in potentiated Müller glial activation after ONC and, whilst unable to directly induce a reactive gliosis, siRTP801 promoted longer neurite growth *in vitro* in the presence of $GFAP^+$ activated retinal glia, a response associated with potentiated secretion of glial-derived NTF including BDNF, NGF, NT-3 and CNTF. The enhanced RGC neurite elongation induced by siRTP801 in the presence of $GFAP^+$ glia was abolished by the potent pan-Trk receptor antagonist K252a, implicating glial-derived Trk-dependent NTF signalling as the underlying mechanism of siRTP801-induced axon/neurite elongation through indirect, paracrine effects.

6.1.4 Hypothesis 4: Inhibition of GSK3β promotes RGC survival and axon growth

It was apparent from experiments in Chapters 3 and 4 that mTORC1-independent factors contributed to siRTP801-dependent effects, and also that the axon regeneration results achieved with siRNA were inferior to previously reported genetic manipulations of the PI3K/Akt/mTOR pathway, for example by *pten* gene deletion (Park *et al.*, 2010; Park *et al.*, 2008). The constitutively active GSK3β is regulated by PI3K/Akt activity, and has also been implicated as an important regulator of cell survival,

gene transcription and axonal growth cone dynamics (Hur and Zhou, 2010; Seira and Del Rio, 2014), and thus was a potential additional therapeutic target. As with siRTP801, inhibition of GSK3β with siRNA was directly RGC neuroprotective, both after ONC *in vivo* and in a culture paradigm, irrespective of whether activated retinal glia were present, in keeping with reports that GSK3β directly and negatively regulates neuronal survival in response to cell stress (Beurel and Jope, 2006; Jacobs *et al.*, 2012). The experimental findings of Chapter 5 further demonstrated that GSK3β inhibition promoted the initiation of neurite outgrowth on a permissive laminin substrate *in vitro*, but was unable to positively influence initiation of axon regeneration after ONC *in vivo*. Also, siGSK3β supported growth of longer RGC neurites only in the presence of activated retinal glia *in vitro* and after ONC *in vivo* without significantly affecting the reactive glial response, suggesting that GSK3β suppression permits disinhibited axon growth induced by external factors. Other results demonstrated that GSK3β inhibition was neuroprotective in an mTORC1-dependent, pS6-independent manner, thus implicating 4E-BP1 as a regulator of RGC survival after GSK3β inhibition. Furthermore, siGSK3β enabled RGC to overcome the growth-inhibitory action of the CNS myelin-derived factor Nogo, providing evidence that axon growth after GSK3β knock-down is at least partly due to reduced sensitivity of axonal growth cones to extrinsic CNS inhibitors, although the GSK3β substrates sub-serving this effect remain to be determined.

6.1.5 Hypothesis 5: Combined siRNA-mediated knock-down of both RTP801 and GSK3β potentiates RGC survival and axon regeneration

Combinatorial approaches have consistently yielded superior RGC survival and axon regeneration results compared to single-target manipulations in the literature (Sun *et al.*, 2011; de Lima *et al.*, 2012; Geoffroy *et al.*, 2015; Yungher *et al.*, 2015), hence the positive results of siRTP801 and siGSK3β observed individually provided the basis for a combined siRNA approach to further optimise RGC

survival and axon regeneration. The *in vitro* experiments demonstrated that using a combination of unequal concentrations of siRNA (50nM siGSK3β + 20nM siRTP801) did not enable dual target knock-down, suggesting a degree of competition between individual siRNA components for the RISC (Tanudji *et al.*, 2010), and also that a high total siRNA load was not favourable to RGC viability and neurite outgrowth (Read *et al.*, 2009; Suggate *et al.*, 2009). Refinement of the combination formulation *in vitro* to 25nM/25nM enabled dual-target knock-down, with positive effects on RGC survival and neurite growth, albeit with no significant advantage of the combination over the individual components alone. The combination treatment similarly conferred no advantage over the component treatments for RGC survival after ONC *in vivo*, with siRTP801 as the major neuroprotective influence with little benefit of additional GSK3β knock-down. However, the combination treatment enabled significantly more $GAP43^{+}$ regenerating axons at all measured distances in the distal nerve segment after ONC, indicating enhanced initiation and elongation of axon regeneration. This finding strongly suggests that a 'double-hit' approach with simultaneous knock-down of both RTP801 and GSK3β targets multiple aspects of the regulation neuronal survival and axon growth, for example: (1) promoting a pro-survival balance of apoptotic regulators; (2) enabling potentiation of the $GFAP^{+}$ retinal glial response with increased NTF production; (3) maintenance of mTOR-dependent protein synthesis to provide the raw materials for the elongation of regenerating axons; and (4) modulation of axonal growth cone responses to intrinsic growth-associated signals and reduced sensitivity to external inhibitory influences.

6.2 CHALLENGES FOR CLINICAL TRANSLATION OF CELLULAR-SIGNALLING BASED THERAPIES

6.2.1 Optimising conditions for RGC survival and axon regeneration

The findings of the experiments presented here largely support the growing body of literature relating to the role of the PI3K signalling pathway in CNS neuronal survival and axon regeneration (Park *et al.*, 2010; Fischer and Leibinger, 2012), and highlight some important factors that may enable cellular signalling to be further optimised. It is increasingly clear that a single targeted manipulation is insufficient to fully maximise both RGC survival and axonal growth, as different factors underlie these different facets of the injury response. Up-regulation of mTORC1/2 activity is robustly neuroprotective, and plays a major role in the maintenance of the regenerative growth state that enables axon elongation, probably by permitting continued protein synthesis after injury (Park *et al.*, 2010; Park *et al.*, 2008; Fischer and Leibinger, 2012). However, additional stimuli are required for the induction of CNS axonal growth after injury, and it is likely that inflammatory cells (Benowitz and Popovich, 2011; Kurimoto *et al.*, 2013) and retinal glia are major contributors, for example through CNTF/LIF-dependent JAK-STAT signalling (Leibinger *et al.*, 2012; Leibinger *et al.*, 2009; Ahmed *et al.*, 2010). Although not investigated in this thesis, cAMP levels are also relevant in determining neuronal responsiveness to growth factors, the threshold for intrinsic growth capacity, and sensitivity to external inhibitory factors (Cai *et al.*, 2001; Gao *et al.*, 2003; Hellstrom and Harvey, 2014; Ma *et al.*, 2014; Yang and Yang, 2012; Park *et al.*, 2009; de Lima *et al.*, 2012; Kurimoto *et al.*, 2010). In addition to initiating and driving axon growth, optimal therapeutic strategies also require a mechanism of overcoming CNS myelin- and scar-derived inhibitory factors. Limited axon regeneration is possible after neutralisation of extrinsic inhibitory ligands like Nogo or downstream signalling components such as RhoA/ROCK (Alabed *et al.*, 2006; Domeniconi *et al.*, 2002; Fournier *et al.*, 2003; Sandvig *et al.*, 2004; Vajda *et al.*, 2015; Lehmann *et al.*, 1999; Lingor *et al.*, 2007), consistent with the very limited

enhancement in axon growth reported here after siGSK3β, but axon regeneration is only likely to be optimised when targeting CNS extrinsic inhibitors is part of a broader, multi-target strategy (Geoffroy *et al.*, 2015; Wang *et al.*, 2012; Ahmed *et al.*, 2009; Fischer *et al.*, 2004b; Lingor *et al.*, 2008; Chen *et al.*, 2009).

6.2.2 Unlocking axon regeneration in non-responding RGC

Despite an increasing understanding of the molecular mechanisms surrounding axon regenerative failure in the mature CNS, and promising experimental approaches to overcome these to induce RGC survival and axon regeneration after ON injury, at present only a small proportion of RGC have been stimulated to regenerate axons. Even with the best genetic techniques, only around 10% of surviving RGC regenerate axons despite manipulation of many candidate signalling pathways, including up-regulation of mTOR activity and as part of combinatorial strategies (Park *et al.*, 2008; Sun *et al.*, 2011; Kurimoto *et al.*, 2010), and the results presented here are just a fraction of that. Understanding why the majority of RGC do not regenerate axons after these treatments may hold the key to visual recovery for patients blinded by ON injury, and answers may lie in differential responses of RGC sub-types. It was reported over twenty years ago that a specific population of large RGC with somal area over 250μm^2 were most responsive to intravitreal NTF (Mey and Thanos, 1993). It is now known that many different RGC sub-types exist (Sanes and Masland, 2015), with the α- and M1-ipRGC surviving preferentially after axotomy, and αRGC accounting for the vast majority of pS6$^+$ and regenerating RGC after *pten* gene deletion (Duan *et al.*, 2015). Selective regeneration of this particular RGC sub-type after *pten* deletion was clearly not fully replicated in the experiments presented here using siRTP801 to promote mTOR signalling, as pS6$^+$ expression was not exclusively associated with neurite-bearing RGC after siRTP801. Furthermore, given that αRGC make up approximately 6% of the RGC population (Duan *et al.*, 2015), the current data suggested that maximal regeneration of αRGC

was not even achieved after siRTP801 (± siGSK3β) as the *in vivo* regenerative response seen here was less than 1% of the total RGC number. It is very possible that different RGC sub-types respond selectively to different regenerative stimuli, and further work is required to more completely understand whether targeting other signalling mediators, such as MAPK, GSK3β, CNTF/LIF, cAMP and RhoA/ROCK, for example, may enable more robust axon regenerative responses among different RGC classes to elicit clinically relevant functional regeneration. The current results clearly support a role for retinal glia in modulating the RGC regenerative response, but a deeper understanding of the glial contribution and of more subtle control mechanisms of cellular signalling is required. Temporal dynamics of pathway activation may be relevant, as the duration of receptor signalling mediates specific effects in response to activation by different ligands (Braun *et al.*, 2013). Epigenetic changes and micro-RNA modulation of gene expression, including those related to mTOR signalling, have pivotal roles in neuronal survival and axon growth, and require further investigation (Yea and Fruman, 2013; Strickland *et al.*, 2011; Zhang *et al.*, 2013).

6.2.3 Forming the right connections: axon guidance and synaptogenesis

Even if the goal of ON axon regeneration is realised, RGC axons may not be guided appropriately to their central targets (Luo *et al.*, 2013), aberrant functional synapses may be formed, and topographic representations mismatched (Moore and Goldberg, 2010). Anatomically conserved functional synaptic connections are possible after nerve regeneration in hippocampal neurons (Li *et al.*, 1996; Li *et al.*, 1994; Zhou *et al.*, 1998), and target-specific axon regeneration has been reported in the murine visual system using a combination of *pten* deletion, zymosan and a cAMP analogue (de Lima *et al.*, 2012). However, utilising the same combinatorial treatment strategy, recent imaging studies using light sheet fluorescence microscopy for 3-dimensional evaluation of regenerating axons could not detect the same degree of central innervation, and reported significant aberrant axon growth

trajectories into the ipsilateral optic tract, both the ipsilateral and contralateral ON, and the hypothalamus (Luo *et al.*, 2013). The reason for the discrepancy in these findings is unclear, although aberrant growth of regenerating axons in the ON has also been reported after intravitreal PN implant as the growth stimulus (Berry *et al.*, 1999) and genetic up-regulation of CNTF release (Pernet *et al.*, 2013). Reduction of growth cone sensitivity to extrinsic growth inhibitory ligands and associated signalling pathways, such as NgR, $p75^{NTR}$, RhoA/ROCK and GSK3β to promote axon growth may simultaneously render RGC unresponsive to attractive and repellent axon guidance molecules and paradoxically encourage disorganised axon growth (Koeberle and Bahr, 2004; Pernet and Schwab, 2014), although functional plasticity of the CNS may overcome deficiencies in anatomic connections (Quadrato and Di Giovanni, 2013).

6.2.4 Translating molecular biology to the ophthalmic clinic: clinical potential for siRNA therapy

Once the optimal biochemical conditions for RGC survival and axon regeneration are elucidated, a further challenge remains in translating them into a clinical approach. Many genetic and laboratory techniques are not clinically translatable, but siRNA-based therapies to knock-down target gene function may offer the potential for more rapid delivery to patients (Guzman-Aranguez *et al.*, 2013). Experiments described in this thesis have demonstrated significant RGC neuroprotection with a siRNA approach, enabling tissue-specific gene knock-down whilst minimizing non-specific, off-target, and immunogenic effects. The axon regeneration obtained was very limited, but further refinement of siRNA technology to optimise tissue delivery and stability plus better selection of targets for knock-down may enable siRNA therapies to promote clinically relevant axon regeneration and become a mainstay for the treatment of ocular conditions such as TON (Guzman-Aranguez *et al.*, 2013; Shim and Kwon, 2010; Thakur *et al.*, 2012; Campochiaro, 2006). Clinical trials of siRNA treatments, including those targeting RTP801, already have been reported for ocular disorders, such

as diabetic macular oedema and age-related macular degeneration (Nguyen *et al.*, 2012a; Nguyen *et al.*, 2012b; Nguyen *et al.*, 2012c; Kaiser *et al.*, 2010). Combination siRNA treatment may also become a viable therapeutic option if multiple target knock-down is required for optimal results (Sriram *et al.*, 2013).

6.2.5 Potential adverse effects of up-regulating PI3K/Akt/mTOR signalling

Despite the enthusiasm for up-regulating mTOR activity as a component of a therapeutic approach for TON, a note of caution should be sounded. Hyper-activation of PI3K/Akt/mTOR is found in many malignant diseases (Don and Zheng, 2011; Alayev and Holz, 2013; Hay, 2005). Sustained mTOR over-activity is associated with aberrant protein translation and nerve growth, linked to epilepsy, adverse inflammatory responses in traumatic brain injury, and intellectual disorders, such as autism and cognitive decline in dementia (Don *et al.*, 2012; O'Neill, 2013). Furthermore, dysregulation of GSK3β is also associated with CNS disorders, particularly Alzheimer's disease, schizophrenia and mood disorders (Hernandez *et al.*, 2009; Cole, 2013; Eldar-Finkelman and Martinez, 2011). Achieving the balance of neuroprotection and regenerative growth promotion without inducing malignant proliferation or dysregulated sprouting remains a formidable challenge. Therefore, development of treatments based upon modulation of mTOR and related pathways must be mindful of potential adverse and off-target effects, although there have been no reports of tumour development in the relatively short time-frame of CNS axon regeneration studies, and tissue-specific drug delivery and short-term signal up-regulation may protect against possible detrimental outcomes.

6.3 EXPERIMENTAL LIMITATIONS

The ONC model is a popular experimental paradigm for studying RGC responses to injury and testing therapeutic substances for neuroprotective and axon regenerative effects (Blanch *et al.*, 2012; Berry *et al.*, 2008). RGC structure and the environment within the retina are well defined, RGC are very accessible *in vivo*, and are the only retinal neurons to extend axons along the ON. RGC survival and axon regeneration analyses can therefore be undertaken in a relatively straightforward fashion, either using anterograde/retrograde tracing studies (Berry *et al.*, 2008; Gao *et al.*, 2012), or immunohistochemical analyses of retinal and ON sections as utilised here, which provide robust and reliable results whilst minimising surgical intervention (Mead *et al.*, 2014; Vigneswara *et al.*, 2014). Related studies using dissociated retinal cultures are useful for investigating neuronal responses to changes in the cellular environment, such as the addition of siRNA treatments, and multiple conditions can be studied in parallel with ease (Romano and Hicks, 2007; Levin, 2005; Lilley and Robbins, 2005).

6.3.1 Limitations of *in vivo* procedures

Differential RGC loss with lesions at different anatomical sites along the ON (Berkelaar *et al.*, 1994), as well as species- and development-dependent variation in survival and regenerative responses (Cui *et al.*, 2007; So and Yip, 1998; Cai *et al.*, 2001; Chen *et al.*, 1995; Goldberg, 2003; Mar *et al.*, 2014; Zhou and Snider, 2006) makes comparison between studies worthy of careful consideration. The ONC procedures undertaken here were performed to a standard technique, and with the same operating surgeon for each batch of animals irrespective of treatment group (Section 2.3.1), but it is possible that some surgical variation occurred. Delivery of agents by intravitreal injections was also performed by a standard technique, with care taken not to injure the lens. Lens injury is associated

with a pro-regenerative state (Fischer *et al.*, 2000; Fischer *et al.*, 2004b; Leon *et al.*, 2000) and, whilst it is possible that injection-induced intraocular inflammation may have contributed to the observed survival/regeneration effects, any overt signs of lens injury were obvious in the post-operative period and affected animals excluded from analyses.

A limitation in the use of *in vivo* studies for RGC survival and ON regeneration is that tissue processing between animal killing and immunohistochemistry of tissue sections requires several technical steps, with a risk of tissue loss. Rat eye dissection is relatively straightforward, but the preparation of ON samples for analysis is technically more challenging. Local adherent scar tissue in the area of the ONC lesion makes nerve dissection difficult and crushed ON are vulnerable to breaking at the lesion site, making subsequent analysis of axon regeneration across an ONC lesion impossible and reducing the intended treatment group size. Despite some tissue loss during processing, in the reported studies sufficient tissue for each group of animals was available for analysis to be undertaken. Identification of RGC for *in vivo* survival analyses can be problematic. Traditional phenotypic markers like βIII-tubulin also immunostain other cells of the GCL, such as amacrine cells, whereas Brn3a is more RGC specific and provides an accurate representation of RGC loss across treatment groups, but does not localise to ipRGC sub-types that are more injury resistant (Nadal-Nicolas *et al.*, 2012; Nadal-Nicolas *et al.*, 2009; Mead *et al.*, 2014). The consistent use of Brn3a in RGC survival analyses presented here should support valid inter-group treatment comparisons.

It has previously been reported that unilateral ONC lesions induce reactive glial changes in the contralateral retina, cautioning against the use of contralateral intact controls in RGC survival and axon regeneration analyses (Bodeutsch *et al.*, 1999). In these studies intact controls were not used for axon regeneration analyses, with comparisons undertaken between treatments after ONC only, and separate rats were used as intact/uninjured controls for RGC survival analysis. In animals

undergoing ONC, bilateral ONC was always performed, followed by different treatment/control agents injected into each eye, in keeping with previous studies in our laboratory (Mead *et al.*, 2013), including after siRNA treatment (Neuregenix, unpublished data). It is possible that systemic absorption of an agent delivered to one eye could have had an effect on the fellow eye, but the observations that targeted-siRNA treatments delivered significantly different results from PBS and siEGFP controls suggested that differences observed could be attributable to the individual treatments. In addition, the use of individual eyes for each treatment facilitates comparison of multiple treatment groups whilst minimising unnecessary animal usage.

6.3.2 Limitations of *in vitro* procedures

Despite the advantages of using dissociated primary retinal cultures, there are several limitations inherent in their use. Preparing dissociated retinal cultures often produces a variable yield of RGC, which can lead to some variation in later analyses, but attempts to minimise this were undertaken, including limiting delay between the various steps of the cultures protocol and using fresh reagents. The relatively consistent RGC survival and neurite outgrowth results obtained in control wells demonstrated that these attempts were largely successful. The preparation of primary retinal cultures by necessity results in axotomy, and so even 'untreated' control cultures may not truly represent the uninjured *in vivo* condition. However, there is no avoiding axotomy in the retinal culture process, and in order to more accurately model the injury condition separate cultures were prepared 5d after ONC injury (for glial-activation) and subsequently exposed to treatment conditions. The anatomical arrangement and cellular connections are not maintained *in vitro*, making it difficult to accurately assess inter-cellular relationships, but the dissociated retinal culture paradigm used contains a mixed cell population, and so does enable some investigation as to the contributions of retinal glia, for example. Techniques are available for evaluation of RGC-specific responses, such as

laser capture microdissection (Chung *et al.*, 2013; Huang *et al.*, 2006) or immunopanning (Meyer-Franke *et al.*, 1998; Butowt and von Bartheld, 2005) to isolate RGC, but as experiments in this thesis have demonstrated, the contribution and interactions of multiple cell populations is probably more relevant when trying to develop a translatable therapy. Finally, using dissociated retinal cultures to obtain RNA for qPCR requires pooling of retinae for adequate RNA yield, necessitating the use of several animals/condition for each experiment, leading to potentially large numbers of animals especially when there are multiple treatment groups for comparison. The qPCR experiments reported here thus used RNA obtained from mixed retinal cells, potentially diluting the measured degree of siRNA-mediated target knock-down. To specifically isolate RGC for analysis of specific gene changes with qPCR would require an unacceptable number of animals, and although an RGC cell line has been described that may have helped this process (Krishnamoorthy *et al.*, 2001), it was subsequently determined not to be of RGC origin (Krishnamoorthy *et al.*, 2013).

6.4 FUTURE DIRECTIONS

The experiments undertaken and reported here have clearly demonstrated the potential for the use of a targeted siRNA approach for RGC neuroprotection, and that a combination therapy may yield superior results and be associated with more robust axon regeneration after injury. In order to move this work forward, two broad areas should be considered: (1) optimisation of the combinatorial treatment and (2) measurement of anatomical and functional outputs.

6.4.1 Development of an optimal targeted combination treatment

It is clear both from the experiments presented in this thesis and in the published literature that knock-down or inhibition of a single cellular signalling complex is insufficient to promote both RGC

neuroprotection and vigorous axon regeneration after ON injury. Promotion of PI3K/Akt/mTOR signalling is neuroprotective, and may itself be a feasible option to prevent RGC loss after ON injury, but additional targets are required for induction and maintenance of a robust axon regenerative response. Additional factors that could be targeted with siRNA include PTEN and TSC, which are situated at different levels of the PI3K/Akt/mTOR cascade, and would therefore provide valuable data on the relative importance of the upstream/downstream location of complex inhibition in the mTOR pathway with regard to RGC survival and axon regeneration. Furthermore, addition of NTF such as CNTF or neurotrophins to initiate and drive the axon growth response may enable a more potent regenerative response after ONC, which may be further enhanced by suppression of other intrinsic negative regulators like SOCS3, or by the addition of a cAMP analogue. The inclusion of a specific component to neutralise external CNS myelin-derived inhibition, for example targeting the NgR (± its co-receptors) or the RhoA/ROCK pathway, may also usefully form an integral part of an optimised treatment combination. These factors could be very easily studied both in the established *in vivo* ONC model, and in the dissociated retinal culture models, with the glial-activated culture paradigm providing the most relevant *in vitro* model for building an understanding of underlying mechanisms. Specific inhibitors of mTORC2 and activated retinal glia or their dependent factors would also facilitate understanding of mechanistic aspects, and identification of RGC sub-types would enable correlation of axon regenerative responses with particular RGC populations.

In addition, it is likely that temporal factors play an important role in determining RGC survival and axon regeneration after ON injury, and so the timing and duration of intervention(s) should also be investigated. It may be that a critical window of opportunity exists for initiation of a regenerative response, and that certain aspects of a combinatorial approach are only required or viable for a limited period after the initial insult. This aspect may have pivotal importance in translating molecular biology to the ophthalmic clinic, as treatment protocols will need to be defined.

6.4.2 Measurement of anatomical and functional outputs

Ultimately, functional recovery of vision is of critical importance for patients requiring treatment of ON injury. Repeatable, reliable results for improvement in visual function after laboratory ONC experiments are currently lacking. Advances in anatomical measures, such as optical coherence tomography (OCT), light sheet microscopy and axon tracing will enable more accurate assessment of retinal NFL/GCL integrity and axon trajectory, particularly if long-distance axon regeneration can be achieved with translatable techniques *in vivo*. Physiological measures of visual recovery, such as pupillometry, electroretinography, visual evoked potentials and behavioural testing could be employed to investigate aspects of functionally relevant improvement after clinical intervention.

6.5 CONCLUSIONS

With no clinically effective treatments for TON, patients are at risk of lifelong visual impairment. Laboratory studies are unlocking the relevance of multiple extrinsic and intrinsic factors to post-injury responses, and the candidate signalling pathways responsible for RGC death and axon regenerative failure in the adult visual system are becoming potential targets for the development of future clinical treatments. The PI3K/Akt pathway, which mediates neuronal viability, axon growth and protein synthesis through complexes such as mTORC1/2 and GSK3β, is a promising candidate pathway. Complementing the increasing body of literature in this research field, work presented here has demonstrated that siRNA mediated knock-down of the mTOR negative regulator RTP801 promotes RGC neuroprotection, supports elongation of some regenerating axons and potentiates a pro-regenerative reactive glial response to injury. Suppression of GSK3β is also RGC neuroprotective, and contributes to enhanced axon regeneration, and a combinatorial approach with dual RTP801/GSK3β knock-down delivers superior anatomical results, particularly with regard to axon

regeneration after ONC. The data also contribute to a more detailed understanding of the underlying cellular signalling mechanisms, although a thorough comprehension of the pro-survival and regenerative determinants remains to be achieved. Altering the balance of cellular signalling to promote clinically relevant RGC survival and axon regeneration after ON injury and translating laboratory studies into the clinic remain significant challenges although increasing evidence suggests that the task may not be insurmountable.

REFERENCES

Abe, N., Borson, S. H., Gambello, M. J., Wang, F., and Cavalli, V. (2010) Mammalian target of rapamycin (mTOR) activation increases axonal growth capacity of injured peripheral nerves. *J Biol Chem,* 285**,** 28034-43.

Adami, C., Sorci, G., Blasi, E., Agneletti, A. L., Bistoni, F., and Donato, R. (2001) S100B expression in and effects on microglia. *Glia,* 33**,** 131-42.

Aguayo, A. J., Vidal-Sanz, M., Villegas-Perez, M. P., and Bray, G. M. (1987) Growth and connectivity of axotomized retinal neurons in adult rats with optic nerves substituted by PNS grafts linking the eye and the midbrain. *Ann N Y Acad Sci,* 495**,** 1-9.

Aguirre, A., Maturana, C. J., Harcha, P. A., and Saez, J. C. (2013) Possible involvement of TLRs and hemichannels in stress-induced CNS dysfunction via mastocytes, and glia activation. *Mediators Inflamm,* 2013**,** 893521.

Ahmed, Z., Aslam, M., Lorber, B., Suggate, E. L., Berry, M., and Logan, A. (2010) Optic nerve and vitreal inflammation are both RGC neuroprotective but only the latter is RGC axogenic. *Neurobiol Dis,* 37**,** 441-54.

Ahmed, Z., Berry, M., and Logan, A. (2009) ROCK inhibition promotes adult retinal ganglion cell neurite outgrowth only in the presence of growth promoting factors. *Mol Cell Neurosci,* 42**,** 128-33.

Ahmed, Z., Dent, R. G., Suggate, E. L., Barrett, L. B., Seabright, R. J., Berry, M., and Logan, A. (2005) Disinhibition of neurotrophin-induced dorsal root ganglion cell neurite outgrowth on CNS myelin by siRNA-mediated knockdown of NgR, p75NTR and Rho-A. *Mol Cell Neurosci,* 28**,** 509-23.

Ahmed, Z., Douglas, M. R., John, G., Berry, M., and Logan, A. (2013) AMIGO3 is an NgR1/p75 co-receptor signalling axon growth inhibition in the acute phase of adult central nervous system injury. *PLoS One,* 8**,** e61878.

Ahmed, Z., Kalinski, H., Berry, M., Almasieh, M., Ashush, H., Slager, N., Brafman, A., Spivak, I., Prasad, N., Mett, I., Shalom, E., Alpert, E., Di Polo, A., Feinstein, E., and Logan, A. (2011) Ocular neuroprotection by siRNA targeting caspase-2. *Cell Death Dis,* 2**,** e173.

Ahmed, Z., Suggate, E. L., Brown, E. R., Dent, R. G., Armstrong, S. J., Barrett, L. B., Berry, M., and Logan, A. (2006) Schwann cell-derived factor-induced modulation of the NgR/p75NTR/EGFR axis disinhibits axon growth through CNS myelin in vivo and in vitro. *Brain,* 129**,** 1517-33.

Alabed, Y. Z., Grados-Munro, E., Ferraro, G. B., Hsieh, S. H., and Fournier, A. E. (2006) Neuronal responses to myelin are mediated by rho kinase. *J Neurochem,* 96**,** 1616-25.

Alabed, Y. Z., Pool, M., Ong Tone, S., Sutherland, C., and Fournier, A. E. (2010) GSK3 beta regulates myelin-dependent axon outgrowth inhibition through CRMP4. *J Neurosci,* 30**,** 5635-43.

Alayev, A., and Holz, M. K. (2013) mTOR signaling for biological control and cancer. *J Cell Physiol,* 228**,** 1658-64.

Ali, A., Hoeflich, K. P., and Woodgett, J. R. (2001) Glycogen synthase kinase-3: properties, functions, and regulation. *Chem Rev,* 101**,** 2527-40.

Angliker, N., and Ruegg, M. A. (2013) In vivo evidence for mTORC2-mediated actin cytoskeleton rearrangement in neurons. *Bioarchitecture,* 3**,** 113-118.

Arevalo, M. A., and Rodriguez-Tebar, A. (2006) Activation of casein kinase II and inhibition of phosphatase and tensin homologue deleted on chromosome 10 phosphatase by nerve growth factor/p75NTR inhibit glycogen synthase kinase-3beta and stimulate axonal growth. *Mol Biol Cell,* 17**,** 3369-77.

Armstrong, J. S. (2006) Mitochondrial membrane permeabilization: the sine qua non for cell death. *Bioessays,* 28**,** 253-60.

Arsham, A. M., Howell, J. J., and Simon, M. C. (2003) A novel hypoxia-inducible factor-independent hypoxic response regulating mammalian target of rapamycin and its targets. *J Biol Chem,* 278**,** 29655-60.

Bader, A. G., Brown, D., and Winkler, M. (2010) The promise of microRNA replacement therapy. *Cancer Res,* 70**,** 7027-30.

Bahr, M., Vanselow, J., and Thanos, S. (1988) In vitro regeneration of adult rat ganglion cell axons from retinal explants. *Exp Brain Res,* 73**,** 393-401.

Barbacid, M. (1994) The Trk family of neurotrophin receptors. *J Neurobiol,* 25**,** 1386-403.

Barbacid, M. (1995) Structural and functional properties of the TRK family of neurotrophin receptors. *Ann N Y Acad Sci,* 766**,** 442-58.

Benowitz, L. I., and Popovich, P. G. (2011) Inflammation and axon regeneration. *Curr Opin Neurol,* 24**,** 577-83.

Benowitz, L. I., and Yin, Y. (2010) Optic nerve regeneration. *Arch Ophthalmol,* 128**,** 1059-64.

Berkelaar, M., Clarke, D. B., Wang, Y. C., Bray, G. M., and Aguayo, A. J. (1994) Axotomy results in delayed death and apoptosis of retinal ganglion cells in adult rats. *J Neurosci,* 14**,** 4368-74.

Berry, M., Ahmed, Z., Lorber, B., Douglas, M., and Logan, A. (2008) Regeneration of axons in the visual system. *Restor Neurol Neurosci,* 26**,** 147-74.

Berry, M., Carlile, J., and Hunter, A. (1996) Peripheral nerve explants grafted into the vitreous body of the eye promote the regeneration of retinal ganglion cell axons severed in the optic nerve. *J Neurocytol,* 25**,** 147-70.

Berry, M., Carlile, J., Hunter, A., Tsang, W., Rosenstiel, P., and Sievers, J. (1999) Optic nerve regeneration after intravitreal peripheral nerve implants: trajectories of axons regrowing through the optic chiasm into the optic tracts. *J Neurocytol,* 28**,** 721-41.

Bertrand, J., Winton, M. J., Rodriguez-Hernandez, N., Campenot, R. B., and Mckerracher, L. (2005) Application of Rho antagonist to neuronal cell bodies promotes neurite growth in compartmented cultures and regeneration of retinal ganglion cell axons in the optic nerve of adult rats. *J Neurosci,* 25**,** 1113-21.

Beurel, E., and Jope, R. S. (2006) The paradoxical pro- and anti-apoptotic actions of GSK3 in the intrinsic and extrinsic apoptosis signaling pathways. *Prog Neurobiol,* 79**,** 173-89.

Blanch, R. J., Ahmed, Z., Berry, M., Scott, R. A., and Logan, A. (2012) Animal models of retinal injury. *Invest Ophthalmol Vis Sci,* 53**,** 2913-20.

Blanch, R. J., Bindra, M. S., Jacks, A. S., and Scott, R. A. (2011) Ophthalmic injuries in British Armed Forces in Iraq and Afghanistan. *Eye (Lond),* 25**,** 218-23.

Bodeutsch, N., Siebert, H., Dermon, C., and Thanos, S. (1999) Unilateral injury to the adult rat optic nerve causes multiple cellular responses in the contralateral site. *J Neurobiol,* 38**,** 116-28.

Bonfanti, L., Strettoi, E., Chierzi, S., Cenni, M. C., Liu, X. H., Martinou, J. C., Maffei, L., and Rabacchi, S. A. (1996) Protection of retinal ganglion cells from natural and axotomy-induced cell death in neonatal transgenic mice overexpressing bcl-2. *J Neurosci,* 16**,** 4186-94.

Bracken, M. B., Shepard, M. J., Collins, W. F., Holford, T. R., Young, W., Baskin, D. S., Eisenberg, H. M., Flamm, E., Leo-Summers, L., Maroon, J., and Et Al. (1990) A randomized, controlled trial of methylprednisolone or naloxone in the treatment of acute spinal-cord injury. Results of the Second National Acute Spinal Cord Injury Study. *N Engl J Med,* 322**,** 1405-11.

Brafman, A., Mett, I., Shafir, M., Gottlieb, H., Damari, G., Gozlan-Kelner, S., Vishnevskia-Dai, V., Skaliter, R., Einat, P., Faerman, A., Feinstein, E., and Shoshani, T. (2004) Inhibition of oxygen-induced retinopathy in RTP801-deficient mice. *Invest Ophthalmol Vis Sci,* 45**,** 3796-805.

Braun, D. A., Fribourg, M., and Sealfon, S. C. (2013) Cytokine response is determined by duration of receptor and signal transducers and activators of transcription 3 (STAT3) activation. *J Biol Chem,* 288**,** 2986-93.

Bray, G. M., Vidal-Sanz, M., and Aguayo, A. J. (1987a) Regeneration of axons from the central nervous system of adult rats. *Prog Brain Res,* 71**,** 373-9.

Bray, G. M., Villegas-Perez, M. P., Vidal-Sanz, M., and Aguayo, A. J. (1987b) The use of peripheral nerve grafts to enhance neuronal survival, promote growth and permit terminal reconnections in the central nervous system of adult rats. *J Exp Biol,* 132**,** 5-19.

Brewer, G. J. (1995) Serum-free B27/neurobasal medium supports differentiated growth of neurons from the striatum, substantia nigra, septum, cerebral cortex, cerebellum, and dentate gyrus. *J Neurosci Res,* 42**,** 674-83.

Brosius Lutz, A., and Barres, B. A. (2014) Contrasting the glial response to axon injury in the central and peripheral nervous systems. *Dev Cell,* 28**,** 7-17.

Brugarolas, J., Lei, K., Hurley, R. L., Manning, B. D., Reiling, J. H., Hafen, E., Witters, L. A., Ellisen, L. W., and Kaelin, W. G., Jr. (2004) Regulation of mTOR function in response to hypoxia by REDD1 and the TSC1/TSC2 tumor suppressor complex. *Genes Dev,* 18**,** 2893-904.

Budanov, A. V., and Karin, M. (2008) p53 target genes sestrin1 and sestrin2 connect genotoxic stress and mTOR signaling. *Cell,* 134**,** 451-60.

Burgaya, F., Fontana, X., Martinez, A., Montolio, M., Mingorance, A., Simo, S., Del Rio, J. A., and Soriano, E. (2006) Semaphorin 6C leads to GSK-3-dependent growth cone collapse and redistributes after entorhino-hippocampal axotomy. *Mol Cell Neurosci,* 33**,** 321-34.

Butowt, R., and Von Bartheld, C. S. (2005) Anterograde axonal transport of BDNF and NT-3 by retinal ganglion cells: roles of neurotrophin receptors. *Mol Cell Neurosci,* 29**,** 11-25.

Cai, D., Qiu, J., Cao, Z., Mcatee, M., Bregman, B. S., and Filbin, M. T. (2001) Neuronal cyclic AMP controls the developmental loss in ability of axons to regenerate. *J Neurosci,* 21**,** 4731-9.

Campochiaro, P. A. (2006) Potential applications for RNAi to probe pathogenesis and develop new treatments for ocular disorders. *Gene Ther,* 13**,** 559-62.

Canal, M., Romani-Aumedes, J., Martin-Flores, N., Perez-Fernandez, V., and Malagelada, C. (2014) RTP801/REDD1: a stress coping regulator that turns into a troublemaker in neurodegenerative disorders. *Front Cell Neurosci,* 8**,** 313.

Carriere, A., Romeo, Y., Acosta-Jaquez, H. A., Moreau, J., Bonneil, E., Thibault, P., Fingar, D. C., and Roux, P. P. (2011) ERK1/2 phosphorylate Raptor to promote Ras-dependent activation of mTOR complex 1 (mTORC1). *J Biol Chem,* 286**,** 567-77.

Cenni, M. C., Bonfanti, L., Martinou, J. C., Ratto, G. M., Strettoi, E., and Maffei, L. (1996) Long-term survival of retinal ganglion cells following optic nerve section in adult bcl-2 transgenic mice. *Eur J Neurosci,* 8**,** 1735-45.

Chen, C., Chen, X., Yin, X., Yuan, R., Wang, B., and Ye, J. (2009) NgR RNA interference, combined with zymosan intravitreal injection, enhances optic nerve regeneration. *J Neurochem,* 110**,** 1628-34.

Chen, D. F., Jhaveri, S., and Schneider, G. E. (1995) Intrinsic changes in developing retinal neurons result in regenerative failure of their axons. *Proc Natl Acad Sci U S A,* 92**,** 7287-91.

Chen, Z. L., Yu, W. M., and Strickland, S. (2007) Peripheral regeneration. *Annu Rev Neurosci,* 30**,** 209-33.

Cheung, Z. H., Chan, Y. M., Siu, F. K., Yip, H. K., Wu, W., Leung, M. C., and So, K. F. (2004) Regulation of caspase activation in axotomized retinal ganglion cells. *Mol Cell Neurosci,* 25**,** 383-93.

Chong, Z. Z., Shang, Y. C., Wang, S., and Maiese, K. (2012) Shedding new light on neurodegenerative diseases through the mammalian target of rapamycin. *Prog Neurobiol,* 99**,** 128-48.

Christie, K. J., Webber, C. A., Martinez, J. A., Singh, B., and Zochodne, D. W. (2010) PTEN inhibition to facilitate intrinsic regenerative outgrowth of adult peripheral axons. *J Neurosci,* 30**,** 9306-15.

Chuang, D. M., Wang, Z., and Chiu, C. T. (2011) GSK-3 as a Target for Lithium-Induced Neuroprotection Against Excitotoxicity in Neuronal Cultures and Animal Models of Ischemic Stroke. *Front Mol Neurosci,* 4**,** 15.

Chung, S. H., Shen, W., and Gillies, M. C. (2013) Laser capture microdissection-directed profiling of glycolytic and mTOR pathways in areas of selectively ablated Muller cells in the murine retina. *Invest Ophthalmol Vis Sci,* 54**,** 6578-85.

Cimarosti, H., Rodnight, R., Tavares, A., Paiva, R., Valentim, L., Rocha, E., and Salbego, C. (2001) An investigation of the neuroprotective effect of lithium in organotypic slice cultures of rat hippocampus exposed to oxygen and glucose deprivation. *Neurosci Lett,* 315**,** 33-6.

Codeluppi, S., Svensson, C. I., Hefferan, M. P., Valencia, F., Silldorff, M. D., Oshiro, M., Marsala, M., and Pasquale, E. B. (2009) The Rheb-mTOR pathway is upregulated in reactive astrocytes of the injured spinal cord. *J Neurosci,* 29**,** 1093-104.

Cole, A. R. (2013) Glycogen synthase kinase 3 substrates in mood disorders and schizophrenia. *FEBS J,* 280**,** 5213-27.

Corradetti, M. N., Inoki, K., and Guan, K. L. (2005) The stress-inducted proteins RTP801 and RTP801L are negative regulators of the mammalian target of rapamycin pathway. *J Biol Chem,* 280**,** 9769-72.

Cross, D. A., Alessi, D. R., Cohen, P., Andjelkovich, M., and Hemmings, B. A. (1995) Inhibition of glycogen synthase kinase-3 by insulin mediated by protein kinase B. *Nature,* 378**,** 785-9.

Crowder, R. J., and Freeman, R. S. (2000) Glycogen synthase kinase-3 beta activity is critical for neuronal death caused by inhibiting phosphatidylinositol 3-kinase or Akt but not for death caused by nerve growth factor withdrawal. *J Biol Chem,* 275**,** 34266-71.

Crowther, J. R. (1995) ELISA. Theory and practice. *Methods Mol Biol,* 42**,** 1-218.

Cui, Q., Benowitz, L., and Yin, Y. (2008) Does CNTF mediate the effect of intraocular inflammation on optic nerve regeneration? *Brain,* 131**,** e96; author reply e97.

Cui, Q., Hodgetts, S. I., Hu, Y., Luo, J. M., and Harvey, A. R. (2007) Strain-specific differences in the effects of cyclosporin A and FK506 on the survival and regeneration of axotomized retinal ganglion cells in adult rats. *Neuroscience,* 146**,** 986-99.

Cui, Q., Lu, Q., So, K. F., and Yip, H. K. (1999) CNTF, not other trophic factors, promotes axonal regeneration of axotomized retinal ganglion cells in adult hamsters. *Invest Ophthalmol Vis Sci,* 40**,** 760-6.

Cui, Q., Ren, C., Sollars, P. J., Pickard, G. E., and So, K. F. (2015) The injury resistant ability of melanopsin-expressing intrinsically photosensitive retinal ganglion cells. *Neuroscience,* 284**,** 845-53.

Cui, Q., Yin, Y., and Benowitz, L. I. (2009) The role of macrophages in optic nerve regeneration. *Neuroscience,* 158**,** 1039-48.

Cui, Z., Kang, J., Hu, D., Zhou, J., and Wang, Y. (2014) Oncomodulin/truncated protamine-mediated Nogo-66 receptor small interference RNA delivery promotes axon regeneration in retinal ganglion cells. *Mol Cells,* 37**,** 613-9.

Cumming, G., Fidler, F., and Vaux, D. L. (2007) Error bars in experimental biology. *J Cell Biol,* 177**,** 7-11.

Czauderna, F., Fechtner, M., Dames, S., Aygun, H., Klippel, A., Pronk, G. J., Giese, K., and Kaufmann, J. (2003) Structural variations and stabilising modifications of synthetic siRNAs in mammalian cells. *Nucleic Acids Res,* 31**,** 2705-16.

Danilov, C. A., and Steward, O. (2015) Conditional genetic deletion of PTEN after a spinal cord injury enhances regenerative growth of CST axons and motor function recovery in mice. *Exp Neurol,* 266**,** 147-60.

David, S., and Aguayo, A. J. (1985) Axonal regeneration after crush injury of rat central nervous system fibres innervating peripheral nerve grafts. *J Neurocytol,* 14**,** 1-12.

David, S., Bouchard, C., Tsatas, O., and Giftochristos, N. (1990) Macrophages can modify the nonpermissive nature of the adult mammalian central nervous system. *Neuron,* 5**,** 463-9.

De Lima, S., Koriyama, Y., Kurimoto, T., Oliveira, J. T., Yin, Y., Li, Y., Gilbert, H. Y., Fagiolini, M., Martinez, A. M., and Benowitz, L. (2012) Full-length axon regeneration in the adult mouse optic nerve and partial recovery of simple visual behaviors. *Proc Natl Acad Sci U S A,* 109**,** 9149-54.

Del Olmo-Aguado, S., Nunez-Alvarez, C., Ji, D., Manso, A. G., and Osborne, N. N. (2013) RTP801 immunoreactivity in retinal ganglion cells and its down-regulation in cultured cells protect them from light and cobalt chloride. *Brain Res Bull,* 98**,** 132-44.

Dennis, M. D., Coleman, C. S., Berg, A., Jefferson, L. S., and Kimball, S. R. (2014) REDD1 enhances protein phosphatase 2A-mediated dephosphorylation of Akt to repress mTORC1 signaling. *Sci Signal,* 7**,** ra68.

Deyoung, M. P., Horak, P., Sofer, A., Sgroi, D., and Ellisen, L. W. (2008) Hypoxia regulates TSC1/2-mTOR signaling and tumor suppression through REDD1-mediated 14-3-3 shuttling. *Genes Dev,* 22**,** 239-51.

Dill, J., Wang, H., Zhou, F., and Li, S. (2008) Inactivation of glycogen synthase kinase 3 promotes axonal growth and recovery in the CNS. *J Neurosci,* 28**,** 8914-28.

Domeniconi, M., Cao, Z., Spencer, T., Sivasankaran, R., Wang, K., Nikulina, E., Kimura, N., Cai, H., Deng, K., Gao, Y., He, Z., and Filbin, M. (2002) Myelin-associated glycoprotein interacts with the Nogo66 receptor to inhibit neurite outgrowth. *Neuron,* 35**,** 283-90.

Don, A. S., Tsang, C. K., Kazdoba, T. M., D'arcangelo, G., Young, W., and Zheng, X. F. (2012) Targeting mTOR as a novel therapeutic strategy for traumatic CNS injuries. *Drug Discov Today,* 17**,** 861-8.

Don, A. S., and Zheng, X. F. (2011) Recent clinical trials of mTOR-targeted cancer therapies. *Rev Recent Clin Trials,* 6**,** 24-35.

Douglas, M. R., Morrison, K. C., Jacques, S. J., Leadbeater, W. E., Gonzalez, A. M., Berry, M., Logan, A., and Ahmed, Z. (2009) Off-target effects of epidermal growth factor receptor antagonists mediate retinal ganglion cell disinhibited axon growth. *Brain,* 132**,** 3102-21.

Duan, X., Qiao, M., Bei, F., Kim, I. J., He, Z., and Sanes, J. R. (2015) Subtype-Specific Regeneration of Retinal Ganglion Cells following Axotomy: Effects of Osteopontin and mTOR Signaling. *Neuron,* 85**,** 1244-56.

Eickholt, B. J., Walsh, F. S., and Doherty, P. (2002) An inactive pool of GSK-3 at the leading edge of growth cones is implicated in Semaphorin 3A signaling. *J Cell Biol,* 157**,** 211-7.

Elbashir, S. M., Harborth, J., Lendeckel, W., Yalcin, A., Weber, K., and Tuschl, T. (2001) Duplexes of 21-nucleotide RNAs mediate RNA interference in cultured mammalian cells. *Nature,* 411**,** 494-8.

Eldar-Finkelman, H., and Martinez, A. (2011) GSK-3 Inhibitors: Preclinical and Clinical Focus on CNS. *Front Mol Neurosci,* 4**,** 32.

Ennos, R. 2007. *Statistical and Data Handling Skills in Biology,* Harlow, Essex, UK, Pearson Education Limited.

Ergorul, C., Ray, A., Huang, W., Wang, D. Y., Ben, Y., Cantuti-Castelvetri, I., and Grosskreutz, C. L. (2010) Hypoxia inducible factor-1alpha (HIF-1alpha) and some HIF-1 target genes are elevated in experimental glaucoma. *J Mol Neurosci,* 42**,** 183-91.

Fedorov, Y., Anderson, E. M., Birmingham, A., Reynolds, A., Karpilow, J., Robinson, K., Leake, D., Marshall, W. S., and Khvorova, A. (2006) Off-target effects by siRNA can induce toxic phenotype. *RNA,* 12**,** 1188-96.

Feinstein, E., Ashush, H., Kleinman, M. E., Nozaki, M., Kalinski, H., Mett, I., and Ambati, J. 2009. PF-0423655 (REDD14), an siRNA Compound Targeting RTP801, Penetrates Retinal Cells Producing Target Gene Knockdown and Avoiding TLR Activation. *Association for Research in Vision and Ophthalmology (ARVO).* ARVO.

Fenrich, K., and Gordon, T. (2004) Canadian Association of Neuroscience review: axonal regeneration in the peripheral and central nervous systems--current issues and advances. *Can J Neurol Sci,* 31**,** 142-56.

Fire, A., Xu, S., Montgomery, M. K., Kostas, S. A., Driver, S. E., and Mello, C. C. (1998) Potent and specific genetic interference by double-stranded RNA in Caenorhabditis elegans. *Nature,* 391**,** 806-11.

Fischer, A. B. (1975) Gentamicin as a bactericidal antibiotic in tissue culture. *Med Microbiol Immunol,* 161**,** 23-39.

Fischer, D., Hauk, T. G., Muller, A., and Thanos, S. (2008) Crystallins of the beta/gamma-superfamily mimic the effects of lens injury and promote axon regeneration. *Mol Cell Neurosci,* 37**,** 471-9.

Fischer, D., He, Z., and Benowitz, L. I. (2004a) Counteracting the Nogo receptor enhances optic nerve regeneration if retinal ganglion cells are in an active growth state. *J Neurosci,* 24**,** 1646-51.

Fischer, D., and Leibinger, M. (2012) Promoting optic nerve regeneration. *Prog Retin Eye Res,* 31**,** 688-701.

Fischer, D., Pavlidis, M., and Thanos, S. (2000) Cataractogenic lens injury prevents traumatic ganglion cell death and promotes axonal regeneration both in vivo and in culture. *Invest Ophthalmol Vis Sci,* 41**,** 3943-54.

Fischer, D., Petkova, V., Thanos, S., and Benowitz, L. I. (2004b) Switching mature retinal ganglion cells to a robust growth state in vivo: gene expression and synergy with RhoA inactivation. *J Neurosci,* 24**,** 8726-40.

Forsbach, A., Nemorin, J. G., Montino, C., Muller, C., Samulowitz, U., Vicari, A. P., Jurk, M., Mutwiri, G. K., Krieg, A. M., Lipford, G. B., and Vollmer, J. (2008) Identification of RNA sequence motifs stimulating sequence-specific TLR8-dependent immune responses. *J Immunol,* 180**,** 3729-38.

Fournier, A. E., Takizawa, B. T., and Strittmatter, S. M. (2003) Rho kinase inhibition enhances axonal regeneration in the injured CNS. *J Neurosci,* 23**,** 1416-23.

Fujita, Y., and Yamashita, T. (2014) Axon growth inhibition by RhoA/ROCK in the central nervous system. *Front Neurosci,* 8**,** 338.

Fukata, Y., Itoh, T. J., Kimura, T., Menager, C., Nishimura, T., Shiromizu, T., Watanabe, H., Inagaki, N., Iwamatsu, A., Hotani, H., and Kaibuchi, K. (2002) CRMP-2 binds to tubulin heterodimers to promote microtubule assembly. *Nat Cell Biol,* 4**,** 583-91.

Gallant, P. E. (2000) Axonal protein synthesis and transport. *J Neurocytol,* 29**,** 779-82.

Gao, H., Zhang, H. L., Shou, J., Chen, L., Shen, Y., Tang, Q., Huang, J., and Zhu, J. (2012) Towards retinal ganglion cell regeneration. *Regen Med,* 7**,** 865-75.

Gao, Y., Nikulina, E., Mellado, W., and Filbin, M. T. (2003) Neurotrophins elevate cAMP to reach a threshold required to overcome inhibition by MAG through extracellular signal-regulated kinase-dependent inhibition of phosphodiesterase. *J Neurosci,* 23**,** 11770-7.

Garrido, J. J., Simon, D., Varea, O., and Wandosell, F. (2007) GSK3 alpha and GSK3 beta are necessary for axon formation. *FEBS Lett,* 581**,** 1579-86.

Geoffroy, C. G., Lorenzana, A. O., Kwan, J. P., Lin, K., Ghassemi, O., Ma, A., Xu, N., Creger, D., Liu, K., He, Z., and Zheng, B. (2015) Effects of PTEN and Nogo Codeletion on Corticospinal Axon Sprouting and Regeneration in Mice. *J Neurosci,* 35**,** 6413-28.

Geoffroy, C. G., and Zheng, B. (2014) Myelin-associated inhibitors in axonal growth after CNS injury. *Curr Opin Neurobiol,* 27C**,** 31-38.

Gingras, A. C., Kennedy, S. G., O'leary, M. A., Sonenberg, N., and Hay, N. (1998) 4E-BP1, a repressor of mRNA translation, is phosphorylated and inactivated by the Akt(PKB) signaling pathway. *Genes Dev,* 12**,** 502-13.

Gobrecht, P., Leibinger, M., Andreadaki, A., and Fischer, D. (2014) Sustained GSK3 activity markedly facilitates nerve regeneration. *Nat Commun,* 5**,** 4561.

Goldberg, J. L. (2003) How does an axon grow? *Genes Dev,* 17**,** 941-58.

Goldberg, J. L., Espinosa, J. S., Xu, Y., Davidson, N., Kovacs, G. T., and Barres, B. A. (2002a) Retinal ganglion cells do not extend axons by default: promotion by neurotrophic signaling and electrical activity. *Neuron,* 33**,** 689-702.

Goldberg, J. L., Klassen, M. P., Hua, Y., and Barres, B. A. (2002b) Amacrine-signaled loss of intrinsic axon growth ability by retinal ganglion cells. *Science,* 296**,** 1860-4.

Goold, R. G., and Gordon-Weeks, P. R. (2004) Glycogen synthase kinase 3beta and the regulation of axon growth. *Biochem Soc Trans,* 32**,** 809-11.

Goold, R. G., Owen, R., and Gordon-Weeks, P. R. (1999) Glycogen synthase kinase 3beta phosphorylation of microtubule-associated protein 1B regulates the stability of microtubules in growth cones. *J Cell Sci,* 112 (Pt 19)**,** 3373-84.

Gordon, B. S., Williamson, D. L., Lang, C. H., Jefferson, L. S., and Kimball, S. R. (2015) Nutrient-Induced Stimulation of Protein Synthesis in Mouse Skeletal Muscle Is Limited by the mTORC1 Repressor REDD1. *J Nutr*.

Gouti, M., Tsakiridis, A., Wymeersch, F. J., Huang, Y., Kleinjung, J., Wilson, V., and Briscoe, J. (2014) In vitro generation of neuromesodermal progenitors reveals distinct roles for wnt signalling in the specification of spinal cord and paraxial mesoderm identity. *PLoS Biol,* 12**,** e1001937.

Grandpre, T., Nakamura, F., Vartanian, T., and Strittmatter, S. M. (2000) Identification of the Nogo inhibitor of axon regeneration as a Reticulon protein. *Nature,* 403**,** 439-44.

Grimm, D., Wang, L., Lee, J. S., Schurmann, N., Gu, S., Borner, K., Storm, T. A., and Kay, M. A. (2010) Argonaute proteins are key determinants of RNAi efficacy, toxicity, and persistence in the adult mouse liver. *J Clin Invest,* 120**,** 3106-19.

Guenther, E., Schmid, S., Grantyn, R., and Zrenner, E. (1994) In vitro identification of retinal ganglion cells in culture without the need of dye labeling. *J Neurosci Methods,* 51**,** 177-81.

Guzman-Aranguez, A., Loma, P., and Pintor, J. (2013) Small-interfering RNAs (siRNAs) as a promising tool for ocular therapy. *Br J Pharmacol,* 170**,** 730-47.

Gwinn, D. M., Shackelford, D. B., Egan, D. F., Mihaylova, M. M., Mery, A., Vasquez, D. S., Turk, B. E., and Shaw, R. J. (2008) AMPK phosphorylation of raptor mediates a metabolic checkpoint. *Mol Cell,* 30**,** 214-26.

Hamano, K., Kiyama, H., Emson, P. C., Manabe, R., Nakauchi, M., and Tohyama, M. (1990) Localization of two calcium binding proteins, calbindin (28 kD) and parvalbumin (12 kD), in the vertebrate retina. *J Comp Neurol,* 302**,** 417-24.

Hamar, P., Song, E., Kokeny, G., Chen, A., Ouyang, N., and Lieberman, J. (2004) Small interfering RNA targeting Fas protects mice against renal ischemia-reperfusion injury. *Proc Natl Acad Sci U S A,* 101**,** 14883-8.

Hara, K., Yonezawa, K., Weng, Q. P., Kozlowski, M. T., Belham, C., and Avruch, J. (1998) Amino acid sufficiency and mTOR regulate p70 S6 kinase and eIF-4E BP1 through a common effector mechanism. *J Biol Chem,* 273**,** 14484-94.

Harada, T., Harada, C., Kohsaka, S., Wada, E., Yoshida, K., Ohno, S., Mamada, H., Tanaka, K., Parada, L. F., and Wada, K. (2002) Microglia-Muller glia cell interactions control neurotrophic factor production during light-induced retinal degeneration. *J Neurosci,* 22**,** 9228-36.

Hattar, S., Liao, H. W., Takao, M., Berson, D. M., and Yau, K. W. (2002) Melanopsin-containing retinal ganglion cells: architecture, projections, and intrinsic photosensitivity. *Science,* 295**,** 1065-70.

Hauk, T. G., Leibinger, M., Muller, A., Andreadaki, A., Knippschild, U., and Fischer, D. (2010) Stimulation of axon regeneration in the mature optic nerve by intravitreal application of the toll-like receptor 2 agonist Pam3Cys. *Invest Ophthalmol Vis Sci,* 51**,** 459-64.

Hauk, T. G., Muller, A., Lee, J., Schwendener, R., and Fischer, D. (2008) Neuroprotective and axon growth promoting effects of intraocular inflammation do not depend on oncomodulin or the presence of large numbers of activated macrophages. *Exp Neurol,* 209**,** 469-82.

Hay, N. (2005) The Akt-mTOR tango and its relevance to cancer. *Cancer Cell,* 8**,** 179-83.

Hay, N., and Sonenberg, N. (2004) Upstream and downstream of mTOR. *Genes Dev,* 18**,** 1926-45.

Hellstrom, M., and Harvey, A. R. (2014) Cyclic AMP and the regeneration of retinal ganglion cell axons. *Int J Biochem Cell Biol*.

Hellstrom, M., Muhling, J., Ehlert, E. M., Verhaagen, J., Pollett, M. A., Hu, Y., and Harvey, A. R. (2011) Negative impact of rAAV2 mediated expression of SOCS3 on the regeneration of adult retinal ganglion cell axons. *Mol Cell Neurosci,* 46**,** 507-15.

Hernandez, F., De Barreda, E. G., Fuster-Matanzo, A., Goni-Oliver, P., Lucas, J. J., and Avila, J. (2009) The role of GSK3 in Alzheimer disease. *Brain Res Bull,* 80**,** 248-50.

Heskamp, A., Leibinger, M., Andreadaki, A., Gobrecht, P., Diekmann, H., and Fischer, D. (2013) CXCL12 facilitates optic nerve regeneration. *Neurobiol Dis*.

Hetman, M., Cavanaugh, J. E., Kimelman, D., and Xia, Z. (2000) Role of glycogen synthase kinase-3beta in neuronal apoptosis induced by trophic withdrawal. *J Neurosci,* 20**,** 2567-74.

Hida, T., Yamashita, N., Usui, H., Nakamura, F., Sasaki, Y., Kikuchi, A., and Goshima, Y. (2012) GSK3beta/axin-1/beta-catenin complex is involved in semaphorin3A signaling. *J Neurosci,* 32**,** 11905-18.

Hoeffer, C. A., and Klann, E. (2010) mTOR signaling: at the crossroads of plasticity, memory and disease. *Trends Neurosci,* 33**,** 67-75.

Hoeflich, K. P., Luo, J., Rubie, E. A., Tsao, M. S., Jin, O., and Woodgett, J. R. (2000) Requirement for glycogen synthase kinase-3beta in cell survival and NF-kappaB activation. *Nature,* 406**,** 86-90.

Huang, W., Fileta, J., Guo, Y., and Grosskreutz, C. L. (2006) Downregulation of Thy1 in retinal ganglion cells in experimental glaucoma. *Curr Eye Res,* 31**,** 265-71.

Huettner, J. E., and Baughman, R. W. (1986) Primary culture of identified neurons from the visual cortex of postnatal rats. *J Neurosci,* 6**,** 3044-60.

Hughes, K., Nikolakaki, E., Plyte, S. E., Totty, N. F., and Woodgett, J. R. (1993) Modulation of the glycogen synthase kinase-3 family by tyrosine phosphorylation. *EMBO J,* 12**,** 803-8.

Hur, E. M., Saijilafu, Lee, B. D., Kim, S. J., Xu, W. L., and Zhou, F. Q. (2011) GSK3 controls axon growth via CLASP-mediated regulation of growth cone microtubules. *Genes Dev,* 25**,** 1968-81.

Hur, E. M., and Zhou, F. Q. (2010) GSK3 signalling in neural development. *Nat Rev Neurosci,* 11**,** 539-51.

Ichikawa, A., Nakahara, T., Kurauchi, Y., Mori, A., Sakamoto, K., and Ishii, K. (2014) Rapamycin prevents N-methyl-D-aspartate-induced retinal damage through an ERK-dependent mechanism in rats. *J Neurosci Res,* 92**,** 692-702.

Ikenoue, T., Hong, S., and Inoki, K. (2009) Monitoring mammalian target of rapamycin (mTOR) activity. *Methods Enzymol,* 452**,** 165-80.

Inoki, K., Li, Y., Xu, T., and Guan, K. L. (2003a) Rheb GTPase is a direct target of TSC2 GAP activity and regulates mTOR signaling. *Genes Dev,* 17**,** 1829-34.

Inoki, K., Ouyang, H., Zhu, T., Lindvall, C., Wang, Y., Zhang, X., Yang, Q., Bennett, C., Harada, Y., Stankunas, K., Wang, C. Y., He, X., Macdougald, O. A., You, M., Williams, B. O., and Guan, K. L. (2006) TSC2 integrates Wnt and energy signals via a coordinated phosphorylation by AMPK and GSK3 to regulate cell growth. *Cell,* 126**,** 955-68.

Inoki, K., Zhu, T., and Guan, K. L. (2003b) TSC2 mediates cellular energy response to control cell growth and survival. *Cell,* 115**,** 577-90.

Irwin, N., Li, Y. M., O'toole, J. E., and Benowitz, L. I. (2006) Mst3b, a purine-sensitive Ste20-like protein kinase, regulates axon outgrowth. *Proc Natl Acad Sci U S A,* 103**,** 18320-5.

Ishizuka, Y., Kakiya, N., Witters, L. A., Oshiro, N., Shirao, T., Nawa, H., and Takei, N. (2013) AMP-activated protein kinase counteracts brain-derived neurotrophic factor-induced mammalian target of rapamycin complex 1 signaling in neurons. *J Neurochem,* 127**,** 66-77.

Jacinto, E., Facchinetti, V., Liu, D., Soto, N., Wei, S., Jung, S. Y., Huang, Q., Qin, J., and Su, B. (2006) SIN1/MIP1 maintains rictor-mTOR complex integrity and regulates Akt phosphorylation and substrate specificity. *Cell,* 127**,** 125-37.

Jacobs, K. M., Bhave, S. R., Ferraro, D. J., Jaboin, J. J., Hallahan, D. E., and Thotala, D. (2012) GSK-3beta: A Bifunctional Role in Cell Death Pathways. *Int J Cell Biol,* 2012**,** 930710.

Jacobs, S. M., and Van Stavern, G. P. (2013) Neuro-ophthalmic deficits after head trauma. *Curr Neurol Neurosci Rep,* 13**,** 389.

Jaworski, J., and Sheng, M. (2006) The growing role of mTOR in neuronal development and plasticity. *Mol Neurobiol,* 34**,** 205-19.

Jayarama, S., Li, L. C., Ganesh, L., Mardi, D., Kanteti, P., Hay, N., Li, P., and Prabhakar, B. S. (2014) MADD is a downstream target of PTEN in triggering apoptosis. *J Cell Biochem,* 115**,** 261-70.

Jefferies, H. B., Fumagalli, S., Dennis, P. B., Reinhard, C., Pearson, R. B., and Thomas, G. (1997) Rapamycin suppresses 5'TOP mRNA translation through inhibition of p70s6k. *EMBO J,* 16**,** 3693-704.

Jewell, J. L., and Guan, K. L. (2013) Nutrient signaling to mTOR and cell growth. *Trends Biochem Sci,* 38**,** 233-42.

Jo, S. A., Wang, E., and Benowitz, L. I. (1999) Ciliary neurotrophic factor is an axogenesis factor for retinal ganglion cells. *Neuroscience,* 89**,** 579-91.

Johnson, S. C., Rabinovitch, P. S., and Kaeberlein, M. (2013) mTOR is a key modulator of ageing and age-related disease. *Nature,* 493**,** 338-45.

Joos, K. M., Li, C., and Sappington, R. M. (2010) Morphometric changes in the rat optic nerve following short-term intermittent elevations in intraocular pressure. *Invest Ophthalmol Vis Sci,* 51**,** 6431-40.

Kaiser, P. K., Symons, R. C., Shah, S. M., Quinlan, E. J., Tabandeh, H., Do, D. V., Reisen, G., Lockridge, J. A., Short, B., Guerciolini, R., Nguyen, Q. D., and Sirna-027 Study, I. (2010) RNAi-based treatment for neovascular age-related macular degeneration by Sirna-027. *Am J Ophthalmol,* 150**,** 33-39 e2.

Kanamori, A., Catrinescu, M. M., Kanamori, N., Mears, K. A., Beaubien, R., and Levin, L. A. (2010) Superoxide is an associated signal for apoptosis in axonal injury. *Brain,* 133**,** 2612-25.

Kermer, P., Ankerhold, R., Klocker, N., Krajewski, S., Reed, J. C., and Bahr, M. (2000) Caspase-9: involvement in secondary death of axotomized rat retinal ganglion cells in vivo. *Brain Res Mol Brain Res,* 85**,** 144-50.

Kermer, P., Klocker, N., Labes, M., Thomsen, S., Srinivasan, A., and Bahr, M. (1999) Activation of caspase-3 in axotomized rat retinal ganglion cells in vivo. *FEBS Lett,* 453**,** 361-4.

Ketting, R. F., Fischer, S. E., Bernstein, E., Sijen, T., Hannon, G. J., and Plasterk, R. H. (2001) Dicer functions in RNA interference and in synthesis of small RNA involved in developmental timing in C. elegans. *Genes Dev,* 15**,** 2654-9.

Ki, K. H., Park Do, Y., Lee, S. H., Kim, N. Y., Choi, B. M., and Noh, G. J. (2010) The optimal concentration of siRNA for gene silencing in primary cultured astrocytes and microglial cells of rats. *Korean J Anesthesiol,* 59**,** 403-10.

King, T. D., Bijur, G. N., and Jope, R. S. (2001) Caspase-3 activation induced by inhibition of mitochondrial complex I is facilitated by glycogen synthase kinase-3beta and attenuated by lithium. *Brain Res,* 919**,** 106-14.

Kirshenboim, N., Plotkin, B., Shlomo, S. B., Kaidanovich-Beilin, O., and Eldar-Finkelman, H. (2004) Lithium-mediated phosphorylation of glycogen synthase kinase-3beta involves PI3 kinase-dependent activation of protein kinase C-alpha. *J Mol Neurosci,* 24**,** 237-45.

Kleinman, M. E., Yamada, K., Takeda, A., Chandrasekaran, V., Nozaki, M., Baffi, J. Z., Albuquerque, R. J., Yamasaki, S., Itaya, M., Pan, Y., Appukuttan, B., Gibbs, D., Yang, Z., Kariko, K., Ambati, B. K., Wilgus,

T. A., Dipietro, L. A., Sakurai, E., Zhang, K., Smith, J. R., Taylor, E. W., and Ambati, J. (2008) Sequence- and target-independent angiogenesis suppression by siRNA via TLR3. *Nature,* 452**,** 591-7.

Koch, J. C., Tonges, L., Barski, E., Michel, U., Bahr, M., and Lingor, P. (2014a) ROCK2 is a major regulator of axonal degeneration, neuronal death and axonal regeneration in the CNS. *Cell Death Dis,* 5**,** e1225.

Koch, J. C., Tonges, L., Michel, U., Bahr, M., and Lingor, P. (2014b) Viral vector-mediated downregulation of RhoA increases survival and axonal regeneration of retinal ganglion cells. *Front Cell Neurosci,* 8**,** 273.

Koeberle, P. D., and Bahr, M. (2004) Growth and guidance cues for regenerating axons: where have they gone? *J Neurobiol,* 59**,** 162-80.

Koeberle, P. D., and Ball, A. K. (1998) Effects of GDNF on retinal ganglion cell survival following axotomy. *Vision Res,* 38**,** 1505-15.

Koeberle, P. D., and Ball, A. K. (2002) Neurturin enhances the survival of axotomized retinal ganglion cells in vivo: combined effects with glial cell line-derived neurotrophic factor and brain-derived neurotrophic factor. *Neuroscience,* 110**,** 555-67.

Krishnamoorthy, R. R., Agarwal, P., Prasanna, G., Vopat, K., Lambert, W., Sheedlo, H. J., Pang, I. H., Shade, D., Wordinger, R. J., Yorio, T., Clark, A. F., and Agarwal, N. (2001) Characterization of a transformed rat retinal ganglion cell line. *Brain Res Mol Brain Res,* 86**,** 1-12.

Krishnamoorthy, R. R., Clark, A. F., Daudt, D., Vishwanatha, J. K., and Yorio, T. (2013) A forensic path to RGC-5 cell line identification: lessons learned. *Invest Ophthalmol Vis Sci,* 54**,** 5712-9.

Kurimoto, T., Yin, Y., Habboub, G., Gilbert, H. Y., Li, Y., Nakao, S., Hafezi-Moghadam, A., and Benowitz, L. I. (2013) Neutrophils express oncomodulin and promote optic nerve regeneration. *J Neurosci,* 33**,** 14816-24.

Kurimoto, T., Yin, Y., Omura, K., Gilbert, H. Y., Kim, D., Cen, L. P., Moko, L., Kugler, S., and Benowitz, L. I. (2010) Long-distance axon regeneration in the mature optic nerve: contributions of oncomodulin, cAMP, and pten gene deletion. *J Neurosci,* 30**,** 15654-63.

Laplante, M., and Sabatini, D. M. (2012) mTOR signaling in growth control and disease. *Cell,* 149**,** 274-93.

Laplante, M., and Sabatini, D. M. (2013) Regulation of mTORC1 and its impact on gene expression at a glance. *J Cell Sci,* 126**,** 1713-9.

Lasham, A., Herbert, M., Coppieters 'T Wallant, N., Patel, R., Feng, S., Eszes, M., Cao, H., and Reid, G. (2010) A rapid and sensitive method to detect siRNA-mediated mRNA cleavage in vivo using 5' RACE and a molecular beacon probe. *Nucleic Acids Res,* 38**,** e19.

Lazic, S. E. (2010) The problem of pseudoreplication in neuroscientific studies: is it affecting your analysis? *BMC Neurosci,* 11**,** 5.

Leaver, S. G., Cui, Q., Plant, G. W., Arulpragasam, A., Hisheh, S., Verhaagen, J., and Harvey, A. R. (2006) AAV-mediated expression of CNTF promotes long-term survival and regeneration of adult rat retinal ganglion cells. *Gene Ther,* 13**,** 1328-41.

Lee, D. H., Luo, X., Yungher, B. J., Bray, E., Lee, J. K., and Park, K. K. (2014) Mammalian Target of Rapamycin's Distinct Roles and Effectiveness in Promoting Compensatory Axonal Sprouting in the Injured CNS. *J Neurosci,* 34**,** 15347-55.

Lee, D. U., Huang, W., Rittenhouse, K. D., and Jessen, B. (2012) Retina expression and cross-species validation of gene silencing by PF-655, a small interfering RNA against RTP801 for the treatment of ocular disease. *J Ocul Pharmacol Ther,* 28**,** 222-30.

Lee, V., Ford, R. L., Xing, W., Bunce, C., and Foot, B. (2010) Surveillance of traumatic optic neuropathy in the UK. *Eye (Lond),* 24**,** 240-50.

Legacy, J., Hanea, S., Theoret, J., and Smith, P. D. (2013) Granulocyte macrophage colony-stimulating factor promotes regeneration of retinal ganglion cells in vitro through a mammalian target of rapamycin-dependent mechanism. *J Neurosci Res,* 91**,** 771-9.

Lehmann, M., Fournier, A., Selles-Navarro, I., Dergham, P., Sebok, A., Leclerc, N., Tigyi, G., and Mckerracher, L. (1999) Inactivation of Rho signaling pathway promotes CNS axon regeneration. *J Neurosci,* 19**,** 7537-47.

Leibinger, M., Andreadaki, A., and Fischer, D. (2012) Role of mTOR in neuroprotection and axon regeneration after inflammatory stimulation. *Neurobiol Dis,* 46**,** 314-24.

Leibinger, M., Muller, A., Andreadaki, A., Hauk, T. G., Kirsch, M., and Fischer, D. (2009) Neuroprotective and axon growth-promoting effects following inflammatory stimulation on mature retinal ganglion cells in mice depend on ciliary neurotrophic factor and leukemia inhibitory factor. *J Neurosci,* 29**,** 14334-41.

Leon, S., Yin, Y., Nguyen, J., Irwin, N., and Benowitz, L. I. (2000) Lens injury stimulates axon regeneration in the mature rat optic nerve. *J Neurosci,* 20**,** 4615-26.

Levere, T. E. (1978) The primary visual system of the rat: A primer of its anatomy. *Physiological Psychology,* 6**,** 142-169.

Levin, L. A. (2005) Retinal ganglion cells and supporting elements in culture. *J Glaucoma,* 14**,** 305-7.

Levin, L. A., Beck, R. W., Joseph, M. P., Seiff, S., and Kraker, R. (1999) The treatment of traumatic optic neuropathy: the International Optic Nerve Trauma Study. *Ophthalmology,* 106**,** 1268-77.

Lewis, G. M., and Kucenas, S. (2014) Perineurial glia are essential for motor axon regrowth following nerve injury. *J Neurosci,* 34**,** 12762-77.

Li, C. Y., Li, X., Liu, S. F., Qu, W. S., Wang, W., and Tian, D. S. (2015) Inhibition of mTOR pathway restrains astrocyte proliferation, migration and production of inflammatory mediators after oxygen-glucose deprivation and reoxygenation. *Neurochem Int,* 83-84**,** 9-18.

Li, D., Field, P. M., and Raisman, G. (1996) Connectional specification of regenerating entorhinal projection neuron classes cannot be overridden by altered target availability in postnatal organotypic slice co-culture. *Exp Neurol,* 142**,** 151-60.

Li, D., Field, P. M., Yoshioka, N., and Raisman, G. (1994) Axons regenerate with correct specificity in horizontal slice culture of the postnatal rat entorhino-hippocampal system. *Eur J Neurosci,* 6**,** 1026-37.

Li, R. S., Chen, B. Y., Tay, D. K., Chan, H. H., Pu, M. L., and So, K. F. (2006) Melanopsin-expressing retinal ganglion cells are more injury-resistant in a chronic ocular hypertension model. *Invest Ophthalmol Vis Sci,* 47**,** 2951-8.

Li, S. Y., Yau, S. Y., Chen, B. Y., Tay, D. K., Lee, V. W., Pu, M. L., Chan, H. H., and So, K. F. (2008) Enhanced survival of melanopsin-expressing retinal ganglion cells after injury is associated with the PI3 K/Akt pathway. *Cell Mol Neurobiol,* 28**,** 1095-107.

Liang, M. H., and Chuang, D. M. (2007) Regulation and function of glycogen synthase kinase-3 isoforms in neuronal survival. *J Biol Chem,* 282**,** 3904-17.

Lichtman, J. W., and Conchello, J. A. (2005) Fluorescence microscopy. *Nat Methods,* 2**,** 910-9.

Lilley, S., and Robbins, J. (2005) The rat retinal ganglion cell in culture: an accessible CNS neurone. *J Pharmacol Toxicol Methods,* 51**,** 209-20.

Lin, Y., and Wen, L. (2013) Inflammatory response following diffuse axonal injury. *Int J Med Sci,* 10**,** 515-21.

Lindqvist, N., Liu, Q., Zajadacz, J., Franze, K., and Reichenbach, A. (2010) Retinal glial (Muller) cells: sensing and responding to tissue stretch. *Invest Ophthalmol Vis Sci,* 51**,** 1683-90.

Lingor, P., Teusch, N., Schwarz, K., Mueller, R., Mack, H., Bahr, M., and Mueller, B. K. (2007) Inhibition of Rho kinase (ROCK) increases neurite outgrowth on chondroitin sulphate proteoglycan in vitro and axonal regeneration in the adult optic nerve in vivo. *J Neurochem,* 103**,** 181-9.

Lingor, P., Tonges, L., Pieper, N., Bermel, C., Barski, E., Planchamp, V., and Bahr, M. (2008) ROCK inhibition and CNTF interact on intrinsic signalling pathways and differentially regulate survival and regeneration in retinal ganglion cells. *Brain,* 131**,** 250-63.

Liu, C. M., Hur, E. M., and Zhou, F. Q. (2012) Coordinating Gene Expression and Axon Assembly to Control Axon Growth: Potential Role of GSK3 Signaling. *Front Mol Neurosci,* 5**,** 3.

Liu, K., Lu, Y., Lee, J. K., Samara, R., Willenberg, R., Sears-Kraxberger, I., Tedeschi, A., Park, K. K., Jin, D., Cai, B., Xu, B., Connolly, L., Steward, O., Zheng, B., and He, Z. (2010a) PTEN deletion enhances the regenerative ability of adult corticospinal neurons. *Nat Neurosci,* 13**,** 1075-81.

Liu, K., Tedeschi, A., Park, K. K., and He, Z. (2011) Neuronal intrinsic mechanisms of axon regeneration. *Annu Rev Neurosci,* 34**,** 131-52.

Liu, L., Luo, Y., Chen, L., Shen, T., Xu, B., Chen, W., Zhou, H., Han, X., and Huang, S. (2010b) Rapamycin inhibits cytoskeleton reorganization and cell motility by suppressing RhoA expression and activity. *J Biol Chem,* 285**,** 38362-73.

Livak, K. J., and Schmittgen, T. D. (2001) Analysis of relative gene expression data using real-time quantitative PCR and the 2(-Delta Delta C(T)) Method. *Methods,* 25**,** 402-8.

Liz, M. A., Mar, F. M., Santos, T. E., Pimentel, H. I., Marques, A. M., Morgado, M. M., Vieira, S., Sousa, V. F., Pemble, H., Wittmann, T., Sutherland, C., Woodgett, J. R., and Sousa, M. M. (2014) Neuronal deletion of GSK3beta increases microtubule speed in the growth cone and enhances axon regeneration via CRMP-2 and independently of MAP1B and CLASP2. *BMC Biol,* 12**,** 47.

Loberg, R. D., Vesely, E., and Brosius, F. C., 3rd (2002) Enhanced glycogen synthase kinase-3beta activity mediates hypoxia-induced apoptosis of vascular smooth muscle cells and is prevented by glucose transport and metabolism. *J Biol Chem,* 277**,** 41667-73.

Logan, A., Ahmed, Z., Baird, A., Gonzalez, A. M., and Berry, M. (2006) Neurotrophic factor synergy is required for neuronal survival and disinhibited axon regeneration after CNS injury. *Brain,* 129**,** 490-502.

Logan, A., and Berry, M. (2002) Cellular and molecular determinants of glial scar formation. *Adv Exp Med Biol,* 513**,** 115-58.

Logan, A., Oliver, J. J., and Berry, M. (1994) Growth factors in CNS repair and regeneration. *Prog Growth Factor Res,* 5**,** 379-405.

Lonze, B. E., and Ginty, D. D. (2002) Function and regulation of CREB family transcription factors in the nervous system. *Neuron,* 35**,** 605-23.

Lonze, B. E., Riccio, A., Cohen, S., and Ginty, D. D. (2002) Apoptosis, axonal growth defects, and degeneration of peripheral neurons in mice lacking CREB. *Neuron,* 34**,** 371-85.

Lorber, B., Berry, M., Douglas, M. R., Nakazawa, T., and Logan, A. (2009a) Activated retinal glia promote neurite outgrowth of retinal ganglion cells via apolipoprotein E. *J Neurosci Res,* 87**,** 2645-52.

Lorber, B., Berry, M., and Logan, A. (2005) Lens injury stimulates adult mouse retinal ganglion cell axon regeneration via both macrophage- and lens-derived factors. *Eur J Neurosci,* 21**,** 2029-34.

Lorber, B., Berry, M., and Logan, A. (2008) Different factors promote axonal regeneration of adult rat retinal ganglion cells after lens injury and intravitreal peripheral nerve grafting. *J Neurosci Res,* 86**,** 894-903.

Lorber, B., Berry, M., Logan, A., and Tonge, D. (2002) Effect of lens lesion on neurite outgrowth of retinal ganglion cells in vitro. *Mol Cell Neurosci,* 21**,** 301-11.

Lorber, B., Guidi, A., Fawcett, J. W., and Martin, K. R. (2012) Activated retinal glia mediated axon regeneration in experimental glaucoma. *Neurobiol Dis,* 45**,** 243-52.

Lorber, B., Howe, M. L., Benowitz, L. I., and Irwin, N. (2009b) Mst3b, an Ste20-like kinase, regulates axon regeneration in mature CNS and PNS pathways. *Nat Neurosci,* 12**,** 1407-14.

Lund, R. D. (1965) Uncrossed Visual Pathways of Hooded and Albino Rats. *Science,* 149**,** 1506-7.

Luo, X., Salgueiro, Y., Beckerman, S. R., Lemmon, V. P., Tsoulfas, P., and Park, K. K. (2013) Three-dimensional evaluation of retinal ganglion cell axon regeneration and pathfinding in whole mouse tissue after injury. *Exp Neurol*.

Ma, L., Chen, Z., Erdjument-Bromage, H., Tempst, P., and Pandolfi, P. P. (2005) Phosphorylation and functional inactivation of TSC2 by Erk implications for tuberous sclerosis and cancer pathogenesis. *Cell,* 121**,** 179-93.

Ma, T. C., Barco, A., Ratan, R. R., and Willis, D. E. (2014) cAMP-responsive element-binding protein (CREB) and cAMP co-regulate activator protein 1 (AP1)-dependent regeneration-associated gene expression and neurite growth. *J Biol Chem,* 289**,** 32914-25.

Ma, X. M., and Blenis, J. (2009) Molecular mechanisms of mTOR-mediated translational control. *Nat Rev Mol Cell Biol,* 10**,** 307-18.

Mahapatra, A. K., and Tandon, D. A. (1993) Traumatic optic neuropathy in children: a prospective study. *Pediatr Neurosurg,* 19**,** 34-9.

Maiese, K. (2014) Driving neural regeneration through the mammalian target of rapamycin. *Neural Regen Res,* 9**,** 1413-7.

Maiese, K., Chong, Z. Z., Shang, Y. C., and Wang, S. (2013) mTOR: on target for novel therapeutic strategies in the nervous system. *Trends Mol Med,* 19**,** 51-60.

Maiese, K., Li, F., Chong, Z. Z., and Shang, Y. C. (2008) The Wnt signaling pathway: aging gracefully as a protectionist? *Pharmacol Ther,* 118**,** 58-81.

Malagelada, C., Jin, Z. H., and Greene, L. A. (2008) RTP801 is induced in Parkinson's disease and mediates neuron death by inhibiting Akt phosphorylation/activation. *J Neurosci,* 28**,** 14363-71.

Malagelada, C., Jin, Z. H., Jackson-Lewis, V., Przedborski, S., and Greene, L. A. (2010) Rapamycin protects against neuron death in in vitro and in vivo models of Parkinson's disease. *J Neurosci,* 30**,** 1166-75.

Malagelada, C., Lopez-Toledano, M. A., Willett, R. T., Jin, Z. H., Shelanski, M. L., and Greene, L. A. (2011) RTP801/REDD1 regulates the timing of cortical neurogenesis and neuron migration. *J Neurosci,* 31**,** 3186-96.

Malagelada, C., Ryu, E. J., Biswas, S. C., Jackson-Lewis, V., and Greene, L. A. (2006) RTP801 is elevated in Parkinson brain substantia nigral neurons and mediates death in cellular models of Parkinson's disease by a mechanism involving mammalian target of rapamycin inactivation. *J Neurosci,* 26**,** 9996-10005.

Malik, A. R., Urbanska, M., Macias, M., Skalecka, A., and Jaworski, J. (2012) Beyond control of protein translation: What we have learned about the non-canonical regulation and function of mammalian target of rapamycin (mTOR). *Biochim Biophys Acta*.

Malik, J. M., Shevtsova, Z., Bahr, M., and Kugler, S. (2005) Long-term in vivo inhibition of CNS neurodegeneration by Bcl-XL gene transfer. *Mol Ther,* 11**,** 373-81.

Manns, R. P., Cook, G. M., Holt, C. E., and Keynes, R. J. (2012) Differing semaphorin 3A concentrations trigger distinct signaling mechanisms in growth cone collapse. *J Neurosci,* 32**,** 8554-9.

Manthorpe, M., Engvall, E., Ruoslahti, E., Longo, F. M., Davis, G. E., and Varon, S. (1983) Laminin promotes neuritic regeneration from cultured peripheral and central neurons. *J Cell Biol,* 97**,** 1882-90.

Mar, F. M., Bonni, A., and Sousa, M. M. (2014) Cell intrinsic control of axon regeneration. *EMBO Rep,* 15**,** 254-63.

Marcus, R. C., Wang, L. C., and Mason, C. A. (1996) Retinal axon divergence in the optic chiasm: midline cells are unaffected by the albino mutation. *Development,* 122**,** 859-68.

Martin, K. J., Shpiro, N., Traynor, R., Elliott, M., and Arthur, J. S. (2011) Comparison of the specificity of Trk inhibitors in recombinant and neuronal assays. *Neuropharmacology,* 61**,** 148-55.

Mcmanus, E. J., Sakamoto, K., Armit, L. J., Ronaldson, L., Shpiro, N., Marquez, R., and Alessi, D. R. (2005) Role that phosphorylation of GSK3 plays in insulin and Wnt signalling defined by knockin analysis. *EMBO J,* 24**,** 1571-83.

Mead, B., Logan, A., Berry, M., Leadbeater, W., and Scheven, B. A. (2013) Intravitreally transplanted dental pulp stem cells promote neuroprotection and axon regeneration of retinal ganglion cells after optic nerve injury. *Invest Ophthalmol Vis Sci,* 54**,** 7544-56.

Mead, B., Thompson, A., Scheven, B. A., Logan, A., Berry, M., and Leadbeater, W. (2014) Comparative evaluation of methods for estimating retinal ganglion cell loss in retinal sections and wholemounts. *PLoS One,* 9**,** e110612.

Meijer, L., Flajolet, M., and Greengard, P. (2004) Pharmacological inhibitors of glycogen synthase kinase 3. *Trends Pharmacol Sci,* 25**,** 471-80.

Mendes, C. T., Mury, F. B., De Sa Moreira, E., Alberto, F. L., Forlenza, O. V., Dias-Neto, E., and Gattaz, W. F. (2009) Lithium reduces Gsk3b mRNA levels: implications for Alzheimer Disease. *Eur Arch Psychiatry Clin Neurosci,* 259**,** 16-22.

Mey, J., and Thanos, S. (1993) Intravitreal injections of neurotrophic factors support the survival of axotomized retinal ganglion cells in adult rats in vivo. *Brain Res,* 602**,** 304-17.

Meyer-Franke, A., Wilkinson, G. A., Kruttgen, A., Hu, M., Munro, E., Hanson, M. G., Jr., Reichardt, L. F., and Barres, B. A. (1998) Depolarization and cAMP elevation rapidly recruit TrkB to the plasma membrane of CNS neurons. *Neuron,* 21**,** 681-93.

Meyuhas, O. (2000) Synthesis of the translational apparatus is regulated at the translational level. *Eur J Biochem,* 267**,** 6321-30.

Mi, S., Sandrock, A., and Miller, R. H. (2008) LINGO-1 and its role in CNS repair. *Int J Biochem Cell Biol,* 40**,** 1971-8.

Mills, C. N., Nowsheen, S., Bonner, J. A., and Yang, E. S. (2011) Emerging roles of glycogen synthase kinase 3 in the treatment of brain tumors. *Front Mol Neurosci,* 4**,** 47.

Mimura, F., Yamagishi, S., Arimura, N., Fujitani, M., Kubo, T., Kaibuchi, K., and Yamashita, T. (2006) Myelin-associated glycoprotein inhibits microtubule assembly by a Rho-kinase-dependent mechanism. *J Biol Chem,* 281**,** 15970-9.

Monnier, P. P., D'onofrio, P. M., Magharious, M., Hollander, A. C., Tassew, N., Szydlowska, K., Tymianski, M., and Koeberle, P. D. (2011) Involvement of caspase-6 and caspase-8 in neuronal apoptosis and the regenerative failure of injured retinal ganglion cells. *J Neurosci,* 31**,** 10494-505.

Monsul, N. T., Geisendorfer, A. R., Han, P. J., Banik, R., Pease, M. E., Skolasky, R. L., Jr., and Hoffman, P. N. (2004) Intraocular injection of dibutyryl cyclic AMP promotes axon regeneration in rat optic nerve. *Exp Neurol,* 186**,** 124-33.

Moore, D. L., Blackmore, M. G., Hu, Y., Kaestner, K. H., Bixby, J. L., Lemmon, V. P., and Goldberg, J. L. (2009) KLF family members regulate intrinsic axon regeneration ability. *Science,* 326**,** 298-301.

Moore, D. L., and Goldberg, J. L. (2010) Four steps to optic nerve regeneration. *J Neuroophthalmol,* 30**,** 347-60.

Morotti, A., Mila, S., Accornero, P., Tagliabue, E., and Ponzetto, C. (2002) K252a inhibits the oncogenic properties of Met, the HGF receptor. *Oncogene,* 21**,** 4885-93.

Morquette, B., Morquette, P., Agostinone, J., Feinstein, E., Mckinney, R. A., Kolta, A., and Di Polo, A. (2014) REDD2-mediated inhibition of mTOR promotes dendrite retraction induced by axonal injury. *Cell Death Differ*.

Muller, A., Hauk, T. G., and Fischer, D. (2007) Astrocyte-derived CNTF switches mature RGCs to a regenerative state following inflammatory stimulation. *Brain,* 130**,** 3308-20.

Muller, A., Hauk, T. G., Leibinger, M., Marienfeld, R., and Fischer, D. (2009) Exogenous CNTF stimulates axon regeneration of retinal ganglion cells partially via endogenous CNTF. *Mol Cell Neurosci,* 41**,** 233-46.

Murray, A. J., and Shewan, D. A. (2008) Epac mediates cyclic AMP-dependent axon growth, guidance and regeneration. *Mol Cell Neurosci,* 38**,** 578-88.

Murray, A. J., Tucker, S. J., and Shewan, D. A. (2009) cAMP-dependent axon guidance is distinctly regulated by Epac and protein kinase A. *J Neurosci,* 29**,** 15434-44.

Nadal-Nicolas, F. M., Jimenez-Lopez, M., Salinas-Navarro, M., Sobrado-Calvo, P., Alburquerque-Bejar, J. J., Vidal-Sanz, M., and Agudo-Barriuso, M. (2012) Whole number, distribution and co-expression of brn3 transcription factors in retinal ganglion cells of adult albino and pigmented rats. *PLoS One,* 7**,** e49830.

Nadal-Nicolas, F. M., Jimenez-Lopez, M., Sobrado-Calvo, P., Nieto-Lopez, L., Canovas-Martinez, I., Salinas-Navarro, M., Vidal-Sanz, M., and Agudo, M. (2009) Brn3a as a marker of retinal ganglion cells: qualitative and quantitative time course studies in naive and optic nerve-injured retinas. *Invest Ophthalmol Vis Sci,* 50**,** 3860-8.

Newman, E., and Reichenbach, A. (1996) The Muller cell: a functional element of the retina. *Trends Neurosci,* 19**,** 307-12.

Nguyen, Q. D., Schachar, R. A., Nduaka, C. I., Sperling, M., Basile, A. S., Klamerus, K. J., Chi-Burris, K., Yan, E., Paggiarino, D. A., Rosenblatt, I., Aitchison, R., Erlich, S. S., and Group, D. C. S. (2012a) Dose-ranging evaluation of intravitreal siRNA PF-04523655 for diabetic macular edema (the DEGAS study). *Invest Ophthalmol Vis Sci,* 53**,** 7666-74.

Nguyen, Q. D., Schachar, R. A., Nduaka, C. I., Sperling, M., Basile, A. S., Klamerus, K. J., Chi-Burris, K., Yan, E., Paggiarino, D. A., Rosenblatt, I., Khan, A., Aitchison, R., Erlich, S. S., and Group, P. F. S. (2012b) Phase 1 dose-escalation study of a siRNA targeting the RTP801 gene in age-related macular degeneration patients. *Eye (Lond),* 26**,** 1099-105.

Nguyen, Q. D., Schachar, R. A., Nduaka, C. I., Sperling, M., Klamerus, K. J., Chi-Burris, K., Yan, E., Paggiarino, D. A., Rosenblatt, I., Aitchison, R., Erlich, S. S., and Group, M. C. S. (2012c) Evaluation of

the siRNA PF-04523655 versus ranibizumab for the treatment of neovascular age-related macular degeneration (MONET Study). *Ophthalmology,* 119**,** 1867-73.

Niederost, B. P., Zimmermann, D. R., Schwab, M. E., and Bandtlow, C. E. (1999) Bovine CNS myelin contains neurite growth-inhibitory activity associated with chondroitin sulfate proteoglycans. *J Neurosci,* 19**,** 8979-89.

Ning, K., Drepper, C., Valori, C. F., Ahsan, M., Wyles, M., Higginbottom, A., Herrmann, T., Shaw, P., Azzouz, M., and Sendtner, M. (2010) PTEN depletion rescues axonal growth defect and improves survival in SMN-deficient motor neurons. *Hum Mol Genet,* 19**,** 3159-68.

Nonaka, S., Hough, C. J., and Chuang, D. M. (1998) Chronic lithium treatment robustly protects neurons in the central nervous system against excitotoxicity by inhibiting N-methyl-D-aspartate receptor-mediated calcium influx. *Proc Natl Acad Sci U S A,* 95**,** 2642-7.

Noseda, R., Belin, S., Piguet, F., Vaccari, I., Scarlino, S., Brambilla, P., Martinelli Boneschi, F., Feltri, M. L., Wrabetz, L., Quattrini, A., Feinstein, E., Huganir, R. L., and Bolino, A. (2013) DDIT4/REDD1/RTP801 is a novel negative regulator of Schwann cell myelination. *J Neurosci,* 33**,** 15295-305.

O'neill, C. (2013) PI3-kinase/Akt/mTOR signaling: Impaired on/off switches in aging, cognitive decline and Alzheimer's disease. *Exp Gerontol,* 48**,** 647-653.

Obara, I., and Hunt, S. P. (2014) Axonal protein synthesis and the regulation of primary afferent function. *Dev Neurobiol,* 74**,** 269-78.

Odell, I. D., and Cook, D. (2013) Immunofluorescence techniques. *J Invest Dermatol,* 133**,** e4.

Ohtake, Y., Park, D., Abdul-Muneer, P. M., Li, H., Xu, B., Sharma, K., Smith, G. M., Selzer, M. E., and Li, S. (2014) The effect of systemic PTEN antagonist peptides on axon growth and functional recovery after spinal cord injury. *Biomaterials,* 35**,** 4610-26.

Owen, R., and Gordon-Weeks, P. R. (2003) Inhibition of glycogen synthase kinase 3beta in sensory neurons in culture alters filopodia dynamics and microtubule distribution in growth cones. *Mol Cell Neurosci,* 23**,** 626-37.

Pap, M., and Cooper, G. M. (1998) Role of glycogen synthase kinase-3 in the phosphatidylinositol 3-Kinase/Akt cell survival pathway. *J Biol Chem,* 273**,** 19929-32.

Papageorgiou, A., Rapley, J., Mesirov, J. P., Tamayo, P., and Avruch, J. (2015) A Genome-Wide siRNA Screen in Mammalian Cells for Regulators of S6 Phosphorylation. *PLoS One,* 10**,** e0116096.

Park, J., Kim, S., Park, S. I., Choe, Y., Li, J., and Han, A. (2014) A microchip for quantitative analysis of CNS axon growth under localized biomolecular treatments. *J Neurosci Methods,* 221**,** 166-74.

Park, K. K., Hu, Y., Muhling, J., Pollett, M. A., Dallimore, E. J., Turnley, A. M., Cui, Q., and Harvey, A. R. (2009) Cytokine-induced SOCS expression is inhibited by cAMP analogue: impact on regeneration in injured retina. *Mol Cell Neurosci,* 41**,** 313-24.

Park, K. K., Liu, K., Hu, Y., Kanter, J. L., and He, Z. (2010) PTEN/mTOR and axon regeneration. *Exp Neurol,* 223**,** 45-50.

Park, K. K., Liu, K., Hu, Y., Smith, P. D., Wang, C., Cai, B., Xu, B., Connolly, L., Kramvis, I., Sahin, M., and He, Z. (2008) Promoting axon regeneration in the adult CNS by modulation of the PTEN/mTOR pathway. *Science,* 322**,** 963-6.

Parrilla-Reverter, G., Agudo, M., Sobrado-Calvo, P., Salinas-Navarro, M., Villegas-Perez, M. P., and Vidal-Sanz, M. (2009) Effects of different neurotrophic factors on the survival of retinal ganglion cells after a complete intraorbital nerve crush injury: a quantitative in vivo study. *Exp Eye Res,* 89**,** 32-41.

Pasieka, A. E., and Morgan, J. F. (1959) Glutamine metabolism of normal and malignant cells cultivated in synthetic media. *Nature,* 183**,** 1201-2.

Pastor, M. D., Garcia-Yebenes, I., Fradejas, N., Perez-Ortiz, J. M., Mora-Lee, S., Tranque, P., Moro, M. A., Pende, M., and Calvo, S. (2009) mTOR/S6 kinase pathway contributes to astrocyte survival during ischemia. *J Biol Chem,* 284**,** 22067-78.

Peace, A. G., and Shewan, D. A. (2011) New perspectives in cyclic AMP-mediated axon growth and guidance: The emerging epoch of Epac. *Brain Res Bull,* 84**,** 280-8.

Pekny, M., and Nilsson, M. (2005) Astrocyte activation and reactive gliosis. *Glia,* 50**,** 427-34.

Pende, M., Um, S. H., Mieulet, V., Sticker, M., Goss, V. L., Mestan, J., Mueller, M., Fumagalli, S., Kozma, S. C., and Thomas, G. (2004) S6K1(-/-)/S6K2(-/-) mice exhibit perinatal lethality and rapamycin-sensitive 5'-terminal oligopyrimidine mRNA translation and reveal a mitogen-activated protein kinase-dependent S6 kinase pathway. *Mol Cell Biol,* 24**,** 3112-24.

Perluigi, M., Di Domenico, F., and Butterfield, D. A. (2015) mTOR signaling in aging and neurodegeneration: At the crossroad between metabolism dysfunction and impairment of autophagy. *Neurobiol Dis*.

Pernet, V., and Di Polo, A. (2006) Synergistic action of brain-derived neurotrophic factor and lens injury promotes retinal ganglion cell survival, but leads to optic nerve dystrophy in vivo. *Brain,* 129**,** 1014-26.

Pernet, V., Joly, S., Dalkara, D., Jordi, N., Schwarz, O., Christ, F., Schaffer, D. V., Flannery, J. G., and Schwab, M. E. (2013) Long-distance axonal regeneration induced by CNTF gene transfer is impaired by axonal misguidance in the injured adult optic nerve. *Neurobiol Dis,* 51**,** 202-13.

Pernet, V., and Schwab, M. E. (2014) Lost in the jungle: new hurdles for optic nerve axon regeneration. *Trends Neurosci*.

Pochet, R., Pasteels, B., Seto-Ohshima, A., Bastianelli, E., Kitajima, S., and Van Eldik, L. J. (1991) Calmodulin and calbindin localization in retina from six vertebrate species. *J Comp Neurol,* 314**,** 750-62.

Polleux, F., and Snider, W. (2010) Initiating and growing an axon. *Cold Spring Harb Perspect Biol,* 2**,** a001925.

Prasad, S., and Galetta, S. L. (2011) Anatomy and physiology of the afferent visual system. *Handb Clin Neurol,* 102**,** 3-19.

Qin, Q., Patil, K., and Sharma, S. C. (2004) The role of Bax-inhibiting peptide in retinal ganglion cell apoptosis after optic nerve transection. *Neurosci Lett,* 372**,** 17-21.

Qu, J., and Jakobs, T. C. (2013) The Time Course of Gene Expression during Reactive Gliosis in the Optic Nerve. *PLoS One,* 8**,** e67094.

Quadrato, G., and Di Giovanni, S. (2013) Waking up the sleepers: shared transcriptional pathways in axonal regeneration and neurogenesis. *Cell Mol Life Sci,* 70**,** 993-1007.

Ramos-Vara, J. A. (2011) Principles and methods of immunohistochemistry. *Methods Mol Biol,* 691**,** 83-96.

Rand, T. A., Ginalski, K., Grishin, N. V., and Wang, X. (2004) Biochemical identification of Argonaute 2 as the sole protein required for RNA-induced silencing complex activity. *Proc Natl Acad Sci U S A,* 101**,** 14385-9.

Rane, S. G., and Reddy, E. P. (2000) Janus kinases: components of multiple signaling pathways. *Oncogene,* 19**,** 5662-79.

Razmara, M., Heldin, C. H., and Lennartsson, J. (2013) Platelet-derived growth factor-induced Akt phosphorylation requires mTOR/Rictor and phospholipase C-gamma1, whereas S6 phosphorylation depends on mTOR/Raptor and phospholipase D. *Cell Commun Signal,* 11**,** 3.

Read, M. L., Mir, S., Spice, R., Seabright, R. J., Suggate, E. L., Ahmed, Z., Berry, M., and Logan, A. (2009) Profiling RNA interference (RNAi)-mediated toxicity in neural cultures for effective short interfering RNA design. *J Gene Med,* 11**,** 523-34.

Richardson, P. M., Mcguinness, U. M., and Aguayo, A. J. (1980) Axons from CNS neurons regenerate into PNS grafts. *Nature,* 284**,** 264-5.

Riechenbach, A., Wolburg, H. 2013. Astrocytes and Ependymal Glia. *In:* KEFFENMANN, H., RANSOM, BR (ed.) *Neuroglia.* 3rd ed.: Oxford University Press.

Ririe, K. M., Rasmussen, R. P., and Wittwer, C. T. (1997) Product differentiation by analysis of DNA melting curves during the polymerase chain reaction. *Anal Biochem,* 245**,** 154-60.

Rittenhouse, K. D., Johnson, T. R., Vicini, P., Hirakawa, B., Kalabat, D., Yang, A. H., Huang, W., and Basile, A. S. (2014) RTP801 gene expression is differentially upregulated in retinopathy and is silenced by PF-04523655, a 19-Mer siRNA directed against RTP801. *Invest Ophthalmol Vis Sci,* 55**,** 1232-40.

Robbins, M., Judge, A., Ambegia, E., Choi, C., Yaworski, E., Palmer, L., Mcclintock, K., and Maclachlan, I. (2008) Misinterpreting the therapeutic effects of small interfering RNA caused by immune stimulation. *Hum Gene Ther,* 19**,** 991-9.

Roberti, G., Mantelli, F., Macchi, I., Massaro-Giordano, M., and Centofanti, M. (2014) Nerve growth factor modulation of retinal ganglion cell physiology. *J Cell Physiol,* 229**,** 1130-3.

Roberts, I., Yates, D., Sandercock, P., Farrell, B., Wasserberg, J., Lomas, G., Cottingham, R., Svoboda, P., Brayley, N., Mazairac, G., Laloe, V., Munoz-Sanchez, A., Arango, M., Hartzenberg, B., Khamis, H., Yutthakasemsunt, S., Komolafe, E., Olldashi, F., Yadav, Y., Murillo-Cabezas, F., Shakur, H., Edwards, P., and Collaborators, C. T. (2004) Effect of intravenous corticosteroids on death within 14 days in 10008 adults with clinically significant head injury (MRC CRASH trial): randomised placebo-controlled trial. *Lancet,* 364**,** 1321-8.

Romano, C., and Hicks, D. (2007) Adult retinal neuronal cell culture. *Prog Retin Eye Res,* 26**,** 379-97.

Roux, P. P., Shahbazian, D., Vu, H., Holz, M. K., Cohen, M. S., Taunton, J., Sonenberg, N., and Blenis, J. (2007) RAS/ERK signaling promotes site-specific ribosomal protein S6 phosphorylation via RSK and stimulates cap-dependent translation. *J Biol Chem,* 282**,** 14056-64.

Rui, Y., Myers, K. R., Yu, K., Wise, A., De Blas, A. L., Hartzell, H. C., and Zheng, J. Q. (2013) Activity-dependent regulation of dendritic growth and maintenance by glycogen synthase kinase 3β. *Nat Commun,* 4.

Saijilafu, Hur, E. M., Liu, C. M., Jiao, Z., Xu, W. L., and Zhou, F. Q. (2013) PI3K-GSK3 signalling regulates mammalian axon regeneration by inducing the expression of Smad1. *Nat Commun,* 4**,** 2690.

Saitoh, M., Pullen, N., Brennan, P., Cantrell, D., Dennis, P. B., and Thomas, G. (2002) Regulation of an activated S6 kinase 1 variant reveals a novel mammalian target of rapamycin phosphorylation site. *J Biol Chem,* 277**,** 20104-12.

Sanchez-Migallon, M. C., Nadal-Nicolas, F. M., Jimenez-Lopez, M., Sobrado-Calvo, P., Vidal-Sanz, M., and Agudo-Barriuso, M. (2011) Brain derived neurotrophic factor maintains Brn3a expression in axotomized rat retinal ganglion cells. *Exp Eye Res,* 92**,** 260-7.

Sandvig, A., Berry, M., Barrett, L. B., Butt, A., and Logan, A. (2004) Myelin-, reactive glia-, and scar-derived CNS axon growth inhibitors: expression, receptor signaling, and correlation with axon regeneration. *Glia,* 46**,** 225-51.

Sanes, J. R., and Masland, R. H. (2015) The Types of Retinal Ganglion Cells: Current Status and Implications for Neuronal Classification. *Annu Rev Neurosci*.

Sarbassov, D. D., Ali, S. M., Sengupta, S., Sheen, J. H., Hsu, P. P., Bagley, A. F., Markhard, A. L., and Sabatini, D. M. (2006) Prolonged rapamycin treatment inhibits mTORC2 assembly and Akt/PKB. *Mol Cell,* 22**,** 159-68.

Schwabe, R. F., and Brenner, D. A. (2002) Role of glycogen synthase kinase-3 in TNF-alpha-induced NF-kappaB activation and apoptosis in hepatocytes. *Am J Physiol Gastrointest Liver Physiol,* 283**,** G204-11.

Sedding, D. G., Widmer-Teske, R., Mueller, A., Stieger, P., Daniel, J. M., Gunduz, D., Pullamsetti, S., Nef, H., Moellmann, H., Troidl, C., Hamm, C., and Braun-Dullaeus, R. (2013) Role of the Phosphatase PTEN in Early Vascular Remodeling. *PLoS One,* 8**,** e55445.

Seira, O., and Del Rio, J. A. (2014) Glycogen synthase kinase 3 beta (GSK3beta) at the tip of neuronal development and regeneration. *Mol Neurobiol,* 49**,** 931-44.

Seki, M., Tanaka, T., Sakai, Y., Fukuchi, T., Abe, H., Nawa, H., and Takei, N. (2005) Muller Cells as a source of brain-derived neurotrophic factor in the retina: noradrenaline upregulates brain-derived neurotrophic factor levels in cultured rat Muller cells. *Neurochem Res,* 30**,** 1163-70.

Selles-Navarro, I., Ellezam, B., Fajardo, R., Latour, M., and Mckerracher, L. (2001) Retinal ganglion cell and nonneuronal cell responses to a microcrush lesion of adult rat optic nerve. *Exp Neurol,* 167**,** 282-9.

Shao, Z., Browning, J. L., Lee, X., Scott, M. L., Shulga-Morskaya, S., Allaire, N., Thill, G., Levesque, M., Sah, D., Mccoy, J. M., Murray, B., Jung, V., Pepinsky, R. B., and Mi, S. (2005) TAJ/TROY, an orphan TNF receptor family member, binds Nogo-66 receptor 1 and regulates axonal regeneration. *Neuron,* 45**,** 353-9.

Sharma, B., Gupta, R., Anand, R., and Ingle, R. (2014) Ocular manifestations of head injury and incidence of post-traumatic ocular motor nerve involvement in cases of head injury: a clinical review. *Int Ophthalmol*.

Shen, J. Y., Yi, X. X., Xiong, N. X., Wang, H. J., Duan, X. W., and Zhao, H. Y. (2011) GSK-3beta activation mediates Nogo-66-induced inhibition of neurite outgrowth in N2a cells. *Neurosci Lett,* 505**,** 165-70.

Shen, S., Wiemelt, A. P., Mcmorris, F. A., and Barres, B. A. (1999) Retinal ganglion cells lose trophic responsiveness after axotomy. *Neuron,* 23**,** 285-95.

Shim, M. S., and Kwon, Y. J. (2010) Efficient and targeted delivery of siRNA in vivo. *FEBS J,* 277**,** 4814-27.

Shin, S., Wolgamott, L., Tcherkezian, J., Vallabhapurapu, S., Yu, Y., Roux, P. P., and Yoon, S. O. (2014) Glycogen synthase kinase-3beta positively regulates protein synthesis and cell proliferation through the regulation of translation initiation factor 4E-binding protein 1. *Oncogene,* 33**,** 1690-9.

Shoshani, T., Faerman, A., Mett, I., Zelin, E., Tenne, T., Gorodin, S., Moshel, Y., Elbaz, S., Budanov, A., Chajut, A., Kalinski, H., Kamer, I., Rozen, A., Mor, O., Keshet, E., Leshkowitz, D., Einat, P., Skaliter, R., and Feinstein, E. (2002) Identification of a novel hypoxia-inducible factor 1-responsive gene, RTP801, involved in apoptosis. *Mol Cell Biol,* 22**,** 2283-93.

Silver, J., and Miller, J. H. (2004) Regeneration beyond the glial scar. *Nat Rev Neurosci,* 5**,** 146-56.

Singh, B., Singh, V., Krishnan, A., Koshy, K., Martinez, J. A., Cheng, C., Almquist, C., and Zochodne, D. W. (2014) Regeneration of diabetic axons is enhanced by selective knockdown of the PTEN gene. *Brain,* 137**,** 1051-67.

Smith, P. D., Sun, F., Park, K. K., Cai, B., Wang, C., Kuwako, K., Martinez-Carrasco, I., Connolly, L., and He, Z. (2009) SOCS3 deletion promotes optic nerve regeneration in vivo. *Neuron,* 64**,** 617-23.

Snell, R. S. 1998. The Eyeball. *Clinical Anatomy of the Eye.* 2nd ed. Oxford, UK: Blackwell Science, Inc.

So, K. F., and Yip, H. K. (1998) Regenerative capacity of retinal ganglion cells in mammals. *Vision Res,* 38**,** 1525-35.

Somervaille, T. C., Linch, D. C., and Khwaja, A. (2001) Growth factor withdrawal from primary human erythroid progenitors induces apoptosis through a pathway involving glycogen synthase kinase-3 and Bax. *Blood,* 98**,** 1374-81.

Song, L., Zhou, T., and Jope, R. S. (2004) Lithium facilitates apoptotic signaling induced by activation of the Fas death domain-containing receptor. *BMC Neurosci,* 5**,** 20.

Sriram, S., Robinson, P., Pi, L., Lewin, A. S., and Schultz, G. (2013) Triple combination of siRNAs targeting TGFbeta1, TGFbetaR2, and CTGF enhances reduction of collagen I and smooth muscle actin in corneal fibroblasts. *Invest Ophthalmol Vis Sci,* 54**,** 8214-23.

Stahl, N., Boulton, T. G., Farruggella, T., Ip, N. Y., Davis, S., Witthuhn, B. A., Quelle, F. W., Silvennoinen, O., Barbieri, G., Pellegrini, S., and Et Al. (1994) Association and activation of Jak-Tyk kinases by CNTF-LIF-OSM-IL-6 beta receptor components. *Science,* 263**,** 92-5.

Steinsapir, K. D., and Goldberg, R. A. (1994) Traumatic optic neuropathy. *Surv Ophthalmol,* 38**,** 487-518.

Steinsapir, K. D., and Goldberg, R. A. (2011) Traumatic optic neuropathy: an evolving understanding. *Am J Ophthalmol,* 151**,** 928-933 e2.

Steinsapir, K. D., Goldberg, R. A., Sinha, S., and Hovda, D. A. (2000) Methylprednisolone exacerbates axonal loss following optic nerve trauma in rats. *Restor Neurol Neurosci,* 17**,** 157-163.

Strickland, I. T., Richards, L., Holmes, F. E., Wynick, D., Uney, J. B., and Wong, L. F. (2011) Axotomy-induced miR-21 promotes axon growth in adult dorsal root ganglion neurons. *PLoS One,* 6**,** e23423.

Strober, W. (2001) Trypan blue exclusion test of cell viability. *Curr Protoc Immunol,* Appendix 3**,** Appendix 3B.

Su, H., Yuan, Q., Qin, D., Yang, X., Wong, W. M., So, K. F., and Wu, W. (2014) Lithium enhances axonal regeneration in peripheral nerve by inhibiting glycogen synthase kinase 3beta activation. *Biomed Res Int,* 2014**,** 658753.

Suggate, E. L., Ahmed, Z., Read, M. L., Eaton-Charnock, K., Douglas, M. R., Gonzalez, A. M., Berry, M., and Logan, A. (2009) Optimisation of siRNA-mediated RhoA silencing in neuronal cultures. *Mol Cell Neurosci,* 40**,** 451-62.

Sun, F., Park, K. K., Belin, S., Wang, D., Lu, T., Chen, G., Zhang, K., Yeung, C., Feng, G., Yankner, B. A., and He, Z. (2011) Sustained axon regeneration induced by co-deletion of PTEN and SOCS3. *Nature,* 480**,** 372-5.

Taga, T., and Kishimoto, T. (1997) Gp130 and the interleukin-6 family of cytokines. *Annu Rev Immunol,* 15**,** 797-819.

Tan, H. B., Zhong, Y. S., Cheng, Y., and Shen, X. (2011) Rho/ROCK pathway and neural regeneration: a potential therapeutic target for central nervous system and optic nerve damage. *Int J Ophthalmol,* 4**,** 652-7.

Tang, B. L. (2003) Inhibitors of neuronal regeneration: mediators and signaling mechanisms. *Neurochem Int,* 42**,** 189-203.

Tang, Z., Baykal, A. T., Gao, H., Quezada, H. C., Zhang, H., Bereczki, E., Serhatli, M., Baykal, B., Acioglu, C., Wang, S., Ioja, E., Ji, X., Zhang, Y., Guan, Z., Winblad, B., and Pei, J. J. (2014) mTor Is a Signaling Hub in Cell Survival: A Mass-Spectrometry-Based Proteomics Investigation. *J Proteome Res*.

Tanudji, M., Machalek, D., Arndt, G. M., and Rivory, L. (2010) Competition between siRNA duplexes: impact of RNA-induced silencing complex loading efficiency and comparison between conventional-21 bp and Dicer-substrate siRNAs. *Oligonucleotides,* 20**,** 27-32.

Tapley, P., Lamballe, F., and Barbacid, M. (1992) K252a is a selective inhibitor of the tyrosine protein kinase activity of the trk family of oncogenes and neurotrophin receptors. *Oncogene,* 7**,** 371-81.

Tato, I., Bartrons, R., Ventura, F., and Rosa, J. L. (2011) Amino acids activate mammalian target of rapamycin complex 2 (mTORC2) via PI3K/Akt signaling. *J Biol Chem,* 286**,** 6128-42.

Taylor, S., Srinivasan, B., Wordinger, R. J., and Roque, R. S. (2003) Glutamate stimulates neurotrophin expression in cultured Muller cells. *Brain Res Mol Brain Res,* 111**,** 189-97.

Taylor, S., Wakem, M., Dijkman, G., Alsarraj, M., and Nguyen, M. (2010) A practical approach to RT-qPCR-Publishing data that conform to the MIQE guidelines. *Methods,* 50**,** S1-5.

Technologies, L. 2012. Real-time PCR handbook. 2nd Edition ed.: Life Technologies.

Thakur, A., Fitzpatrick, S., Zaman, A., Kugathasan, K., Muirhead, B., Hortelano, G., and Sheardown, H. (2012) Strategies for ocular siRNA delivery: Potential and limitations of non-viral nanocarriers. *J Biol Eng,* 6**,** 7.

Thanos, S., Bohm, M. R., Schallenberg, M., and Oellers, P. (2012) Traumatology of the optic nerve and contribution of crystallins to axonal regeneration. *Cell Tissue Res,* 349**,** 49-69.

Toy, D., and Namgung, U. (2013) Role of glial cells in axonal regeneration. *Exp Neurobiol,* 22**,** 68-76.

Trivedi, N., Marsh, P., Goold, R. G., Wood-Kaczmar, A., and Gordon-Weeks, P. R. (2005) Glycogen synthase kinase-3beta phosphorylation of MAP1B at Ser1260 and Thr1265 is spatially restricted to growing axons. *J Cell Sci,* 118**,** 993-1005.

Tsang, C. K., Qi, H., Liu, L. F., and Zheng, X. F. (2007) Targeting mammalian target of rapamycin (mTOR) for health and diseases. *Drug Discov Today,* 12**,** 112-24.

Tsokas, P., Grace, E. A., Chan, P., Ma, T., Sealfon, S. C., Iyengar, R., Landau, E. M., and Blitzer, R. D. (2005) Local protein synthesis mediates a rapid increase in dendritic elongation factor 1A after induction of late long-term potentiation. *J Neurosci,* 25**,** 5833-43.

Turenne, G. A., and Price, B. D. (2001) Glycogen synthase kinase3 beta phosphorylates serine 33 of p53 and activates p53's transcriptional activity. *BMC Cell Biol,* 2**,** 12.

Ueki, Y., and Reh, T. A. (2012) Activation of BMP-Smad1/5/8 signaling promotes survival of retinal ganglion cells after damage in vivo. *PLoS One,* 7**,** e38690.

Vajda, F., Jordi, N., Dalkara, D., Joly, S., Christ, F., Tews, B., Schwab, M. E., and Pernet, V. (2015) Cell type-specific Nogo-A gene ablation promotes axonal regeneration in the injured adult optic nerve. *Cell Death Differ,* 22**,** 323-35.

Van Stavern, G. P., Biousse, V., Lynn, M. J., Simon, D. J., and Newman, N. J. (2001) Neuro-ophthalmic manifestations of head trauma. *J Neuroophthalmol,* 21**,** 112-7.

Vega-Rubin-De-Celis, S., Abdallah, Z., Kinch, L., Grishin, N. V., Brugarolas, J., and Zhang, X. (2010) Structural analysis and functional implications of the negative mTORC1 regulator REDD1. *Biochemistry,* 49**,** 2491-501.

Veldman, M. B., Bemben, M. A., Thompson, R. C., and Goldman, D. (2007) Gene expression analysis of zebrafish retinal ganglion cells during optic nerve regeneration identifies KLF6a and KLF7a as important regulators of axon regeneration. *Dev Biol,* 312**,** 596-612.

Vezina, C., Kudelski, A., and Sehgal, S. N. (1975) Rapamycin (AY-22,989), a new antifungal antibiotic. I. Taxonomy of the producing streptomycete and isolation of the active principle. *J Antibiot (Tokyo),* 28**,** 721-6.

Vidal-Sanz, M., Bray, G. M., Villegas-Perez, M. P., Thanos, S., and Aguayo, A. J. (1987) Axonal regeneration and synapse formation in the superior colliculus by retinal ganglion cells in the adult rat. *J Neurosci,* 7**,** 2894-909.

Vigneswara, V., Akpan, N., Berry, M., Logan, A., Troy, C. M., and Ahmed, Z. (2014) Combined suppression of CASP2 and CASP6 protects retinal ganglion cells from apoptosis and promotes axon regeneration through CNTF-mediated JAK/STAT signalling. *Brain,* 137**,** 1656-75.

Vigneswara, V., Berry, M., Logan, A., and Ahmed, Z. (2012) Pharmacological inhibition of caspase-2 protects axotomised retinal ganglion cells from apoptosis in adult rats. *PLoS One,* 7**,** e53473.

Vigneswara, V., Berry, M., Logan, A., and Ahmed, Z. (2013) Pigment epithelium-derived factor is retinal ganglion cell neuroprotective and axogenic after optic nerve crush injury. *Invest Ophthalmol Vis Sci,* 54**,** 2624-33.

Wahl, S. E., Mclane, L. E., Bercury, K. K., Macklin, W. B., and Wood, T. L. (2014) Mammalian target of rapamycin promotes oligodendrocyte differentiation, initiation and extent of CNS myelination. *J Neurosci,* 34**,** 4453-65.

Wahlin, K. J., Campochiaro, P. A., Zack, D. J., and Adler, R. (2000) Neurotrophic factors cause activation of intracellular signaling pathways in Muller cells and other cells of the inner retina, but not photoreceptors. *Invest Ophthalmol Vis Sci,* 41**,** 927-36.

Wahlin, K. J., Lim, L., Grice, E. A., Campochiaro, P. A., Zack, D. J., and Adler, R. (2004) A method for analysis of gene expression in isolated mouse photoreceptor and Muller cells. *Mol Vis,* 10**,** 366-75.

Walker, C. L., Liu, N. K., and Xu, X. M. (2013) PTEN/PI3K and MAPK signaling in protection and pathology following CNS injuries. *Front Biol (Beijing),* 8.

Wang, F., and Zhu, Y. (2008) The interaction of Nogo-66 receptor with Nogo-p4 inhibits the neuronal differentiation of neural stem cells. *Neuroscience,* 151**,** 74-81.

Wang, H., Shen, J., Xiong, N., Zhao, H., and Chen, Y. (2011) Protein kinase B is involved in Nogo-66 inhibiting neurite outgrowth in PC12 cells. *Neuroreport,* 22**,** 733-8.

Wang, K. C., Kim, J. A., Sivasankaran, R., Segal, R., and He, Z. (2002) P75 interacts with the Nogo receptor as a co-receptor for Nogo, MAG and OMgp. *Nature,* 420**,** 74-8.

Wang, X., Hasan, O., Arzeno, A., Benowitz, L. I., Cafferty, W. B., and Strittmatter, S. M. (2012) Axonal regeneration induced by blockade of glial inhibitors coupled with activation of intrinsic neuronal growth pathways. *Exp Neurol,* 237**,** 55-69.

Weichel, E. D., Colyer, M. H., Ludlow, S. E., Bower, K. S., and Eiseman, A. S. (2008) Combat ocular trauma visual outcomes during operations iraqi and enduring freedom. *Ophthalmology,* 115**,** 2235-45.

Weise, J., Isenmann, S., Klocker, N., Kugler, S., Hirsch, S., Gravel, C., and Bahr, M. (2000) Adenovirus-mediated expression of ciliary neurotrophic factor (CNTF) rescues axotomized rat retinal ganglion cells but does not support axonal regeneration in vivo. *Neurobiol Dis,* 7**,** 212-23.

Weishaupt, J. H., Diem, R., Kermer, P., Krajewski, S., Reed, J. C., and Bahr, M. (2003) Contribution of caspase-8 to apoptosis of axotomized rat retinal ganglion cells in vivo. *Neurobiol Dis,* 13**,** 124-35.

Weng, Q. P., Kozlowski, M., Belham, C., Zhang, A., Comb, M. J., and Avruch, J. (1998) Regulation of the p70 S6 kinase by phosphorylation in vivo. Analysis using site-specific anti-phosphopeptide antibodies. *J Biol Chem,* 273**,** 16621-9.

Wigley, C. B., and Berry, M. (1988) Regeneration of adult rat retinal ganglion cell processes in monolayer culture: comparisons between cultures of adult and neonatal neurons. *Brain Res,* 470**,** 85-98.

Wittwer, C. T., Herrmann, M. G., Moss, A. A., and Rasmussen, R. P. (1997) Continuous fluorescence monitoring of rapid cycle DNA amplification. *Biotechniques,* 22**,** 130-1, 134-8.

Wolin, M. J., and Lavin, P. J. (1990) Spontaneous visual recovery from traumatic optic neuropathy after blunt head injury. *Am J Ophthalmol,* 109**,** 430-5.

Wong, M. L., and Medrano, J. F. (2005) Real-time PCR for mRNA quantitation. *Biotechniques,* 39**,** 75-85.

Worby, C. A., Vega, Q. C., Zhao, Y., Chao, H. H., Seasholtz, A. F., and Dixon, J. E. (1996) Glial cell line-derived neurotrophic factor signals through the RET receptor and activates mitogen-activated protein kinase. *J Biol Chem,* 271**,** 23619-22.

Wu, J. H., Zhang, S. H., Gao, F. J., Lei, Y., Chen, X. Y., Gao, F., Zhang, S. J., and Sun, X. H. (2013) RNAi screening identifies GSK3beta as a regulator of DRP1 and the neuroprotection of lithium chloride against elevated pressure involved in downregulation of DRP1. *Neurosci Lett,* 554**,** 99-104.

Wu, M. M., Zhu, T. T., Wang, P., Kuang, F., Hao, D. J., You, S. W., and Li, Y. Y. (2014) Dose-dependent protective effect of lithium chloride on retinal ganglion cells is interrelated with an upregulated intraretinal BDNF after optic nerve transection in adult rats. *Int J Mol Sci,* 15**,** 13550-63.

Yang, L., Miao, L., Liang, F., Huang, H., Teng, X., Li, S., Nuriddinov, J., Selzer, M. E., and Hu, Y. (2014) The mTORC1 effectors S6K1 and 4E-BP play different roles in CNS axon regeneration. *Nat Commun,* 5**,** 5416.

Yang, P., and Yang, Z. (2012) Enhancing intrinsic growth capacity promotes adult CNS regeneration. *J Neurol Sci,* 312**,** 1-6.

Ye, S., Tan, L., Yang, R., Fang, B., Qu, S., Schulze, E. N., Song, H., Ying, Q., and Li, P. (2012) Pleiotropy of glycogen synthase kinase-3 inhibition by CHIR99021 promotes self-renewal of embryonic stem cells from refractory mouse strains. *PLoS One,* 7**,** e35892.

Yea, S. S., and Fruman, D. A. (2013) Achieving cancer cell death with PI3K/mTOR-targeted therapies. *Ann N Y Acad Sci,* 1280**,** 15-8.

Yin, Y., Cui, Q., Gilbert, H. Y., Yang, Y., Yang, Z., Berlinicke, C., Li, Z., Zaverucha-Do-Valle, C., He, H., Petkova, V., Zack, D. J., and Benowitz, L. I. (2009) Oncomodulin links inflammation to optic nerve regeneration. *Proc Natl Acad Sci U S A,* 106**,** 19587-92.

Yin, Y., Cui, Q., Li, Y., Irwin, N., Fischer, D., Harvey, A. R., and Benowitz, L. I. (2003) Macrophage-derived factors stimulate optic nerve regeneration. *J Neurosci,* 23**,** 2284-93.

Yin, Y., Henzl, M. T., Lorber, B., Nakazawa, T., Thomas, T. T., Jiang, F., Langer, R., and Benowitz, L. I. (2006) Oncomodulin is a macrophage-derived signal for axon regeneration in retinal ganglion cells. *Nat Neurosci,* 9**,** 843-52.

Yiu, G., and He, Z. (2003) Signaling mechanisms of the myelin inhibitors of axon regeneration. *Curr Opin Neurobiol,* 13**,** 545-51.

Yiu, G., and He, Z. (2006) Glial inhibition of CNS axon regeneration. *Nat Rev Neurosci,* 7**,** 617-27.

Yokogami, K., Wakisaka, S., Avruch, J., and Reeves, S. A. (2000) Serine phosphorylation and maximal activation of STAT3 during CNTF signaling is mediated by the rapamycin target mTOR. *Curr Biol,* 10**,** 47-50.

Yoshimura, T., Kawano, Y., Arimura, N., Kawabata, S., Kikuchi, A., and Kaibuchi, K. (2005) GSK-3beta regulates phosphorylation of CRMP-2 and neuronal polarity. *Cell,* 120**,** 137-49.

Yu-Wai-Man, P., and Griffiths, P. G. (2013a) Steroids for traumatic optic neuropathy. *Cochrane Database Syst Rev,* 6**,** CD006032.

Yu-Wai-Man, P., and Griffiths, P. G. (2013b) Surgery for traumatic optic neuropathy. *Cochrane Database Syst Rev,* 6**,** CD005024.

Yungher, B. J., Luo, X., Salgueiro, Y., Blackmore, M. G., and Park, K. K. (2015) Viral vector-based improvement of optic nerve regeneration: characterization of individual axons' growth patterns and synaptogenesis in a visual target. *Gene Ther*.

Zhang, C. W., Lu, Q., You, S. W., Zhi, Y., Yip, H. K., Wu, W., So, K. F., and Cui, Q. (2005) CNTF and BDNF have similar effects on retinal ganglion cell survival but differential effects on nitric oxide synthase expression soon after optic nerve injury. *Invest Ophthalmol Vis Sci,* 46**,** 1497-503.

Zhang, X., Tang, N., Hadden, T. J., and Rishi, A. K. (2011) Akt, FoxO and regulation of apoptosis. *Biochim Biophys Acta,* 1813**,** 1978-86.

Zhang, Y., Ueno, Y., Liu, X. S., Buller, B., Wang, X., Chopp, M., and Zhang, Z. G. (2013) The MicroRNA-17-92 Cluster Enhances Axonal Outgrowth in Embryonic Cortical Neurons. *J Neurosci,* 33**,** 6885-94.

Zhao, J., Qu, Y., Wu, J., Cao, M., Ferriero, D. M., Zhang, L., and Mu, D. (2013) PTEN inhibition prevents rat cortical neuron injury after hypoxia-ischemia. *Neuroscience,* 238**,** 242-51.

Zhen, X., Torres, C., and Friedman, E. (2002) Lithium regulates protein tyrosine phosphatase activity in vitro and in vivo. *Psychopharmacology (Berl),* 162**,** 379-84.

Zheng, J. Q., Kelly, T. K., Chang, B., Ryazantsev, S., Rajasekaran, A. K., Martin, K. C., and Twiss, J. L. (2001) A functional role for intra-axonal protein synthesis during axonal regeneration from adult sensory neurons. *J Neurosci,* 21**,** 9291-303.

Zhong, J., and Zou, H. (2014) BMP signaling in axon regeneration. *Curr Opin Neurobiol,* 27C**,** 127-134.

Zhou, F. Q., and Snider, W. D. (2005a) Cell biology. GSK-3beta and microtubule assembly in axons. *Science,* 308**,** 211-4.

Zhou, F. Q., and Snider, W. D. (2005b) CELL BIOLOGY: GSK-3beta and Microtubule Assembly in Axons. *Science,* 308**,** 211-214.

Zhou, F. Q., and Snider, W. D. (2006) Intracellular control of developmental and regenerative axon growth. *Philos Trans R Soc Lond B Biol Sci,* 361**,** 1575-92.

Zhou, F. Q., Zhou, J., Dedhar, S., Wu, Y. H., and Snider, W. D. (2004) NGF-induced axon growth is mediated by localized inactivation of GSK-3beta and functions of the microtubule plus end binding protein APC. *Neuron,* 42**,** 897-912.

Zhou, W., Raisman, G., and Zhou, C. (1998) Transplanted embryonic entorhinal neurons make functional synapses in adult host hippocampus. *Brain Res,* 788**,** 202-6.

Zimmer, D. B., Cornwall, E. H., Landar, A., and Song, W. (1995) The S100 protein family: history, function, and expression. *Brain Res Bull,* 37**,** 417-29.

Zou, H., Lai, Y., Zhao, X., Yan, G., Ma, D., Cardenes, N., Shiva, S., Liu, Y., Bai, X., Jiang, Y., and Jiang, Y. (2013) Regulation of mammalian target of rapamycin complex 1 by Bcl-2 and Bcl-XL proteins. *J Biol Chem,* 288**,** 28824-30.

Zukor, K., Belin, S., Wang, C., Keelan, N., Wang, X., and He, Z. (2013) Short hairpin RNA against PTEN enhances regenerative growth of corticospinal tract axons after spinal cord injury. *J Neurosci,* 33**,** 15350-61.

APPENDIX

Elements of work presented in this thesis have been published in:

Morgan-Warren PJ, Berry M, Ahmed Z, Scott RAH, Logan A. Exploiting mTOR signaling: a novel translatable treatment strategy for traumatic optic neuropathy? *Invest Ophthalmol Vis Sci.* 2013; 54: 6903-6916

Morgan-Warren PJ, O'Neill J, De Cogan F, Spivak K, Ashush H, Kalinski H, Ahmed Z, Berry B, Feinstein E, Scott RAH, Logan A. siRNA mediated knockdown of the mTOR inhibitor RTP801 promotes retinal ganglion cell survival and axon elongation by direct and indirect mechanisms. *Invest Ophthalmol Vis Sci.* 2016 (in press). DOI:10.1167/iovs.15-17511